

Systemic iron distribution during hemochromatosis and inflammation

By

Bill Andriopoulos

Department of Medicine

Division of Experimental Medicine

McGill University

Montreal, Quebec, Canada

October 2007

A thesis submitted to the Faculty of Graduate Studies and Research in partial fulfillment of the requirements for the degree of Doctor of Philosophy

© Bill Andriopoulos 2007

ABSTRACT	5
RESUME	8
PREFACE AND CONTRIBUTIONS OF AUTHORS	11
ACKNOWLEDGEMENTS	15
CLAIM TO ORIGINALITY	17
CHAPTER I. GENERAL INTRODUCTION	18
1. Iron Homeostasis	19
2. Chemistry of Iron	19
3. Biology of Iron	20
4. Iron's Toxicity	20
5. Body Iron	21
6. Iron Absorption	22
7. Cellular Iron Uptake	24
8. Iron Storage	25
9. Regulation of Iron Uptake and Storage Proteins	26
9.1. IRP1	28
9.2. IRP2	29
10. Iron and Disease	30
11. Heparin, the master hormonal regulator of iron stores	31
11.1 Expression and Biochemical Properties	31
11.2. Mouse model studies	32
11.2.1. Heparin silencing	32
11.2.2. Heparin overexpression	33
11.3. Molecular mechanism of heparin action	33
11.3.2. Mechanism of ferroportin internalization and degradation	34
11.4. Heparin Stimuli	35
11.4.1 Heparin regulation by iron	35
11.4.1.1. HFE	36
11.4.1.2. TfR2	37
11.4.1.3. Hju	37
11.4.1.3.1. Expression and Biochemical Properties	38
11.4.1.3.2. RNA encoding Hju	38
11.4.1.3.3. Hju protein features	38
11.4.1.3.4. Hju mutations in JH	40
11.4.1.3.5. Processing of Hju	41
11.4.1.3.5.1 Defective Hju Processing	43
11.4.1.3.6. Function of Hju	44
11.4.1.3.6.1. Regulation of heparin	44
11.4.1.3.6.2. Hju and cell signaling	45
11.4.1.3.6.3. Soluble Hju	46
11.4.1.3.7. Regulation of Hju	47
11.4.1.3.7.1. Hju and iron	48
11.4.1.3.7.2. Hju and inflammation	49
11.4.1.3.7.3. Hju and neogenin	49
11.5.1. Heparin regulation by inflammation	50
11.5.1.1. Localized responses	51

11.5.1.2. Systemic response	51
11.5.1.2.1. Hypoferremia of inflammation	51
11.5.1.2.1.1. Cytokine induction of hepcidin	51
11.5.1.2.1.2. Physiology of hepcidin's action	53
11.5.1.3. ACD	54
11.5.1.3.1. Diseases responsible for ACD	54
11.5.1.3.2. Oxidative Burst	55
11.5.1.3.3. Alterations in iron homeostasis	55
11.5.1.3.4. Alterations in erythropoiesis	56
11.5.1.3.5. Treating ACD	57
11.6.1. Hepcidin regulation by erythropoietic demand	57
12. Hemolysis	59
12.1. Mechanisms of Hemolysis	59
12.2. Hemoglobin scavenging	60
12.3. Hemolytic anemias	60
13. Hypothesis and objectives of this work	61
FIGURES	63
FIGURE LEGENDS	73
CHAPTER II. HEMOLYSIS PROMOTES THE RELEASE OF A NOVEL POSITIVE REGULATOR OF HEPCIDIN EXPRESSION, SOLUBLE HJV	76
PREFACE	77
ABSTRACT	78
INTRODUCTION	80
MATERIALS AND METHODS	83
RESULTS	89
DISCUSSION	99
FIGURES	104
FIGURE LEGENDS	122
CHAPTER III. HEPCIDIN GENERATED BY HEPATOMA CELLS INHIBITS IRON EXPORT FROM CO-CULTURED THP1 MONOCYTES	129
PREFACE	130
ABSTRACT	131
INTRODUCTION	132
MATERIALS AND METHODS	134
RESULTS	138
DISCUSSION	142
FIGURES	145
FIGURE LEGENDS	152
CHAPTER IV. SUSTAINED HYDROGEN PEROXIDE INDUCES IRON UPTAKE BY TFR1-1 INDEPENDENT OF THE IRP/IRE NETWORK	155
PREFACE	156
ABSTRACT	157
INTRODUCTION	158

MATERIALS AND METHODS	161
RESULTS	166
DISCUSSION	171
FIGURES	175
FIGURE LEGENDS	188
CHAPTER V. DISCUSSION	192
REFERENCES	201
ABBREVIATIONS	217
REFEREED PAPERS IN PUBLISHED FORMAT	222

ABSTRACT

Juvenile hemochromatosis (JH), anemia of chronic disease (ACD) and various inflammatory conditions such as Hepatitis C and alcoholic steatohepatitis exhibit improper handling of systemic iron.

Patients with JH have mutations in either the hemojuvelin (Hjv) or hepcidin genes. Thus far, Hjv appears to control the levels of hepatic hepcidin, the master hormonal regulator of iron stores. Interestingly, Hjv exists in both a cellular and soluble form [1] that is expressed primarily in the muscle and to a lesser extent in the liver [2]. Cellular Hjv (cHjv), localized in the liver, is a GPI-anchored protein that enhances bone morphogenic protein (BMP) mediated induction of hepcidin [3]. On the other hand, soluble Hjv (sHjv) is a negative regulator of hepatic hepcidin expression [1, 4, 5].

We hypothesize that sHjv plays an important systemic role in regulating iron homeostasis. Thus, our goal was to 1) investigate the signals regulating shedding of muscle sHjv and 2) study the hormonal function of sHjv in the target liver. Surprisingly, using in vitro and in vivo models, we observed elevated release of Hjv during hemolytic conditions. Furthermore, in contrast to previously published reports, both cell culture and animal model studies reveal sHjv as a positive regulator of hepatic hepcidin.

Upon induction of hepcidin expression in the liver, the hormonal peptide exerts its actions by binding and internalizing the iron exporter ferroportin in the reticuloendothelial system (RES) and duodenum [6, 7]. Using a co-culture system, we investigated the effects of secreted hepatic hepcidin on the iron metabolism of target monocytes. As a result, hepatic hepcidin was shown to inhibit iron export and promote iron retention within monocytes.

Inappropriate levels of hepcidin, whether low or high, results in improper handling of iron stores which may potentially cause disease, on both sides of the iron spectrum. On one side of the scale, such as in hemochromatosis, inappropriately low hepcidin expression permits elevated mobilization of iron stores from the RES. Increased mobilization eventually saturates serum transferrin leading to iron accumulation in the liver parenchyma. On the other side of the spectrum, such as in ACD, higher than normal levels of hepcidin is associated with increased containment of iron within the RES which subsequently elicits hypoferremia.

In addition to increased iron retention in the RES, various forms of inflammation display elevated iron accumulation in the liver parenchyma. Interestingly, the expression of transferrin receptor (TfR1) is induced in some of these livers [8, 9]. Previously published reports suggest a link between inflammation and iron homeostasis through hydrogen peroxide (H_2O_2) and iron regulatory protein 1 (IRP1). Transient pulses of H_2O_2 , a dismutated product of superoxide released during an oxidative burst from macrophage and neutrophils, is capable of activating IRP1 in cultured cells [10]. We hypothesize that sustained and non-toxic exposure of H_2O_2 to fibroblasts will induce iron uptake in an IRP dependent mechanism. As expected, we observed an increase in iron uptake but surprisingly independent of IRP1 activity. Thus, we identified a novel mechanism of iron accumulation by sustained H_2O_2 , via direct translational activation of TfR1 during periods of inflammation.

Taken together, in this thesis, we show that the release of sHjv is a regulated process where intravascular hemolysis may provide a physiological stimulus for this response. In turn, sHjv is necessary for inducing hepcidin expression in the liver.

Increased levels of hepcidin will inhibit iron export from the RES and subsequently lead to hypoferremia. In addition to elevated iron retention within the RES, certain inflammatory conditions display increased iron accumulation in the parenchyma. Continuous release of H_2O_2 by inflammatory cells directly stimulates TfR1 translation which subsequently increases iron uptake in the parenchyma.

RESUME

L'hémochromatose juvénile (HJ), anémie de maladie chronique (ACD) et des conditions inflammatoires variées, telles que l'Hépatite C et la stéatopathie de l'alcoolique démontrent la mauvaise manipulation du fer systémique.

Les patients atteints de l'HJ ont des mutations dans soit, les gènes hemojuvelin (Hjv) ou hepcidine. Jusqu'à maintenant, Hjv semble contrôler les niveaux d'hepcidine hépatique, le régulateur maître pour les réserves de fer. Nous avons observé que l'Hjv existe autant sous forme cellulaire que soluble [1] qui s'exprime surtout dans le muscle et de façon moins prononcée dans le foie [2]. L'Hjv cellulaire (Hjvc), située dans le foie, est une protéine ancrée par GPI qui améliore la « Bone Morphogenic Protein » arbitrée par l'induction d'hepcidine [3]. D'autre part, l'Hjv soluble (sHjv) est un régulateur négatif d'expression d'hepcidine hépatique [1, 4, 5].

Nous avons élaboré l'hypothèse que le sHjv joue un rôle systémique important dans la régulation d'homeostasie du fer. Alors, notre objectif était de 1) rechercher les signaux régulant la perte de muscle sHjv et 2) d'étudier la fonction hormonale du sHjv dans le foie cible. Étonnement, en utilisant des modèles *in vitro* et *in vivo*, nous avons observé la perte élevée de Hjv pendant des conditions hémolytiques. De plus, en contraste à des rapports précédemment publiés, les cultures cellulaires ainsi que les modèles basés sur les animaux révèlent que la sHjv et un régulateur positif d'hepcidine hépatique.

Dès l'induction d'expression d'hepcidine dans le foie, la peptide hormonale exerce son action en fusionnant et en internalisant l'exportateur de fer, ferroportine dans le système réticuloendothélial (RES) [6, 7]. En utilisant un système de co-culture, nous

avons cherché les effets d'hepcidine hépatique secrétée sur le métabolisme du fer de monocytes cibles.

Des niveaux inappropriés de hepcidine, soit bas ou élevés, résultent dans la manipulation inappropriée des réserves de fer qui peuvent potentiellement mener à des maladies, des deux côtés du spectre de fer. D'un côté de la balance, tel que dans l'hémochromatose, des niveaux bas d'expression d'hepcidine permettent des niveaux de mobilisation élevés dans les réserves de fer du RES. La mobilisation accrue sature éventuellement le sérum transferrin menant à l'accumulation de fer dans le parenchyme du foie. De l'autre côté du spectre, tel que dans l'ACD, des niveaux plus élevés que d'habitude de hepcidine en association avec la rétention accrue de fer dans le RES qui inflige subséquemment l'hypoferremie.

En plus de la rétention accrue du fer dans le RES, des formes variées d'inflammation démontrent une accumulation élevée de fer dans le parenchyme du foie. Il est intéressant de constater que l'expression du récepteur de transferrin (TfR) est induite dans quelques uns de ses foies [8, 9]. Des rapports précédemment publiés suggèrent un lien entre l'inflammation et l'homeostasie du fer à travers le peroxyde d'hydrogène (H_2O_2) et la protéine régulatrice du fer 1 (IRP1). Des pulsations transientes de H_2O_2 , un produit démuté de superoxyde relâché pendant une réaction oxydative des macrophages et neutrophiles, est capable d'activer IRP1 dans des cellules cultivées [10]. Notre hypothèse est que l'exposition soutenue et non-toxique de H_2O_2 à des fibroblastes induiront l'internalisation de fer dans un mécanisme dépendant de l'IRP. Tel qu'attendu, nous avons observé une augmentation d'internalisation de fer, mais de

façon surprenante elle était indépendante d'activité du IRP1. Nous avons identifié un nouveau mécanisme d'accumulation de fer par l'exposition soutenue du H₂O₂, par activation translationnelle de TfR pendant des périodes d'inflammation.

Ensemble, dans cette thèse, nous démontrons que la relâche de sHjv est un processus régulé où hemolyse inter vasculaire peut offrir un stimulus physiologique pour cette réponse. De plus, Hjvs est un activateur hormonal de hepcidine dans le foie. Des niveaux accru de hepcidine empêcheront l'exportation du fer du RES et mèneront subséquemment à l'hypoferremie. En plus de la rétention élevée dans le RES, certaines conditions inflammatoires démontrent une accumulation de fer dans le parenchyme. La relâche constante de H₂O₂ par des cellules inflammatoires stimules la translation du TfR qui augmente subséquemment l'internalisation du fer dans le parenchyme.

PREFACE AND CONTRIBUTIONS OF AUTHORS

“As an alternative to the traditional thesis format, the thesis can consist of a collection of papers of which the student is an author or co-author.”

(Quoted from McGill University guidelines for submitting a doctoral thesis at: <http://www.mcgill.ca/gps/programs/thesis/guidelines/preparation/>).

In accordance with the above guidelines for thesis preparation and submission, I have included the following papers as the core of my thesis (CHAPTER II, III and IV).

- **Andriopoulos B**, Palaiologou D, Fillebeen C, Daba A, Robinson M, Hadjis A, Papanikolaou G Pantopoulos K. Hemolysis promotes the release of a novel positive regulator of hepcidin expression, soluble HJV. (Manuscript to be submitted)
- **Andriopoulos B**, Pantopoulos K. Hepcidin generated by hepatoma cells inhibits iron export from co-cultured THP1 monocytes. *J Hepatol.* 2006 Jun;44(6):1125-31. Epub 2005 Dec 5.
- **Andriopoulos B**, Hegedusch S, Mangin J, Riedel HD, Hebling U, Wang J, Pantopoulos K, Mueller S. Sustained hydrogen peroxide induces iron uptake by TfR1-1 independent of the iron regulatory protein/iron-responsive element network. *J Biol Chem.* 2007 Jul 13;282(28):20301-8. Epub 2007 May 21.

I have included as the first chapter, an extensive literature review as an introduction to the thesis. Chapter II, Hemolysis promotes the release of a novel positive regulator of hepcidin expression, soluble HJV, is a first author manuscript in which I performed most of the experiments and wrote the manuscript in collaboration with my

supervisor Dr. Kostas Pantopoulos. The paper will soon be submitted for publication. Chapter III, Heparin generated by hepatoma cells inhibits iron export from co-cultured THP1 monocytes is a first author manuscript to which I performed all the experiments. The paper was written in association with my supervisor, Dr. Kostas Pantopoulos. A reprint copy is included in the appendix. Chapter IV, Sustained hydrogen peroxide induces iron uptake by TfR1 independent of the iron regulatory protein/iron-responsive element network, is a first author paper to which I completed many of the experiments and wrote the manuscript in close collaboration with Dr. Sebastian Mueller and Dr. Kostas Pantopoulos. A reprint copy is included in the appendix. I have not included the following five publications to which I have made a substantial contribution:

- Fillebeen C, Muckenthaler M, **Andriopoulos B**, Bisailon M, Mounir Z, Hentze MW, Koromilas AE, Pantopoulos K. Expression of the subgenomic hepatitis C virus replicon alters iron homeostasis in Huh7 cells. *J Hepatol*. Epub March 2, 2007.
- Harrison-Findik DD, Schafer D, Klein E, Timchenko NA, Kulaksiz H, Clemens D, Fein E, **Andriopoulos B**, Pantopoulos K, Gollan J. Alcohol metabolism-mediated oxidative stress down-regulates hepcidin transcription and leads to increased duodenal iron transporter expression. *J Biol Chem*. 2006 Aug 11;281(32):22974-82. Epub 2006 May 31.
- Wang J, Fillebeen C, Chen G, **Andriopoulos B**, Pantopoulos K. Sodium nitroprusside promotes IRP2 degradation via an increase in intracellular iron and in the absence of S nitrosylation at C178. *Mol Cell Biol*. 2006 Mar;26(5):1948-54.

- Kiemer AK, Forniges AC, Pantopoulos K, Bilzer M, **Andriopoulos B**, Gerwig T, Kenngott S, Gerbes AL, Vollmar AM. ANP-induced decrease of iron regulatory protein activity is independent of HO-1 induction. *Am J Physiol Gastrointest Liver Physiol*. 2004 Sep;287(3):G518-26. Epub 2004 Apr 15.
- **Andriopoulos, B.** and Pantopoulos, K. (2004): Regulation of iron metabolism at the cellular and systemic level. *Recent Res. Devel. Mol. Cell. Biol.*: 5 1-22. Pages 1-22.

For the Journal of Hepatology paper I performed iron release and accumulation studies in Huh7 replicon cells. In both the Journal of Biological Chemistry and American Journal of Physiology: Gastrointestinal Liver Physiology papers, I performed IRP bandshift assays from cell lysates provided by the corresponding authors. In the Molecular and Cellular Biology paper, I measured, using the Greiss reagent, levels of nitrite in cell culture supernatant of cells treated with freshly prepared and photodegraded sodium nitroprusside. Finally, the Recent Research Development in Molecular and Cellular Biology paper was a review for a chapter in a book.

The following is how the co-authors contributed to my first author papers. Danaï Palaiologou, Carine Fillebeen, and Alina Daba assisted with the real-time PCR analysis and mouse experiments in Chapter II. Matthew Robinson and Alexis Hadjis were summer students who were instrumental in helping with everyday experiments. Dr. George Papanikolaou's lab in Greece performed the experiments depicted in Fig. 10A of Chapter II. Chapter IV was the result of work done in close collaboration with our lab and that of Dr. Sebastian Mueller (Hegedusch S, Mangin J, Riedel HD, Hebling U). Both of our labs separately reproduced Figs. 1, 2 and 5. Figs. 3 and 4 were done in Dr. Sebastian Mueller's lab whereas I performed the experiments for Figs. 6 and 7. Jian

Wang from our lab originally did Fig. 5A, which I and Dr. Sebastian Mueller's lab reproduced.

ACKNOWLEDGEMENTS

On a hot summer day in June 2003, Dr. Kostas Pantopoulos granted me permission to pursue my doctoral studies in his lab. In the 4 years since then, I have had the absolute pleasure of being mentored by Dr. Pantopoulos. With his door always open, Dr. Pantopoulos and I have shared many scientific discussions. Since 2003, he has taught me to think critically and to keep an open mind to scientific observations and debate. He has included me in many collaborations and has sent me to places all around the world so that I may share my work with others. I am forever indebted to him for his teachings and opportunities he has granted me.

Our collaborators Dr. Sebastian Mueller and Dr. George Papanikolaou were essential in the work presented in this thesis.

I would also like to acknowledge my lab co-workers throughout the years, Annie Caltagirone, Dr. Carine Fillebeen, Dr. Jian Wang and Dr. Guohua Chen. Each taught me multiple lab techniques that were essential in my publications. Alina Daba, Julie Lee, Danai Palaiologou, and Dr. Anja Haussman have helped me with multiple experiments.

In addition to our lab, Dr. Prem Ponka and his lab made significant contributions in scientific discussions and experimental techniques. Since undergraduate school, Dr. Prem Ponka has been especially helpful with his feedback and advice. Importantly, whenever I worked late into the night, my good friend Marc Mikhael always kept me company and in good spirit with his humor. In addition, Aleric Cirella who helped in the translation of the abstract clearly defined the meaning of friendship with his support during my years as a PhD student.

I would also like to acknowledge the Canadian Liver Foundation and McGill Experimental Medicine for salary support. In particular, Dr. Hugh Bennett has been incredibly supportive during my years as a PhD student.

Furthermore, my brother George constantly made sure I was in a good mood no matter how tough research was. My oldest brother Andre and his wife Effie always supported me with advice and encouragement.

Instead of acknowledging my parents I would like to make a dedication. This thesis is not only a result of my hard work, but a life time of theirs. I aim only to make them proud with this thesis.

Last and foremost, I full heartedly acknowledge my love Dr. Eftihia Cocolakis. Throughout the last 4 years, Eftihia has supported me in everyway possible with incredible love, kindness and care.

CLAIM TO ORIGINALITY

The present thesis, consisting of five chapters, was written by me, Bill Andriopoulos, under the supervision of my thesis director, Dr. Kostas Pantopoulos. The manuscript presented in Chapter II, will be submitted for publication and consists of original and unpublished data. Chapters III and IV contain refereed published papers which were at the time original and unpublished data.

The major novel findings of the presented thesis are as follows:

1. Hemolysis promotes the release of a novel positive regulator of hepcidin expression, soluble HJV.
2. Hepcidin generated by hepatoma cells inhibits iron export from co-cultured THP1 monocytes.
3. Sustained hydrogen peroxide induces iron uptake by TfR1 independent of the iron regulatory protein/iron-responsive element network

CHAPTER I. GENERAL INTRODUCTION

1. Iron Homeostasis

Iron is one of the most useful metals on our planet. Since the middle bronze age, mankind has always benefited from its abundance and versatile applicability. For instance, whether in its elemental or steel form, iron has produced innumerable indispensable tools and destructive weapons. Similarly in biology, all vertebrates utilize iron as an essential molecular tool and potent weapon. The ruinous power of iron in organisms is not only observed against a foreign pathogen, but to the host. When present in excess, iron essentially becomes a toxin capable of inflicting organ damage. On the other side, a scarcity of iron within an organism prevents multiple biological tools from carrying out vital survival tasks. To ensure appropriate handling of iron, organisms have evolved elegant mechanisms to maintain a delicate iron balance, defined as iron homeostasis.

2. Chemistry of Iron

Iron is essential to all living cells. Iron's biological importance stems from its ability to transition between a ferrous (Fe(II)) (soluble) to ferric (Fe(III)) (insoluble) state where it may either donate (oxidation) or accept (reduction) electrons, respectively. Such an elemental transition defined as an electrochemical redox potential is vital in carrying out cellular processes such as oxygen transport, electron transfer and catalytic reactions. At physiological oxygen tension and pH, Fe(II) is readily oxidized to Fe(III). Subsequently, Fe(III) is further hydrated to form insoluble ferric hydroxide and oxyhydroxide polymers.

3. Biology of Iron

Iron is *au fait* for forming a complex with either heme or non-heme proteins. Heme is an important prosthetic group that is composed of the protoporphyrin IX ring that constrains iron within its center. The synthesis of protoporphyrin IX occurs in multiple steps within the cytosol and mitochondria of a cell. The final step incorporates ferrous iron into the protoporphyrin ring at the inner mitochondrial layer by the enzyme ferrochelatase. Upon heme-iron assembly in the mitochondrial matrix, heme assimilates into proteins to form oxygen carriers such as hemoglobin or myoglobin. It also participates in electron transfer reactions by assembling into cytochromes. Furthermore, it constitutes the active sites of enzymes such as oxidases, peroxidases, catalases or NO-synthases. In contrast, iron also interacts with non-heme substrates such as iron-sulfur clusters, mononuclear iron centers or iron-oxo clusters.

4. Iron's Toxicity

Iron is essential, however when present in excess has the potential to be toxic. Its toxicity resides in its ability to catalyze the formation of potentially dangerous hydroxyl ($\text{OH}\cdot$) and organic radicals (Fig. 1.). Iron catalyzed generation of $\text{OH}\cdot$ is accomplished in the presence of two reactive oxygen intermediates (ROIs), hydrogen peroxide (H_2O_2) and superoxide anion ($\text{O}_2^{\cdot-}$). ROIs may originate from byproducts of mitochondrial aerobic respiration or enzyme reactions in the peroxisome, endoplasmic reticulum and cytoplasm. Iron also reacts with organic peroxides to generate organic radicals such as alkoxyl peroxy, thiyl and thiyl-peroxy.

Mechanisms have evolved to protect against ROIs such as peroxidases and catalase which decompose (H_2O_2). However, if the defense mechanisms against free radicals are compromised, free radicals will evoke cellular damage via protein oxidation, membrane lipid peroxidation and nucleic acid damage or mutagenesis. Damage caused by oxidative stress leads to cell death and tissue degeneration which are both observed in aging [11] and various pathological conditions such as inflammation, ischemia-reperfusion injury, diabetes, pulmonary disease, and neurodegeneration [12].

During inflammation (infection induced or not), ROIs are generated as a defense mechanism against bacteria by membrane bound nicotinamide adenine dinucleotide phosphate (NADPH) oxidase. This process, defined as an oxidative burst, results in a direct $\text{O}_2^{\cdot-}$ targeted attack against bacteria. Furthermore, in the presence of nitric oxide, $\text{O}_2^{\cdot-}$ may spontaneously form a more potent oxidant called peroxynitrite (ONOO^-). $\text{O}_2^{\cdot-}$ could also form H_2O_2 , either spontaneously or enzymatically which in turn, may produce hypochlorite (OCl^-) through myeloperoxidase. Thus infection or inflammation induced production of ROIs serves as a beneficial role in defending against invading bacteria. In addition, ROIs which arise from by-products of metabolic pathways may function as important second messengers in various signaling pathways [13]. Taken together, ROIs may be damaging, protective or direct participants in signaling pathways.

5. Body Iron

Humans contain approximately 3-5 g of iron from which males have 55 mg per kilogram body weight whereas females have a lesser 45 mg per kilogram body weight. Both males and females absorb approximately 1-2 mg of iron from a daily western diet of

15-20 mg. Iron absorption occurs in enterocytic cells of the duodenum where once internalized, it may be utilized, stored or exported into the circulation. Exported iron is delivered to the transporter protein transferrin in the circulation. Once in the circulation, iron may be distributed to a variety of areas in our body such as the muscle, liver or bone marrow (Fig. 2). Approximately 3 mg of iron is bound to transferrin in the plasma at any given time. Turnover of plasma transferrin iron is in the region of 25 mg/24 hour. On average, 80% of transferrin bound iron is destined mostly to the bone marrow where iron is used for hemoglobin synthesis during erythropoiesis. Upon release from the bone marrow and spleen, normal reticulocytes have a life span of 120 days. Senescent or damaged reticulocytes are erythrophagocytosed by macrophages which in turn break down hemoglobin and recycle iron back into the circulation. The remaining 20% of plasma transferrin iron is delivered to non-erythroid tissues namely the muscle and liver. The muscle contains approximately 300 mg of functional iron in the form of myoglobin. In addition, transferrin bound iron may be distributed to liver hepatocytes (and to a far lesser extent liver macrophages) where it is mostly stored. Importantly, only a small portion of the 1000 mg of iron in the liver is functional.

Iron loss occurs through non-specific mechanisms such as cell desquamation, bleeding or menstruation and accounts for 1-2 mg per day. There exists no regulated mechanism for iron excretion. With no specific mechanisms to lose iron, its distribution, utilization and storage is tightly regulated.

6. Iron Absorption

Approximately 1-2 mg of ingested iron is absorbed in the duodenum, more specifically by a mature enterocyte. Approximately 2/3 of the daily ingested iron is heme iron while the remaining 1/3 is a non-heme form. To date, the mechanisms by which heme iron absorption occurs remains elusive. In contrast, extensive progress has recently been made in understanding the means and regulation of non-heme iron absorption.

Iron absorption commences via transport from the duodenal lumen across the apical membrane of mature enterocytes (Fig. 3). More specifically, ingested Fe(III) is reduced to Fe(II) by the apical membrane bound reductase, duodenal cytochrome B (DcytB). Following a catalyzed reduction, Fe(II) is transported across the apical membrane into the cell by the Divalent Metal Transporter (DMT1). In addition to importing Fe(II) into the enterocyte, DMT1 may also deliver the divalent cations Zn^{2+} , Mn^{2+} , Co^{2+} , Cd^{2+} , Cu^{2+} , Ni^{2+} and Pb^{2+} [14]. Transport across the membrane is pH dependent and defined as a parallel proton symport. Unlike DcytB, DMT1 expression has been found in all cell types in which it has been sought [15]. Alongside serving as an importer at the apical side of an enterocyte, DMT1 is also an iron transporter within a cell's endosome. More specifically, iron uptake via the transferrin cycle is released from an acidified endosome by DMT1. Animal models possessing a mutation in DMT1 such as the microcytic anemia (MK) mice or Belgrade rats display a severe microcytic anemia phenotype. Furthermore, humans possessing a DMT1 mutation exhibit a similar severe microcytic anemia that is observed in mouse models [16]. Taken together, DMT1 has a dual transporter function either in absorption of iron or the transferrin cycle.

Once transported into the enterocyte, iron's movement within the cell remains elusive. However, iron is transported out of the enterocyte into the portal circulation via

ferroportin. Initially identified by 3 independent groups as ferroportin [17], IREG1[18] and MTP1[19], ferroportin is the sole iron exporter identified to date. Ferroportin is also expressed in macrophages where it serves to recycle iron obtained from senescent red blood cells back into the circulation. In addition, the iron exporter is expressed in placental syncytiotrophoblasts where it serves to deliver iron to the fetus.

Importantly, ferrous iron exported from enterocytes via ferroportin is oxidized by the blue copper ferroxidase ceruloplasmin (this is true for both heme non-heme iron that has been absorbed). This ferroxidase is produced in the liver and secreted into the plasma [20]. Interestingly a Glycosylphosphatidylinositol (GPI) -anchored form co-localizes with ferroportin on the membrane of astrocytes and neurons [21]. In addition there exists the membrane bound ferroxidase hephaestin which is a ceruloplasmin homolog.

Ceruloplasmin oxidation of Fe(II) to Fe(III) permits binding onto transferrin's two high affinity binding sites. Iron, now in its oxidized and transferrin bound state, is non-toxic and ready for transport within the circulation. Iron bound to transferrin whether it is monoferric or diferric (~2-3 μM) is referred to as holo-transferrin (holo-Tf) and accounts for 30% of total transferrin. The remaining 70% of circulating transferrin is called apo-transferrin. Taken together, approximately 18 μM of the 56 μM of plasma transferrin, is holo-Tf [22].

7. Cellular Iron Uptake

Circulating holo-Tf delivers iron to target cells via a transferrin/TfR1 mediated pathway (Fig. 4). More specifically, binding of transferrin to TfR1 initiates endocytosis via clathrin coated pit formation. Upon internalization, the clathrin coat disassociates

from the endosome and leads to acidification of this newly formed compartment. Endosomal acidification occurs via a proton pump that sets the pH to approximately 5.5. Low endosomal pH permits disassociation of diferric iron from transferrin. Liberated iron is subsequently exported from the endosome into the cytosol by DMT1 where its fate will largely depend on the type and state in which the cell is in. Ultimately, iron is mostly utilized for various metabolic purposes and stored in ferritin when present in excess.

In addition to TfR1, there exists additional iron uptake mechanisms that are either transferrin receptor 2 (TfR2) [23, 24] or siderophore mediated. TfR2 is capable of binding transferrin but at a lower affinity than TfR1. The importance of TfR2 in iron uptake seems to be relatively minor as illustrated by its inability to rescue the E12.5 embryonic lethality TfR1 $-/-$ [25]. Furthermore, TfR2 does not seem to improve the microcytic hypochromic erythrocytes phenotype observed in TfR1 $+/-$ mice [25]. In contrast, bacteria have evolved uptake mechanisms that utilize siderophores. Siderophore, Greek for iron carrier, is an organic macromolecule that is synthesized and released by either bacteria or fungi to scavenge iron.

8. Iron Storage

Excess of cellular iron that is not utilized for metabolic purposes is stored and detoxified in the iron storage protein ferritin.

Cytosolic ferritin is ubiquitously expressed and may store approximately 4500 Fe(III) ions in the form of ferric oxy-hydroxide [26, 27]. This storage protein consists of 24 subunits of H- and L chains that form a shell-like structure. The H-chain is expressed

mostly in the heart and its ferroxidase activity functions to oxidize iron from the ferrous to ferric form. Homozygous H-chain knockout in mice reveals embryonic lethality in E3 - E9.5 [28] whereas heterozygous knockouts display no phenotypic abnormalities [29]. In contrast, L-chain ferritin is expressed primarily in the liver and is involved in the nucleation of ferric iron. The specific signals and mechanisms by which iron is liberated are not yet fully understood. However, iron liberated to meet metabolic demands may occur either through structural rearrangements [30] or lysosomal degradation [31].

Mitochondrial ferritin also possesses both oxidase and storage properties [32]. Recently, it was shown that erythroid cells in patients with sideroblastic anemia possess iron overloaded mitochondria with high ferritin [33]. This form of anemia is characterized by inappropriately elevated iron in the mitochondria [33].

A glycosylated and soluble form of ferritin exists in our circulation and has been shown to contain very little iron [22]. Although its function remains elusive, levels of plasma iron serve as an indirect measurement of body iron stores. For example, males exhibit approximately $< 300 \mu\text{g/L}$ whereas females display $< 200 \mu\text{g/L}$. Understandably, this is useful in clinically diagnosing patients with anemia or hemochromatosis. Importantly, this measurement does not reflect body iron stores from those suffering from acute and chronic forms of inflammation or the hyperferritinemia/cataract syndrome [34].

9. Regulation of Iron Uptake and Storage Proteins

The mechanisms that control the expression of iron uptake and storage proteins exist at multiple levels including *au niveau* transcriptional and post-transcriptional. Regulation at the post-transcriptional level is accomplished by protein/mRNA

interactions via the cytosolic iron regulatory protein/iron regulatory element (IRP/IRE) system (Fig. 5). IREs are hairpin structures composed of a 30 nucleotide stem and a 5'-CAGUGU-3' looped sequence. Iron regulatory proteins 1 (IRP1) belongs to the family of iron-sulfur cluster isomerases and is highly homologous to mitochondrial aconitase. Post-transcriptional control is accomplished through IRP interaction with IRE on the messenger ribonucleic acids (mRNA). mRNA containing IREs that exert post-transcriptional control include proteins such as TfR1, ferritin (H and L), erythroid 5-aminolevulinate synthase (ALAS2), DMT1, ferroportin and mitochondrial aconitase.

IREs are found in either the 5' or 3' untranslated region (UTR) of the mRNA (Fig. 5). 5' IREs exist in H and L ferritin chains, ALAS2 and mitochondrial aconitase mRNAs. During periods of low cytosolic iron, IRP binds a single IRE which subsequently prevents the translational machinery from binding to mRNA. As a consequence, protein translation is inhibited. Thus, upon IRP/IRE interaction, the decrease in ferritin, eALAS and mitochondrial aconitase synthesis reflects the cell's ability to reduce iron storage, utilization and mitochondrial activity in an iron depleted cytosol. In contrast, in an iron replete cell, translation of the aforementioned proteins proceeds which subsequently permits augmented storage and utilization of iron in the cell (Fig. 5).

Interactions among IRP/IRE may also occur on the 3' UTR of both TfR1 (5 IREs) and DMT1 (1 IRE) mRNA (Fig. 5). In contrast to the 5' UTR, translational control of both TfR1 and DMT1 is at the level of mRNA stability. In an iron depleted cytosol, IRP/IRE interaction prevents endonucleases from targeted degradation of mRNA. Aversion of mRNA truncation permits translational machinery to bind and subsequently

proceed with the expression of both TfR1 and DMT1. As a consequence, an increase in the expression of TfR1 and DMT1 in iron depletes cells leads to elevated iron intake. In contrast to TfR1 and DMT1, the relationship between the IRP/IRE system and ferroportin remains elusive.

Surprisingly, IRP1 and iron regulatory protein 2 (IRP2) knockout mice display dramatically different phenotypes. IRP1^{-/-} mice exhibit no phenotypic abnormalities [35] whereas IRP2^{-/-} mice possess a progressive neurodegenerative disorder and iron overload in the intestinal mucosa and central nervous system [36].

9.1. IRP1

IRP1 is ubiquitously expressed and a vital component in the regulation of iron metabolism [37]. In the cell, IRP1 is capable of providing two highly distinct cytosolic functions. In iron starved cells, IRP1 serves as an IRE binding protein whereas in iron loaded cells, it functions as a cytosolic aconitase. The ability to switch from an mRNA binding protein to an aconitase is mechanistically possible through the use of a 4Fe-4S iron-sulfur cluster. In conditions of low cytosolic iron, the cleft region between its domains 1-3 and 4 is narrow thus impeding interactions with IRE through steric hindrance. Despite the disallowance of IRE binding, IRP recruits an iron sulfur cluster which subsequently enables the protein to perform aconitase activity. In contrast, during conditions of high cytosolic iron, the cleft region within the domains 1-3 and 4 is wider and permits interactions with IRE.

The activation of IRP1 as an IRE binding protein may also occur via an iron independent manner. For instance, IRP/IRE interactions are elevated when exposed to

nitric oxide (NO) and/or hydrogen peroxide [38, 39]. The physiological role of NO in the context of iron metabolism remains unclear, however, it has been suggested that the rise in IRP1 activation may be due to the direct or indirect dismantling of the 4Fe-4S [40]. It has also been suggested that NO may somehow influence chelatable iron within the labile iron pool [40].

Moreover, response to non-iron stimuli may also be achieved via exposure to hydrogen peroxide (H_2O_2). The transition of IRP1 into an IRE binding protein via a H_2O_2 dependent manner is rapid (30-60 min) [41, 42]. Furthermore, IRP1 activation by H_2O_2 is not the result of either H_2O_2 acting on the 4Fe-4S cluster or an increase in intracellular H_2O_2 . Thus the integrity of the cell is required for IRP1 activation through H_2O_2 .

9.2. IRP2

Although the structures of IRP1 and IRP2 are homologous, the functions and mechanisms by which they are regulated are dissimilar. IRP1 may transition between an IRE binding protein and mitochondrial aconitase. In contrast, IRP2 lacks aconitase activity and is regulated at the level of protein stability. In an iron depleted cell, IRP2 is synthesized de novo and is a stable IRE binding protein [43, 44]. In contrast, in an iron replete cell, iron has been reported to bind an iron sensing domain of the protein and subsequently initiate IRP2 degradation [45, 46]. Upon binding and oxidation, IRP2 is ubiquitinated and subsequently undergoes degradation.

Similar to IRP1, IRP2 and IRE interaction may be influenced in response to non-iron related stimuli such as NO [38, 39]. The effect of NO on IRP2 binding activity

appears to vary in response to the type of NO donor and perhaps the cell type [47-51]. Unlike IRP1, IRP2 was unresponsive to extracellular H₂O₂ [52].

10. Iron and Disease

Tightly controlled mechanisms for maintaining systemic and cellular iron homeostasis is essential in the prevention of iron related disease. Pathological conditions caused by inappropriate levels of iron may be elicited by either a deficiency or excess of iron.

Iron deficiency anemia (IDA) is one of the most common diseases in third world countries and is due to insufficient iron in the diet [53]. Another form of anemia called “anemia of chronic disease” (ACD) or “anemia of inflammation” (AI) is common in patients with chronic inflammation, infections, autoimmune diseases and cancer [54]. Contrast to IDA, iron is retained within the reticuloendothelial system which in turn deprives erythropoiesis of iron.

In contrast to anemia, iron overload is a perturbation in iron homeostasis at the other end of the spectrum [55, 56]. Iron overload is etiologically categorized into either a primary or secondary form. Primary iron overload is defined as a genetically heterogeneous disorder with defects in iron absorption and handling. In contrast, secondary iron overload results from multiple blood transfusions used to correct for ineffective erythropoiesis.

Taken together, iron may cause disease at both ends of the spectrum, whether it is anemia or hereditary hemochromatosis (HH). Heparin, a circulating hormonal peptide,

is now widely accepted as the systemic regulator of iron absorption and stores which, if present in inappropriate amounts, may elicit either anemia or HH.

11. Hepcidin, the master hormonal regulator of iron stores

Hepcidin is an antimicrobial and iron regulatory peptide. It is synthesized mostly in the liver in response to iron. Upon synthesis, hepcidin is released into the circulation where it will seek and bind the iron exporter ferroportin on target cells such as enterocytes and macrophages. More specifically, hepcidin binding leads to ferroportin internalization and lysosomal degradation. As a consequence of ferroportin degradation, iron is retained within the cell and thwarted from entering the circulation. The principal regulators of hepcidin expression are iron, inflammatory cytokines and erythropoietic activity (Fig. 6).

11.1 Expression and Biochemical Properties

Hepcidin was initially discovered in the plasma ultrafiltrate and labeled liver-expressed antimicrobial peptide (LEAP-1) [57]. It was characterized as a novel human antimicrobial peptide synthesized primarily in the liver and containing multiple di-sulfide bonds [57]. To a much lesser extent, hepcidin expression is localized in the brain and heart. In humans, the hepcidin gene is 2.5-kilobases (kb) and located on chromosome 19. A 0.4-kb mRNA is expressed from 3 exons and encodes an 84-amino acid prepropeptide. Mature hepcidin peptides, isolated in the liver are 25, 22, and 20 amino acids long. The mechanism, regulation and location of hepcidin processing remain unresolved.

Nuclear magnetic resonance spectrometry revealed that hepcidin consists of two beta strands that form a hairpin whose two arms are linked together by 4 disulfide bonds. Among the disulfide bonds exists a highly strained bond between two cysteines located in close proximity to the turn of the hairpin. The importance of this highly strained bond remains elusive.

Hepcidin's hydrophobic and positively charged side chains are located at opposite ends of each other. This distal separation is characteristic of antimicrobial peptides capable of disrupting bacterial membrane walls. In contrast to most antimicrobial peptides, hepcidin is highly conserved among species.

11.2. Mouse model studies

11.2.1. Hepcidin silencing

In 2001, an unexpected discovery revealed the potency of hepcidin as a regulator of iron metabolism [58]. Researchers observed that disruption of the murine transcription factor “upstream stimulatory factor 2” (USF2), also silenced the downstream hepcidin gene [58]. Excitingly, these USF2^{-/-} mice developed an iron overload phenotype characterized by multivisceral iron overload, high plasma transferrin saturation and non-transferrin bound iron accumulation in the pancreas and heart [58]. Furthermore, splenic iron in USF2^{-/-} mice was significantly lower than in wild type (WT) mice [58]. This observed iron overload phenotype was strikingly similar to that seen in HFE knockout mice and patients suffering from HH [58].

11.2.2. Hepcidin overexpression

In 2002, the same group of scientists developed an overexpressing hepcidin transgenic mouse model using a liver-specific transthyretin promoter [59]. The majority of transgenic mice died within a few hours after birth displaying pale skin, diminished body iron and severe microcytic hypochromic anemia [59]. At the time of publication, only 3 transgenic mice survived but were severely ill exhibiting reduced body size, pallor, hairless and crumpled skin [59]. In addition, red blood cell abnormalities such as anisocytosis, poikilocytosis and hypochromia were markedly observed [59]. Taken together, the overexpression of hepcidin seemed to display iron metabolism phenotypes similar to those seen in IDA and AI.

11.3. Molecular mechanism of hepcidin action

As illustrated in the aforementioned Section 11.2, the systemic effect of hepcidin is indisputable and extremely potent. The molecular mechanism by which hepcidin exerts its effects was unraveled in 2004 with the discovery of the iron exporter ferroportin as its receptor. In this unique case, ligand-receptor binding leads to internalization and subsequent degradation of the receptor. Interestingly, this is the first and so far only case in biology where a hormone binds and initiates degradation of a transporter/receptor.

11.3.1. Regions in the hepcidin peptide important for ferroportin

Determining the regions in hepcidin responsible for the internalization and degradation of ferroportin utilized an experimental model consisting of overexpressing mouse ferroportin (green fluorescent protein (GFP) fused to the c-terminus) in 293

human kidney epithelial cell line and chemically synthesized human hepcidin [6]. This model allows for the measurement of ferroportin on the cell membrane and iron retention in cells, before and after hepcidin treatment. More specifically, “hepcidin activity” is defined as 1) the amount of GFP detected on the cell surface as determined by flow cytometry and cell sorting analysis; 2) quantity of the iron storage protein ferritin measured by enzyme-linked immunosorbent assay [60]. Using these methods, a negative relationship between hepcidin activity and a serial deletion of the first 5 amino acids was observed [60]. Furthermore, complete deletion of these 5 amino acids resulted in complete loss of hepcidin activity whereas chemically synthesized 3 and 6 amino acid peptides from the N-terminal did not exert any hepcidin activity [60]. Mutations in hepcidin’s cysteines did not effect its function in vitro but appeared to be important when injected into mice [60]. Lack of activity of the mutated cysteine form in mice is most likely because it is less stable. Thus, although the first 5 amino acids on the N-terminus of hepcidin are vital, they are inactive by themselves.

11.3.2. Mechanism of ferroportin internalization and degradation

The precise molecular mechanism by which hepcidin mediates ferroportin internalization involves a string of events that ultimately leads to ferroportin degradation. At a concentration as low as 0.1 μ M, human hepcidin is able to internalize overexpressing mouse ferroportin-GFP in the 293 cell line within 1 hour [6]. Using this model, it was determined that upon hepcidin binding, ferroportin undergoes tyrosine phosphorylation at the plasma membrane [61]. Once phosphorylated, ferroportin is internalized and undergoes dephosphorylation followed by ubiquitination [61]. The addition of ubiquitin

moieties to the internalized transporter enables it to be targeted for degradation in the late endosome/lysosome, via the multivesicular body pathway [61].

11.4. Hepcidin Stimuli

To date, stimuli controlling the expression of hepcidin in the liver may be categorized into 3 non-mutually exclusive parts. Hepcidin may be positively regulated by iron or inflammation (infection induced or not) or negatively regulated by erythropoietic demand. Mechanisms of misregulation of hepcidin expression by iron or inflammatory cytokines define the pathophysiology of HH and ACD, respectively.

11.4.1 Hepcidin regulation by iron

The positive regulatory effect of iron on hepcidin has been clearly demonstrated by 2 simple *in vivo* experiments. Firstly, iron loaded mice either by oral or parenteral administration exhibit a strong induction of hepcidin mRNA expression [62, 63]. Secondly, humans who ingest a single dose of 65 mg of FeSO₄ reveal a peak in urinary hepcidin excretion 24 hours after ingestion [62]. The mechanism by which iron induces liver hepcidin expression is complex, involves many intermediaries and has been defined primarily by mapping the multiple genetic defects in patients with the different types of HH. The different types of the autosomal recessive disorder HH have mutations in either the HFE, TfR2, hepcidin or HJV genes. All types of HH display a similar phenotype of varying severity and are summarized in figure 8 [2, 64-66]. Patients with the aforementioned forms of HH display pathological iron deposits in the parenchyma of the liver, pancreas, heart and other tissues. Interestingly, these patients retain less iron in

their macrophages than normal individuals. Furthermore, of most interest, patients display inappropriately low expression of hepcidin in each type of HH suggesting that HFE, Tfr2 and HJV encode upstream regulators of hepcidin expression.

11.4.1.1. HFE

The most common form of hemochromatosis is type I HH which is widespread and especially frequent in people of North European Descent. Approximately 1:300 individuals are affected by this disorder. In 1996, researchers identified HFE as the hemochromatosis gene via linkage analysis [65]. The HFE gene expresses an unusual major histocompatibility complex class I protein. Upon processing in the golgi, HFE is localized to the plasma membrane where it binds beta 2 microglobulin (β 2M). The most common mutation in type I HH patients is C282Y which impedes disulfide interaction between HFE and β 2M. Lack of interaction prevents localization to the plasma membrane [67]. Patients with this mutation display variable clinical penetrance and inappropriately low expression of hepcidin. Furthermore, knockout mice [68, 69] or transgenic C282Y [70] mutants develop progressive iron overload but vary in phenotype in relation to their genetic strain [71, 72].

In vitro studies revealed that HFE has the ability to bind Tfr1 [73, 74] and prevent transferrin/Tfr1 iron uptake [75, 76]. In addition, data have suggested that HFE may play a role in the programming of crypt cells to mature enterocytes in the crypt-villus axis of the duodenum [77]. In contrast, a duodenal specific knockout of HFE revealed no changes in iron metabolism in comparison to WT mice [78]. Thus, to date, the mechanism by which HFE controls the expression of hepcidin remains unresolved.

11.4.1.2. TfR2

In 1999, a second receptor for transferrin called TfR2 was identified and cloned from chromosome 7 [79]. Autosomal recessive mutations in TfR2 are responsible for type 3 HH in which patients display a similar iron overload phenotype observed in that of type I. Human TfR2 is expressed highly in the liver and to a lesser extent in the spleen, muscle, lung, prostate, peripheral mononuclear cells and erythroid precursor cells [79, 80].

TfR2 has the ability to bind (at a much lower affinity than TfR1) and internalize holo-Tf [81]. In cultured hepatomas, dose dependent treatment of differic iron appears to stabilize TfR2 [82]. More specifically, holo-Tf binds and stabilizes TfR2 by redirecting it from a degradation to recycling pathway [83]. In contrast to TfR1, TfR2 does not respond to intracellular iron stores but to both differic transferrin [82] and in conformity of the cell cycle [80, 84].

Although TfR2 may internalize iron, it is not sufficient to rescue TfR1 knockout mice from dying at embryonic day 12.5 due to neurological abnormalities and severe anemia [25]. TfR2 knockout mice display inappropriately low levels of hepcidin expression and also fail to achieve hepcidin induction upon iron challenge [85]. Taken together, the primary function of hepatic TfR2 may be to regulate hepcidin expression by sensing circulating holo-Tf.

11.4.1.3. Hju

Homozygous or compound heterozygous mutations of either the hepcidin or HJV genes display a severe type of iron overload called JH. Interestingly, patients with HJV derived JH and HJV knockout mice display inappropriately low hepcidin peptide and mRNA levels respectively [2, 86, 87]. Thus, similar to HFE and TfR2, HJV is an upstream regulator of hepcidin expression.

11.4.1.3.1. Expression and Biochemical Properties

Discovered as recently as 2004, the HJV gene was mapped to chromosome 1q21 [2] and is identical to repulsive guidance molecule c (RGMc) found in mice. HJV is expressed primarily in skeletal muscle and to a lesser extent in the liver [2], heart [2] and esophagus [88].

11.4.1.3.2. RNA encoding HJV

Initially, using expressed sequence tags (EST) database searches, it was suggested that the four exons in the human HJV gene are transcribed and processed into five distinct mRNAs that contain alternative coding sequences [2]. More specifically, it was suggested that differentially spliced transcripts encode multiple forms of HJV that vary in size [2]. In contrast, using reverse transcription polymerase chain reaction (RT-PCR) with exon specific primer pairs, differentiating muscle cells displayed only one HJV transcript [89]. These new data imply that multiple protein isoforms are expressed from a single protein precursor [89].

11.4.1.3.3. HJV protein features

Full length H₁v is comprised of 426 amino acids and has multiple protein features. More specifically, it consists of an N-terminal signal peptide, an RGD tri-amino acid motif, a partial von Willebrand factor (vWF) type D domain and a GPI-linked site [2, 90]. In addition to these domains, H₁v contains 3 consensus sequences for N-linked glycosylation, 12 conserved cysteine residues and 1 predicted acid sensitive autocatalytic cleavage site [90] (Fig. 7).

According to the Signal Hypothesis, initially formulated by Gunter Blobel, Cesar Milstein and David Sabatini, a signal peptide targets a protein for either secretion or membrane localization [91]. A signal peptide is approximately 13-46 residues where 7-13 residues consist of a hydrophobic core flanked by hydrophilic residues that usually include one or more basic residues close to the N-terminus.

An RGD motif is composed of the amino acids arginine, glycine and aspartate and is found on proteins of the extracellular matrix. For example, fibronectin (an RGD containing protein) interacts through integrin to link the intracellular cytoskeleton with the extracellular matrix. Interestingly, an RGD motif within the C1 domain of the vWF activates platelets via integrin binding during coagulation. In addition, RGDs are also in latency associated peptides (LAPs) which bind integrins [92]. Interestingly, during iron deprivation integrin α 6 is dramatically induced, suggesting a possible role in iron metabolism [93].

A partial vWF type D domain exists in the core of full length H₁v. At wound sites, the function of the multi-domain vWF is to mediate platelet adhesion through interactions with other factors. The type D domain of the vWF specifically binds to and

stabilizes factor VIII. Factor VIII remains stable when bound to vWF but through the action of thrombin, is released and rapidly degraded.

A predicted GPI-linked site is located at the C-terminus of full length H_{ijv}. A GPI-anchor is a glycolipid located on the C-terminus of a protein that is responsible for anchoring it to the plasma membrane. The mechanism by which GPI synthesis and attachment occurs is complex. Essentially, attachment of GPI to a precursor protein is initiated by GPI transamidase which cleaves off a C-terminal signal sequence. This in turn forms an enzyme-substrate intermediate linked by a thioester which subsequently undergoes a nucleophilic attack by the terminal amino group in GPI. In turn, the protein undergoes inositol deacylation in the endoplasmic reticulum which sensitizes it for phosphatidylinositol-specific phospholipase C (PI-PLC) cleavage [94].

11.4.1.3.4. H_{ijv} mutations in JH

The onset of the autosomal recessive disease, JH, occurs in patients with mutations in the H_{ijv} gene that are either homozygous or compound heterozygous. Within a short time frame since the discovery of H_{ijv}, approximately 33 different types of mutations have been identified [2, 95-104] figure 9A and 9B. With the exception of G320V, most mutations are representative of one patient. Whether in homozygous or compound heterozygous form, the 33 different types of mutations account for 31 possible combinations. Of the 33 different types of mutations, 17 involve mutations in areas of the protein described in the aforementioned Section 11.4.1.3.3. More specifically (Figure 9A), 2 mutations are located in the signal peptide [101, 102], 4 are cysteine substitutions [96, 97, 101, 104] which includes an amino acid of an N-linked

glycosylation site [96], 2 are different substitutions of the G in the RGD [2, 95], 1 is the first amino acid after RGD [95, 97] and as many as 7 mutations are located within the partial vWF type D domain [2, 95, 97, 100] which also includes 1 mutation of the acid sensitive autocatalytic cleavage site [95].

Most of the families affected by JH possess the G320V mutation. Interestingly, the G320V mutation is part of a highly conserved LCVXGCP region [105]. The origins of these families are in Greece [2], Canada [2, 95], Italy [95], France [2, 95], Croatia [96], Germany [96], Slovakia [96], Ireland [99] and United States [97, 98, 104] (Figure 9B). Interestingly, the sole Italian homozygote lives in an area of southern Italy where the Greek language and traditions are alive [95]. Families possessing mutations other than that of G320V are found in the previously mentioned areas (with the exception of Croatia) and in Australia [95], Great Britain [95, 102], Albania [95], Japan [100] and Romania [103] (Figure 9B).

11.4.1.3.5. Processing of H_{jv}

As mentioned earlier, H_{jv} is primarily expressed in the muscle and to a lesser extent the liver. Upon translation, H_{jv} is localized either inside the cell, on the plasma membrane or in a released soluble form. Thus far, various groups have reported different data pertaining to the processing of H_{jv}.

In muscle cells, a full length endogenous H_{jv} protein is translated from a single RNA [89]. Full length cellular H_{jv} is also expressed in cells transfected with full length cDNA. More specifically, full length cellular H_{jv} is observed in the transfected cell lines: HeLa [106], HepG2 [106], Hep3B[1], Cos-7 [89], C2 myoblasts [89], C3H10T1/2

mouse embryonic fibroblasts [89] and HEK293 [1, 90]. Full length cellular H_{jv}, which includes all the protein features described above in “*H_{jv} Protein Features*” migrates at a size of approximately 50 kDa [1, 89, 90, 106, 107].

During translation, the signal peptide is removed from cellular H_{jv} and the carboxyl-terminus is modified to allow for GPI linked anchorage to the membrane. Upon translation, cellular H_{jv} may undergo cleavage at the GDPH site located at amino acids 172-175. Cleavage occurs naturally under mildly acidic conditions presumably in the late secretory pathway [90]. Other proteins that undergo GDPH cleavage include MUC2 mucin, sialomucin complex and heavy chain 3 of pre- α -inhibitor [90]. Subsequently, cellular H_{jv} is either targeted to the plasma membrane or released from cells via the secretory pathway [89, 90, 106].

Because of the presence of disulfide bonds, different forms of H_{jv} have been reported using either reducing or non-reducing gels [89, 90]. As a result of cleavage at the GDPH site, cellular H_{jv} forms a heterodimer that localizes to the membrane [89]. The heterodimer consists of both a 15 kDa N-terminal and 35 kDa C-terminal fragments that were cleaved at GDPH and observed under reducing conditions [89, 90]. These two fragments are linked together by disulfide bridges but the exact cysteines involved in the linkage remains to be determined. Under non-reducing conditions, both cellular and membrane associated H_{jv} migrate at 50 kDa (35 + 15 kDa fragments still bound by disulfide bridges). In addition, H_{jv} may undergo a varying degree of post-translational modification such as Asn-linked glycosylation [89]. The life span of H_{jv} within the whole cell extract and purified membrane fractions in transfected cells is approximately 24 hours and is reduced by roughly 75% in only 4 hours [89].

Upon localization to the plasma membrane, H₁v may be cleaved by either PI-PLC or an unidentified protease [89, 90]. When using a non-reducing gel, H₁v either released from cells or present in rodent serum ranges from 40-50 kDa [1, 89, 106, 107]. This molecular weight range accounts for the heterodimer linked together by disulfide bonds (35 + 15 kDa with varying degree of glycosylation). In contrast, when using a reducing gel, additional 35 and 15 kDa fragments with the 40-50 kDa protein are detected as soluble H₁v [89, 90, 106]. The appearance of the 35 and 15 kDa fragments is due to the reduction of the disulfide bonds by a reducing agent found in the separating gel of a western blot. Interestingly, the presence of the 50 kDa soluble protein, in the absence of PI-PLC and in the presence of a reducing agent (multiple agents have been tested) suggests constitutive release of a *full length* H₁v (minus the signal peptide) via the secretory pathway independent of proteolytic cleavage [89, 108]. Furthermore, transfection of H₁v lacking the GPI anchor is also released from cells [89].

Interestingly, in contrast to transfected H₁v found in both whole cell extracts and purified membrane fraction, the life span of soluble H₁v in the media was found to be constant for 36 hours [89].

11.4.1.3.5.1 Defective H₁v Processing

The effect of disease associated mutations in H₁v processing was recently studied using transient transfections of WT and various mutant forms of H₁v in cultured HeLa and HepG2 cells [106]. Transfected WT H₁v was compared with mutants G320V, W191C and F170S for their glycosylation, autoproteolytic cleavage and cellular localization [106]. Employing enzymatic deglycosylation assays, it was observed that all 3 cellular

Hjv mutants displayed differing glycosylation in comparison to WT [106]. Furthermore, using reducing gels for a western blot, it was shown that WT cellular Hjv displayed 2 bands of 33 and 15 kDa suggesting autoproteolytic cleavage [106]. In contrast, the mutant forms did not undergo cleavage and exhibited only a 50 kDa form [106]. Interestingly, those proteins incapable of autoproteolytic cleavage were less efficient in reaching the plasma membrane [106]. In agreement with these data, it was previously reported using immunocytochemistry in transfected 293T cells that G320V Hjv failed to reach the plasma membrane [90]. Localization experiments with an electron microscope showed that these mutants formed a cluster within the endoplasmic reticulum [106]. Taken together, recent in vitro data studying G320V, W191C and F170S Hjv revealed altered glycosylation, no autoproteolytic cleavage and little localization to the plasma membrane [106]. Thus, the processing of Hjv in patients with any of these 3 forms of JH may be affected by these 3 mutations [106].

11.4.1.3.6. Function of Hjv

11.4.1.3.6.1. Regulation of hepcidin

Patients with Hjv associated JH display inappropriately low levels of hepcidin in the urine [2]. This blunted hepcidin response during iron overload of this magnitude, suggests that Hjv acts upstream of hepcidin and may positively regulate its expression. Hjv knockout mice display inappropriately low expression of liver hepcidin thus confirming observations seen in human patients [86, 87]. Furthermore, presumably as a result of low hepcidin expression, knockout mice display an iron overload phenotype

characterized by iron deposition in the liver, pancreas, and heart in addition to depressed levels of iron in tissue macrophages [86, 87, 109]. Moreover, ferroportin levels were greatly elevated in both intestinal epithelial cells and macrophages [86]. Taken together, *in vivo*, as studied in human patients and knockout mice, HJV acts as a positive upstream regulator of hepcidin expression.

Cellular work using cultured hepatomas further corroborates HJV's involvement in regulating hepcidin expression. Using siRNA to silence HJV expression in cultured Hep3B hepatomas, hepcidin expression decreased in a dose dependent manner with HJV siRNA treatment [1]. This suggests that cellular HJV is involved in positively regulating hepcidin expression [1]. The mechanism by which cellular HJV positively regulates hepcidin expression in the liver was recently discovered to be via a bone morphogenic/Smad (BMP/Smad) mediated pathway [3].

11.4.1.3.6.2. HJV and cell signaling

HJV belongs to the Repulsive Guidance Molecule (RGM) family of molecules. HJV, also called RGMc, is the third member of the family, which includes RGMa and RGMb (also referred to as DRAGON). Prior to the discovery of HJV, RGMa and RGMb were found to be co-receptors that enhance BMP signaling [110, 111]. Signaling pathways are finely tuned by co-receptors to either enhance signaling or inhibit ligand binding [112]. Recently, HJV was identified as a BMP co-receptor capable of enhancing hepcidin expression in liver cells [3]. More specifically, HJV activation of a BMP responsive element (BRE) requires receptors Activin like kinase 3 (Alk3) and Alk6. Interestingly, BMP 2 has a higher binding affinity to HJV than BMP 4 [3]. In addition,

disease associated mutations G313V (murine G320V equivalent) and G99V of HJV are incapable of activating BRE [3]. Furthermore, it was shown that HJV enhanced BMP 2 mediated induction of hepcidin expression and that enhancement was lost with disease associated HJV constructs [3]. Dominant negative Smad1 coexpression with HJV failed to induce BRE activity suggesting Smad1 involvement in the HJV pathway [3]. Recently, a separate group showed that BMP 2, 4 and 9 were capable of stimulating liver hepcidin in mice independently of HFE, TFR2 and IL-6 (inflammatory stimulus of hepcidin expression) [113].

In agreement with recent signal transduction data describing hepcidin regulation by a BMP/Smad pathway, liver specific Smad 4 knockout mice resulted in markedly decreased liver hepcidin expression and elevated intestinal ferroportin [114]. Furthermore, these mice displayed an iron overload phenotype characterized by iron accumulation in the liver, pancreas and proximal tubule of the kidney [114]. In addition, BMP 4 and to a much lesser extent TGF β induction of hepcidin in primary hepatocytes was blunted in these Smad4 knockout mice [114]. Interestingly, in a separate study using HepG2 hepatomas, HJV was found not to signal through TGF β [3]. Taken together, HJV enhancement of BMP mediated induction of hepcidin involves both Smad1 and Smad4.

Recently, using freshly isolated murine primary hepatocytes, holo-Tf was shown to modestly upregulate hepcidin expression in a BMP 2/4 dependent and BMP9 independent mechanism [5]. In addition, recombinant soluble HJV blunted this response [5].

11.4.1.3.6.3. Soluble HJV

Thus far, 3 types of recombinant soluble HJV have been used to study its function [1, 4, 5].

The first recombinant form is comprised of amino acids 1-402 (from the full 1-426) which lacks the GPI sequence from human hemojuvelin. It is purified from baculovirus/insect cells and is linked by disulfide bonds to form a 2 chain structure [1]. This form of soluble HJV was able to suppress hepcidin expression in primary human hepatocytes in a dose dependent manner [1]. Furthermore, large doses of recombinant soluble HJV (1-3 µg/mL) greatly reversed induction of hepcidin via IL-6 [1].

The second form is comprised of amino acids 33-328 (from the full 1-420) of murine hemojuvelin. It was purified using a viral overexpressing system in a permanent human cell line [5]. Interestingly, this recombinant murine soluble HJV was shown to block the induction of hepcidin by either holo-Tf or BMP [5].

The third type is a human soluble HJV fusion protein [4]. More specifically, the N-terminal signal sequence was replaced with a preprotrypsin fragment, a FLAG tag supplants the GPI domain and this form was fused to the Fc portion of human IgG [4]. This recombinant/fusion protein inhibits BMP mediated induction of hepcidin expression in hepatomas [4]. Furthermore, when injected into mice, a decrease in hepcidin expression, increase in ferroportin expression, mobilization of splenic stores and increases in serum iron were observed [4].

Taken together, the 3 types of truncated and recombinant forms of soluble HJV appear to negatively regulate hepcidin expression.

11.4.1.3.7. Regulation of HJV

11.4.1.3.7.1. HJV and iron

To date, iron has been shown to effect HJV's localization to the membrane and subsequent shedding. More specifically, cultured Hela cells treated with 50 μM of ferric ammonium citrate increased localization of transiently transfected HJV to the plasma membrane whereas G99V and C119F mutants failed to [106]. Membrane shedding in these same transiently transfected cells was significantly decreased upon treatment with 50 μM of ferric ammonium citrate [106]. In contrast, G320V HJV shedding was not significantly decreased upon iron treatment, however, it should be noted that these mutant transfectants displayed minimal shedding when not treated with iron [106]. Taken together, Hela cells transiently transfected with HJV and treated with 50 μM of ferric ammonium citrate display amplified localization to the plasma membrane and reduced membrane shedding. Furthermore, disease associated mutations respond differently to iron treatment than WT HJV.

Data showing depressed HJV shedding upon iron treatment was corroborated in experiments done in transfected 293T and Hep3B cell lines [1]. Holo-Tf treatment of these cell lines at a concentration range of 30-100 μM significantly decreased soluble HJV in a dose dependent manner [1]. A separate group reported that liver HepG2 and muscle C2C12 cell lines treated with up to 30 μM holo-Tf decreased HJV shedding [107]. Interestingly, this group saw no effect on shedding upon ferric ammonium citrate treatment.

The inverse relationship between iron levels and HJV shedding was recently shown *in vivo* [107]. More specifically, mice fed an iron deficient diet displayed

elevated levels of soluble HJV and decreased hepcidin expression [107]. Interestingly, another group reported that upon iron injection into mice, hepatic HJV mRNA remained unchanged while the expected hepcidin induction was present [115].

11.4.1.3.7.2. HJV and inflammation

Hepcidin was initially described as an antimicrobial peptide regulated by inflammatory cytokines [116, 117]. Since its initial discovery which implied that HJV is an upstream regulator of hepcidin expression, various groups sought to investigate whether HJV is involved in regulating hepcidin during inflammation. Thus far, inflammatory mediated induction of hepcidin seems to be independent of HJV [1]. However, it appears that liver HJV is negatively regulated by lipopolysaccharide (LPS) [115]. More specifically, mice administered LPS display depressed hepatic [87, 115] and unaffected muscle [115] HJV mRNA. A possible involvement of HJV in LPS mediated liver hepcidin induction was ruled out approximately two years ago [87]. More specifically, HJV knockout mice administered LPS were still capable of inducing hepcidin expression to the same extent as WT mice [87].

11.4.1.3.7.3. HJV and neogenin

As previously mentioned in the “HJV and cell signaling” section, HJV shares significant sequence resemblance with the RGMs [2]. Murine RGMA and RGMB are mostly expressed in developing and adult central nervous systems [118-120]. RGMA in mouse embryos is essential in controlling the formation of afferent connections in the dentate gyrus and cephalic neural tube closure [120, 121]. In addition, chicken RGM, an

ortholog of mouse RGM is critical in the retinotectal map formation of chick embryos [122]. Recently, the chicken and mouse RGMs receptor was identified as neogenin and that this high affinity interaction is necessary for neuronal survival [123, 124]. With the exception of the spleen, thymus and pancreas, neogenin is ubiquitously expressed [88].

In 2005, neogenin was found to interact with Hvjv in the 293 cell line [90]. In contrast, disease associated G320V Hvjv lacked interaction with neogenin. Furthermore, co-overexpression of Hvjv and neogenin in human 293 cells by transient transfection brought about iron accumulation within these cells [90]. Neogenin was also recently shown to mediate Hvjv shedding in response to iron [107]. More specifically, iron treatment significantly depressed Hvjv shedding but this inhibition was less when overexpressed with neogenin. Neogenin mediated shedding of Hvjv was also observed in C2C12 muscle cells [107]. Interestingly, neogenin mediated shedding of Hvjv was found to be independent of the BMP signaling pathway [107].

11.5.1. Hepcidin regulation by inflammation

During periods of infection, foreign pathogens survive by acquiring and utilizing iron for their metabolic processes. For example, iron is a key constituent for cytochromes involved in their respiratory chains. Vertebrates have evolved various mechanisms to protect against microbial invaders by depriving them of their necessary iron.

These mechanisms may be separated into two groups. The first utilizes homologs of iron distribution and transport proteins to restrict iron from invading pathogens. The second group initiates a rapid and potent hypoferremic response by stimulation of hepcidin via inflammatory cytokines.

11.5.1.1. Localized responses

Homologs that restrict iron from pathogens in inflammation include natural resistance-associated macrophage protein 1 (Nramp1) and lactoferrin. Nramp1 is a homolog of the iron transporter DMT1. Nramp1 has been proposed to export iron removed from pathogens within phagocytic vacuoles [125]. Lactoferrin is a transferrin homolog and during inflammation is released from both epithelial and white cells. In addition to these homologs, the recently discovered neutrophil-derived protein neutral gelatinase-associated lipocalin (NGAL) [126, 127] and lipocalin 2 [128] deliver iron loaded siderophores into cells. Taken together, vertebrates may employ multiple localized mechanisms to deprive pathogens of iron.

11.5.1.2. Systemic response

Vertebrates also possess a more systemic response to deprive pathogens of iron by causing a rapid drop in plasma iron concentration. This rapid hypoferremic response sequesters and restricts iron to storage sites. The master hormonal mediator of this response is hepcidin. Clinically, the role of hepcidin in host defence is evident in patients with HH that are more susceptible to several types of infection [129-131].

11.5.1.2.1. Hypoferremia of inflammation

11.5.1.2.1.1. Cytokine induction of hepcidin

In humans, as well as in mice and fish, hepcidin is dramatically upregulated during periods of infection and inflammation [63, 116, 132, 133]. Hepcidin induction occurs primarily by the cytokine interleukin 6 (IL-6) in human hepatocytes [62]. In addition, interleukin 1 α (IL-1 α) [134, 135] and tumor necrosis factor (TNF) α [116] have been demonstrated to induce and repress hepcidin expression, respectively. Although IL-1 α and TNF α are able to modulate hepcidin expression, four key experiments define IL-6 as the most important [62]. Firstly, in the presence of anti-IL-6 antibodies, primary human hepatocytes treated with either bacterial endotoxins (LPS) or peptidoglycan had a blunted hepcidin response. Secondly, anti-IL-6 antibodies prevented hepcidin stimulation when treated with conditioned media from LPS or peptidoglycan treated macrophages. Thirdly, IL-6 knockout mice were unable to induce hepcidin expression upon induction of inflammation via turpentine injection. Fourthly, healthy humans infused with IL-6 excrete 7.5 fold more hepcidin in the urine than control patients. Interestingly, IL-6 induced hepcidin expression is independent of HFE [117], Tfr2 [117] and HJV [1].

Recently it was discovered, using mouse models and primary mouse hepatocytes, that IL-6 induces hepcidin expression via the IL-6 receptor glycoprotein (gp) 130 and through Janus kinases/Signal Transducers and Activators of Transcription 3, JAK/STAT3 signaling [136-138]. The signal transduction pathway mediating IL-6 induction of hepcidin begins with IL-6 binding its membrane bound receptor gp80. Upon binding, gp80 interacts with gp130 and subsequently leads to phosphorylation of tyrosines in the cytoplasmic domain of gp130 by intracellular JAKs. Phosphorylation enables gp130 to dimerize and activate STAT1 and STAT3. Once activated, STAT3 translocates to the

nucleus and binds base pairs -64/-72 of the proximal promoter region of the hepcidin gene [137].

11.5.1.2.1.2. Physiology of hepcidin's action

Upon induction in hepatocytes, hepcidin is secreted into the circulation where it will target ferroportin on macrophages and enterocytes. In turn, binding will initiate internalization and subsequent degradation of the iron exporter ferroportin. As a consequence, iron is retained within these cells and restricted from entering the circulation. As observed in both mice and humans, inflammation is capable of causing a remarkable hypoferremic phenotype. More specifically, mice injected with turpentine to induce inflammation display a severe drop in serum iron [62, 132]. In contrast, no drop in serum iron is observed when injected into either IL-6 or hepcidin deficient mice. In agreement with mice data, humans who underwent IL-6 infusion for 3 hours, had a 34% reduction in serum iron and a 33% decrease in transferrin saturation 2 hours post-infusion [62]. Such a dramatic and rapid drop in serum iron may be explained by considering the amount of iron that hepcidin is restraining from the circulation. Every 24 hours, approximately 20 mg of iron flows through a plasma transferrin compartment that contains at any moment about 3 mg of iron. Iron flowing in this transit compartment is derived mostly from iron recycled from senescent erythrocytes. Once in this compartment, iron transferrin is primarily targeted for erythropoiesis. Taken together, every 3-4 hours there is a complete turnover of plasma iron at an approximate rate of 0.83 mg/hour. Thus, if hepcidin is capable of causing a 100% inhibition of iron export from macrophages, this means 0.83 mg of iron will be deprived from the serum every hour.

Thus, total inhibition of iron export from macrophages by hepcidin can produce a staggering ~25% plunge in serum iron, every hour.

11.5.1.3. ACD

ACD is the most common form of anemia in hospitalized patients and second most prevalent form of anemia in humans next to IDA. What distinguishes IDA from ACD is that serum ferritin (accepted clinical marker of body iron stores) is normal or elevated in the latter. Thus in this unique form of anemia, iron is both retained and distributed into iron storage sites, primarily the RES. This hypoferremic state acts to deprive an invading pathogen of iron. This response arises from either an acute or chronic activation of the immune system [54, 139, 140]. Immune activation in this disease leads to inflammatory cells unleashing an oxidative burst against invading pathogens causing alterations in both systemic iron homeostasis and erythropoiesis.

11.5.1.3.1. Diseases responsible for ACD

ACD in hospitalized patients may originate from infections [141-143], autoimmune disorders [142, 144-146], cancer [142, 147-149], chronic kidney disease and inflammation [150] and chronic rejection following solid-organ transplantation [151-153]. Infections primarily responsible for causing ACD may be acute or chronic and be of viral, bacterial, parasitic or fungal origin. Autoimmune diseases shown to inflict this type of anemia are inflammatory bowel disease, rheumatoid arthritis, sarcoidosis, systemic lupus erythematosus and vasculitis. In addition, cancer patients with solid tumors or hematologic cancer may develop ACD.

11.5.1.3.2. Oxidative Burst

Activation of the immune system initiates the mobilization of various defense mechanisms such as an oxidative burst from inflammatory cells. In a protective role to kill invading pathogens, neutrophils and macrophages release reactive oxygen species. More specifically, superoxide is initially produced by the membrane-associated NADPH-oxidase and then rapidly dismutated to the more stable H_2O_2 by superoxide dismutases [154]. As a result, surrounding tissue and cells are under chronic exposure to the potentially dangerous H_2O_2 . In combination with iron, H_2O_2 may form tissue damaging hydroxyl radicals via the Fenton Haber-Weiss reactions. Thus, tight control of iron homeostasis during inflammatory conditions is imperative in preventing hydroxyl radical formation. IRP1 is rapidly induced when exposed to transient pulses of H_2O_2 both in vitro and in mouse models [10, 155-157]. Furthermore, IRP1 activation in cell lines exposed to transient pulses of H_2O_2 leads to a significant increase in TfR1 expression [158]. Thus, during inflammation, it has been proposed that H_2O_2 signals an increase in TfR1 expression which may relocalize iron from the circulation to intracellular compartments.

11.5.1.3.3. Alterations in iron homeostasis

ACD displays dramatic changes in systemic iron homeostasis. This systemic alteration is cytokine driven and is defined by an increase in iron retention and uptake in the RES. Recently, the discovery of hepcidin as being the master hormonal regulator of iron stores has provided a mechanistic explanation to the observed iron mishandling in

ACD [116]. Recent data suggest that during inflammatory conditions, IL-6 is upregulated and induces the expression and release of hepcidin from the liver [62]. Subsequently, hepcidin will target the iron exporter ferroportin in the RES [6, 7]. As a consequence, iron being recycled through erythrophagocytosis from senescent red blood cells will be retained within macrophages. As described in detail in the section “*Physiology of hepcidin’s action 11.5.2.1.2*”, inhibition of iron export from these cells is potent enough to enable a hypoferremic phenotype in vertebrates. As a consequence of this inflammatory driven hypoferremic state, pathogens are deprived of iron that is vital for their survival.

In addition to hepcidin driven hypoferremia, various cytokines may elicit redistribution of iron into the RES. In contrast to hepcidin’s iron retention effect, cytokines such as interferon (IFN) γ , LPS, TNF α and IL-10 are capable of driving iron accumulation in the RES. More specifically, IFN γ , LPS and TNF α upregulate the iron importer DMT1 in macrophages [159]. In addition, IL-10 may increase iron transferrin mediated uptake in macrophages [160]. Interestingly, patients with chronic liver pathologies, such as alcoholic steatohepatitis and hepatitis C display iron accumulation in the parenchymal cells of the liver [8, 161-165]. Taken together, iron may be deprived from a pathogen by either an iron retention or accumulation mechanism in both the RES and parenchyma.

11.5.1.3.4. Alterations in erythropoiesis

ACD exhibits defective erythropoiesis which accounts for patients with a low reticulocyte count [166, 167]. Although a reduced number of red blood cells exists,

patients are normochromic and normocytic. The lower than normal count of red blood cells is defined by diminished proliferation and differentiation of erythroid burst-forming units and erythroid colony forming units [166]. Inhibition of proliferation and differentiation of both these erythroid forming units is accomplished through the inhibitory activity of cytokines IFN α , IFN β , IFN γ , TNF α and IL-1 [166]. The mechanism by which cytokines prevent progenitor cell proliferation is either through directly initiating apoptosis or reducing expression of hematopoietic factors such as stem cell factor and erythropoietin [166, 168-170].

In addition to cytokine mediated inhibition of erythropoiesis, ACD induces the formation of labile free radicals. These toxic radicals are capable of directly damaging erythroid progenitor cells and erythropoietin generating cells [170, 171].

11.5.1.3.5. Treating ACD

Treatment of patients with ACD is unique to the disease responsible for causing the infection based anemia. In some cases, treating the underlying disease causing the anemia is enough to restore normal hemoglobin levels. In addition, treatments such as erythropoietin administration, oral iron medication and transfusion have been used to treat ACD patients [54].

11.6.1. Hepcidin regulation by erythropoietic demand

Prior to the discovery of hepcidin, there existed a notion that both a stores regulator and an erythroid regulator are responsible for controlling iron absorption and mobilization [172]. More specifically, the stores regulator is responsible for maintaining

normal iron needs by controlling iron stores and absorption at a range of approximately 1-2 mg/day. On the other hand, the erythroid regulator has a much greater capacity to alter iron balance. It ensures that iron is continuously providing the needs for erythropoiesis, regardless of the body iron equilibrium. For example, through the erythroid regulator, patients with severe anemia may enhance iron absorption up to 40 mg per day with oral iron supplementation. In contrast, once anemia has subsided, these patients absorb a normal 2 mg per day, presumably through the stores regulator [172].

Hepcidin expression is negatively regulated in anemia and hypoxemia. The drop in hepcidin production during these conditions allows for increased iron absorption in the duodenum and iron release into the circulation from macrophages. Mobilization occurs by decreasing hepcidin mediated degradation of the iron exporter ferroportin.

The signal (s) responsible for suppressing hepcidin during anemia remains to be identified. This long sought erythroid regulator was recently shown to require erythropoietic activity to exert its inhibition of hepcidin during anemia [173, 174]. More specifically, shutting off erythropoiesis with inhibitors such as carboplatin or doxorubicin, and performing a subsequent 'phlebotomy induced anemia' failed to suppress hepcidin in mice [173]. At the same time, a separate group observed that irradiation of the bone marrow followed by a phenylhydrazine induced hemolysis (anemia) also failed to inhibit hepcidin [174]. Interestingly, 16 hours post phenylhydrazine treatment, a 4 fold induction was observed prior to the suppression of hepcidin at 48 hours post treatment [174]. In addition, it was further shown that the suppression of hepcidin was not directly mediated by erythropoietin, anemia or hypoxia [173]. In contrast, cell culture work using hepatoma cell lines HepG2 and Hep3B

demonstrated that when cultured in less than 2% oxygen for 24 hours, hepcidin is dramatically reduced [132].

12. Hemolysis

Hemolysis is defined by the premature destruction of circulating red blood cells and subsequent release of their contents such as hemoglobin into the plasma. Multiple factors initiate hemolysis and many mechanisms exist for handling it. However, when erythropoiesis cannot match the rate of red blood cell breakdown, a number of clinical problems may occur.

12.1. Mechanisms of Hemolysis

Hemolysis may occur in either the intravascular or extravascular (more frequent) milieu. Intravascular hemolysis is defined by the breakdown of red blood cells within the circulation. Damage to erythrocytes may be the result of direct cell destruction or membrane damage by infectious agents, complement activation on the cell surface or mechanical trauma. Interestingly, under normal conditions, 10-20% of senescent erythrocytes undergo hemolysis [175].

Extravascular hemolysis involves the erythrophagocytosis of damaged red blood cells by macrophages in both the spleen and liver. Erythrophagocytosis is usually a process that occurs at a constant rate. Abnormally elevated erythrophagocytosis has the potential to cause anemia such as in hemophagocytic syndrome [176]. Upon erythrophagocytosis, hemoglobin from the red blood cells is broken down to biliverdin, iron and carbon monoxide by HO-1 [177]. The iron is primarily recycled back into the

circulation for use; however a smaller percentage may be stored in ferritin or utilized for other processes in the macrophage [178, 179].

12.2. Hemoglobin scavenging

Hemoglobin (pro-oxidative) released from red blood cells during hemolysis is rapidly cleared from the circulation and delivered to macrophages. Clearance of pro-oxidative hemoglobin is essential in preventing potential oxidative damage. Upon entrance into the circulation, pro-oxidative hemoglobin is rapidly and more or less irreversibly bound to haptoglobin [180, 181]. This abundantly circulating protein is clinically used as a marker for hemolysis. Once bound onto haptoglobin, this hemoglobin-haptoglobin complex is destined to both macrophages and parenchymal cells in various tissues. The complex binds receptor CD163 in macrophages and a yet unidentified receptor in parenchymal cells [182]. Binding of the hemoglobin-haptoglobin complex to CD163 initiates endocytosis and subsequent lysosomal degradation [182]. Similarly to erythrophagocytosis, hemoglobin is degraded by HO-1 to produce biliverdin, iron and carbon monoxide.

12.3. Hemolytic anemias

The risk of developing hemolytic anemia exists when the rate of hemolysis exceeds the rate of erythropoiesis. Hemolytic anemias may be categorized into either acquired or hereditary types.

Acquired hemolytic anemias may be immune-mediated, microangiopathic or caused by certain infections. Immune-mediated hemolytic anemias involve direct

binding of antibodies to antigens on the cell surface of red blood cells such as in autoimmune disorders, infections or transfusions. Microangiopathic hemolytic anemias is defined as mechanical disruption of the erythrocyte in circulation that may be caused by thrombotic thrombocytopenic purpura, hemolytic uremic syndrome, disseminated intravascular coagulation, preclampsia, eclampsia, malignant hypertension or prosthetic valves. Hemolysis induced by infections may be caused by malaria, babesiosis and clostridium [183].

In contrast, hereditary hemolytic anemias may arise from the enzymopathy Glucose-6-phosphate dehydrogenase (G6PD) deficiency, membranopathy hereditary spherocytosis or hemoglobinopathies such as thalassemia or sickle cell disease [183].

13. Hypothesis and objectives of this work

In chapter II, we hypothesize that sHjv plays an important regulatory role in systemic iron homeostasis. Our objectives were to characterize signals involved in the release of sHjv and whether it has a role in the regulation of hepcidin expression.

In chapter III we hypothesize that hepcidin has an important hormonal functional in controlling iron release from target macrophages. To address this hypothesis, we established a co-culture model consisting of hepcidin producing hepatomas and radioactively labeled iron loaded monocytes. With this model, our objectives were to monitor 1) iron release from monocytes in presence of physiologically generated hepcidin and 2) investigate the effects of hepcidin on monocytic iron metabolism.

In chapter IV, we hypothesize that chronic and sustained exposure of H₂O₂ as observed in various inflammatory conditions serves a significant mechanistic role in

promoting iron accumulation in parenchymal cells. Our objective was to employ an enzymatic system for steady-state H_2O_2 generation to monitor the mechanisms responsible for iron accumulation in these cells.

FIGURES

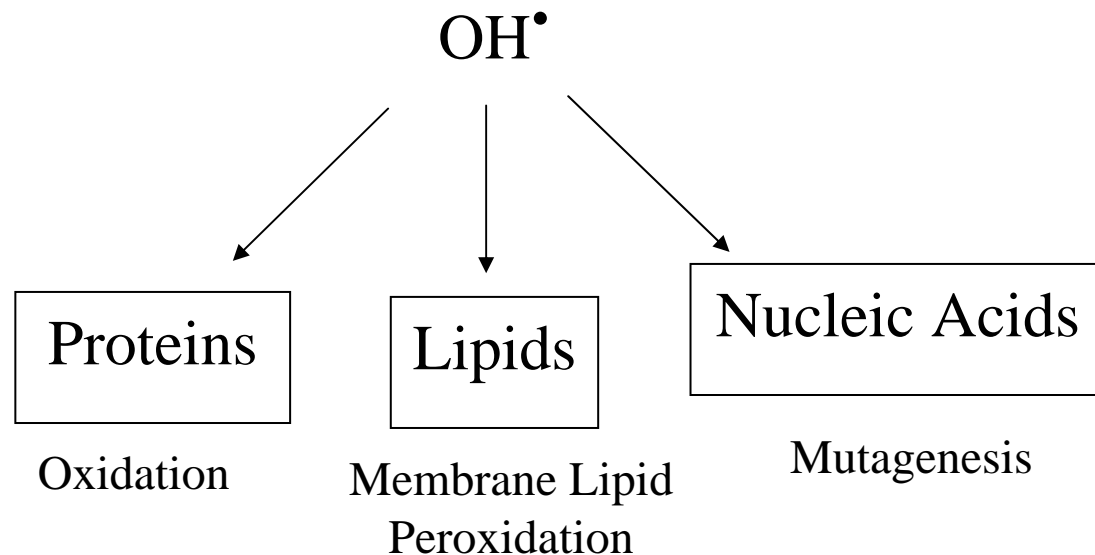
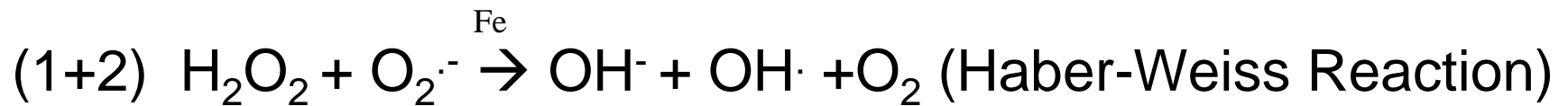
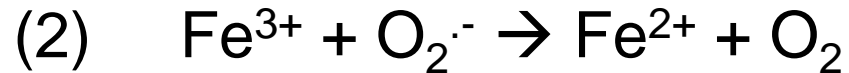


Figure 1

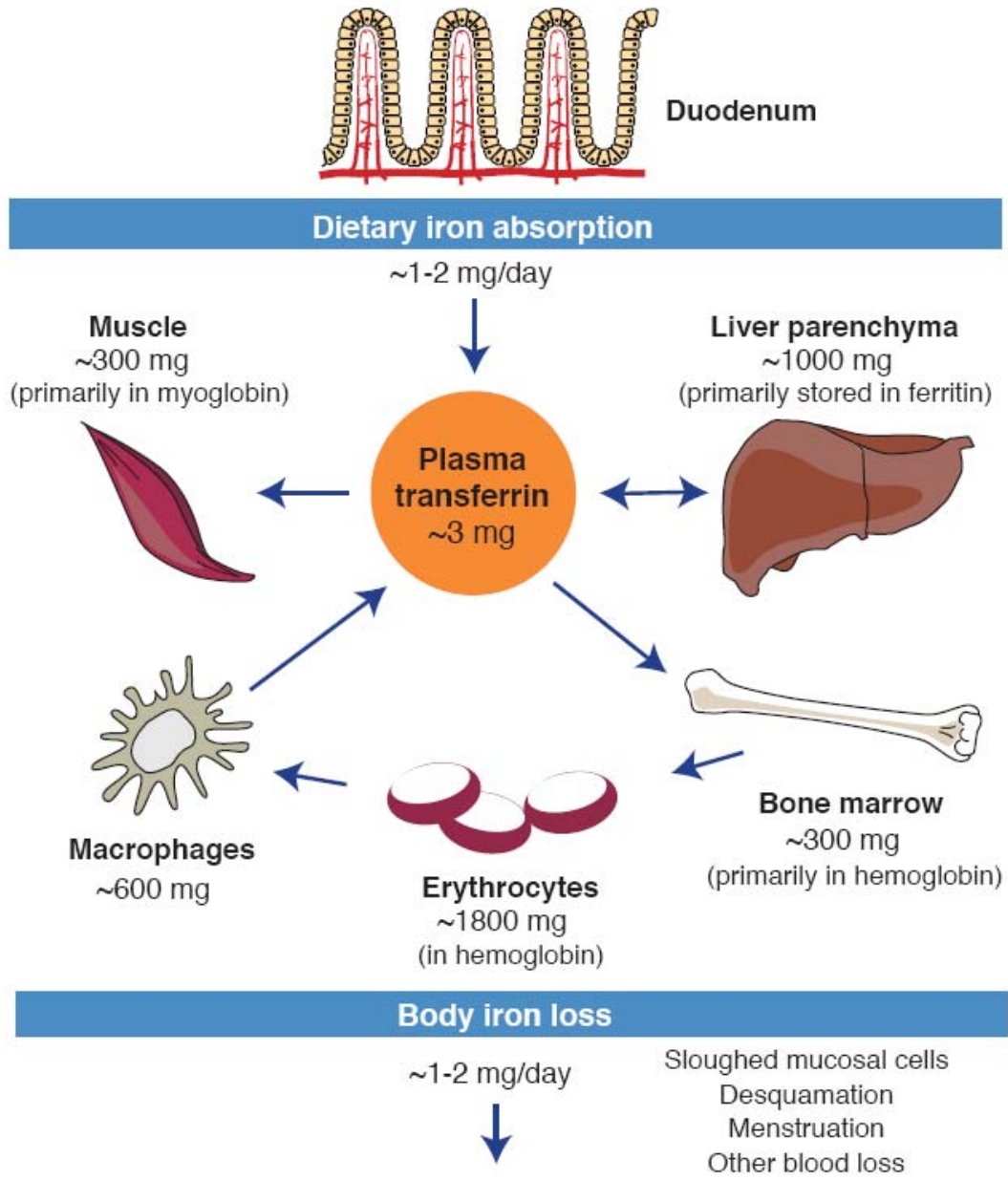
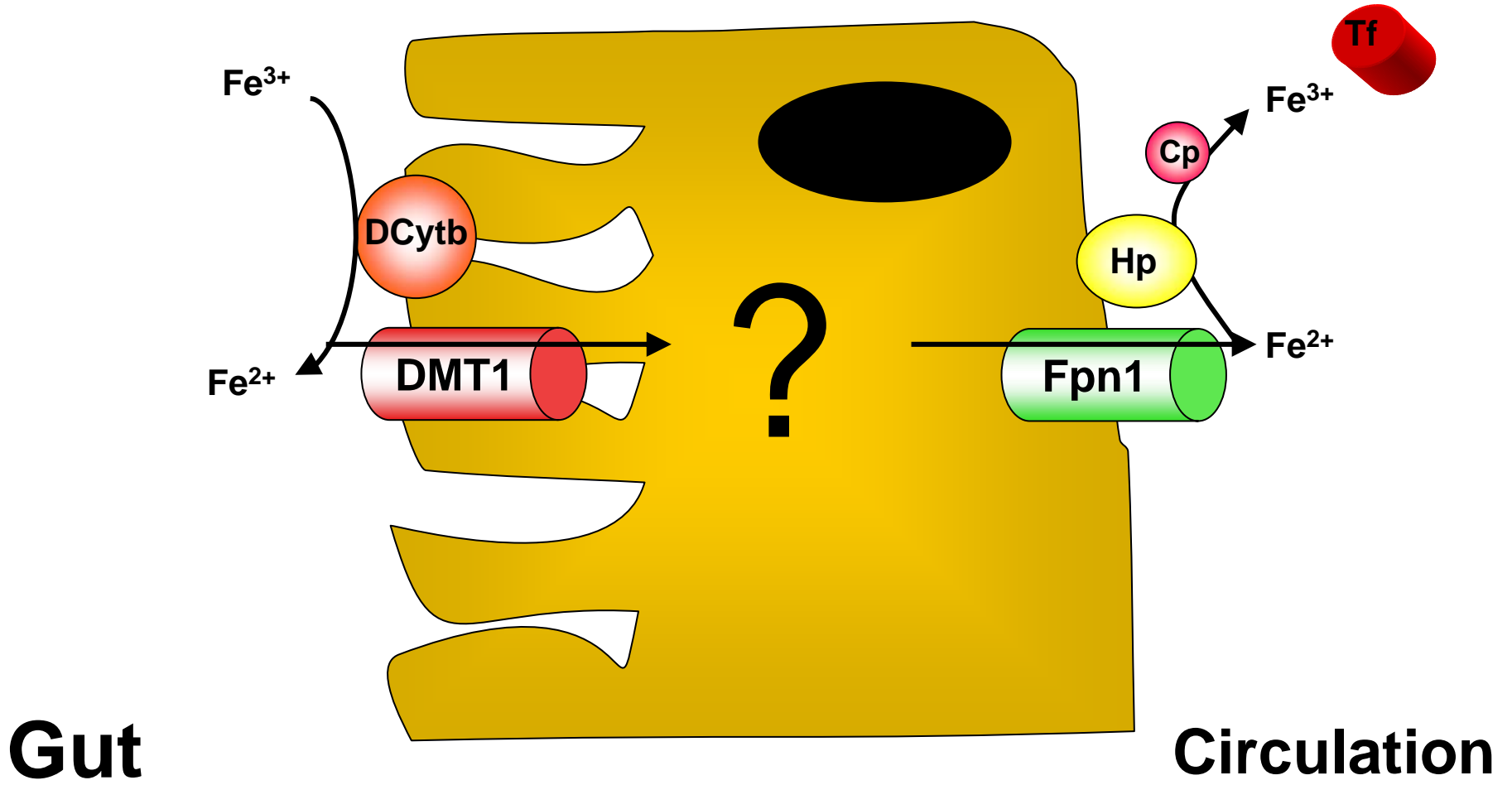


Figure 2



Gut

Circulation

Figure 3

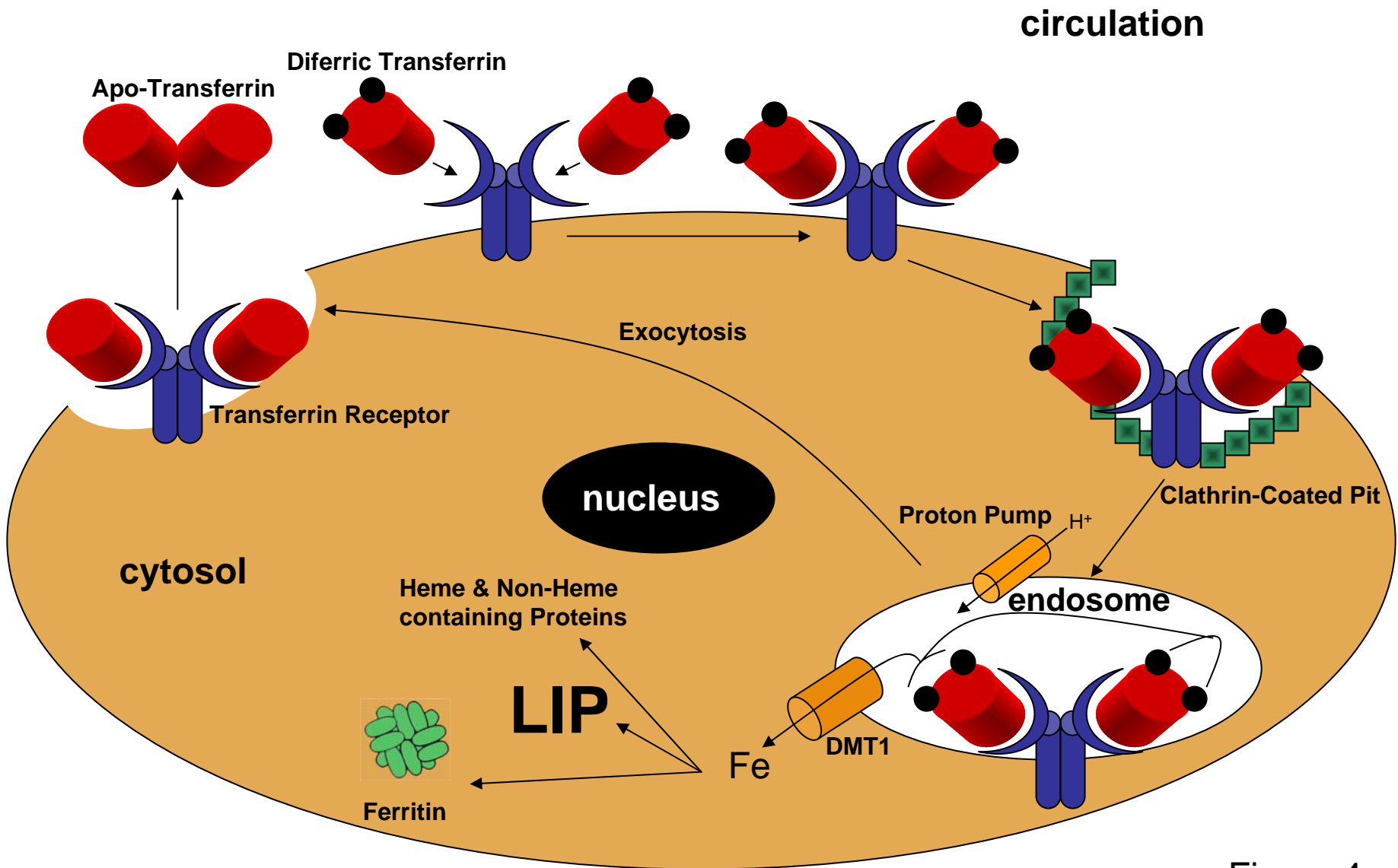


Figure 4

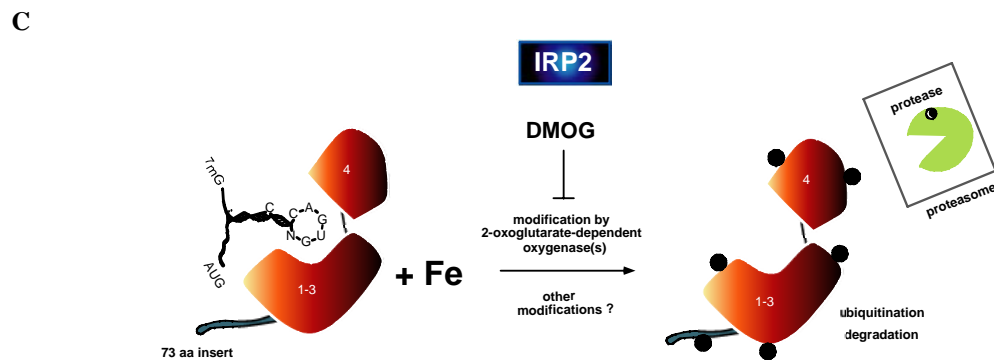
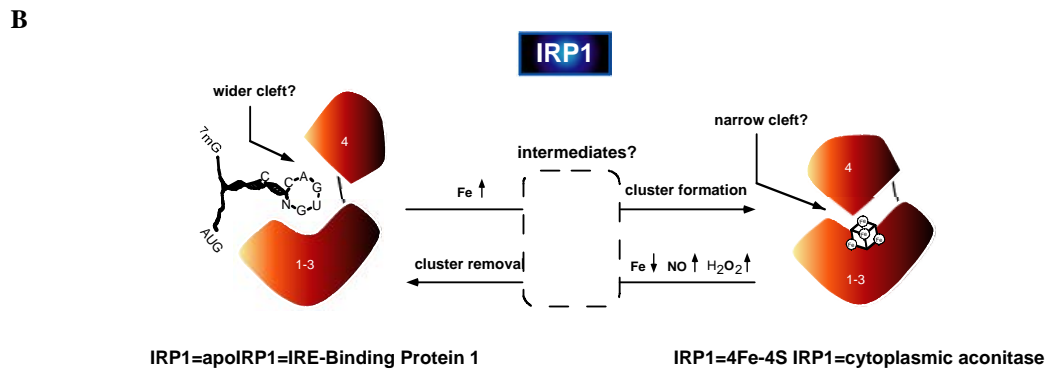
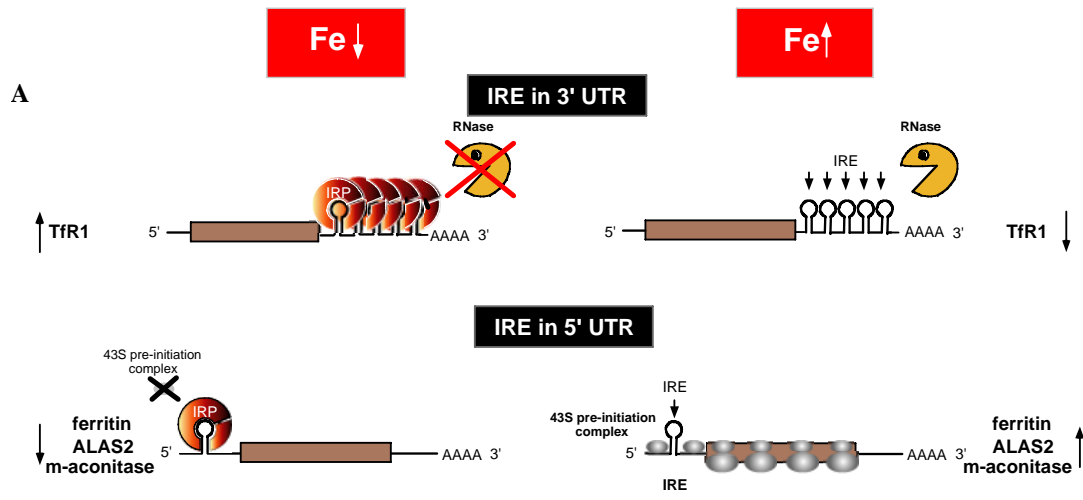


Figure 5

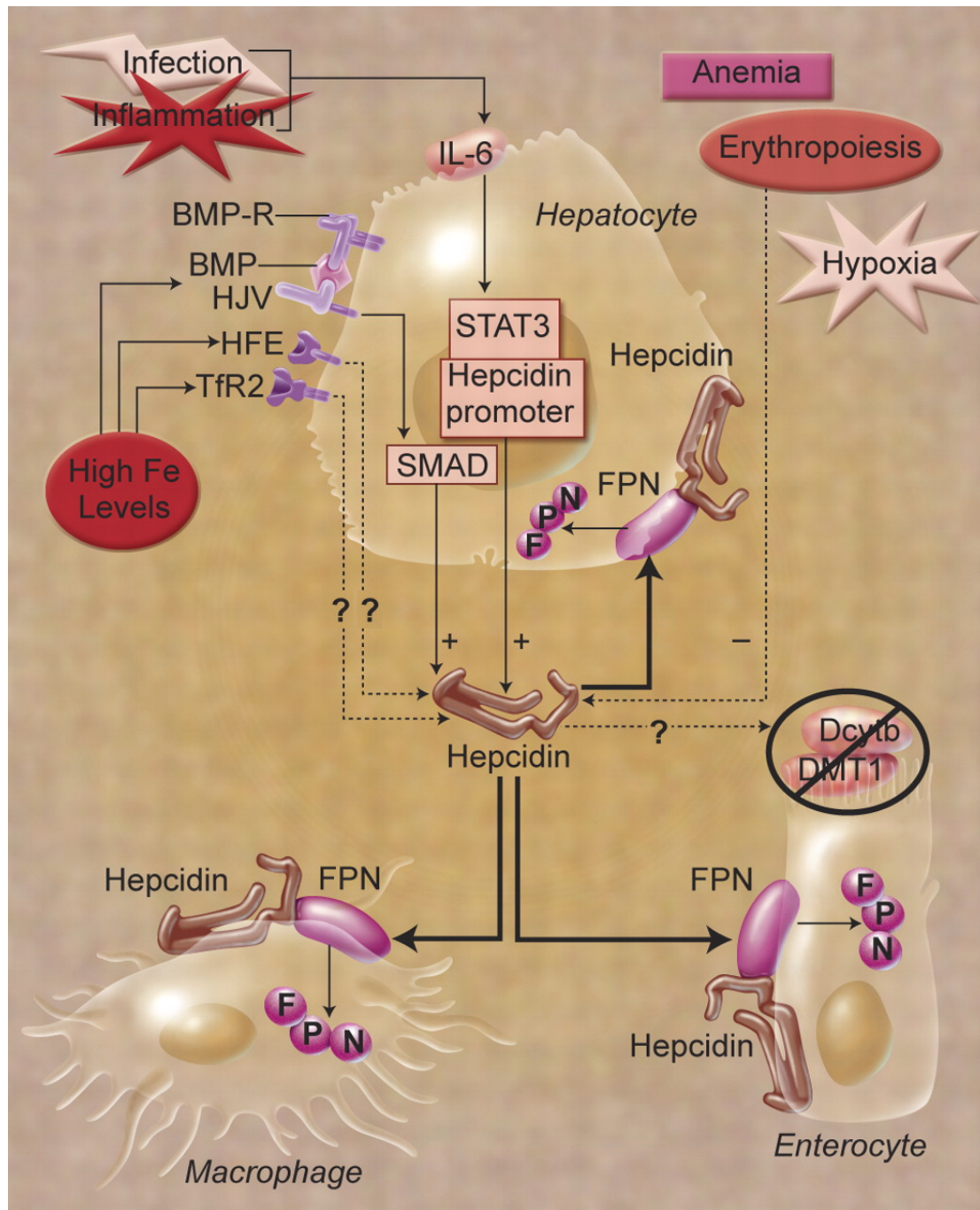


Figure 6

Full Length Human Hemojuvelin



1 MGEPGQSPSPRSSHGSPPPTLSTLTLLLLLLCGHAHSQCKILRC
43 NAEYVSSTLSLRGGGSSGALRGGGGGGGRGGGVGSGGLCR
82 ALRSYALCTRRTARTCRGDLAFHSAVHGIEDLMIQH**NCSR**
122 QGPTAPPPPRGPALPGAGSGLPAPDPCDYEGRFSRLHGRPP
163 GFLHCASF**GDPH**VRSFHHHFHTCRVQGAWPLLDNDFLFV
202 QATSSPMALGAN**NAT**ATRKLTIIFKNMQECIDQKVYQAEVD
243 NLPVAFEDGSINGGDRPGGSSLSIQTANPGNHVEIQAAYIG
284 TTIIRQTAGQLSFSIKVAEDVAMAFSAEQDLQLCVGGCPP
325 SQRLSRSERNRRGAITIDTARRLCKEGLPVEDAYFHSCVFD
366 VLISGDP**NFT**VAAQALEDARAFLPDLEKLHLFPSDAGVP
406 LSSATLLAPLLSGLFVLWLCIQ*

Figure 7

Type	I	IIA	IIB	III	IV
Gene/Chromosome	HFE/6p21.3	HFE2/1q21	HAMP/19q13.1	TfR2/7q22	SLC40A1/2q32
Gene product	HFE	Hemojuvelin	Hepcidin	Transferrin Receptor 2	Ferroportin
Pattern of inheritance	Autosomal recessive	Autosomal recessive	Autosomal recessive	Autosomal recessive	Autosomal dominant
Organs with iron accumulation	Liver, endocrine glands and heart	Liver and spleen			
Cells with iron accumulation	Parenchymal	Parenchymal	Parenchymal	Parenchymal	Reticuloendothelial
Age of organ disease onset (years)	40-50	20-30	20-30	40-50	40-50

Figure 8

A

Protein Features Affected	Mutation	Region
SP	nt 81G deletion	<100
SP	Q6H/ G66X	
	G69-R70 insG	
	V74fsX113/ Cysteine	
	C80R	
	S85P	
RGD	G99R	
RGD	G99V	
1 AA after RGD	L101P	100-199
	Q116X	
N-Glycosylation,Cysteine	C119F	
	I1281T	
	R131fsX245	
	D149fsX245	
vWF	A168D	
vWF	F170S	
vWF Acid Sensitive	D172E	
vWF	W191C	
vWF	S205R/	200-299
vWF	I222N	
vWF	D249H	
vWF	G250V	
	N269fsX311	
	R288W	
	G319fsX341	300-399
	Q312X	
	G320V	
Cysteine	C321X/	
Cysteine	C321W/	
	R326X	
	S328fsX337	
	C361fsX366	
	R385X	
	G486S	>400

B

HJV Mutation	Ethnic Origin
R385X	Italian (Ref. 95)
F170S	Italian (Ref. 95)
W191C	Italian (Ref. 95)
D149fsX245	Italian (Ref. 95)
S205R/G250V	Italian (Ref. 95)
V74fsX113/N269fsX311	English (Ref. 95)
R131fsX245	Italian (Ref. 95)
G320V	Canadian (Ref. 95), Italian (Ref. 95), Greece (Ref. 2), France (Ref. 2), Croatia (Ref. 96), Germany (Ref. 96)
S85P	Italian (Ref. 95)
R288W	France (Ref. 95)
D172E/G319fsX341	Italian (Ref. 95)
A168D	Australian (Ref. 95),English (Ref. 95)
L101P/G99R	Albanian (Ref. 95)
C80R/L101P	United States (Ref. 97)
L101P	United States (Ref. 97)
I222N/G320V	United States (Ref. 97), Canada (Ref. 2)
I1281T	Greece (Ref. 2)
C361fsX366	Greece (Ref. 2)
G99V	Greece (Ref. 2)
G320V/R326X	Greece (Ref. 2)
G486S	? (Ref. 98)
G69-R70 insG	United States (African American) (Ref. 98)
G320V/Q116X	Ireland (Ref. 99)
nt 81G deletion	English/Ireland (Ref. 102)
D249H	Japan (Ref. 100)
Q312X	Japan (Ref. 100)
G320V/S328fsX337	Slovakia (Ref. 96)
C119F	Germany (Ref. 96)
C321X/Q6H/I281T	China (Ref. 101)
G66X	Romania (Ref. 103)
C321W/G320V	United States (Caucasian) (Ref. 104)

Figure 9

FIGURE LEGENDS

Fig. 1. Iron-catalyzed generation of hydroxyl radicals inflicts damage on cellular macromolecules. [184]

Fig. 2. Relative iron distribution in the adult human body [40, 184].

The vast majority (~60-70%) of body iron is utilized in the erythron for hemoglobin synthesis and is recycled by reticuloendothelial macrophages. A significant portion of iron (~7-8%) is utilized in muscle myoglobin and the rest (~20-30%) is stored in the liver parenchyma. Daily absorption of 1-2 mg iron from the diet offset non-specific iron losses.

Fig. 3. Model for the absorption of inorganic iron by enterocytes [184].

Ingested Fe^{3+} is reduced in the lumen to Fe^{2+} via duodenal cytochrome b (Dcytb) and transported across the apical membrane by the divalent metal transporter 1 (DMT1). The intracellular iron transport steps remain elusive. The transport of Fe^{2+} across the basolateral membrane is mediated by ferroportin (Fpn). The delivery of iron to circulating transferrin (Tf) is coupled by its reoxidation to Fe^{3+} by membrane-hephaestin (Hp) and soluble ceruloplasmin (Cp) [184].

Fig. 4. Cellular iron uptake via the transferrin cycle [184].

Diferic transferrin binds to the transferrin receptor and undergoes endocytosis involving clathrin coated pits. Acidification of the endosome by a proton pump results in the release of iron, which is subsequently transported across the endosomal membrane to the

cytosol by DMT1. Internalized iron is utilized for metabolic purposes and excess is stored in ferritin. A fraction of intracellular iron is believed to remain within the “labile iron pool” (LIP). The apo-transferrin/transferrin receptor complex is recycled to the cell surface, where transferrin is released.

Fig. 5. The IRE/IRP regulatory system [40, 184].

(A) Iron deficiency promoted IRE/IRP interactions. These result in stabilization of TfR1 mRNA and translational inhibition of the mRNAs encoding ferritin (H- and L- chains), erythroid aminolevulinate synthase (ALAS2) and mitochondrial aconitase (m-aconitase). Opposite responses occur when iron levels increase.

(B) IRP1 is regulated by an iron-sulfur cluster switch: in iron-loaded cells it assembles a cubane 4Fe-4S cluster that converts it to a cytosolic aconitase. The cluster is lost in response to iron deficiency, NO or H₂O₂.

(C) IRP2 is regulated at the level of protein stability: in iron loaded cells it undergoes proteasomal degradation by a pathway sensitive to dimethyl-oxalyl-glycine (DMOG), an inhibitor of 2-oxoglutarate-dependent oxygenases.

Fig. 6. Central role of hepcidin in organismal iron homeostasis [185]

Cell-associated, GPI-linked hemojuvelin (HJV) is proposed to act as a coreceptor for bone morphogenetic protein (BMP) ligands and BMP receptors (BMP-Rs). Interaction of HJV with BMP ligands and 2 BMP-Rs on the cell surface generates an active signaling complex. This complex subsequently activates the intracellular SMAD signaling pathway to induce hepcidin expression. Hepcidin, a peptide secreted by the liver, promotes

internalization and degradation of the iron exporter ferroportin (FPN). The pathway by which HFE and transferrin receptor 2 (TfR2) control the expression of hepcidin is unclear. Importantly, mutations in HJV, HFE, or TfR2 lead to inappropriately low levels of hepcidin. This figure is a modified version of that published in [186] copyright Elsevier; adapted with permission by Alice Y. Chen.

Fig. 7. Protein features of human hemojuvelin

Human hemojuvelin contains an N-terminal signal peptide (red), an RGD motif (green), partial von willebrand factor type D domain (purple) and a predicted GPI sequence (orange). Hemojuvelin also contains 3 glycosylation sites depicted in brown. In blue, the GDPH sequence represents an autoproteolytic cleavage site.

Fig. 8. Different types of hereditary hemochromatosis.

Fig. 9. Disease associated mutations of hemojuvelin

(A) The regions and protein features affected by disease associated mutations in hemojuvelin.

(B) The ethnic origins of the different disease associated mutations in hemojuvelin.

CHAPTER II. HEMOLYSIS PROMOTES THE RELEASE OF A NOVEL POSITIVE
REGULATOR OF HEPCIDIN EXPRESSION, SOLUBLE HJV

Bill Andriopoulos, Danai Palaiologou, Carine Fillebeen, Alina Daba, Matthew Robinson,
Alexi Hadjis, George Papanikolaou and Kostas Pantopoulos

PREFACE

2004 was a remarkable year for iron metabolism research. The receptor for hepcidin was discovered to be the iron exporter ferroportin [6] and researchers identified the second gene responsible for JH [2]. That gene was *Hjv*. Patients with *Hjv*-derived type II JH display inappropriately low levels of urinary hepcidin [2]. Furthermore, hepcidin regulation was compromised and expression was virtually shut off in *Hjv* knockout mice [86, 87]. Like HFE and Tfr2, it seemed that *Hjv* was an upstream regulator of hepatic hepcidin.

Since its discovery, it is well established that *Hjv* exists in both a cellular and soluble form [1, 90, 106, 107]. The cellular form is membrane bound by GPI-anchorage and is expressed primarily in the muscle and to a lesser extent the liver [2]. To date, cellular *Hjv* appears to function as a co-receptor involved in enhancing induction of hepatic hepcidin transcription via a BMP/SMAD mediated pathway [3].

Thus far, most work published investigating the function of soluble *Hjv* (s*Hjv*) have utilized a recombinant and truncated form of the protein [1, 3-5]. These works, published in high profile journals, define *Hjv* as a negative regulator of hepcidin in both *in vitro* [1, 5] and *in vivo* [4] experiments.

In this chapter we utilize physiologically generated s*Hjv* to show the exact opposite. Furthermore, we identify a novel and quite unexpected link between s*Hjv* and hemolysis.

ABSTRACT

Mutations in the gene encoding HJV (Hjv) are associated with juvenile hemochromatosis and lead to low expression of hepcidin, a hormonal regulator of systemic iron homeostasis. Hjv is primarily expressed in skeletal muscle and the liver, while a soluble form (sHjv) is present in the circulation. To explore mechanisms for sHjv shedding and its regulation of hepcidin expression, we engineered H1299 lung cancer cells for conditional expression of WT Hjv or the disease-associated Hjv_{G320V} mutant. Hemin, hemoglobin and human hemolysates promoted robust release of WT and mutant sHjv within 6-24 h. In contrast, other iron sources or manipulation of intracellular heme synthesis failed to promote shedding. The mechanism was independent of HO-1, did not involve the secretory pathway and most likely involves cleavage from the membrane. Hemin also induced the release of endogenous Hjv from H9C2 myocytes, mimicking a response of differentiated myotubes.

In vivo, a significant increase of serum sHjv levels and hepcidin expression was observed 18 hours following treatment of mice with phenylhydrazine, while iron loaded mice (high iron diet or iron-dextran injection) had no effect on Hjv shedding. Physiologically generated sHjv promoted a robust induction of hepcidin mRNA in target hepatoma cells, while the disease-associated sHjv_{G320V} mutant was considerably less efficient. Importantly, sera from healthy volunteers containing sHjv also activated hepcidin expression in target cells, while sera from JH patients containing similar amounts of mutant sHjv blunted this response. Corroborating a role for sHjv as a positive regulator or at least a necessity for hepcidin induction, we observed a strong positive correlation between sHjv and hepcidin expression in developing mice. Taken together,

our results suggest 1) that the release of sHjv is a regulated process and intravascular hemolysis may provide a physiological stimulus for this response; 2) a novel function for sHjv to directly or indirectly enhance hepcidin expression in the liver.

INTRODUCTION

Juvenile hemochromatosis (JH) is a rare, early-onset hereditary disorder of iron overload with an autosomal recessive transmission pattern [187, 188]. Iron progressively accumulates in parenchymal cells, thereby promoting tissue damage. Clinical manifestations of hypogonadism, cardiomyopathy and diabetes develop mostly in the late teens and early twenties. The major locus of the JH gene was mapped to the 1q chromosome [189, 190], but 1q-unlinked genotypes were also identified [191, 192], underlying the heterogeneity of the disease.

The molecular basis of the 1q-unlinked JH was elucidated first. The disease is caused by mutations in the hepcidin gene [66], encoding the antimicrobial plasma peptide hepcidin, which is secreted by the liver in response to increased iron stores or inflammatory signals, and serves as a key hormonal regulator of systemic iron homeostasis [193]. Hepcidin interacts with and controls the levels of ferroportin [6], a transmembrane iron exporter crucial for dietary iron absorption in the duodenum and iron efflux from reticuloendothelial macrophages [194]. Complete disruption of *HAMP* leads to severe JH, while inappropriately low hepcidin expression is documented in milder conditions of hereditary iron overload, associated with mutations in the *HFE* [195] and *TfR2* [196] genes.

The 1q-linked subset of JH is due to a wide range of mutations in the *HFE2* gene, encoding *Hjv* [2, 95]. *Hjv* is identical to repulsive guidance molecule c (RGMc). The RGMa and RGMb family members are expressed in neuronal cells and control the patterning of retinal axons during development [122]. By contrast, *Hjv* is primarily expressed in striated muscle and to a smaller extent in the liver [2], and apparently exerts

an important regulatory function in systemic iron homeostasis. This view is also reinforced by the iron overload phenotype of $Hjv^{-/-}$ mice [86, 87], which represents an animal model for JH.

Hjv -associated JH patients [2] and $Hjv^{-/-}$ mice [86, 87] fail to mount an increase in hepcidin expression despite pathological iron stores, indicating that Hjv acts upstream of hepcidin and positively regulates its expression (or processing). Hjv functions as a co-receptor of bone morphogenetic proteins (BMPs) and mediates signaling via the BMP pathway. More specifically, Hjv interacts with BMP2 and activates hepcidin mRNA transcription [3]. Likewise, BMP4 and BMP9 also stimulate hepcidin expression [113]. In agreement with these data, mice bearing liver-specific disruption of SMAD4, a downstream component of the BMP pathway, had low hepcidin levels and developed iron overload [114]. Hjv also interacts with neogenin [90], suggesting a potential involvement in additional signaling pathways.

Hjv is associated on the cell surface via a glycosylphosphatidylinositol (GPI) anchor and is also located in perinuclear compartments [89, 90]. It is glycosylated at Asn residues [89] and undergoes processing by complex mechanisms [90]. Differentiating muscle cells release a soluble isoform of Hjv in extracellular media [89], which is also present in human serum and plasma [1]. A treatment of primary human hepatocyte cultures with preparations of recombinant soluble Hjv decreased hepcidin mRNA levels suggesting that cellular (c-) and soluble (s-) Hjv have opposing functions [1]. Furthermore, injection into mice of truncated Hjv that is fused to the Fc portion of IgG elevates and diminishes expression of ferroportin and hepcidin, respectively. In addition, injection of this fusion protein also mobilizes splenic iron stores and increases serum iron

levels [4]. Iron is reported to decrease the shedding of sHjv [1, 106], possibly via neogenin [107]. We show here that extracellular heme is a potent inducer of sHjv shedding. Furthermore, we provide evidence that sHjv is necessary for positive regulation of hepcidin expression.

MATERIALS AND METHODS

Materials.

Hemin, ferric ammonium citrate, succinyl acetone, brefeldin A, monensin, and human holo-Tf were purchased from Sigma (St. Louis, MI). Sodium arsenite was from Fisher Scientific (Waltham, USA) whereas protoporphyrin IX, Sn protoporphyrin IX and δ -aminolevulinic were purchased from Frontier Scientific Inc. (Logan, Utah). Bovine serum albumin was purchased from BioShop (Ontario, Canada)

Cell culture.

Human H1299 lung cancer cells and rat H9C2 myoblasts were maintained in Dulbecco modified Eagle medium (DMEM) supplemented with 10% heat-inactivated fetal bovine serum, 100 units/ml penicillin, and 100 μ g/ml streptomycin. Where indicated, H9C2 were incubated in differentiation media containing 1% horse serum [197].

Construction of plasmids.

Human H_{jv} cDNA was kindly provided by Dr. Paul Goldberg (Xenon Pharmaceuticals). A hemagglutinin (HA) epitope tag was introduced into the C-terminus of H_{jv} using PCR with the forward 5'-GAAGAATTCA TGGGGGAGCC AGGCCAGTCC-3' and reverse 5'-CGATCTCGAG CTAAGCGTAA TCTGGAACAT CGTATGGGTA CTGAATGCAA AGCCACAGAA-3' primers, which amplified the full-length sequence and further introduced EcoR1 and Xho1 restriction enzyme sites on

the 5' and 3' ends, respectively. The 1.32 kb amplicon was cloned into the pcDNA3.1 vector (Invitrogen) to yield pcDNA3.1-Hjv_{WT}. The Hjv sequence was confirmed by sequencing. The G320V point mutation was introduced by site-directed mutagenesis with the ExSite™ PCR-based method (Stratagene, La Jolla, CA), according to the manufacturer's recommendations. The construct pcDNA3.1-Hjv_{WT} was utilized as template with the forward primer 5'-CAGCTCTGTG TTGGGGTGTG CCCTCCAAGT CAG-3' and the reverse complement 5'-CTGACTTGGA GGGCACACCC CAACACAGAG CTG-3'. The introduction of the point mutation was confirmed by sequencing. Finally, WT and mutant Hjv were excised with EcoR1 and Xba1 and ligated into the respective sites of the pUHD10-3 vector, which contains a tetracycline-inducible hCMV minimal promoter [198], to yield pUHD-Hjv_{WT} and pUHD-Hjv_{G320V}, respectively. Promoter constructs -900 bp and -600 bp were prepared as published in [199].

Tetracycline-inducible expression of WT and mutant Hjv in H1299 cells.

The pUHD-Hjv_{WT} and pUHD-Hjv_{G320V} plasmids were co-transfected with the puromycin resistant pBABE in tTA-H1299 cells [198] by using the Lipofectamine Plus reagent (Invitrogen). Stable H1299-Hjv and H1299-Hjv_{G320V} clones were selected in media containing 2 µg/ml tetracycline, 2 µg/ml puromycin and 250 µg/ml G418. The expression of Hjv was induced by removal of tetracycline (tet-off system) for a period of 48 hours.

Western blotting.

Cells were lysed in RIPA buffer, containing phosphate buffered saline (PBS), 1% NP-40, 0.5% sodium deoxycholate, 0.1% SDS and a protease inhibitor cocktail (Sigma). Cell debris was cleared by centrifugation and protein concentration was measured with the Bradford reagent (Biorad). Supernatants obtained from cells were concentrated ~18-fold using Amicon Ultra Centrifugal Filter Devices (Millipore) with a cut-off of 5 kDa. Cell lysates and concentrated supernatants, each containing approximately 50 µg of proteins, were denatured for 10 minutes at 95°C. The proteins were resolved by SDS-PAGE on 12% gels and transferred onto nitrocellulose membranes (Bio-Rad). The blots were saturated with 10% non-fat milk in PBS containing 0.1% Tween (PBS-T) and probed overnight at 4°C with following primary antibodies (diluted in PBS-T with 5% non-fat milk): 1:100 HA (Santa Cruz), 1:500 H₂v (Santa Cruz) or ferritin (Daco), 1:1000 TfR1 (Zymed) or β-actin (Sigma), or 1:2000 HO-1 (Stressgen). Following wash with PBST, the blots with HA, ferritin, β-actin and HO-1 antibodies were incubated with 1:5000 diluted peroxidase-coupled goat anti-rabbit IgG (Sigma). The blots with H₂v and TfR1 antibody were incubated with 1:5000 diluted peroxidase-coupled donkey anti-goat (Santa Cruz) and rabbit anti-mouse IgG (Sigma), respectively. Detection was performed with the enhanced chemiluminescence ECL[®] method (Perkin Elmer). Where indicated, the immunoreactive bands were quantified by densitometric scanning using ImageJ 1,38x National Institute of Health.

Northern Blotting.

Liver and muscle tissues were homogenized in TRizol reagent (Invitrogen), and RNA was prepared according to the manufacturer's recommendations. Total cellular

RNA (10 µg) was electrophoretically resolved on denaturing 1.5% agarose gels, transferred onto nylon membranes, and hybridized to radiolabeled cDNA probes against mouse hepcidin RNA or β-actin. Autoradiograms were quantified by phosphorimaging.

Real time PCR.

Total DNA-free RNA was isolated from approximately 2.5×10^5 Huh7 cells using the Nucleospin RNA II kit (Macherey-Nagel), according to the manufacturer's instructions. cDNA was synthesized by reverse transcription of 1.5 µg of quality-checked RNA using 0.5 µg oligo-dT primers and 200 units of Moloney Murine Leukemia Virus (MMLV) reverse transcriptase (Invitrogen). Real-time quantification of hepcidin mRNA transcripts was performed in the LightCycler (Roche) with SYBR Green I fluorescent dye (Molecular Probes). The values of β-actin mRNA and ribosomal 18S RNA were determined as internal controls. Following gene-specific primers were used: For hepcidin 5'-ATGGCACTGA GCTCCAGAT-3' (forward) and 5'- ACTTTGATCG ATGACAGCA GCCG-3' (reverse); for β-actin 5'-AGGATGCAGA AGGAGATCAC T-3' (forward) and 5'-GGGTGTAACG CAACTAAGTC ATAG-3' (reverse); and for 18S RNA 5'-GTTCCGACCA TAAACGATGC-3' and 5'-AACCAGACAA ATCGCTCCAC-3' (reverse). The reaction conditions were as follows: An initial denaturation at 95°C for 1 min, followed by 40 cycles of amplification (denaturation at 95°C for 1 s, primer annealing at 65°C for 15 s and extension at 72°C for 20 s). Melting curve analysis and agarose electrophoresis were used to verify the specificity of the reaction products. Results from triplicate samples were expressed as hepcidin/β-actin and hepcidin/18S RNA ratios.

Dual luciferase reporter assays.

Firefly luciferase reporter plasmids -900 bp and -600 bp (4 µg each) were co-transfected with 4 µg of Renilla reniformis luciferase control vector pRL-CMV (Promega) into 1 million Huh7 cells in a 10 cm dish by using Lipofectamine™ Plus reagent (Invitrogen). Twenty-four hours post-transfection, cells were equally split into 24 well plates and allowed to grow and attach for 18 hours. Conditioned media was subsequently applied for 6 hours and Dual luciferase assays were performed in cell lysates according to the manufacturer's instructions (Promega).

Preparation of hemolysate.

Peripheral blood (10 ml) from a healthy volunteer was collected in lavender top EDTA tubes and centrifuged at 2,500 rpm for 15 minutes at 25°C, with the centrifuge brake off. The plasma was discarded and the cell pellet was washed twice with PBS and centrifuged at 3,000 rpm for 10 minutes at 25°C. One half of the red blood cell pellet was subjected to hemolysis by addition of 3 ml double distilled water and incubation for 10 minutes at room temperature. Subsequently, the cell lysates were centrifuged at 12,000 rpm for 10 minutes at 25°C. The supernatant (hemolysate), the cell debris pellet, and the other half of intact red blood cells were diluted with culture media to 20 ml.

Mouse experiments.

C57BL/6N male mice (Charles River) were aged for 2 to 3 months and were subjected to a single intraperitoneal injection of phenylhydrazine at a concentration of 50

mg/kg as described in [174]. For the iron diets and iron dextran experiments, female CD-1 retired breeder mice were used. To isolate the plasma, 50-75 μ l of blood was collected from the heart of anesthetized mice in a heparinized microhematocrit tube. The tubes were then spun at 2300 rpm for 3 minutes in a micro-hematocrit centrifuge and the top phase plasma was subsequently collected and 1 μ l was utilized for analysis of sHjv expression by Western blotting. Serum iron parameters were analyzed at the Hematology Department at the Jewish General Hospital. Iron dextran and control PBS were injected into mice as described in [63].

RESULTS

Hjv isoforms

Full length WT or disease-associated (Hjv_{G320V}) mutant human Hjv cDNA, were transiently and stably transfected into tTA-H1299 cells. Both Hjv constructs contained a C-terminal HA epitope tag and overexpression in tTA-H1299 cells was controlled by a “Tet-Off” system. Upon removal of tetracycline for 48 hours, different Hjv isoforms were observed when comparing transient and stable transfections. Using RT-PCR, tTA-H1299 cells were shown to lack endogenous Hjv (data not shown).

In transient transfections, western blot analysis shown in Fig. 1A using a polyclonal HA antibody revealed the presence of 3 Hjv isoforms that were identical in both WT (lanes 1-2) and mutant Hjv_{G320V} (lanes 3-4). More specifically, a predominant ~52 kDa band was detected in addition to 2 much weaker bands of approximately ~49 and ~27 kDa.

Stably transfected clones were isolated and analyzed for Hjv expression. The results from two representative H1299-Hjv and H1299-Hjv_{G320V} clones, which are used throughout this study, are shown in Fig. 1B. Both WT Hjv (lanes 1-2) and Hjv_{G320V} (lanes 3-4) were tightly regulated by tetracycline, while the levels of endogenous β -actin were not affected by the antibiotic (bottom panel). In stably transfected cells, only the major ~52 kDa band was detectable by immunoblotting with the HA antibody and also with Hjv antisera (Supplementary Fig. 1).

Hemin promotes Hjv shedding

To evaluate whether the expression of WT and mutant HJV responds to iron, H1299-HJV and H1299-HJV_{G320V} cells were exposed overnight to either 5 μ M holo-Transferrin (holo-Tf), 50 μ g/ml ferric ammonium citrate (FAC) or 100 μ M hemin. Immunoblot analysis of the cell lysates showed that these treatments did not substantially alter the levels of cHJV (Fig. 2A, top) and cHJV_{G320V} (Fig. 2B, top). However, following treatment with hemin, soluble forms of WT (Fig. 2A, second panel) and to a lesser extent mutant (Fig. 2B, second panel) HJV emerged in concentrated cell supernatants. Both proteins co-migrated with sHJV from mouse serum (lanes 1), with an apparent molecular mass of \sim 50 kDa. They were detected with HJV antisera and did not cross-react with the HA antibody, indicative of a processing event at the C-terminus. HJV antisera also recognizes a \sim 52 kDa band in H1299-HJV and H1299-HJV_{G320V} cells (supplemental Fig. 1A) and a \sim 45 kDa band in mouse muscle tissues and to a much lesser degree in the liver (Fig. 11B, 12C and 12D). To rule out clonal specificity, a second isolated WT clone displayed hemin induced shedding of sHJV (supplementary Fig. 1C).

As expected, the expression of cellular TfR1 and ferritin, which are involved in iron uptake and storage, respectively, were also regulated by hemin, while control β -actin was not (panels 4-6). Interestingly, under these experimental conditions, neither holo-Tf nor FAC had any effect on sHJV release, even though they both induced ferritin expression, albeit to a lesser degree than hemin. Holo-Tf at concentrations of 5-30 μ M failed to elicit any sHJV release (Fig. 3A and 3B). A dose dependent treatment of heme revealed that sHJV and sHJV_{G320V} shedding occurs at approximately 50-100 μ M (Fig. 3C and 3D).

Treatments known to modulate intracellular heme levels (Fig. 2A and 2B) such as addition δ -aminolevulinic acid (lane 7), protoporphyrin IX (lane 8), succinyl acetone (lane 9) and FAC plus δ -aminolevulinic acid (data not shown) did not affect sHjv release.

We conclude that extracellular hemin promotes the shedding of sHjv and sHjv_{G320V} from transfected H1299 cells.

Kinetics of hemin-induced sHjv shedding

The kinetics of hemin-mediated sHjv release was determined in a pulse-chase experiment. We took advantage of the inducible Hjv expression system and analyzed the decay (in the cells) and the release (in the media) of a defined Hjv (or Hjv_{G320V}) pool, in the absence or presence of hemin, following re-addition of tetracycline. In this setting, the half-life of cHjv and cHjv_{G320V} (Figs. 4A and 4B, respectively) was approximately 6 h and was not affected by hemin. WT and mutant sHjv were detectable in media after 2 h and their levels peaked after 24 h of hemin treatment. Even though the release of WT sHjv was generally more robust, the eventual accumulation of sHjv_{G320V} seems to exclude a major defect in the processing of the mutant protein. Overall, the above results suggest that the release of both WT and mutant sHjv is subjected to regulation and identify hemin as an inducer.

Mechanism of hemin-induced sHjv shedding

Hemin (the Fe³⁺ oxidation product of heme) is a potent inducer of heme oxygenase-1 (HO-1) (Figs. 5A and 5B, second panels). This enzyme metabolizes heme

(and hemin, following its reduction into heme) into biliverdin, iron and carbon monoxide, which in turn activates various signaling cascades [200]. To explore a possible involvement of HO-1 signaling in the mechanism of sHjv release, we blocked HO-1 activity with excess tin protoporphyrin IX (SnPPIX), a substrate analogue of heme and inhibitor of HO-1 (lanes 3-4). This, however, failed to inhibit hemin-mediated shedding of sHjv (third panels). Moreover, the hemin-independent induction of HO-1 by arsenite was not sufficient to elicit sHjv release, indicative of a HO-1-independent mechanism (lanes 5-6). Thus, the shedding of sHjv (WT and mutant) in response to hemin does not depend on HO-1 activity. The arsenite treatment was associated with a conversion of cHjv and cHjv_{G320V} to the ~49 kDa isoforms (top panel); the reason for this is unclear.

The mechanism for hemin-induced shedding of sHjv could involve the secretory pathway. However, neither brefeldin A nor monensin, which block the secretion of glycoproteins [201], prevented the accumulation of sHjv (Fig. 5C) or sHjv_{G320V} (Fig. 5D) from hemin-treated cells. As expected, both brefeldin A and monensin induced the phosphorylation of the translation initiation factor eIF2 α (third panels), which, is indicative for activation of the PERK kinase due to ER stress [202]. These results suggest that the hemin-mediated release of sHjv is independent of the secretory pathway and may involve cleavage from the plasma membrane.

We next sought to gain insight into the factors responsible for membrane cleavage during hemin treatment. In cell culture, factors involved in hemin-induced shedding may originate from either the media's fetal bovine serum or the cells themselves. To address this, H1299-Hjv and H1299-Hjv_{G320V} cells were treated with hemin in the presence of either fetal bovine serum or 10% albumin. As a result, hemin mediated shedding of sHjv

was observed in both WT and mutant cells, regardless if they were cultured with media supplemented containing either fetal bovine serum or albumin (Fig. 5E and 5F). Interestingly, in the absence of both fetal bovine serum and albumin, hemin precipitated and did induce release of sHjv and sHjv_{G320V} (supplementary Fig. 1C). Thus, the factor(s) responsible for hemin induced shedding of sHjv and sHjv_{G320V} most likely originates from H1299-Hjv and H1299-Hjv_{G320V} cells. Taken together, the mechanism by which sHjv is most likely shed from the membrane is independent of HO-1, the secretory pathway and factors present in fetal bovine serum.

Hemin-regulated shedding of endogenous sHjv from H9C2 myoblasts

Since Hjv is primarily expressed in skeletal muscle, we investigated whether hemin is capable of inducing sHjv release in a muscle cell line. The growth of H9C2 myoblasts in low-serum (1% horse serum) differentiation media was associated with the release of endogenous sHjv (Fig. 6A and 6B) indicative of differentiation as illustrated in the data obtained with C2 and C2AS12 myoblasts. Importantly, hemin but not its precursor protoporphyrin IX triggered the release of endogenous sHjv from undifferentiated H9C2 cells (Fig. 6B, lanes 3-4) and this effect was more pronounced when the cells were grown in differentiation media (lanes 6-7). A higher loading of the blot indicates that the shedding of sHjv triggered by hemin is dramatic, compared to the differentiation response.

Shedding of sHjv in response to a human hemolysate

Having established that hemin induces shedding of transfected and endogenous sHjv, we sought to recapitulate this effect under more physiologically relevant conditions. More specifically, peripheral blood from a healthy volunteer was obtained and subjected to hemolysis. Subsequently, the hemolysate was cleared by centrifugation and incubated with H1299-Hjv and H1299-Hjv_{G320V} cells. The hemoglobin- and heme-rich soluble fraction of the hemolysate induced the release of sHjv (Fig. 7A, lane 4) and sHjv_{G320V} (Fig. 7B, lane 4), while the pellet (lanes 5), or intact red blood cells (lanes 3) failed to do so (observations supported by a second donor, data not shown). In addition, dose dependent treatment of hemoglobin revealed sHjv and sHjv_{G320V} release at approximately 50-100 μ M (Fig. 7C and 7D). These data imply that the release of sHjv may constitute a pathophysiological response to intravascular hemolysis.

Phenylhydrazine-induced hemolysis in mice is associated with prolonged and transient increases in serum sHjv levels and hepatic hepcidin expression, respectively.

Thus far, in vitro experiments reveal that shedding of sHjv from transfected and muscle cells occurs when treated with human hemolysate, hemoglobin or hemin. The next step was to validate our cell culture data with an in vivo model. More specifically, mice were injected with a single intraperitoneal injection of phenylhydrazine (PHZ) to induce hemolytic anemia. PHZ treatment promoted a statistically significant ($p < 0.05$) 2.1 fold increase in serum sHjv levels and a ($p < 0.05$) 2.4 fold induction of hepatic hepcidin mRNA after 18 hours (Fig. 8). As expected, hepcidin expression subsequently dropped to below basal levels at 48 and 72 hours post injection. As expected, % hematocrit was

significantly lower 18 hours after injection. Other serum parameters are presented in Table 1. Taken together, it is possible that sHjv released 18 hours post-PHZ injection may positively regulate hepcidin expression. We next investigated whether sHjv is capable of inducing hepcidin expression.

WT sHjv released from H1299-Hjv cells activates hepcidin expression in target hepatoma cells

The compromised hepcidin response in humans and animals with Hjv deficiency prompted us to evaluate how sHjv affects the expression of this iron regulatory peptide. Huh7 hepatoma cells were cultured with conditioned media for 6 hours from control tTA-H1299, H1299-Hjv or H1299-Hjv_{G320V} cells, previously treated with hemin to release sHjv. Exposure of Huh7 cells with media containing WT sHjv was associated with a ~4-fold increase in hepcidin mRNA levels; however, media containing sHjv_{G320V} failed to elicit an analogous response (Fig. 9A).

To determine if these responses occur at the level of transcription, hepcidin promoter activity in treated Huh7 hepatomas was measured. Hepcidin promoter regions -600 and -900 base pairs (bp) were each fused to firefly luciferase reporters and transiently transfected into Huh7 hepatomas. Approximately 40 hours post-transfection, hepatomas were treated with conditioned media for 6 hours from tTA-H1299, H1299-Hjv or H1299-Hjv_{G320V} cells, previously treated with hemin to release sHjv. No significant difference in luciferase activity was observed in each promoter under all conditions (Fig9B).

Taken together, these data suggest that sHjv is required to positively regulate hepcidin expression and that this response is blunted in the disease associated sHjv_{G320V}.

Furthermore, regulation of hepcidin expression was independent of promoter activity at 600 and 900 bp upstream from the start of translation.

Sera from healthy volunteers but not JH patients induce hepcidin expression in hepatoma cells

To further assess the function of sHjv, HepG2 hepatoma cells were incubated with media containing either fetal bovine serum, or a mixture of sera from either healthy volunteers or JH patients bearing Hjv mutations. Sera from healthy volunteers stimulated the expression of hepcidin mRNA by ~3-fold and this response was blunted with sera from JH patients (Fig. 10a). Importantly, immunoblot analysis of serum samples from a healthy volunteer and a JH patient (genotyped with Hjv_{G320V} mutation) revealed the presence of WT or mutant sHjv, respectively (Fig. 10b); sHjv was repeatedly undetectable in commercial fetal bovine serum. We conclude that WT sHjv from healthy human sera is necessary to activate hepcidin expression, while mutant sHjv present in patient sera is not. Putative confounding factors in patient sera, such as inflammatory cytokines, though not measured, would have resulted in increased hepcidin expression. Therefore, the blunted response is apparently due to the absence of functional sHjv.

High iron diet or iron dextran injections modulate hepcidin expression independent of sHjv in mice

In vitro findings suggest that hemolytic driven shedding of sHjv is a positive regulator of hepcidin expression. Furthermore, elevated serum sHjv in mice may be the inducer of hepcidin expression, 18 hours post-PHZ-injection. Because patients and mouse

models with HJV defects display misregulated hepcidin expression and severe iron overload, we utilized two mouse models that mimicked the iron overload phenotype. The purpose, more specifically, was to monitor if sHJV plays a role in regulating hepcidin expression during this state of elevated iron levels in the animal.

The iron overload models were mice either fed a high iron diet for 1 month (Fig. 11) or injected with iron-dextran (Fig. 12). After a 1 month high iron diet and 7 days after iron-dextran injection, mice from both mouse models exhibited similar levels of elevated serum iron, total iron binding capacity, transferrin saturation and serum ferritin (Tables 2 and 3). Furthermore, liver ferritin and HO-1 were elevated in high iron diets and iron dextran treatments. Interestingly, muscle ferritin and HO-1 responded identically in the liver upon iron dextran treatment (Fig. 11B) but were absent in the muscles of mice with a high iron diet (Fig. 12C and 12D). In addition, significant hepcidin induction was present in both mice. sHJV was unaltered in both models and in mice fed a low iron diet. This suggests that in these iron overload mouse models, hepcidin induction was independent of sHJV.

Positive correlation between hepatic hepcidin and sHJV in developing mice

It has been reported that throughout mouse development, hepatic hepcidin is differentially expressed. To further investigate the role of sHJV in the regulation of hepatic hepcidin, 3 mice were sacrificed at different stages of life. Liver hepcidin expression and levels of sHJV were measured at the different developmental time points and compared with each other. As illustrated in Fig. 13, a Spearman correlation coefficient of 0.7 was measured and is indicative of a strong positive association. In

accordance with previous reports [59, 203], hepcidin expression exhibits a pattern of low expression in embryonic stage, followed by a slight elevation until a dramatic decrease at days 8 and 15. Following this decrease, hepcidin expression is potentiated until day 56. sHjv appears to positively correlate with hepcidin until day 15. Following day 15, sHjv is unchanged whereas hepcidin continues to increase until day 56. This correlation further corroborates that sHjv is involved in positively regulating hepcidin expression, at least until day 15.

DISCUSSION

Hjv is a recently discovered and still incompletely characterized protein that plays an important role in systemic iron homeostasis [204] by controlling the expression of hepcidin [2, 3, 86, 87]. In order to better understand its regulation and function, we expressed WT Hjv and the JH-associated Hjv_{G320V} mutant in heterologous H1299 cells, under the control of a tetracycline-inducible promoter. We searched for signals that may affect Hjv expression in this system and found that micromolar concentrations of extracellular hemin, but not perturbations of intracellular heme levels, promote the shedding of a soluble isoform of the protein from the cells into the media (Fig. 2). We observed no basal shedding or inhibition by iron treatment, as previously reported [1, 106, 107]. Our data suggest that sHjv released upon hemin treatment is via a different mechanism from those reported in the past.

The release of WT sHjv was generally more robust, compared to sHjv_{G320V}, especially considering that the expression levels of the mutant in the transfected cells were ~3.7-fold higher than those of WT (Fig. 2). This may be related to defective intracellular processing of sHjv_{G320V}, as recently described [106]. Nevertheless, in this experimental setting, high levels of sHjv_{G320V} eventually accumulated in the cell supernatants following prolonged hemin treatments (Fig. 4), suggesting that even though the response is delayed, it can be completed. These findings demonstrate that heme induces the shedding of both WT and mutant sHjv.

A possible involvement of HO-1 in the mechanism can be excluded by the failure of its substrate analogue tin protoporphyrin IX to inhibit, and the inability of hemin-independent induction of this enzyme to promote sHjv and sHjv_{G320V} release (Figs. 5A

and 5B). Because the inhibitors monensin and brefeldin A were unable to antagonize sHjv and sHjv_{G320V} release in hemin-treated cells (Figs. 5C and 5D), it appears that the mechanism does not require an intact secretory pathway. We speculate that the mechanism rather involves proteolytic cleavage of plasma membrane-bound Hjv or, alternatively, cleavage of its GPI anchor by a phospholipase by heme-induced enzymes. Since brefeldin A and monensin disrupt the secretory pathway, Hjv shedding due to hemin could only originate from the pool of Hjv that accumulated 48 hours prior to treatment. Previously published data illustrated that the life span of membrane associated Hjv is 12-24 hours [89]. Thus, accumulation of membrane associated Hjv for 48 hours prior to treatment is stable during the 12 hour inhibition of the secretory pathway.

Furthermore, we exclude fetal bovine serum as possessing any hemin-activating factors that are involved in our observed regulated shedding of sHjv (Fig. 5E and 5F). Taken together, we propose that hemin activated factor(s) originate from the cell and are responsible for cleavage of membrane associated Hjv. Currently, work is under way to isolate these potential factors.

Because all experiments establishing the regulated shedding of sHjv were performed with transfected cells, it was important to examine how cells naturally producing Hjv respond to hemin. The data in Fig. 6 confirm the release of endogenous Hjv from hemin-treated H9C2 myoblasts. Interestingly, since myoblast cells release sHjv during in vitro differentiation into myotubes [89] (see also Fig. 6) it appears that the regulation of Hjv by hemin mimics a biological response. In quantitative terms, hemin is clearly the most potent stimulus for sHjv shedding identified thus far. Furthermore, in

vitro and in vivo experiments presented in this report, rule out any significant relationship between sHjv shedding and different sources of iron.

Aiming to explore the physiological relevance of the above findings, we found that not only “free” extracellular hemin and hemoglobin but also a human hemolysate induces sHjv (and sHjv_{G320V}) release with similar efficiency (Fig. 7). A hemolysate is rich in heme that is bound to hemoglobin and degradation intermediates. Considering that intravascular hemolysis normally occurs for 10%-20% of the red blood cells [175], these results suggest that the shedding of sHjv in response to heme can be a (patho)physiologic process. Experimental support for this hypothesis is provided by the prolonged increase of serum sHjv levels starting at 18 hours post-PHZ-injection in mice (Fig. 6). Interestingly, a transient increase in hepcidin expression was also observed 18 hours post-injection followed by an expected suppression [173, 174, 205]. It is well established that upon PHZ injection, a lag period exists until an increase in duodenal iron absorption is observed [205]. Recently, it was discovered that the lag period is due to a delayed hepcidin response [205]. More specifically, approximately 1-3 days post-PHZ-injection, hepcidin is suppressed to below basal levels which leads to increased iron absorption and mobilization of stores to meet erythropoietic demand. What has received little attention is the early transient increase in hepcidin following injection [174, 205]. Our data suggest that following PHZ-injection, sHjv is increasingly shed from the membrane and targets the liver to directly or indirectly induce transient hepcidin expression. Hepcidin inhibition of both iron absorption in the duodenum and release from macrophages could favor the reutilization of heme iron for erythropoiesis by the haptoglobin and hemopexin scavenging systems [206]. Furthermore, we propose that the subsequent robust

suppression of hepcidin in these mice is due to the overriding effect of the yet to be identified erythroid regulator [173, 174].

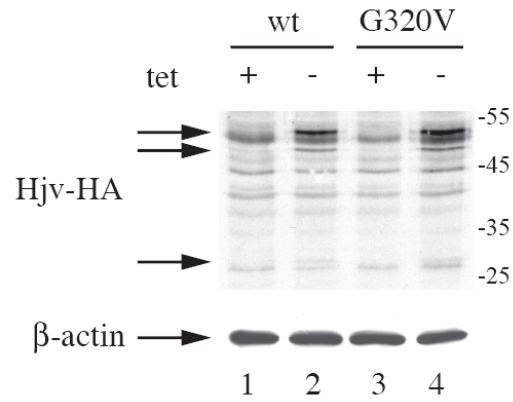
We propose that sHjv is a positive upstream regulator of hepcidin. Conceivably, recombinant sHjv [1, 5] or Hjv-Fc fusion protein [4] may not share similar properties with our full length sHjv that undergoes cellular processing and glycosylation. To address this, we are currently purifying sHjv released upon hemin treatment. We speculate that sHjv may transcriptionally activate hepcidin via a BMP or neogenin signaling pathway, by analogy to cHjv in a promoter region upstream of -900bp [3, 90]. It is also possible that 1) sHjv stimulates other pathways or that 2) sHjv is a necessary co-factor for an unidentified soluble activator of hepcidin expression. The presence of sHjv_{G320V} in a JH serum sample (Fig. 10b) denotes that the misregulation of hepcidin expression in Hjv-associated JH patients [187] is due to defective signaling from mutant sHjv, again by analogy to its cellular precursor [3]. Based on the Hjv mRNA expression pattern [2] and our blots (Fig. 11b, 12c and d), skeletal muscles are the major source of circulating sHjv and this tissue thereby appears to play an unexpected regulatory role in handling hemolysis. Our results are consistent with a novel function of muscle-derived sHjv to directly or indirectly activate hepcidin in the liver. Hjv mRNA is also expressed in the liver [2]; however, the expression of cHjv is weak [88] (Fig. 11b, 12c and d) and very likely restricted to periportal areas [87], while its target hepcidin is ubiquitous within hepatocytes [207]. Circulating sHjv would offer a regulatory signal for hepcidin in hepatocytes lacking cHjv.

Taken together, the function of physiologically produced sHjv in response to hemolysis may be to positively regulate an early transient increase in hepcidin

expression. However, positive regulation of hepcidin expression by sHjv may not only be restricted to hemolytic conditions, as observed in the mouse developmental study.

FIGURES

A



B

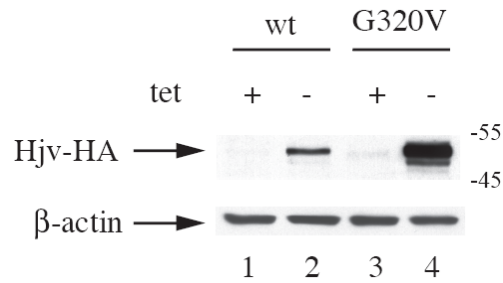
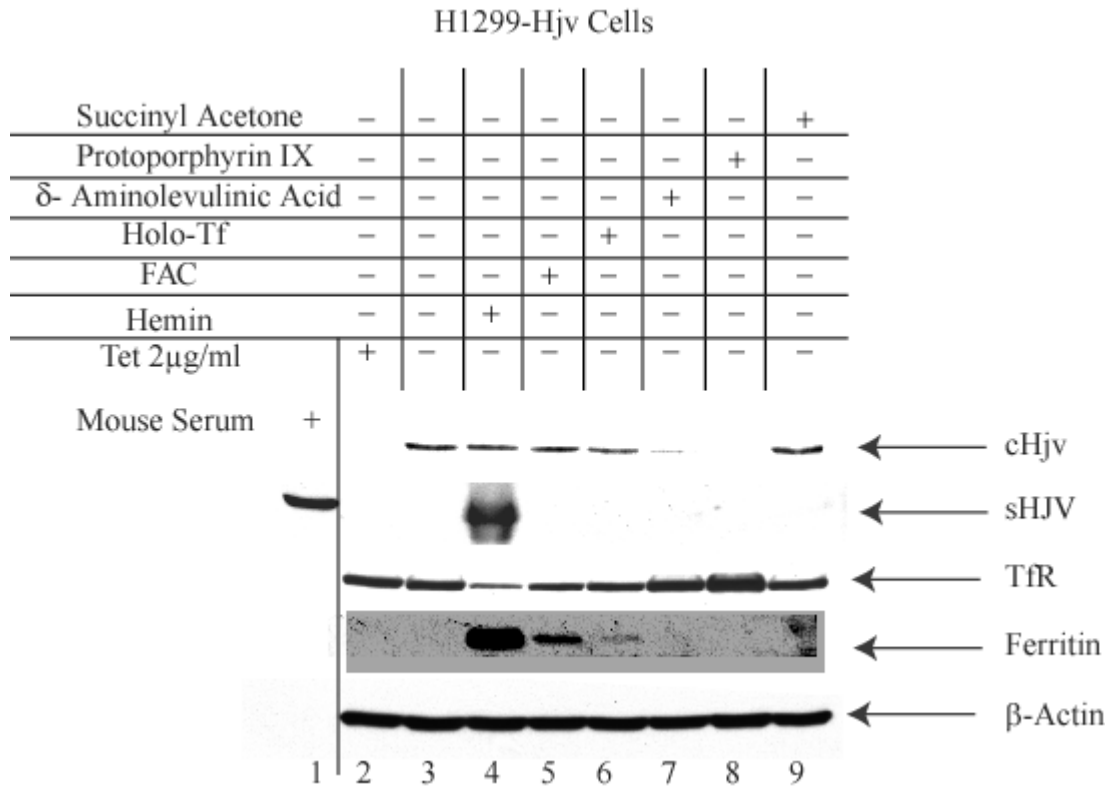


Figure 1

A



B

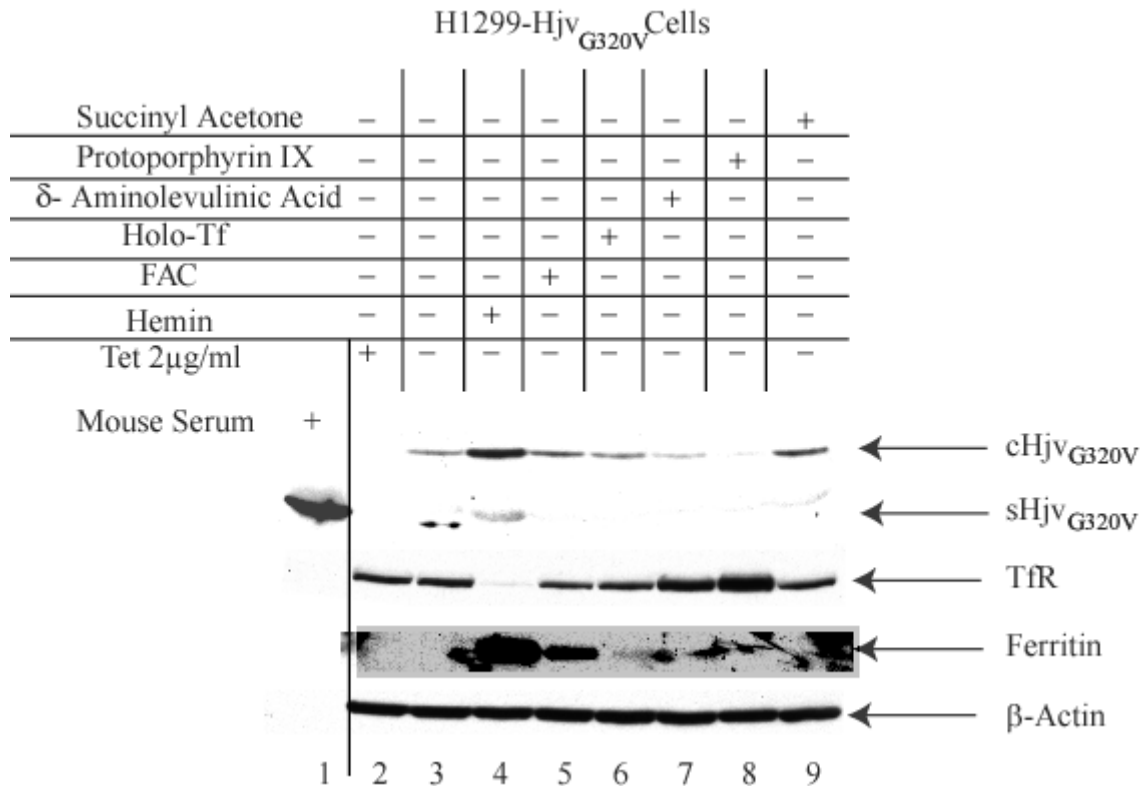
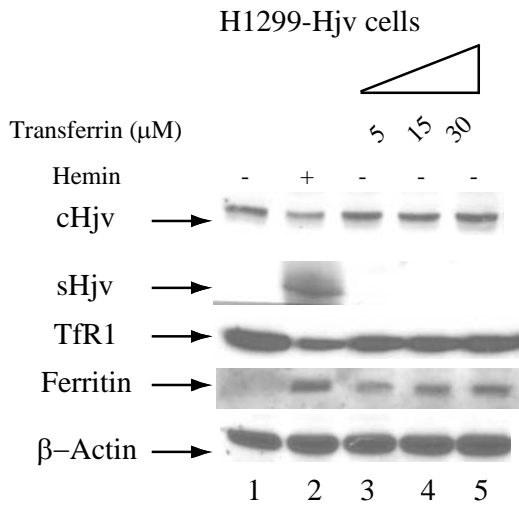
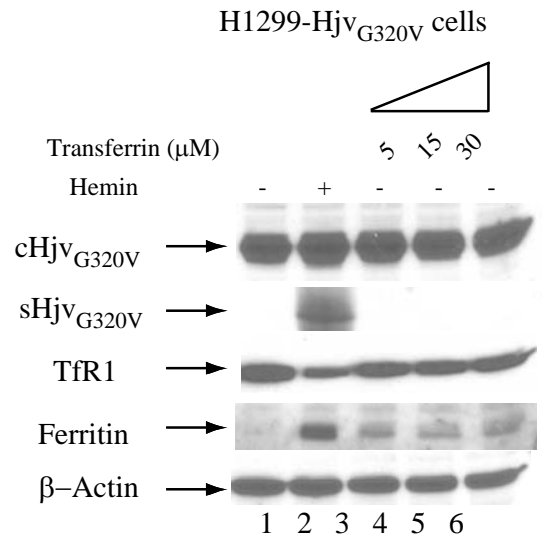


Figure 2

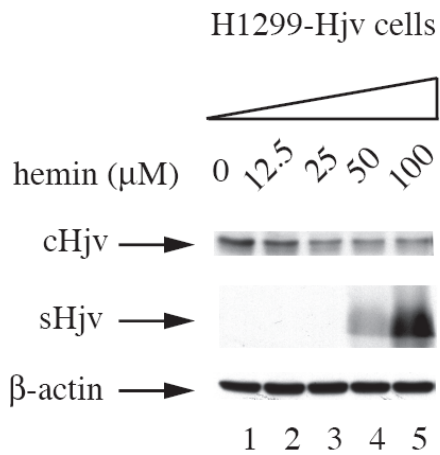
A



B



C



D

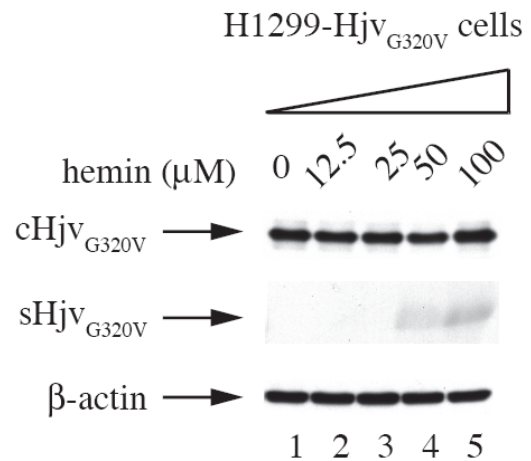
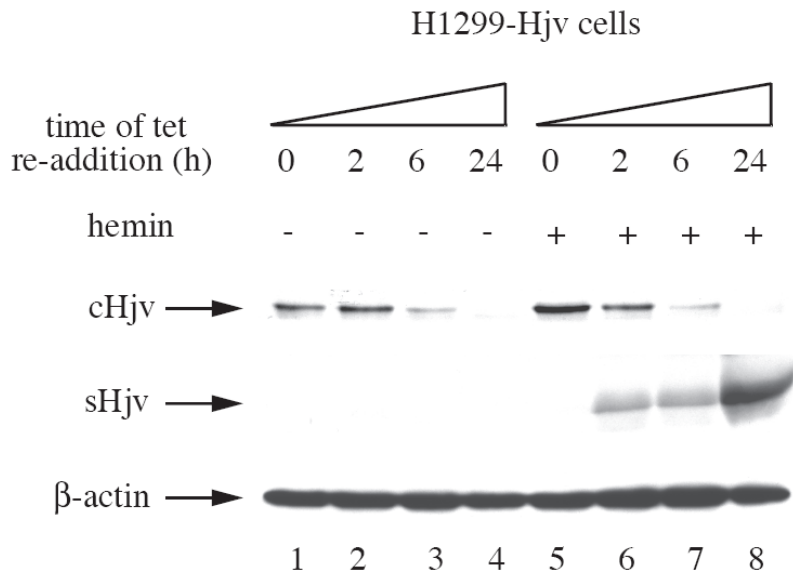
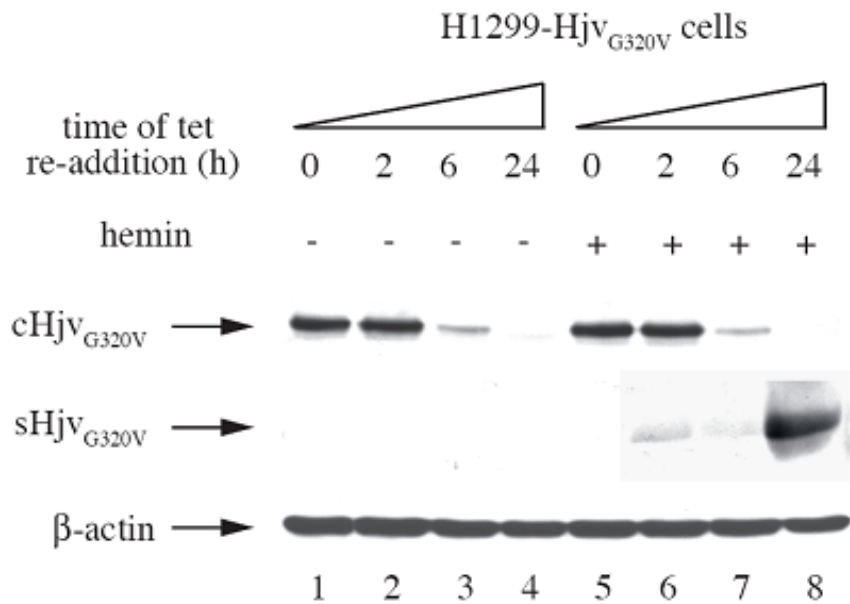


Figure 3

A**B****Figure 4**

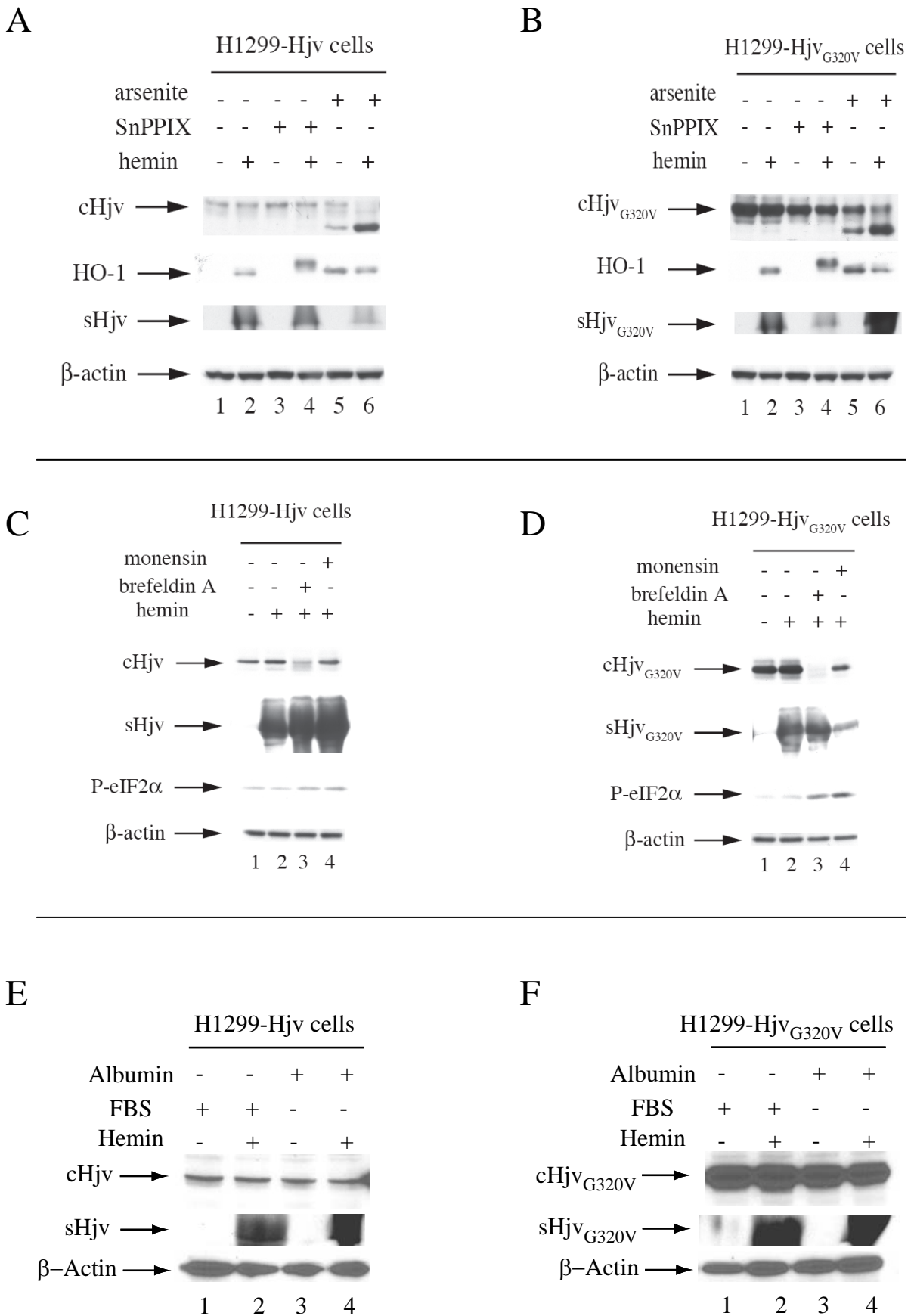
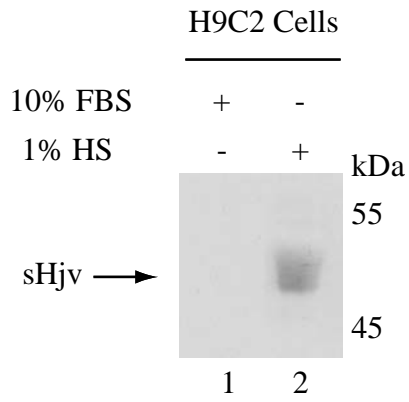


Figure 5

A



B

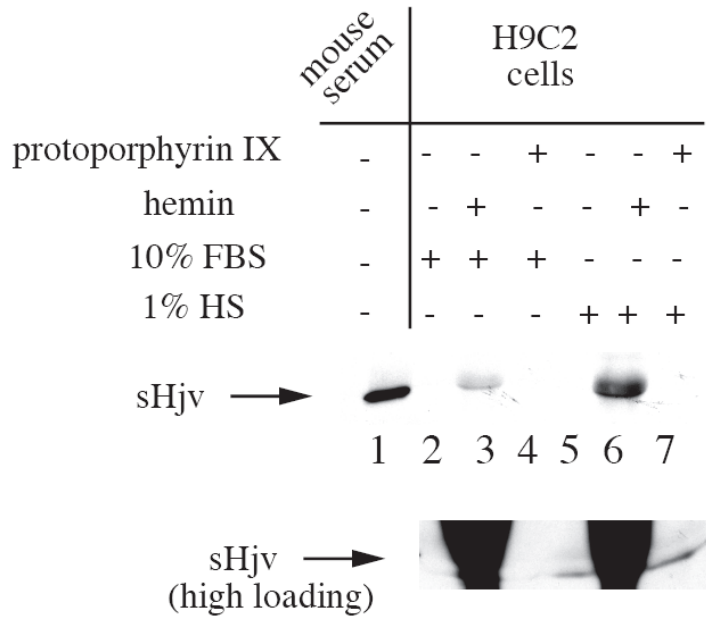


Figure 6

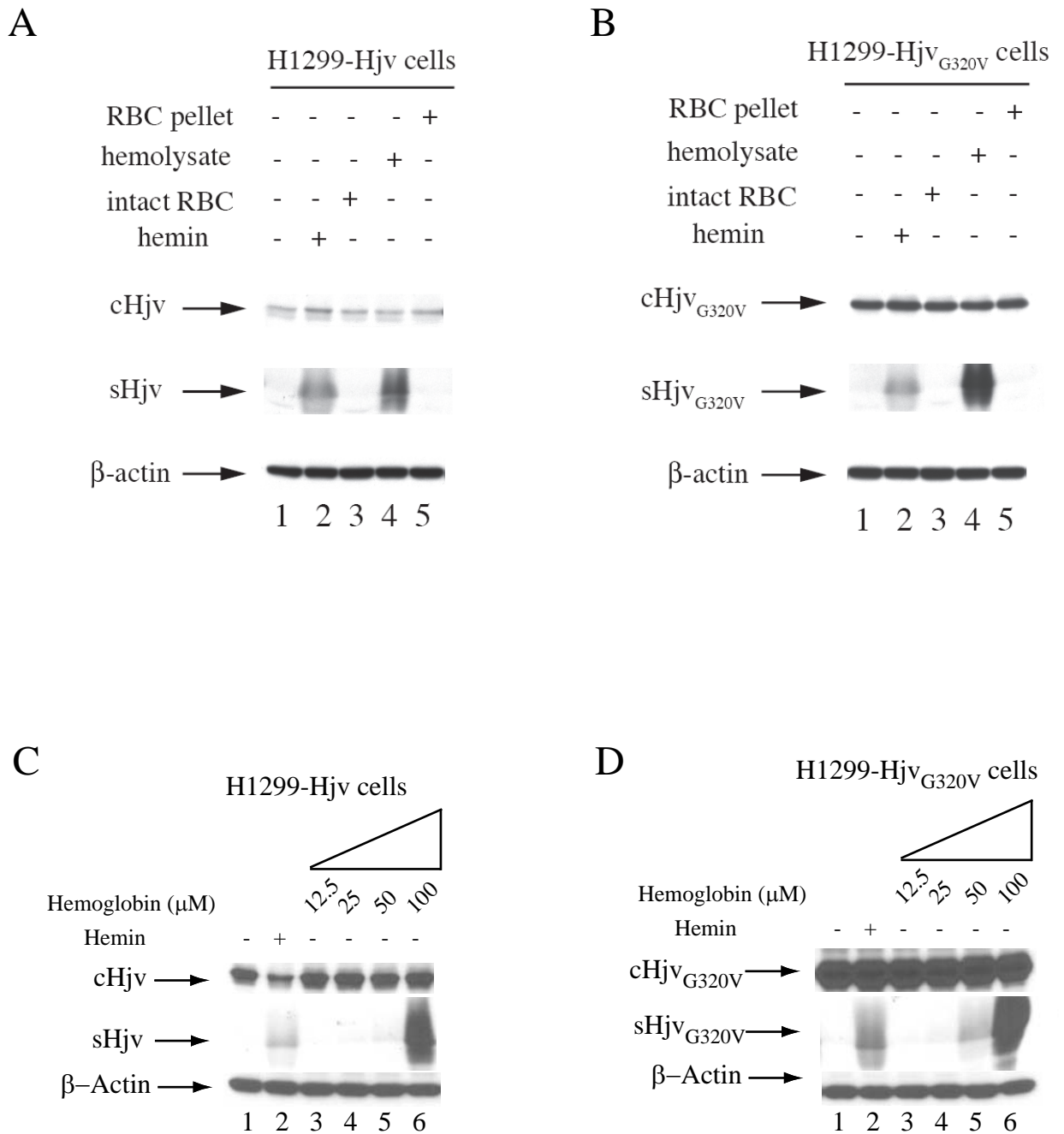


Figure 7

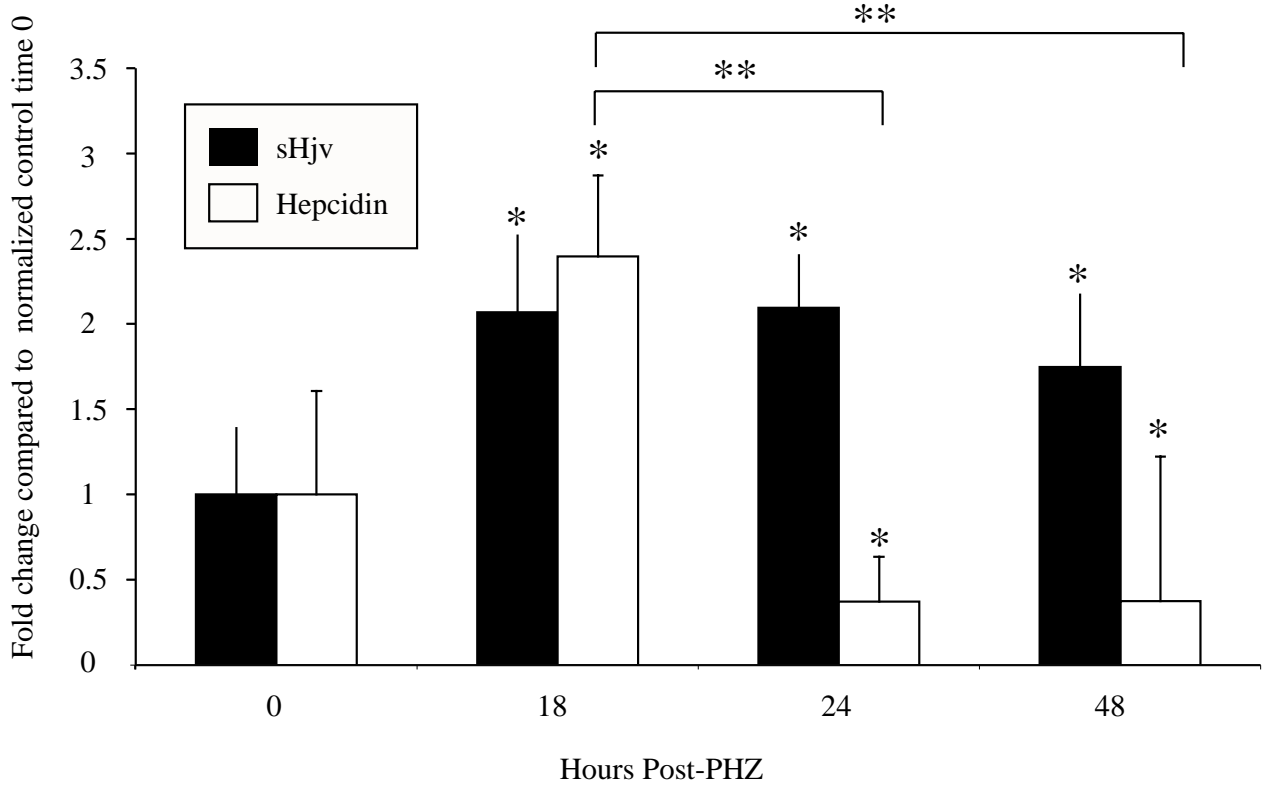
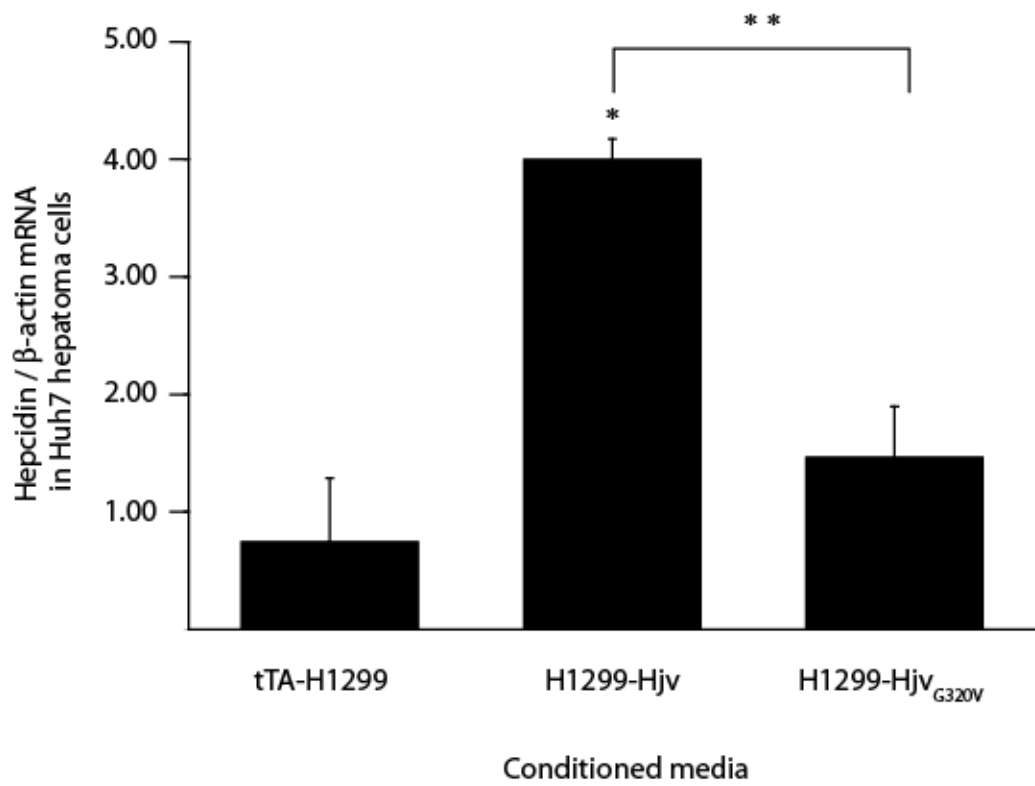


Figure 8

A



B

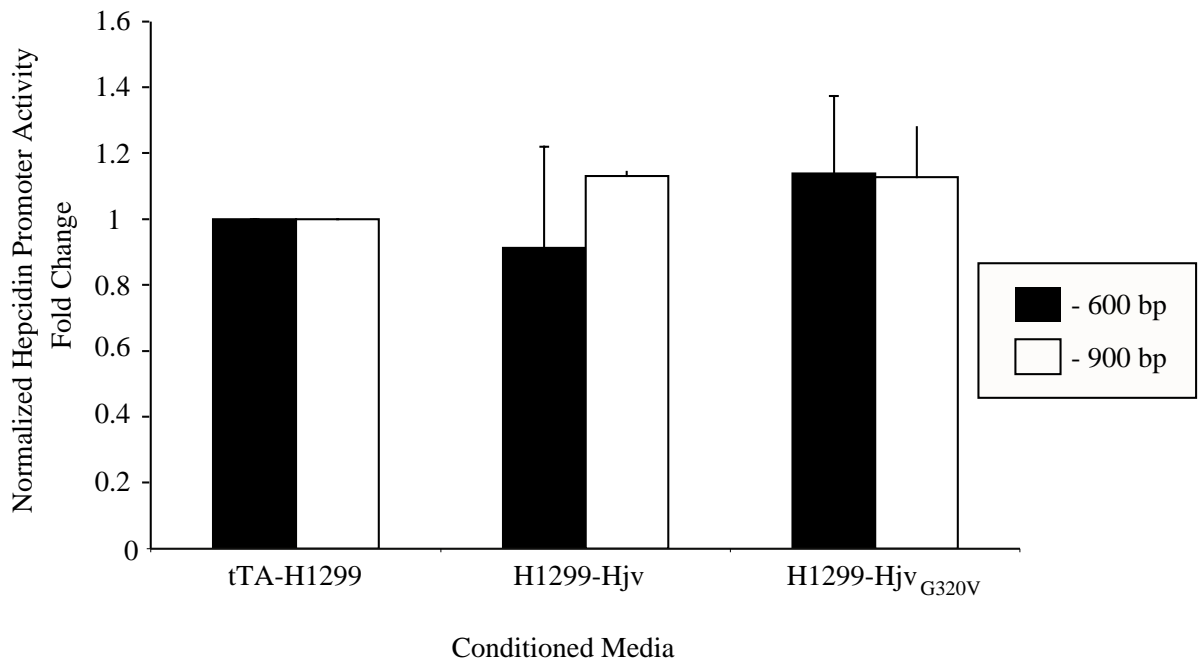
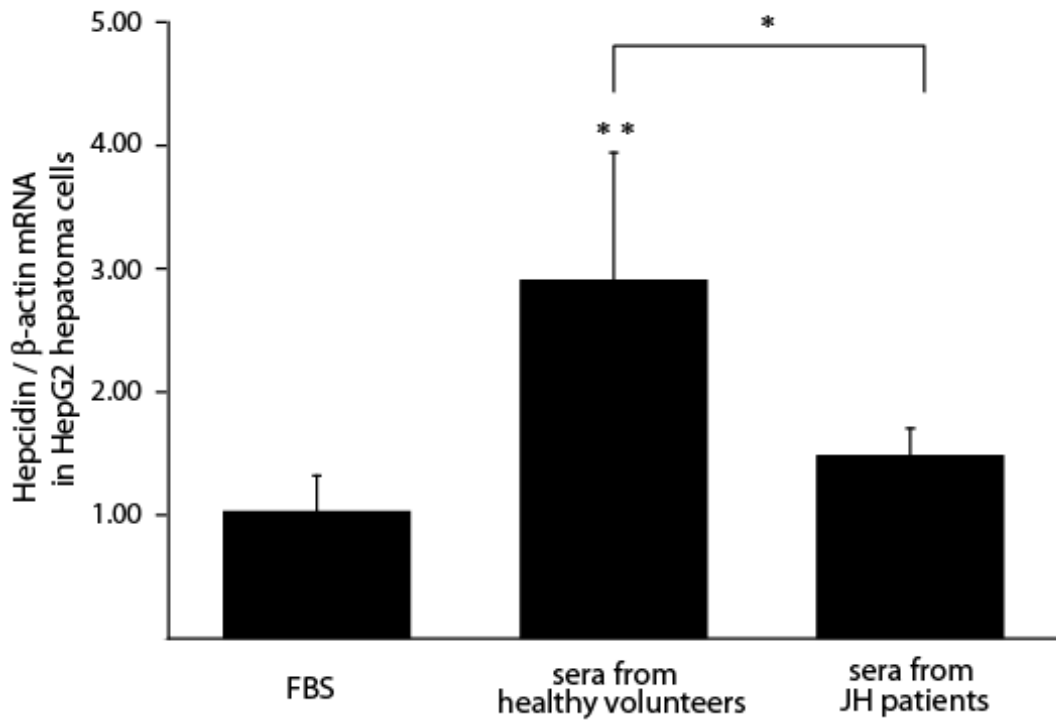


Figure 9

A

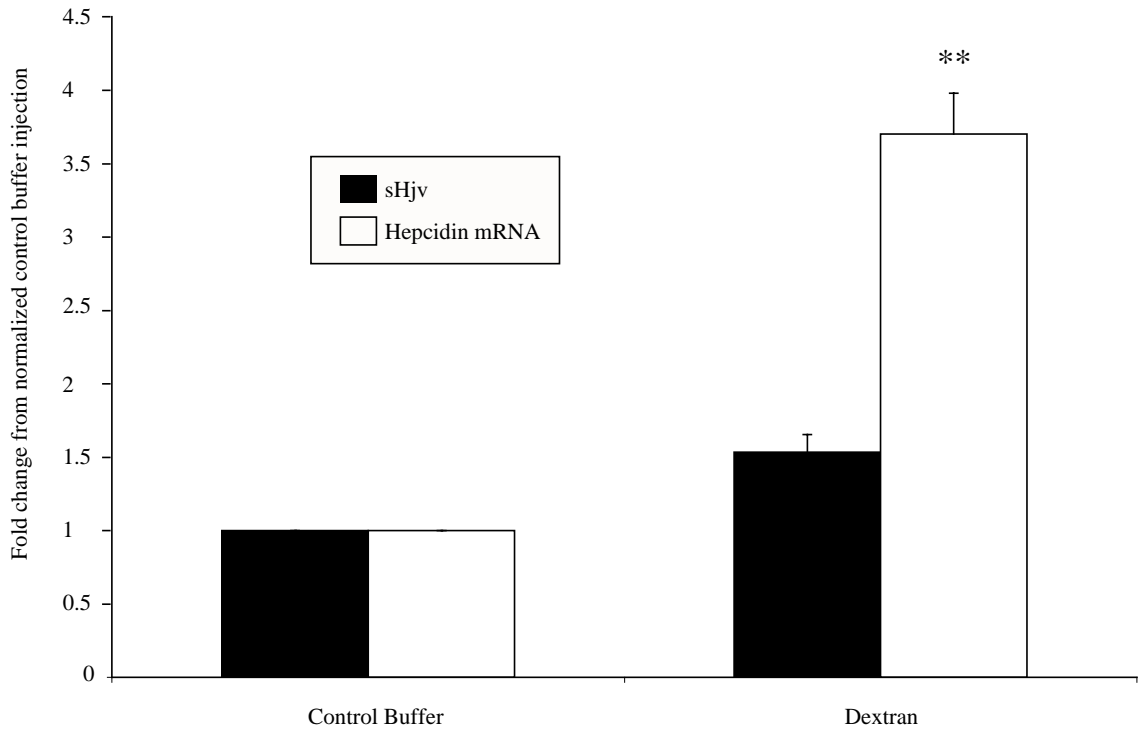


B



Figure 10

A



B

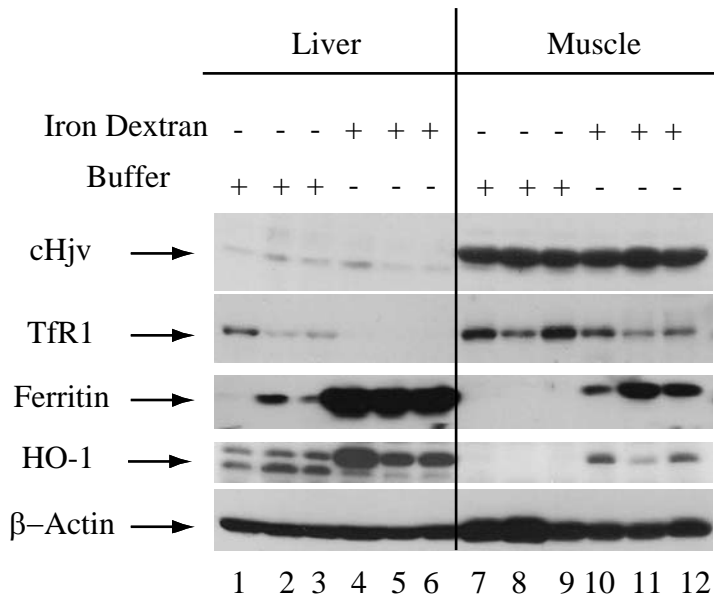
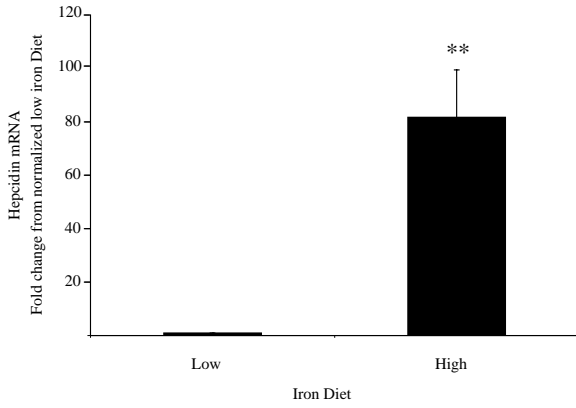
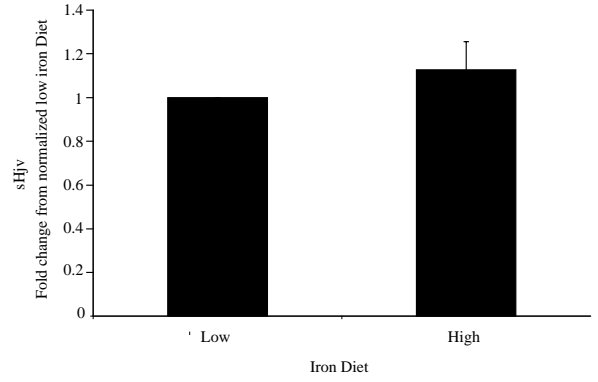


Figure 11

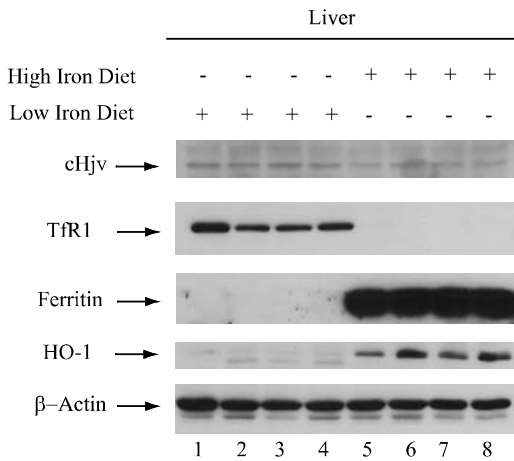
A



B



C



D

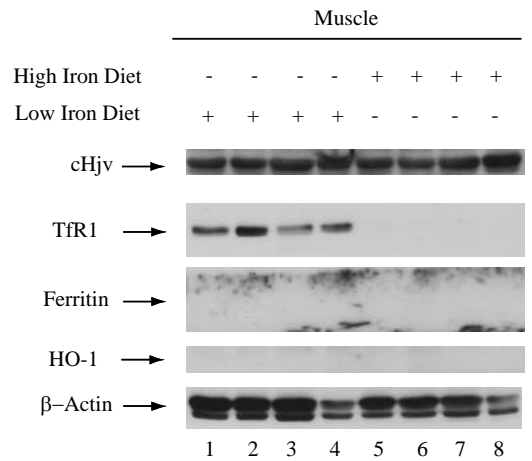


Figure 12

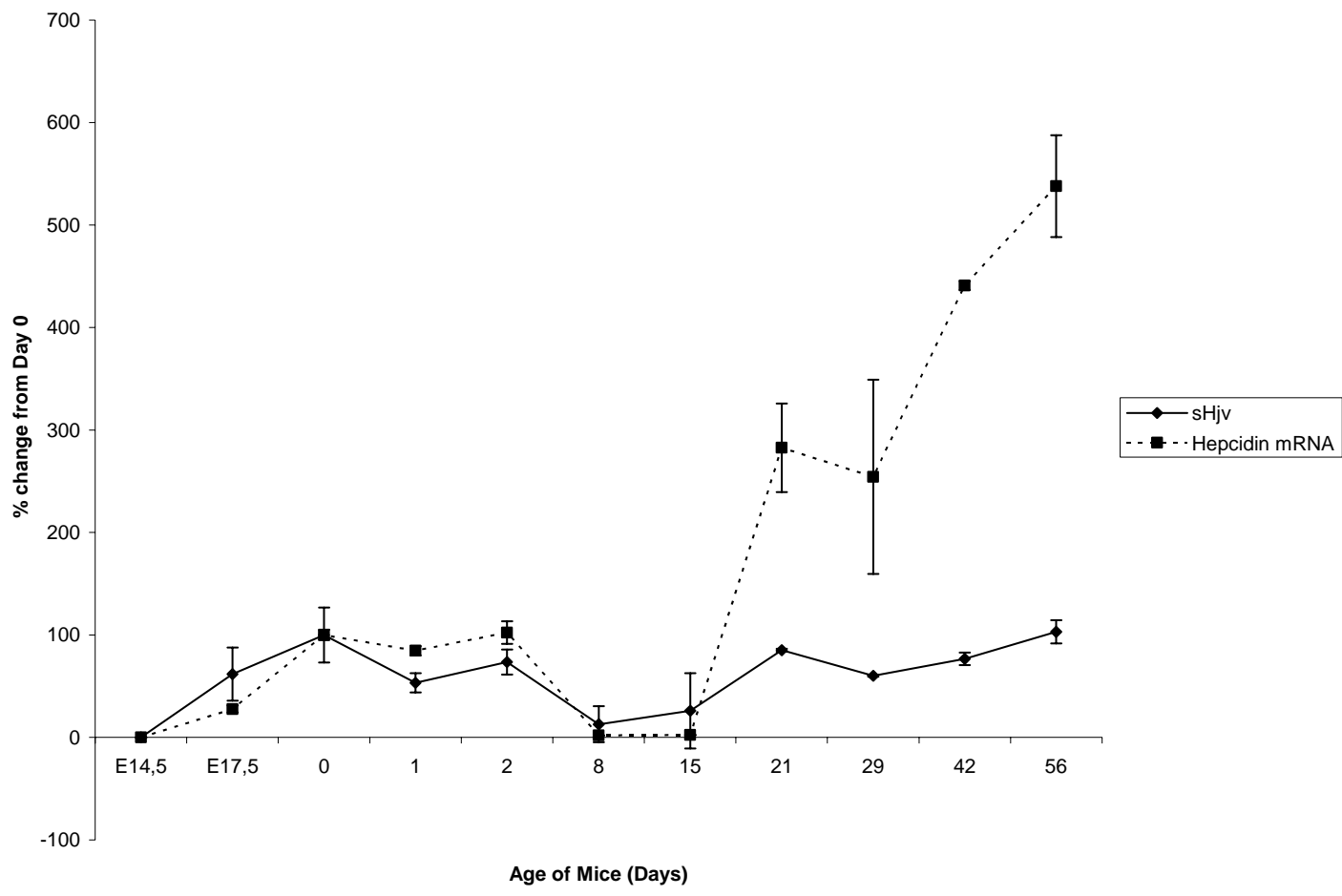
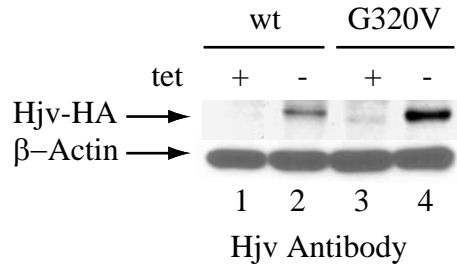
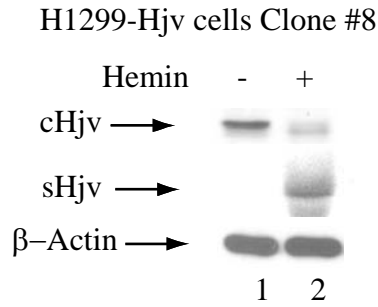


Figure 13

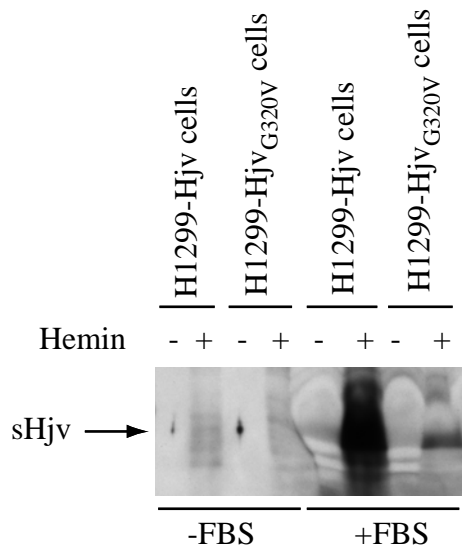
A



B



C



Hours Post Injection	% Hematocrit	Serum Iron (μM)	TIBC (μM)	% Tf Iron Saturation	Serum Ferritin ($\mu\text{g/L}$)
0	46.68 \pm 0.64	31 \pm 5.35	45.25 \pm 2.5	68.75 \pm 10.21	139.25 \pm 14.73
18	38.69 \pm 2.13**	46.75 \pm 6.95	55 \pm 5.72	85.25 \pm 12.42	229.25 \pm 27.66**
24	37.57 \pm 2.08**	21.75 \pm 2.5*	51.75 \pm 3.59*	42.25 \pm 5.74*	321.5 \pm 40.55**
48	35.31 \pm 1.86***	19.75 \pm 6.85	56.5 \pm 9	34.75 \pm 9.91*	316.5 \pm 77*

Table 1

	Serum Iron (μM)	TIBC (μM)	% Tf Iron Saturation	Serum Ferritin ($\mu\text{g/L}$)
Control Buffer	32.33 ± 7.5	52.33 ± 13.42	63.3 ± 14	287.6 ± 211
Iron Dextran	$52 \pm 6.55^*$	53 ± 6.56	98 ± 0	$5867 \pm 0^{***}$

Table 2

	Serum Iron (μM)	TIBC (μM)	% Tf Iron Saturation	Serum Ferritin ($\mu\text{g/L}$)
Low Iron Diet	15.5 ± 6.71	62 ± 8.88	26.3 ± 13	133 ± 30.2
High Iron Diet	$46.33 \pm 3.2^{***}$	$48.33 \pm 3.2^*$	$95.6 \pm 4^{***}$	$5867 \pm 0^{***}$

Table 3

FIGURE LEGENDS

Fig. 1. Tetracycline-inducible expression of HJv in H1299 cells displays different isoforms of WT and mutant sHjv.

Human tTA-H1299 cells were transiently transfected with cDNAs encoding HA epitope-tagged WT HJv, or the disease-associated HJv_{G320V} mutant (A). Stable H1299-HJv and H1299-HJv_{G320V} clones were isolated and utilized in subsequent experiments (B). The cells were grown for 48 h in the absence or presence of 2 µg/ml tetracycline (tet). The expression of WT and mutant HJv were analyzed by Western blotting with an antibody against the HA epitope tag. The membranes were also probed with a β-actin antibody (bottom panels).

Fig. 2. Hemin promotes release of sHJV whereas other sources of iron and heme precursors had no effect on release.

H1299-HJv (A) and H1299-HJv_{G320V} (B) cells were grown in the absence of tetracycline for 48 hours and then treated with 2 mM succinyl acetone, 100 µM protoporphyrin IX, 2 mM δ-aminolevulinic acid, 5 µM holo-transferrin (holo-Tf), 50 µg/ml ferric ammonium citrate (FAC) or 100 µM hemin for 12 hours. Cell lysates were analyzed by Western blotting for the expression of cHjv (top panels), TfR1 (third panels), ferritin (fourth panels) and β-actin (bottom panels). sHjv (second panels) was detected in concentrated culture media. 1 µl of serum obtained from C57B6 mice was loaded on lane 1 as a positive control for sHjv. The apparent increase of HJv_{G320V} in lane 4 was not consistent in multiple experiments and denotes experimental variability.

Fig. 3. Dose curves for holo-Tf and hemin treatment of H1299-HJv and H1299-HJv_{G320V} cells.

H1299-Hjv (A and C) and H1299-Hjv_{G320V} (B and D) cells, grown in the absence of tetracycline for 48 h, were treated with the indicated concentrations of holo-Tf (A and B) and hemin (C and D) for 12 h. The expression of cHjv (top panels) and β -actin (bottom panels) and the release of sHjv (middle panels) were analyzed by Western blotting.

Fig. 4. Kinetics of hemin mediated release of WT and mutant sHjv.

H1299-Hjv (A) and H1299-Hjv_{G320V} (B) cells were grown in the absence of tetracycline for 48 h. Tetracycline (2 μ g/ml) was added back to H1299-Hjv and H1299-Hjv_{G320V} cells and incubation in the absence or presence of 100 μ M hemin was continued for the indicated time intervals. The expression of cHjv (top panels) and β -actin (bottom panels) and the release of sHjv (middle panels) were analyzed by Western blotting.

Fig. 5. Mechanism of Hemin-induced sHjv release is independent of HO-1 activity, the secretory pathway and fetal bovine serum.

(A and B) H1299-Hjv (A) and H1299-Hjv_{G320V} (B) cells, grown in the absence tetracycline for 48 h, were either left untreated, or treated for 12 h with 100 μ M hemin in the absence or presence of 200 μ M tin protoporphyrin IX (SnPPIX) or 20 μ M arsenite. The expression of Hjv (top panels), HO-1 (second panels) and β -actin (bottom panels) and the release of sHjv (middle panels) were analyzed by Western blotting. (C and D) Likewise, H1299-Hjv (C) and H1299-Hjv_{G320V} (D) cells were either left untreated, or treated for 12 h with 100 μ M hemin in the absence or presence of 10 μ M monensin or brefeldin A. The expression of cHjv (top panels), phosphorylated (at Ser-51) eIF2 α (third panels) and β -actin (bottom panels) and the release of sHjv (second panels) were

analyzed by Western blotting. (E and F) H1299-Hjv (E) and H1299-Hjv_{G320V} (F) cells were grown either in the presence of fetal bovine serum (FBS) or albumin and treated with or without 100 μ M hemin for 12 h. The expression of cHjv (top panels), and β -actin (bottom panels) and the release of sHjv (middle panels) were analyzed by Western blotting.

Fig. 6. Hemin promotes the release of endogenous sHjv from H9C2 myocytes.

The cells were grown in the presence of either 10% fetal bovine serum (FBS) or 1% horse serum (HS) for 72 hours. Subsequently, the cells were either left untreated or treated with 100 μ M hemin or protoporphyrin IX for 12 hours. The release of sHjv was analyzed by Western blotting. Mouse serum (1 μ l) was loaded on lanes 1 as a positive control for sHjv. In (B), the lower panel depicts higher loading of the samples.

Fig. 7. Human hemolysate and hemoglobin promote the release of sHjv.

H1299-Hjv (A) and H1299-Hjv_{G320V} (B) cells, grown in the absence of tetracycline for 48 h, were either left untreated, or treated for 6 h with 100 μ M hemin, intact red blood cells (RBC), the pellet fraction or the supernatant of a human hemolysate. H1299-Hjv (C) and H1299-Hjv_{G320V} (D) cells were also treated with the indicated concentrations of hemoglobin. The expression of Hjv (top panels) and β -actin (bottom panels) and the release of sHjv (second panels) were analyzed by Western blotting.

Fig. 8. Increase in liver hepcidin and serum sHjv in response to mice treated with phenylhydrazine (PHZ).

Mice received a single intraperitoneal injection with 50 mg/kg PHZ. (A) Quantification of serum sHjv and hepcidin/ β -actin mRNA levels from western and northern blots respectively, were compared to a normalized time 0. 4 mice were sacrificed and analyzed for each time point and treatment. * $p < 0.05$ and ** $p < 0.01$ (Student's t test).

Fig. 9. WT sHjv released from H1299-Hjv cells activates hepcidin expression in target Huh7 hepatoma cells independent of -600 and -900 bp hepcidin promoters.

(A and B) Parent tTA-H1299, H1299-Hjv and H1299-HjvG320V cells were treated for 15 h with 100 μ M hemin. Subsequently, the conditioned media were collected and applied to Huh7 hepatoma cells for 6 h. (A) The expression of hepcidin mRNA was quantified by using real time RT-PCR with the $\Delta\Delta$ Ct quantification method; values were normalized to those of β -actin. All treatments were performed in triplicate; * $p < 0.05$ and ** $p < 0.01$ (Student's t test). (B) -600 and -900 bp hepcidin promoters were cotransfected with a Renilla luciferase control vector, pRL-CMV, into Huh7 cells. Upon treatment with conditioned media, cell lysates were analysed by dual luciferase assays.

Fig. 10. Sera from healthy volunteers but not JH patients induce hepcidin expression in HepG2 hepatoma cells.

(A) HepG2 cells were cultured in media containing either 10% FBS, or a mixture of sera from either healthy volunteers or JH patients. The expression of hepcidin mRNA was quantified by using real time RT-PCR with the $\Delta\Delta$ Ct quantification method; values were normalized to those of β -actin. All treatments were performed in triplicates; * $p < 0.05$ and ** $p < 0.01$ (Student's t test). (B) FBS (lane 1), serum from a healthy volunteer

(lane 2) and serum from a JH patient with a HJV G320V mutation (lane 3) were analyzed for sHJV expression by Western blotting.

Fig. 11. Mice treated with iron dextran exhibit an increase in liver hepcidin independent of a sHJV response.

(A and B) Mice received a single subcutaneous injection of iron-dextran at a dose of 1 g of iron/kg of body weight. 7 days post-injection, 6 mice in total (3 for each injection) were sacrificed and subsequently analyzed. (A) Quantification of serum sHJV and hepcidin/ β -actin mRNA levels from western and northern blots respectively, were compared to a normalized control buffer injection. (B) In addition, protein extracts from liver and muscle tissues were analyzed for the expression of cHJV (top panels), TfR1 (second panels), ferritin (third panels), HO-1 (fourth panels) and β -actin (bottom panels) by Western blotting. ** $p < 0.01$ (Student's t test).

Fig. 12. Mice fed a high iron diet display robust hepcidin induction independent of a sHJV response.

(A-D) Mice were fed either a low or high iron diet for a period of 1 month. 4 mice per each diet were subsequently sacrificed and analyzed. Quantification of serum sHJV (A) and hepcidin/ β -actin mRNA (B) levels from western and northern blots respectively, were compared to the normalized low iron diet. (C and D) Furthermore, protein extracts from liver (C) and muscle (D) tissues were analyzed for the expression of cHJV (top panels), TfR1 (second panels), ferritin (third panels), HO-1 (fourth panels) and β -actin (bottom panels) were analyzed by Western blotting. ** $p < 0.01$ (Student's t test).

Fig. 13. Levels of sHjv positively correlate with liver hepcidin expression during the course of a mouse's development.

At each time point of the mouse's development, 3 mice were sacrificed and analyzed. Quantification of serum sHjv (A) and hepcidin/ β -actin mRNA (B) levels from western and northern blots respectively, were compared to the normalized age 0 of the mice. A comparison between the levels of sHjv and hepatic hepcidin mRNA at different stages of their development revealed a Pearson's Correlation Coefficient 0.7.

Supplementary Fig. 1.

(A) Hjv antisera detected 1 major ~52 kDa, similar to that detected with a polyclonal HA antibody in Fig. 1A and 1B.

Stable H1299-Hjv and H1299-Hjv_{G320V} clones were grown for 48 h in the absence or presence of 2 μ g/ml tetracycline (tet). The expression of WT and mutant Hjv were analyzed by Western blotting with an antibody against the Hjv antisera (top panels). The membranes were also probed with a β -actin antibody (bottom panels).

(B) Hemin promotes the release of sHjv from a second H1299-Hjv (clone #8).

H1299-Hjv cells were grown in the absence of tetracycline for 48 hours and then treated with 100 μ M hemin for 12 hours. Cell lysates were analyzed by Western blotting for the expression of cHjv (top panels), β -actin (bottom panels). sHjv (second panels) was detected in concentrated culture media.

(C) Hemin induced release of soluble Hjv is blunted in FBS-free media.

H1299-Hjv and H1299-Hjv_{G320V} cells, grown in the absence tetracycline for 48 h, were either left untreated, or treated for 12 h with 100 μ M hemin in the absence or presence of (FBS) for 12 h. The release of sHjv was analyzed by Western blotting.

Table 1: % Hematocrit and serum iron parameters in mice untreated and PHZ injected mice at different time points.

% Hematocrit, serum iron, TIBC, Tf iron saturation and serum ferritin was measured in control mice and mice sacrificed 18, 24 and 48 hours post-PHZ injection. There are 4 mice for each time point and the results are presented as a mean \pm standard deviation. Statistical p values compared time 0 preinjection with time points 18, 24 and 48 hours.

* $p < 0.05$, ** $p < 0.01$ and *** $p < 0.001$ (Student's t test).

Table 2: Serum iron parameters in control and iron dextran injected mice.

Serum iron, TIBC, Tf iron saturation and serum ferritin was measured in mice injected with either a control buffer or iron dextran. There are mice for each time point and the results are presented as a mean \pm standard deviation.

* $p < 0.05$ and *** $p < 0.001$ (Student's t test).

Table 3: Serum iron parameters in mice fed either a low or high iron.

Serum iron, TIBC, Tf iron saturation and serum ferritin was measured in mice fed either a low or a high iron diet. There are 4 mice for each time point and the results are presented as a mean \pm standard deviation.

* $p < 0.05$ and *** $p < 0.001$ (Student's t test).

CHAPTER III. HEPCIDIN GENERATED BY HEPATOMA CELLS INHIBITS IRON
EXPORT FROM CO-CULTURED THP1 MONOCYTES

Bill Andriopoulos and Kostas Pantopoulos

PREFACE

In the previous chapter II, we provided evidence that sHjv is involved in the induction of hepcidin expression. In the following Chapter III we investigate the functional properties of hepcidin. More specifically, we establish a co-culture model consisting of hepcidin producing hepatomas and monocytes. Using this system, we monitor the functional effects of hepcidin on iron handling in the RES.

ABSTRACT

The antimicrobial peptide hepcidin is generated in the liver and released into the circulation in response to iron, oxygen and inflammatory signals. Hepcidin serves as a hormonal regulator of duodenal iron absorption and iron trafficking in the RES. The aim of this study is to explore the effects of this regulatory peptide in macrophage iron metabolism.

Hepcidin-mediated iron efflux and parameters of cellular iron homeostasis were studied in THP1 monocytic cells co-cultured with hepcidin-producing hepatic cells.

Stimulation of hepcidin expression in Huh7 cells with interleukin-6 promoted a significant ~30% decrease in ⁵⁹Fe efflux from THP1 cells, previously loaded with ⁵⁹Fe-transferrin. Similar results were obtained with HepG2 cells transfected with a hepcidin cDNA. Importantly, hepcidin expression from Huh7 cells elicited a decrease in the levels of the iron-sensitive post-transcriptional regulator IRP2 in THP1 cells, accompanied by de novo synthesis of the iron storage protein ferritin.

Physiologically generated hepcidin inhibits iron efflux and promotes iron accumulation in monocytic cells, mimicking a pathophysiological response commonly observed in the anemia of inflammation. Our results highlight the crucial role of hepcidin in the control of macrophage iron homeostasis.

INTRODUCTION

Hepcidin, a conserved cysteine-rich peptide of 20-25 amino acids, is produced in the liver and functions as the principal hormonal regulator of body iron homeostasis [208-210]. Hepcidin negatively regulates iron absorption in the duodenum and transport in reticuloendothelial cells by controlling the levels of the iron exporter ferroportin [6, 61]. The expression of hepcidin is turned off in response to low body iron stores, anemia or hypoxia [132]. On the other hand, hepcidin is induced by iron overload [63] or by inflammatory signals via interleukins IL-1 or IL-6 [62, 135]. Misregulation of hepcidin expression is associated with a broad spectrum of iron-related disorders.

Genetic mutations leading to complete silencing of hepcidin are etiologically linked to a rare form of juvenile hemochromatosis [66], an early onset disease of iron overload characterized by pathological iron absorption and deposition within parenchymal cells with a relative sparing of macrophages [211]. More common forms of hereditary hemochromatosis (caused by mutations in HFE, TfR2 or HJV) [211] correlate with various degrees of hepcidin deficiency [2, 195, 196, 212]. Likewise, hepcidin is suppressed in patients with thalassemia syndromes but increases in patients with “ferroportin disease” [213]. Similar phenotypes have been described in mouse models of hemochromatosis [58, 85-87, 214-216] and thalassemia [217]. Transgenic mice over-expressing hepcidin from a liver-specific promoter show profound defects in materno-foetal iron transport and display severe iron deficiency anemia [59].

Hepcidin levels are normally elevated following iron ingestion or infection [62]. The upregulation of hepcidin expression by inflammatory signals is tightly linked to the “ACD” (ACD) or “anemia of inflammation” (AI) [218, 219]. This condition is

characterized by hypoferremia due to iron retention within macrophages and decreased iron absorption. The withholding of iron may be protective against growing bacteria but eventually limits erythropoiesis. Even though the development of ACD depends on multiple factors [219], hepcidin is considered as the key mediator for the diversion of iron traffic by controlling the stability of ferroportin [6, 61], which is unique in its capacity to export iron from macrophages and intestinal cells [194].

The experimental evidence supporting this mechanism was based on the direct binding of human hepcidin to transfected mouse ferroportin-GFP in HEK293 and HeLa cells, promoting its internalization and lysosomal degradation [6, 61]. In a separate study, synthetic human hepcidin inhibited iron export and decreased the levels of transfected murine ferroportin in J774 macrophages [7]. These data are consistent with a function of hepcidin as a principal regulator of iron efflux from macrophages.

Considering that the effector (hepcidin) and the target (ferroportin) are expressed in different cell types, the above mechanism would require cell-to-cell communication between hepcidin-producing hepatocytes with macrophages. To further validate the molecular basis of hepcidin regulatory activity under physiologically relevant conditions, we establish here a co-culture model of Huh7 or HepG2 hepatoma and THP1 monocytic cells. We demonstrate that hepcidin generated by hepatoma cells is capable of regulating iron metabolism in neighboring monocytes.

MATERIALS AND METHODS

Materials.

Hemin, IL-6 and ceruloplasmin were purchased from Sigma (St. Louis, MI). Desferrioxamine (DFO) was from Novartis (Dorval, QC, Canada). High molecular weight desferrioxamine (HMW-DFO), a non-permeable hydroxyethyl starch conjugate [220], was obtained from Biomedical Frontiers (Minneapolis, MN).

Cell culture.

Human Huh7 and HepG2 hepatoma cells and H1299 lung cancer cells were grown in Dulbecco's modified Eagle's medium supplemented with 10% heat-inactivated fetal bovine serum, 100 units/ml penicillin, and 100 µg/ml streptomycin. Media for Huh7 and HepG2 cells also contained 1% non-essential amino acids. Human THP1 monocytic cells were cultured in supplemented RPMI.

Co-culture experiments.

2×10^6 THP1 suspension cells were inserted into a co-culture cartridge (BD Falcon), which was placed on top of 6-well dishes containing monolayers of 0.2×10^6 Huh7, HepG2 or H1299 cells. Co-culture experiments were performed in serum-free RPMI to avoid possible interference of serum transferrin on iron uptake and release.

Generation of HepG2 hepcidin transfectants.

Human hepcidin cDNA (kindly provided by Dr. M. Muckenthaler, University of Heidelberg, Germany) was digested out of the parent pDNR-LIB vector with EcoR1 and

Xho1 and ligated into pcDNA3. The construct was transfected into HepG2 cells by Lipofectamine Plus (Invitrogen) and stable clones were selected and maintained in the presence of 500 µg/ml G418 (Invitrogen).

Iron release assays.

⁵⁹Fe-labelled transferrin (Tf) was prepared as previously described [158]. THP1 suspension cells were loaded overnight with 5 µM ⁵⁹Fe-Tf in serum-free RPMI. Subsequently, the cells were harvested by centrifugation at 4°C and washed 4x with ice-cold RPMI to remove traces of soluble ⁵⁹Fe-Tf. Under these conditions, less than ~0.1% of radioactivity could be extracted after the second wash, indicating complete removal of non-internalized transferrin. Aliquots of 2x10⁶ cells were resuspended in pre-warmed serum-free RPMI containing 100 µM HMW-DFO and immediately placed into a CO₂ incubator at 37°C either alone, or in co-culture with other cells. Radioactivity in the supernatant, corresponding to ⁵⁹Fe release, and in THP1 cells was monitored at specified time intervals on a γ-counter. To calculate the percentage of ⁵⁹Fe release, the amount of soluble radioactivity was divided by the total amount of radioactivity in media and THP1 cells.

Western blotting.

Cells were lysed in cytoplasmic lysis buffer (1% Triton X-100, 300 mM NaCl and 50 mM Tris/HCl; pH 7.4). Cell debris was cleared by centrifugation and protein concentration was measured with the Bradford reagent (BioRad). Cell lysates (15 µg) were resolved by SDS/PAGE and proteins transferred onto nitrocellulose filters. The

blots were saturated with 10% non-fat milk in Tris-buffered saline (TBS) and probed overnight at 4°C with 1:500 diluted ferritin (DakoCytomation Inc.) or IRP2 [221] antibodies. After 3x washes with TBS containing 0.1% (v/v) Tween 20, the blots were further incubated for 2 h at room temperature with 1:5000 diluted goat anti-rabbit IgG (Sigma). Detection of the peroxidase-coupled secondary antibodies was performed with the ECL[®] method (Amersham). The blots were quantified by densitometry.

Metabolic labeling with ³⁵S-methionine/cysteine and immunoprecipitation of ferritin.

THP1 cells were metabolically labeled during co-culture with (50 µCi/ml) *trans*-[³⁵S]label, a mixture of 70:30 ³⁵S-methionine/cysteine (ICN). Cytoplasmic lysates (160 µg) were subjected to quantitative immunoprecipitation with 5 µl ferritin antibody (Roche). Immunoprecipitated proteins were analysed by SDS/PAGE and visualized by autoradiography. Radioactive bands were quantified by phosphorimaging.

Northern Blotting.

Cells were lysed with the Trizol reagent (Invitrogen) and RNA was prepared according to the manufacturer's recommendations. Total cellular RNA (10 µg) was electrophoretically resolved on a denaturing agarose gel, transferred onto nylon membranes, and hybridized to ³²P-labeled human hepcidin or β-actin cDNA probes. Autoradiograms were quantified by phosphorimaging.

Statistical Analysis.

Data are shown as means \pm SD. Statistical analysis was performed by one-way ANOVA test with the Prism GraphPad Software (version 4.0c).

RESULTS

⁵⁹Fe uptake and release from THP1 monocytic cells.

Human THP1 monocytic cells were utilized as a model to study the effects of hepcidin on the regulation of macrophage iron metabolism. We first established conditions for iron release assays. The cells were loaded overnight with ⁵⁹Fe-Tf and the efflux of ⁵⁹Fe in serum-free media was measured on a γ -counter. In preliminary experiments we noticed that ~20% of released radioactivity could not be recovered and remained attached to the plastic dish. Complete solubilization of released ⁵⁹Fe was accomplished by employing HMW-DFO as an iron acceptor. The addition of bovine ceruloplasmin at concentrations of 0.2 or 0.6 μ g/ml did not appreciably alter the amount of soluble radioactivity (data not shown). A typical time course experiment under optimized conditions is shown in Fig. 1. The efflux of ⁵⁹Fe was fast and reached a plateau within 45-60 min, possibly due to the absence of other iron sources in the serum-free media. The plateau was maintained for up to 5 h. The fraction of released radioactivity corresponded to ~16% of the amount of internalized ⁵⁹Fe. Thus, under these experimental conditions, iron efflux from THP1 cells only occurs for 45-60 min following termination of external iron supply.

Generation of hepcidin by Huh7 or HepG2 hepatoma cells inhibits ⁵⁹Fe release from co-cultured THP1 monocytes.

Because hepcidin is exclusively produced by hepatocytes [208-210], we utilized Huh7 hepatoma cells as physiological source of the peptide. As expected [116], a treatment with 20 ng/ml IL-6 for 2 h dramatically induced hepcidin mRNA expression in

Huh7 cells, but not in control H1299 lung cancer cells (Fig. 2A). In a time course experiment, hepcidin mRNA levels peaked within 1-2 h and remained elevated after 6 h of IL-6 treatment, while under these conditions the expression of control β -actin mRNA did not change (Fig. 2B). We next examined how physiologically generated hepcidin controls macrophage iron efflux. Huh7 cells, previously treated with IL-6, or not, or H1299 cells, were co-cultured with [^{59}Fe -Tf]-loaded THP1 monocytes. When co-cultured with [IL-6]-treated Huh7 cells, THP1 monocytes released ~30% less ^{59}Fe as compared to control (Fig. 2C). The effect was statistically significant ($p < 0.05$) and suggests that hepcidin generated by Huh7 cells in response to IL-6 inhibits iron efflux from THP1 monocytes. In co-cultures with untreated Huh7 cells, which express low levels of hepcidin mRNA (Fig. 2A), a ~15% decrease in ^{59}Fe release from THP1 monocytes was observed. Trypan blue exclusion assays showed that under all experimental conditions cell viability was not affected, confirming that the release of ^{59}Fe was not due to cell decay.

It could be argued that the above described inhibition in ^{59}Fe release may not be directly mediated by hepcidin but rather depend on other, possibly pleiotropic effects of IL-6. To achieve high levels of hepcidin expression in the absence of IL-6 stimulation, a hepcidin cDNA was transfected into HepG2 hepatoma cells and stable clones were selected. Northern blot analysis shows that hepcidin mRNA expression is dramatically upregulated in HepG2 clone #6 (Fig. 3A). The effects of hepcidin on iron release were evaluated in co-culture assays of HepG2 #6, parent HepG2, or control H1299 cells with [^{59}Fe -Tf]-loaded THP1 monocytes. In the presence of HepG2 #6, the release of ^{59}Fe from THP1 monocytes was statistically significantly ($p < 0.05$) decreased by ~35% as compared

to control (Fig. 3B), in agreement with the data obtained with [IL-6]-stimulated Huh7 cells. Likewise, in co-culture with parent HepG2 cells, a smaller (~14%) decrease in ⁵⁹Fe release was apparent, as with untreated Huh7 cells. Taken together, the results in Figs. 2 and 3 suggest that physiologically produced hepcidin inhibits iron efflux from target monocytes.

Hepcidin generated by Huh7 cells elicits responses to iron loading in co-cultured THP1 monocytes.

The hepcidin-mediated inhibition of ⁵⁹Fe release from THP1 cells implies that physiologically generated hepcidin may have the capacity to alter their overall iron status. To examine this, THP1 cells were co-cultured with Huh7 hepatoma or control H1299 cells and the expression of the cytoplasmic post-transcriptional regulator IRP2, which is sensitive to proteasomal degradation in response to iron loading [40], was analyzed by Western blotting. The co-culture with [IL-6]-stimulated Huh7 cells promoted a profound (~66%) decrease in the steady-state levels of IRP2 in THP1 cells (Fig. 4). The decrease was more modest (~13%) in the absence of IL-6 treatment (lane 2). Consistently with the data in Fig. 2, a treatment of control H1299 cells with IL-6 did not affect IRP2 levels in co-cultured THP1 cells (supplemental Fig. 1A). These findings support the idea that hepcidin-mediated inhibition of iron efflux results in accumulation of intracellular iron within THP1 cells, which is sensed by IRP2 and promotes its degradation.

The reduction of IRP2 levels is expected to de-repress ferritin mRNA translation; this in turn leads to storage and detoxification of excess iron [40, 209]. An immunoprecipitation assay with ferritin antibodies following metabolic labeling of the

co-cultured cells with ³⁵S-methionine/cysteine revealed that [IL-6]-stimulated Huh7 cells triggered a 2.1-fold increase in de novo ferritin synthesis in THP1 cells (Fig. 5, lanes 1-3). As expected, a treatment with hemin fully de-repressed ferritin synthesis by 5.3-fold (lane 4), while a co-culture with [IL-6]-stimulated control H1299 cells did not affect ferritin mRNA translation in THP1 cells (supplemental Fig. 1B). We conclude that physiologically generated hepcidin modulates iron homeostasis and yields an iron-rich phenotype in THP1 monocytes via inhibition of iron efflux.

DISCUSSION

The antimicrobial peptide hepcidin has emerged as a major hormonal regulator of systemic iron homeostasis. Overwhelming genetic data, suggested that hepcidin negatively regulates dietary iron absorption in the duodenum and the recycling of iron from senescent red blood cells via reticuloendothelial macrophages [208, 210, 218]. Biochemical experiments revealed that hepcidin binds to transfected GFP-ferroportin and regulates its subcellular localization and stability [6, 61]. The iron exporter ferroportin mediates iron efflux from macrophages, which is crucial for the maintenance of a dynamic pool of transferrin-bound iron in plasma and the delivery of the metal to developing erythroid cells and other tissues [209]. The potential of hepcidin to control ferroportin expression provides a framework to understand the function of this peptide. Nevertheless, the functional characterization of hepcidin is far from completed and important physiological aspects remain largely unexplored. This prompted us to study the effects of hepcidin on macrophage iron efflux and on overall macrophage iron metabolism.

Because hepcidin is generated by hepatocytes and serves as a signal to target macrophages (and enterocytes), we established a physiologically relevant co-culture model of hepcidin-producing hepatoma cells and target THP1 monocytic cells. We previously optimized conditions for an iron release assay: THP1 cells were loaded with $^{59}\text{Fe-Tf}$ and the release of ^{59}Fe in serum-free media was monitored in the presence of HMW-DFO as an iron acceptor (Fig. 1). The induction of endogenous hepcidin by Huh7 cells in response to stimulation with IL-6, or the over-expression of a hepcidin cDNA in transfected HepG2 cells, appreciably reduced the release of ^{59}Fe from co-cultured THP1

monocytes by 30-35% (Figs. 2 and 3). These statistically significant values ($p < 0.05$) compare to ^{59}Fe release in control co-culture experiments with H1299 lung cancer cells. A consistent, yet smaller decrease (~15%) that did not reach statistical significance was apparent when ^{59}Fe release from THP1 monocytes was compared between co-cultures with control H1299 cells that do not express any hepcidin (Fig. 2A), and co-cultures with unstimulated Huh7 or untransfected HepG2 cells. This effect could be attributed to basal expression of hepcidin in the hepatic cells.

The data in Figs. 2 and 3 directly demonstrate that physiologically generated hepcidin controls iron efflux from monocytic cells. They also corroborate biochemical experiments documenting inhibition of iron efflux due to hepcidin-mediated relocalization and lysosomal degradation of transfected ferroportin [6, 7, 61]. Moreover, they strongly suggest that hepcidin produced by hepatoma cells likely targets endogenous ferroportin from co-cultured THP1 cells for degradation. Experiments are underway to validate this hypothesis, which is further supported by recent data showing that exposure of bone marrow-derived macrophages to synthetic hepcidin decreases levels of endogenous ferroportin [222].

Importantly, the capacity of physiologically generated hepcidin to inhibit ^{59}Fe release from THP1 cells correlates with a reduction of IRP2 levels (Fig. 4) and the concomitant de-repression of ferritin synthesis (Fig. 5). Because IRP2 is sensitive to iron-dependent degradation [40], assessment of its steady-state levels serves as a reliable marker of cellular iron status [6]. Thus, low IRP2 levels are indicative of an iron-replete state. The observed increase in de novo synthesis of ferritin, that stores and detoxifies

excess intracellular iron [223], is in agreement with the well-established function of IRP2 as a repressor of ferritin mRNA translation [40, 209].

In summary, the data presented here show that hepcidin generated by hepatic cells inhibits iron efflux from target monocytes and activates homeostatic responses in these cells to handle iron accumulation. These findings are fully consistent with a function of hepcidin in controlling the degree of iron load in macrophages and with the proposed causative relationship of pathological hepcidin expression with the development of ACD.

FIGURES

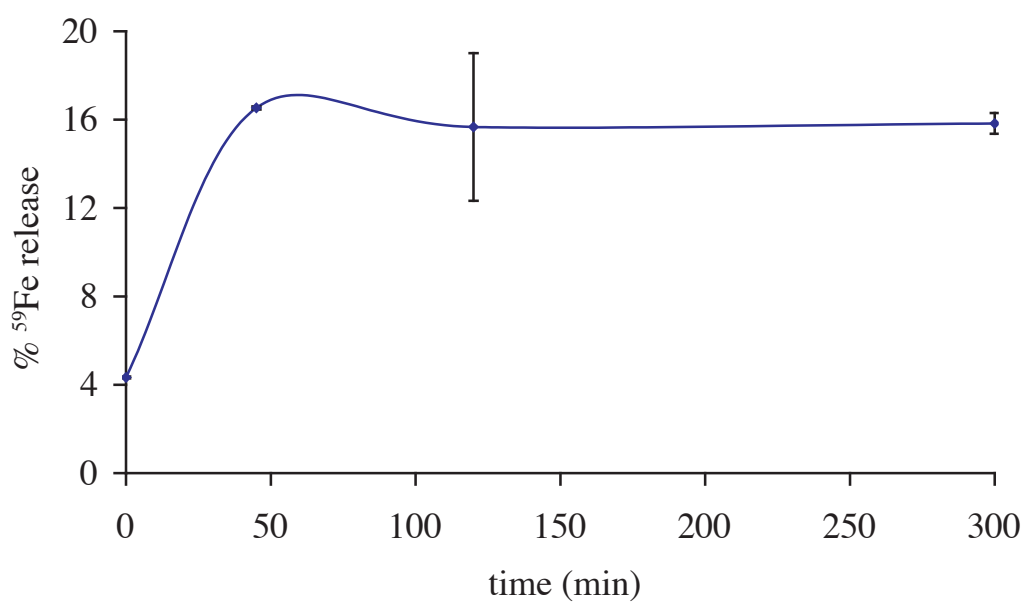


Fig. 1

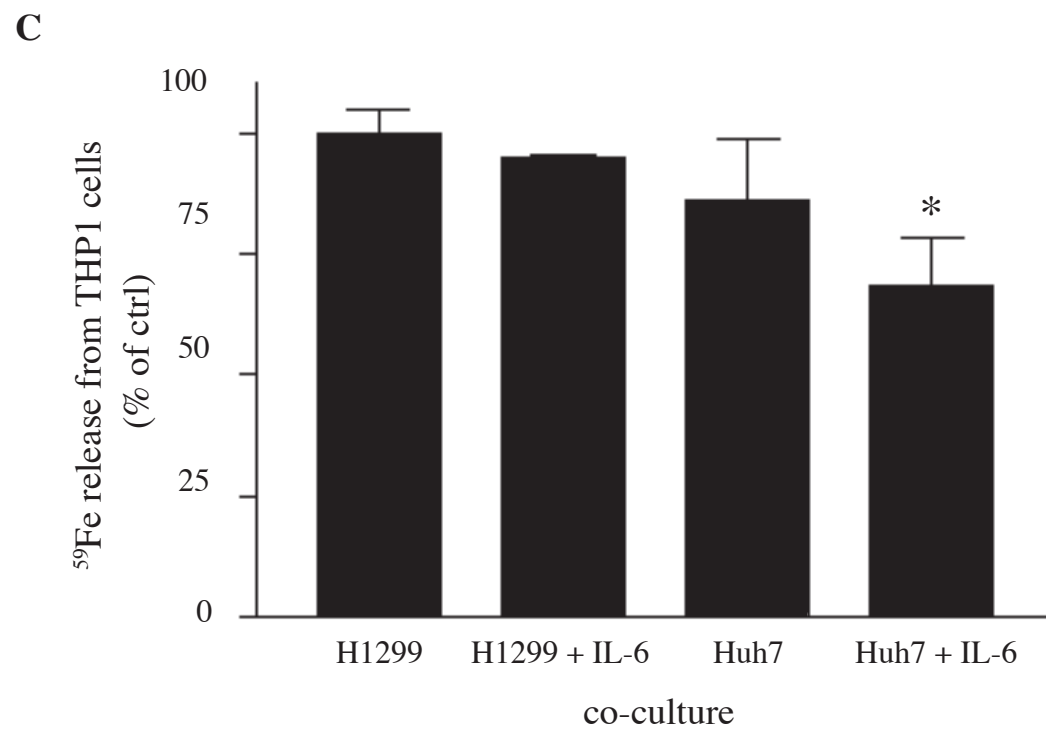
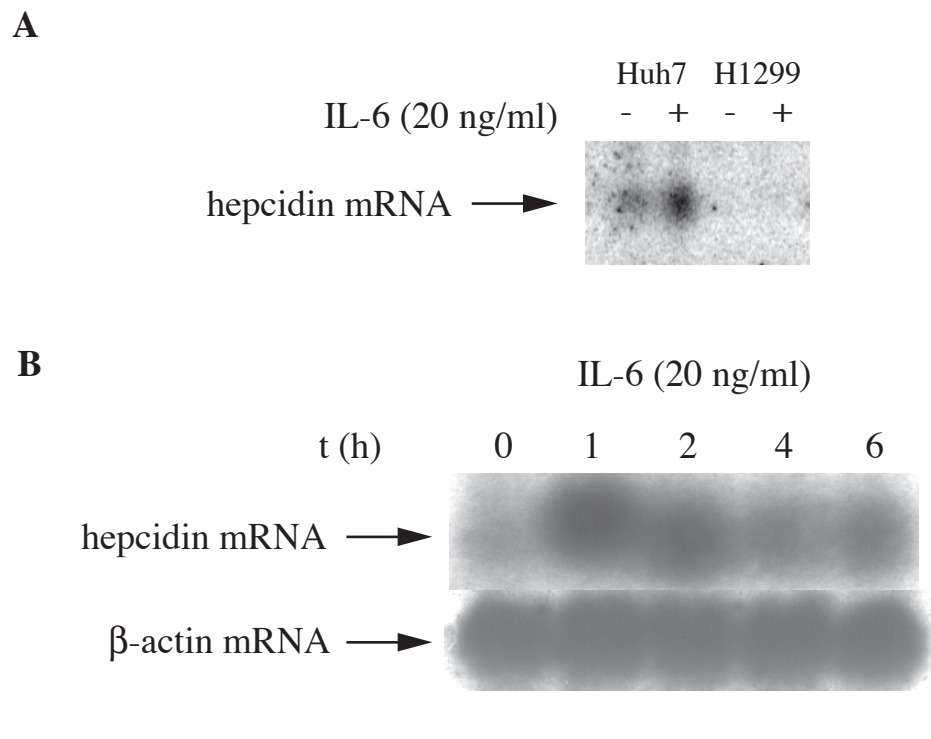
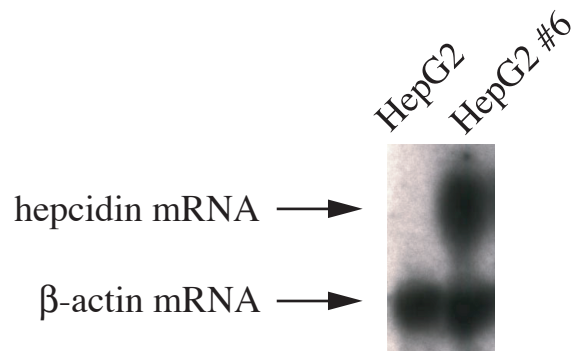


Fig. 2

A



B

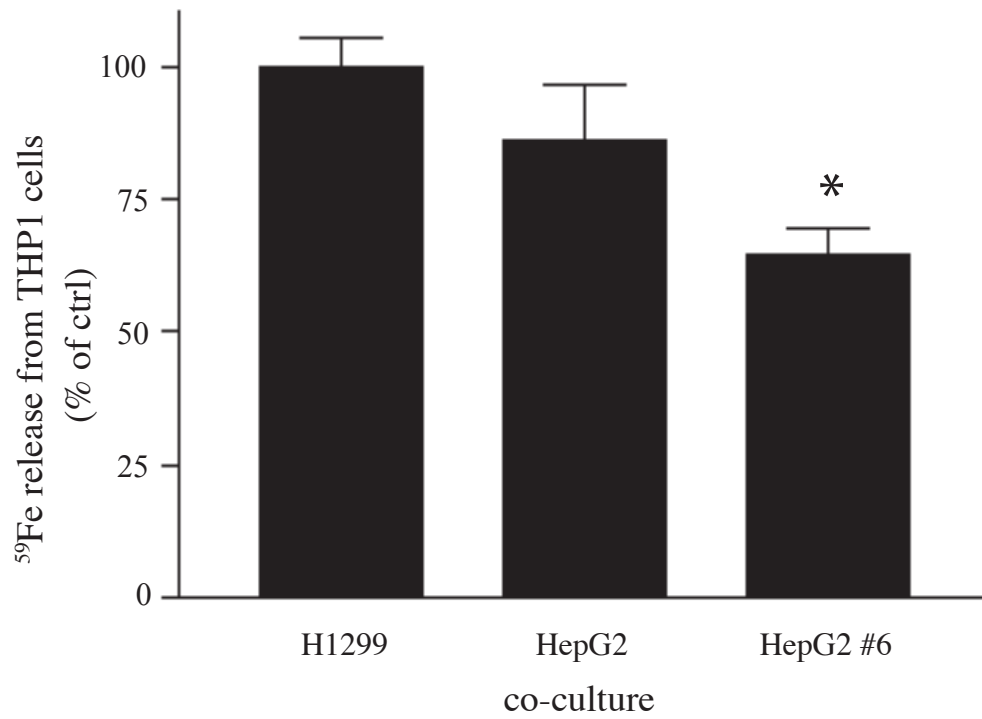


Fig. 3

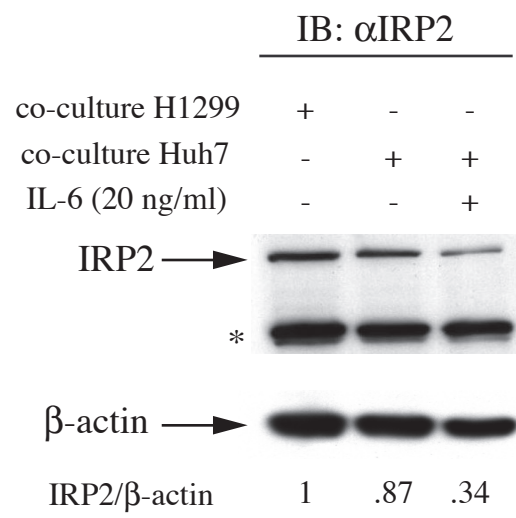


Fig. 4

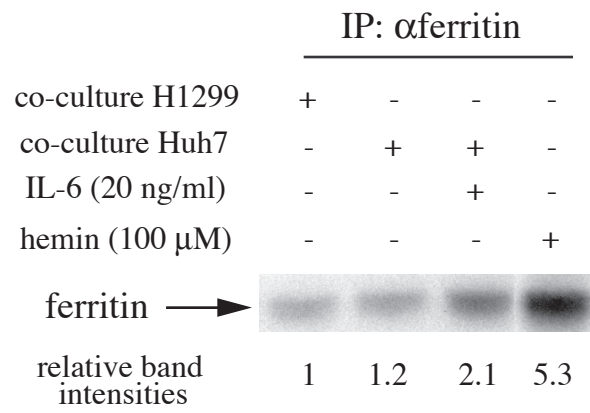
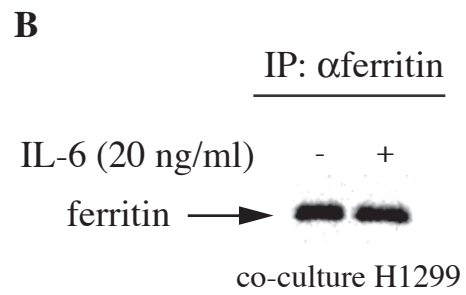
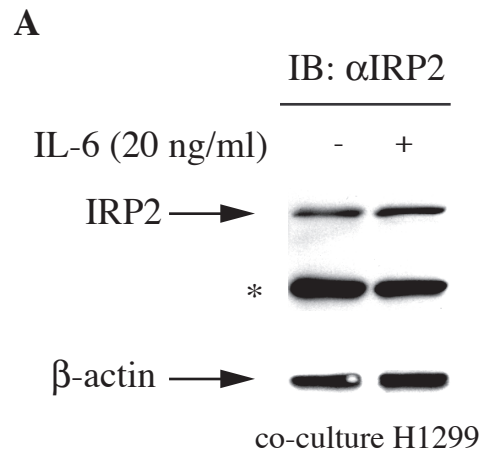


Fig. 5



Suppl. Fig. 1

FIGURE LEGENDS

Fig. 1. Kinetics of ^{59}Fe release from THP1 monocytic cells.

The cells were loaded with 5 μM ^{59}Fe -Tf for 16 h and the release of ^{59}Fe in serum-free media was measured at the indicated time intervals. The media contained 100 μM HMW-DFO to capture and solubilize ^{59}Fe . Iron release is expressed as percentage of the total amount of soluble ^{59}Fe in media divided by ^{59}Fe in both media and cells. Values correspond to triplicate experiments (mean \pm SD).

Fig. 2. The expression of hepcidin from Huh7 hepatoma cells inhibits ^{59}Fe release in THP1 monocytes.

(A) Huh7 hepatoma and H1299 lung cancer cells were treated with 20 ng/ml IL-6 for 2 h and the expression of hepcidin mRNA was analyzed by Northern blotting. (B) Huh7 cells were treated with 20 ng/ml IL-6 and the expression of hepcidin (top) and β -actin (bottom) mRNAs at the indicated time intervals was analyzed by Northern blotting. (C) THP1 monocytes were loaded with 5 μM ^{59}Fe -Tf for 16 h and co-cultured for 4 h with H1299 or Huh7 cells, previously treated with 20 ng/ml IL-6 for 2 h or not. The release of ^{59}Fe was monitored in serum-free media containing 100 μM HMW-DFO. Iron release, calculated from the total amount of soluble ^{59}Fe in media divided by ^{59}Fe in both media and cells, is expressed as percentage of control (co-culture with H1299 cells). Values correspond to triplicate experiments (mean \pm SD).

* $p < 0.05$ versus control (one-way ANOVA test).

Fig. 3. The expression of hepcidin from HepG2 hepatoma cells inhibits ⁵⁹Fe release in THP1 monocytes.

(A) Northern blot analysis of hepcidin (top) and β -actin (bottom) mRNAs in parent HepG2 cells and in HepG2 #6, stably transfected with a hepcidin cDNA. (B) THP1 monocytes were loaded with 5 μ M ⁵⁹Fe-Tf for 16 h and co-cultured for 4 h with either control H1299 lung cancer cells, parent HepG2 cells, or HepG2 #6. The release of ⁵⁹Fe was monitored in serum-free media containing 100 μ M HMW-DFO. Iron release, calculated from the total amount of soluble ⁵⁹Fe in media divided by ⁵⁹Fe in both media and cells, is expressed as percentage of control (co-culture with H1299 cells). Values correspond to triplicate experiments (mean \pm SD).

* $p < 0.05$ versus control (one-way ANOVA test).

Fig. 4. The generation of hepcidin by Huh7 hepatoma cells decreases IRP2 levels in THP1 monocytes.

THP1 monocytes were co-cultured for 4 h with either control H1299 lung cancer cells, Huh7 cells, or Huh7 cells previously treated with 20 ng/ml IL-6 for 2 h. The expression of IRP2 (top) and β -actin (bottom) in THP1 cells was analyzed by Western blotting. IRP2/ β -actin ratios were quantified by densitometry.

* denotes an apparently non-specific band

Fig. 5. The generation of hepcidin by Huh7 hepatoma cells stimulates ferritin synthesis in THP1 monocytes.

THP1 monocytes were co-cultured for 2 h with either control H1299 lung cancer cells, or Huh7 cells, or Huh7 cells previously treated with 20 ng/ml IL-6 for 2 h. Subsequently, the co-cultured cells were metabolically labeled with (50 μ Ci/ml) *trans*-[³⁵S]label for 2 h. Lysates from THP1 cells were subjected to quantitative immunoprecipitation with ferritin antibodies. Immunoprecipitated material was analyzed by SDS-PAGE on a 15% gel and newly synthesized ferritin (arrow) was visualized by autoradiography. The relative band intensities were quantified by phosphorimaging.

Suppl. Fig. 1.

Pre-treatment of control H1299 cells with IL-6 does not affect IRP2 expression (A) and ferritin synthesis (B) in co-cultured THP1 monocytes. Experimental conditions were as described in Figs. 4 and 5, respectively.

CHAPTER IV. SUSTAINED HYDROGEN PEROXIDE INDUCES IRON UPTAKE
BY TFR1-1 INDEPENDENT OF THE IRP/IRE NETWORK

Bill Andriopoulos, Stephan Hegedüs, Julia Mangin, Andreas Welker, Hans-Dieter
Riedel, Ulrike Hebling, Jian Wang, Kostas Pantopoulos, Sebastian Mueller

PREFACE

In the previous Chapter III, we concluded that increased levels of circulating hepcidin leads to increased retention of iron within the RES. The purpose of this action is to deprive an invading pathogen of its necessary iron. As a consequence, as observed in patients with ACD, increased hepcidin may cause hypoferremia. Interestingly, various inflammatory conditions such as hepatitis C or alcoholic steatohepatitis exhibit iron deposits within the liver parenchyma, in addition to increased RES retention.

In Chapter IV we sought to unravel the molecular mechanisms responsible for iron accumulation in liver parenchyma.

ABSTRACT

Local and systemic inflammatory conditions are characterized by the intracellular deposition of excess iron, which may promote tissue damage via Fenton chemistry. Because the Fenton reactant H_2O_2 is continuously released by inflammatory cells, a tight regulation of iron homeostasis is required. Here, we show that exposure of cultured cells to sustained low levels of H_2O_2 that mimic its release by inflammatory cells, leads to upregulation of transferrin receptor 1 (TfR1), the major iron uptake protein. This results in increased transferrin-mediated iron uptake and cellular accumulation of the metal. Although under these conditions iron regulatory protein 1 (IRP1) is transiently activated by H_2O_2 , this response is not sufficient to stabilize TfR1 mRNA and to repress the synthesis of the iron storage protein ferritin. The induction of TfR1 is independent of transcriptional activation via hypoxia inducible factor 1 α (HIF-1 α), or significant protein stabilization. Pulse experiments with [^{35}S]-labeled methionine/cysteine revealed an increased rate of TfR1 synthesis in cells exposed to sustained low H_2O_2 levels. Our results suggest a novel mechanism of iron accumulation by sustained H_2O_2 , based on the translational activation of TfR1, which could provide an important pathophysiological link between iron metabolism and inflammation.

INTRODUCTION

Systemic iron homeostasis undergoes typical changes during inflammatory or infectious conditions. A decrease in plasma iron concentration limits the availability of the metal for erythropoiesis, ultimately leading to the so-called anaemia of chronic disease [224]. Besides iron retention, parenchymal cells also accumulate iron under inflammatory conditions [225-231] and this iron deposition has been identified as important factor in tissue damage by free radicals [232]. In addition, hepatic iron accumulation appears to be an important cofactor in the development of fibrosis and end-stage liver disease in such common chronic liver pathologies such as chronic hepatitis C or alcoholic steatohepatitis [227-231].

Significant progress has been made towards understanding the molecular basis of iron retention within the reticuloendothelial system (RES) during inflammation [233-235]. The mechanism involves the IL-6-mediated induction of the iron-regulatory peptide hepcidin [236, 237], which inhibits iron efflux from macrophages and intestinal enterocytes [238, 239] by binding to and promoting the degradation of the transporter ferroportin 1 (IREG1 or MTP1) [240]. The ensuing hypoferremia is thought to be part of a physiological defence strategy to deplete invading bacteria from the growth-essential iron.

The possibility that inflammation-mediated accumulation of iron in parenchymal cells may also contribute to hypoferremia has not received much attention thus far. Nevertheless, the expression of TfR1, the major iron uptake protein is induced in several models of inflammation [225, 241].

Upon activation, inflammatory cells such as neutrophils and macrophages undergo an ‘oxidative burst’ that results in the release of large amounts of reactive oxygen species to kill invading bacteria [242]. The membrane associated NADPH-oxidase (NOX2) first generates superoxide that is rapidly dismutated to the more stable H_2O_2 by superoxide dismutases [154]. Thus, during inflammation, cells and tissues are exposed to sustained concentrations of H_2O_2 demanding a tight regulation of iron homeostasis to prevent tissue damage via Fenton and Fenton-like reactions. The activation of IRP1 (IRP1) by H_2O_2 has been proposed as a regulatory link between cellular iron homeostasis and inflammation. IRP1 regulates the expression of several proteins by post-transcriptional mechanisms. In iron deficient cells, the mRNA of TfR1 is stabilized upon binding of IRP1 and IRP2 to ‘iron responsive elements’ (IREs) within its 3’ untranslated region [243]. Earlier work showed that the IRE-binding activity of IRP1 is induced by H_2O_2 [244, 245]. Thus, exposure of cultured cells or intact rat liver to H_2O_2 at quantities that are commonly released by inflammatory cells rapidly activate IRP1 within 30-60 min [246, 247]. Importantly, IRP1 activation by H_2O_2 was sufficient to increase TfR1 expression in B6 fibroblasts [248]. TfR1 expression is also controlled transcriptionally; one mechanism involves the hypoxia-inducible factor 1 α (HIF1 α) which binds to a conserved binding site within the TfR1 promoter [249, 250]. HIF1 α is activated in response to hypoxia. The upregulation of HIF1 α has also been linked to mitochondria-derived oxidative stress [251].

Transient pulses of H_2O_2 are commonly employed to study the effects of this reactive oxygen intermediate in biochemical pathways. Such conditions, however, hardly mimic the continuous release of H_2O_2 from inflammatory cells since H_2O_2 is degraded

rapidly by cultured cells [252]. We have previously employed an enzymatic system for H_2O_2 generation at steady-state levels based on glucose oxidase (GOX) and catalase (CAT) [247, 252-254]. For methodological reasons, however, these studies were restricted to relatively short time intervals [246, 247]. In an optimized setting, we expose here cultured cells to a sustained flux of H_2O_2 at low, non-toxic concentrations that mimic the H_2O_2 release by inflammatory cells in terms of time and dose response. We show that such conditions induce the expression of TfR1, which is associated with increased transferrin-mediated iron uptake and intracellular iron accumulation. Neither IRP1 nor HIF1 α are involved in the upregulation of TfR1 in response to such sustained low levels of H_2O_2 . Moreover, H_2O_2 does not block TfR1 turnover. We demonstrate that H_2O_2 significantly stimulates TfR1 expression at the translational level. We suggest that H_2O_2 mediated iron uptake via translational induction of TfR1 could be a general mechanism that contributes to iron accumulation and tissue damage under conditions of inflammation.

MATERIALS AND METHODS

Reagents

Luminol, NaOCl, phosphate buffered saline (PBS), HANKS buffer, H₂O₂, catalase, tetrazolium salt (MTT), glucose oxidase and sodium azide were purchased from Sigma (Deisenhofen, Germany). Dulbecco's modified Eagle's medium (DMEM), McCoy's 5A medium and penicillin/streptomycin were purchased from Gibco (Germany). Foetal calf serum was purchased from Greiner Labortechnik (Germany). Stock solutions of luminol, NaOCl and H₂O₂ were prepared as described recently [254].

Cell culture

Human HepG2, HeLa, and HT29 cells were grown in DMEM supplemented with 2 mM glutamine, 4.5 g/l glucose, 100 units/ml penicillin, 0.1 ng/ml streptomycin, and 10% fetal calf serum. Human colonic carcinoma HCT116 cells were grown in McCoy's 5A medium and murine B6 fibroblasts were grown in supplemented DMEM containing 1000 mg/l glucose. Cells were maintained in an incubator at 37°C with 5 % CO₂.

Determination of enzymatic activities for catalase and GOX

Enzymatic activities of GOX and catalase were determined at very low H₂O₂ concentrations prior to the experiment using a sensitive chemiluminescence technique [253, 255]. Continuous measurements on supernatants of cultured cells confirmed the maintenance of steady-state concentrations of H₂O₂ during each experiment [252].

Electrophoretic Mobility Shift Assay (EMSA)

EMSAs were performed as described previously using a radiolabeled human ferritin H-chain IRE probe [256]. RNA-protein complex formation was quantified by densitometric scanning of the depicted autoradiographs.

Western blotting

Cells were solubilized directly in RIPA lysis buffer and lysates were immediately boiled for 10 min. Equal aliquots were resolved by SDS/PAGE on 8% gels and proteins were transferred on to nitrocellulose filters. The blots were saturated with 5% non-fat milk in PBS and probed with 1:4000 TfR1 (Zymed Laboratories Inc., San Francisco, CA), 1:250 HIF-1 α mouse (Biosciences, Heidelberg, Germany), or 1:500 β -actin (Sigma) antibodies. After washing with TBS containing 0.05% (v/v) Tween 20, the blots were further incubated with HRP-conjugated secondary antibodies using the following dilutions: TfR1 monoclonal antibodies with rabbit anti-mouse IgG 1:6000, β -actin antibodies with goat anti-rabbit IgG 1:10000, HIF-1 α mouse antibodies with goat anti-mouse IgG 1:10000 dilution. Glucose oxidase was detected with a previously developed anti-GOX polyclonal antibody [257] in conjunction with an HRP-conjugated anti-guinea pig secondary antibody (Dianova, Hamburg, Germany) at a dilution of 1:3000. Detection of the HRP-coupled secondary antibodies was performed with the ECL[®] method (Amersham, Piscataway, NJ). The blots were quantified by densitometric scanning using the TotalLab software version 1.11 (Nonlinear Dynamics Inc., Durham, NC).

Determination of the labile iron pool (LIP)

LIP was measured using a modified technique based on the metal-sensitive fluorescence probe calcein [258, 259]. We modified the technique to allow LIP detection of attached cells. Briefly, cells were first treated for over 24 hours in the presence of H₂O₂ or the membrane-impermeable iron chelator desferal (desferrioxamine). Cells were then washed twice with PBS and loaded with calcein-acetoxymethyl ester at a final

concentration of 5 μ M for 30 min (from a 10 mM stock solution in dimethyl sulfoxide). First fluorescence readings (F1) were taken using a Fluostar (BMG Labtechnologies GmbH, Offenburg, Germany) in bottom read technique with a fluorescein optical filter (excitation, 465-495 nm; emission, 505 nm). Subsequently, cells were depleted of iron in the presence of the membrane permeable iron chelator salicylaldehyde isonicotinoyl hydrazone (SIH) for 30 min [260], and a second measurement of fluorescence was performed (F2). After background subtraction, this protocol allowed us to determine the F2/F1 ratio as relative indicator of LIP independent of the cell number and distribution within the wells.

Northern blotting

RNA prepared with the Trizol® reagent (Invitrogen) was analyzed by Northern blotting with ³²P-radiolabeled mouse TfR1, hepcidin or rat β -actin cDNA probes [245].

Oxygen measurements and induction of hypoxia

Oxygen was measured using a computer-driven oxygen electrode Oxi 325-B (WTW, Weilheim, Germany). The electrode was calibrated with air saturated water (21%). Permanent magnetic stirring was necessary to facilitate oxygen exchange at the membrane side of the oxygen electrode. To induce hypoxia, a custom-made oxygen chamber was used and equilibrated with a prepared gas mixture of 3% oxygen, 5% carbon dioxide and 92% nitrogen (Lifegas, USA).

Iron uptake experiments

Transferrin-mediated iron uptake experiments were carried out as described in [261]. Briefly, uptake experiments of ⁵⁹Fe-labeled diferric transferrin (holo-Tf) were performed in 6-cm dishes at 37°C for 30 min in 1 ml of buffer A (140 mM NaCl, 5 mM KCL, 1 mM CaCl₂, 1 mM MgCl₂, 5 mM NaH₂PO₄, and 5 mM HEPES pH 7.4). Cells were washed five times with ice-cold PBS and then lysed with 1 ml of 1 M NaOH. Radioactivity of lysates was determined using a Cobra II Auto Gamma counter (Canberra Packard, Meriden, CT). For all uptake experiments, controls were incubated on ice to determine nonspecific binding of holo-Tf to the cell membrane. The 0°C values were subtracted from the 37°C values to determine net uptake rates.

Analysis of TfR1 mRNA levels by quantitative RT-PCR

Total RNA was isolated from cell culture using the Trizol® reagent (Invitrogen). TfR1 and control β-actin mRNA transcripts were quantified by a 2-step reverse transcriptase-polymerase chain reaction (RT-PCR) with the Applied Biosystems 7500 Real-Time PCR System. cDNA synthesis was performed with the First Strand cDNA Synthesis Kit for RT-PCR (Invitrogen), according to manufacturer's instructions. Transcripts were amplified in duplicates with specific sense and antisense QuantiTect® primers (Qiagen). The thermal cycler profile consisted of a total reaction volume of 50 μl that underwent a 95°C activation for 10 minutes, followed by 40 repetitions of the following 3 steps: 95°C denaturation for 15 seconds, annealing at 55°C for 30 seconds and a 33 second extension period at 72°C. Transcripts were detected with the QuantiTect SYBR® Green kit. TfR1/β-actin ratios were calculated using LightCycler Sequence Detection Software v1.2.

TfR1 protein stability and synthesis

For protein stability, cells were metabolically labeled for 1 hour with (50 μ Ci/ml) trans-[35 S] label, a mixture of 70:30 35 S-methionine/cysteine (ICN) in RPMI methionine/cysteine free media prior to GOX treatment. Following the 1 hour pulse, cells were chased with cold media in the absence or presence of GOX treatment. In contrast, the rate of protein synthesis was determined by first incubating the cells in cold media with or without GOX and subsequently metabolically labeling the cells for 1 hour. Following both the protein stability and synthesis studies, the cells were lysed with RIPA buffer and 1 mg of lysates were subjected to quantitative immunoprecipitation with 2 μ l of mouse monoclonal TfR1 (Zymed Laboratories Inc., San Francisco, CA). Immunoprecipitated proteins were analysed by SDS/PAGE and visualized by autoradiography. Radioactive bands were quantified by phosphorimaging.

Cytotoxicity studies

Cell viability was determined with the MTT assay [262]. Briefly, conversion of the tetrazolium salt (MTT) into a blue formazan product was detected using a 96-well plate reader (Fluostar, BMG Labtechnologies GmbH, Offenburg, Germany) at 570 nm. Cells were treated with different activities of glucose oxidase and catalase in culture medium for 24 hours in 96-well plates at 37°C. After two washing steps with PBS, MTT was added to each well (0.5 mg/ml), cells were incubated for further 4 hours at 37°C and, finally, 10% SDS in 0.01 M HCl was added to lyse the cells. Samples were incubated overnight and the absorbance was measured.

RESULTS

Generation of sustained H₂O₂ in cultured cells at non-toxic conditions

Optimization of the previously developed GOX/CAT system [252-254] allowed us to expand H₂O₂ exposure times up to several days, thus mimicking, with respect to oxidative stress, a chronic inflammatory response. Using an ultra-sensitive H₂O₂ assay [252, 263], we show (Fig. 1A) that the rate of H₂O₂ generation by GOX resembles that of activated leukocytes *in vivo* (0.2 $\mu\text{M s}^{-1}$) [263]. H₂O₂ is maintained at a constant concentration of $\sim 5 \mu\text{M}$ over the entire time interval of 24 h, indicating that GOX remains stable under these experimental conditions and the substrates glucose and oxygen are not depleted. Cell cultures could be exposed to GOX/CAT over several days and such experiments were only limited by cellular confluence and eventual growth arrest. The media were always replaced every twelve hours to renew GOX and substrates. We then examined whether under the above experimental conditions toxicity/growth inhibition was associated with flux or concentration of H₂O₂ by varying GOX amounts or ratios of GOX/CAT [254, 264]. As demonstrated in Fig. 1B, toxicity depended solely on the levels of H₂O₂ and was independent of the flux. Both GOX 1x and GOX 5x inhibited cell growth when H₂O₂ levels exceeded a concentration of 10 $\mu\text{M H}_2\text{O}_2$. Interestingly, B6 cells that were incubated with increasing GOX without additional external catalase, also showed growth inhibition at a steady-state concentration of 10 $\mu\text{M H}_2\text{O}_2$ due to the low cellular catalase activity of 0.001 s^{-1} [253]. Thus, toxicity of a GOX/CAT system only depends on the concentration of H₂O₂ (defined by the ratio of GOX/CAT) and not the H₂O₂ generation rate (defined by the GOX activity), which could be linked to consumption or other metabolites. No changes in cell growth were observed with H₂O₂

concentrations below 1 μM and these non-toxic conditions are tolerated well over 24 hours.

Sustained exposure of cultured cells to non-toxic H_2O_2 concentrations induces TfR1 expression

Long term exposure of B6 fibroblasts over 48 hours to low H_2O_2 concentrations was accompanied by a strong induction of TfR1 expression (Fig. 2A). A slight increase (40%) of TfR1 steady-state levels was observed after 8 hours, while maximal activation (~ 3.5 fold) was manifested after 24 h and sustained up to 48 h. Thus, H_2O_2 not only antagonized the previously reported inhibiting effect of cell growth on TfR1 expression [265] but further increased TfR1 expression. The ratios of TfR1 densities from H_2O_2 -treated and control cells are shown at the bottom panel of Fig. 2A. In contrast to iron depleting conditions, the iron storage protein ferritin was slightly upregulated in H_2O_2 treated cells and more so with iron loading with hemin (see Fig. 2B). Thus, prolonged exposure of B6 cells to non-toxic H_2O_2 concentrations strongly activates TfR1 expression and slightly upregulates ferritin. Importantly, these data were corroborated in additional cell lines of various tissue origin (HeLa, HepG2, HCT116, HT29).

TfR1 up-regulation in cells exposed to GOX/CAT is mediated solely by H_2O_2 and not hypoxia

In the GOX/CAT system, the ratio of GOX/CAT activities determines the concentration of H_2O_2 , while GOX defines the consumption rate of oxygen [252]. At higher concentrations, GOX significantly decreases oxygen levels in the culture medium

(Fig. 3A). Since hypoxia [249, 250] and oxidative stress [251] have been shown to induce TfR1 expression *via* the transcription factor HIF-1 α , we next studied whether exposure of cells to sustained H₂O₂ under our conditions increases expression of HIF1 α . Hepatoma HepG2 cells that express HIF-1 α in response to hypoxia [266], were exposed for 6 hours to different concentrations of H₂O₂ generated by the GOX/CAT system that are known to induce TfR1 (see Fig. 2) and HIF1 α was determined by Western blotting (Fig. 3B). Cells that were incubated with 3% oxygen using an oxygen chamber served as control. As expected, HIF-1 α expression is only induced at 3% oxygen (lane 2) while the application of GOX/CAT at an H₂O₂ flux that results in TfR1 activation (as in Fig. 2) did not stimulate HIF-1 α expression (lane 3 and 4). We conclude that sustained H₂O₂ activates TfR1 specifically and in the absence of hypoxia.

H₂O₂-mediated increase of TfR1 expression is functional and results in intracellular accumulation of iron.

We next addressed whether TfR1 upregulation in response to a sustained H₂O₂ flux is physiologically significant. Transferrin mediated iron uptake was measured by exposing B6 cells to various non-toxic steady-state H₂O₂-concentrations over 24 hours in the presence of ⁵⁹Fe-loaded and purified transferrin. Fig. 4A demonstrates a significant H₂O₂-dependent increase in ⁵⁹Fe uptake by 2.4 times. We then assessed the effects of the prolonged H₂O₂ treatment on the labile iron pool (LIP) using a modified calcein assay [258, 259]. Iron depletion by desferrioxamine was used as negative control. Fig. 4B shows that the LIP is clearly increased in response to exposure of B6 fibroblasts to a H₂O₂ flux over 24 hours. Similar responses of LIP were found with all other cell lines (data not shown).

Stimulated iron uptake by sustained H₂O₂ is independent of the IRE/IRP regulatory system.

Earlier studies showed that H₂O₂ rapidly activates IRP1 in cultured cells [244, 245] and in perfused rat liver [246], and that H₂O₂-mediated activation of IRP1 was sufficient to increase TfR1 mRNA and protein levels [248]. A threshold of ~10 μM was defined as the minimal concentration required for IRP1 activation within 30-60 min [247]; however, methodological constraints did not allow H₂O₂ exposure times longer than 60 min. The optimized H₂O₂ models presented herein enabled us to evaluate IRP1 activity by EMSA after prolonged H₂O₂ treatments. Exposure of B6 cells to steady state concentrations of ~5 μM H₂O₂ was associated with an initial modest activation of IRP1 that was detectable up to 6 hours (Fig. 5A, lanes 1-2). However, IRP1 activity declined within the next 24 h of H₂O₂ treatment (lanes 3-4), to the same degree observed in response to iron-loading with hemin (lane 5). As expected, the iron chelator desferrioxamine drastically activated IRP1 (lane 6). In contrast to iron overload with hemin, however, incubation of cell lysates with 2-mercaptoethanol that activates IRP1 *in vitro* indicated also decreased IRP1 protein levels. Moreover, TfR1 mRNA levels were not increased in response to H₂O₂ as determined by quantitative RT-PCR (Fig. 5B). Thus, it appears that the sustained exposure of cells to such low, non-toxic H₂O₂ concentrations only modestly and transiently induces IRP1 activity, and this response is not sufficient to stabilize TfR1 mRNA.

Increased levels of TfR1 during sustained H₂O₂ is independent of TfR1 stability but involves stimulation of TfR1 synthesis.

Expression of TfR1 is typically controlled at the level of transcription or stabilization of its mRNA via IRPs. Since these mechanisms were excluded, we next studied whether TfR1 levels were affected by either protein stability or synthesis. To measure protein stability in cells with or without sustained H₂O₂ treatment, B6 cells were pulsed with ³⁵S-methionine/cysteine for 1 hour (time 0) and chased for 1, 6.5 and 24 h (fig 6). The cells were then lysed and TfR1 levels were determined by quantitative immunoprecipitation and autoradiography. After 1 and 6 h of chase, TfR1 expression appeared to be slightly higher in cells treated with H₂O₂ than in control cells. However, a 24 h treatment with H₂O₂ did not affect the stability of TfR1. We conclude that the surge of TfR1 levels during H₂O₂ treatment is independent of TfR1 stabilization. We next addressed whether the rate of protein synthesis played a role in the elevated levels of TfR1 during H₂O₂ treatment. Cells were treated with GOX for 1, 6, 12 and 24 hours and subsequently pulsed with the ³⁵S-methionine/cysteine for 1 hour (fig 7). The cells were then lysed and TfR1 synthesis was analyzed by quantitative immunoprecipitation and autoradiography. As shown in Fig. 7, the rate of TfR1 synthesis was relatively unchanged in comparison to non-treated cells following 1 and 6 h of GOX treatment. In contrast, TfR1 mRNA translation was dramatically upregulated in H₂O₂-exposed cells after 12 h of GOX treatment. These findings indicate a novel mechanism, by which sustained H₂O₂ increases iron uptake via translational stimulation of TfR1.

DISCUSSION

The typical changes of iron homeostasis during acute inflammation are considered to be part of the defensive immune response. In chronic inflammation, however, parenchymal cells often show increased deposits of iron that may aggravate disease progression and promote further tissue damage. Under these conditions, iron becomes especially harmful because it catalyzes the generation of free radicals from reactive oxygen species released by inflammatory cells. Here, we show that the exposure of various cell types to sustained H_2O_2 results in the induction of TfR1 expression and accumulation of iron. We also provide evidence that the mechanism for TfR1 activation by H_2O_2 is translational.

The levels of sustained H_2O_2 utilized in our experiments are non-toxic and mimic inflammatory conditions. Thus, our experimental system provides a tool to study the alterations of iron homeostasis observed in chronic inflammation. A diversion of iron from circulation into intracellular compartments is well established. This is associated with impaired erythropoiesis, which eventually leads to the ACD [224, 226, 267, 268]. The antimicrobial peptide hepcidin inhibits iron efflux from macrophages via ferroportin 1 [240, 269]. Considering that hepcidin expression is induced by the pro-inflammatory cytokine IL-6, this pathway is expected to promote tissue iron accumulation and thereby plays a key role in the development of ACD (ACD). It is, however, possible that besides inhibition of iron efflux, increased iron uptake may also contribute to tissue iron accumulation in ACD. Our results suggest that the H_2O_2 -mediated increase of TfR1 may account for this response.

Importantly, increased expression of TfR1 has been observed in animal models of inflammation [225, 241]. In humans, direct evidence of TfR1 upregulation has been recently found in patients with acute respiratory distress syndrome (ARDS)[241]. During acute inflammation, the upregulation of TfR1 may reduce the availability of essential iron to invading bacteria, and is probably beneficial for the host. However, in chronic inflammation, accumulation of iron in tissues is associated with toxicity [232] and seems to drive progression of fibrosis and end-stage liver disease in such common liver pathologies such as chronic hepatitis C or alcoholic liver disease [227-231].

What is the mechanism for TfR1 activation by low, non-toxic doses of H₂O₂? We first explored the role of HIF1 α that is known to transcriptionally activate TfR1 [249, 250] and also responds to reactive oxygen species independently of hypoxia [251, 270]. However, our data clearly show that the GOX system can be calibrated to generate H₂O₂ steady-state levels in the absence of hypoxia (Fig. 3A-B). Moreover, the H₂O₂-mediated activation of TfR1 expression does not require the induction of HIF-1 α . Second, we hypothesized that the mechanism may involve TfR1 mRNA stabilization by IRP1, which is rapidly activated by H₂O₂ within 30 min to bind to IREs [244, 245, 256]. As shown previously in B6 fibroblasts, IRP1 is activated by a bolus of 100 μ M H₂O₂ [248]. In the present study, B6 and other cells were exposed to sustained \sim 5 μ M H₂O₂ (Fig. 1) and IRP1 was only partially and temporarily activated (Fig. 5A), very likely due to H₂O₂ signaling. The absence of full IRP1 activation under these conditions, is fully consistent with previous findings, showing that a concentration of \sim 10 μ M H₂O₂ was a minimum requirement to elicit the complete response [247]. Notably, IRP1 activity decreased at later time intervals (24 h) of GOX treatment, possibly due to increased intracellular iron

accumulation. The observed modest alterations in IRE-binding activity did not affect TfR1 mRNA levels (Fig. 5B), suggesting that the increase in TfR1 expression in GOX-treated B6 cells (Fig. 2A) is independent of IRP-mediated mRNA stabilization. H₂O₂ has been shown to differentially affect protein degradation in mammalian cells [271, 272]. However, pulse-chase experiments with ³⁵S-methionine/cysteine indicate that H₂O₂ does not affect the stability of TfR1 (Fig. 6). Studies of ³⁵S-methionine/cysteine incorporation demonstrate that H₂O₂ directly stimulates TfR1 synthesis.

The direct stimulation of TfR1 protein synthesis by low levels of H₂O₂ is somewhat unexpected. Proteomics data showed that H₂O₂ induces the expression of proteins that are important for translation and RNA processing [273]. However, only few studies on the oxidative modulation of translation exist, which show a rather complex response depending on cell type and conditions [273-278]. H₂O₂ was shown to inhibit translation [273, 274] by mechanisms such as the inhibition of the 70-kDa ribosomal protein S6 kinase [273], dephosphorylation of the eukaryotic initiation factor (eIF) 4E-binding protein 1 (4E-BP1), or increased binding of this repressor protein to eIF4E and concomitant loss of eIF4F complexes [273, 278]. Translation can also be inhibited by H₂O₂ via phosphorylation of the elongation factor eEF2 [273] which was either mediated by activation of the eEF-2 specific, Ca²⁺/calmodulin-dependent protein kinase III [276] or reversible inhibition of the protein phosphatase 1 [277]. On the other side, H₂O₂ has been shown to stimulate translation in cell-free systems [279], plants [280], bacteria [281] and mammalian cells [275]. The latter study interestingly indicated that the effect of H₂O₂ on translation depends on the levels of H₂O₂ and the cell sensitivity towards H₂O₂. Thus, in

Huh7 cells that are moderately sensitive towards H₂O₂, translation was upregulated even at low levels of H₂O₂.

In summary, our study establishes that sustained, non-toxic concentrations of H₂O₂ stimulate TfR1 expression by a novel translational mechanism. Thus, H₂O₂ is able to stimulate TfR1 expression both at the posttranscriptional level via IRP1 and at the translational level which points to a potentially general mechanism of iron internalization in the presence of H₂O₂. In addition to the role of hepcidin and ferroportin on iron homeostasis during inflammation [240, 269], H₂O₂ mediated iron uptake could provide an alternative local mechanism that removes iron from the inflammatory battle field and prevents unspecific collateral tissue damage. Under conditions of chronic inflammation, however, the continued accumulation of iron could itself impose a threat to cells and tissues [225-232]. In addition, translational stimulation of TfR1 expression by H₂O₂ could participate in the toxicity of chemotherapeutic anticancer agents such as doxorubicin that are known to increase TfR1 expression [282, 283]. Our work underlines the importance to study the expression of proteins in clinical and animal trials that are commonly focusing on the mRNA levels because of limited tissue availability. Our novel tool of a sustained exposure of cultured cells to H₂O₂ will help to better understand molecular mechanisms related to oxidative stress in future studies that should also include the complex redox-sensitive regulation of translation.

FIGURES

A

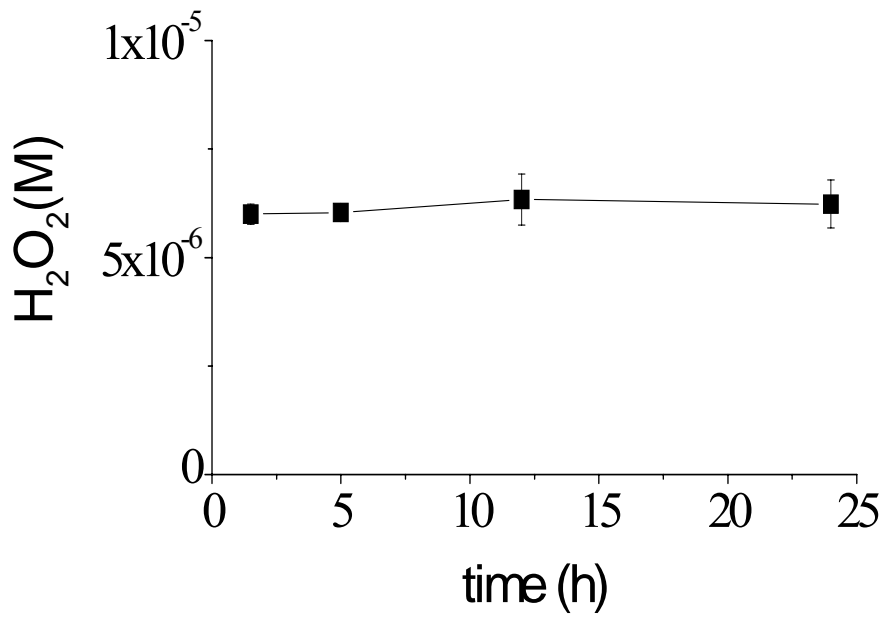


Fig. 1A

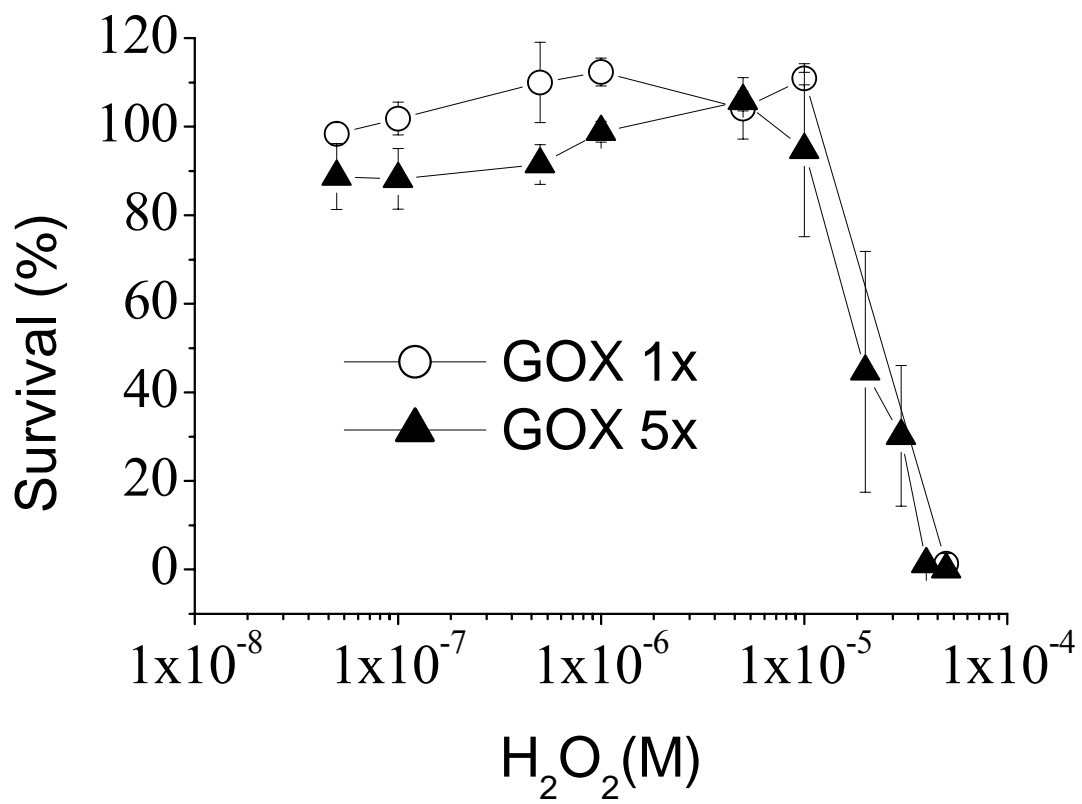


Fig. 1B

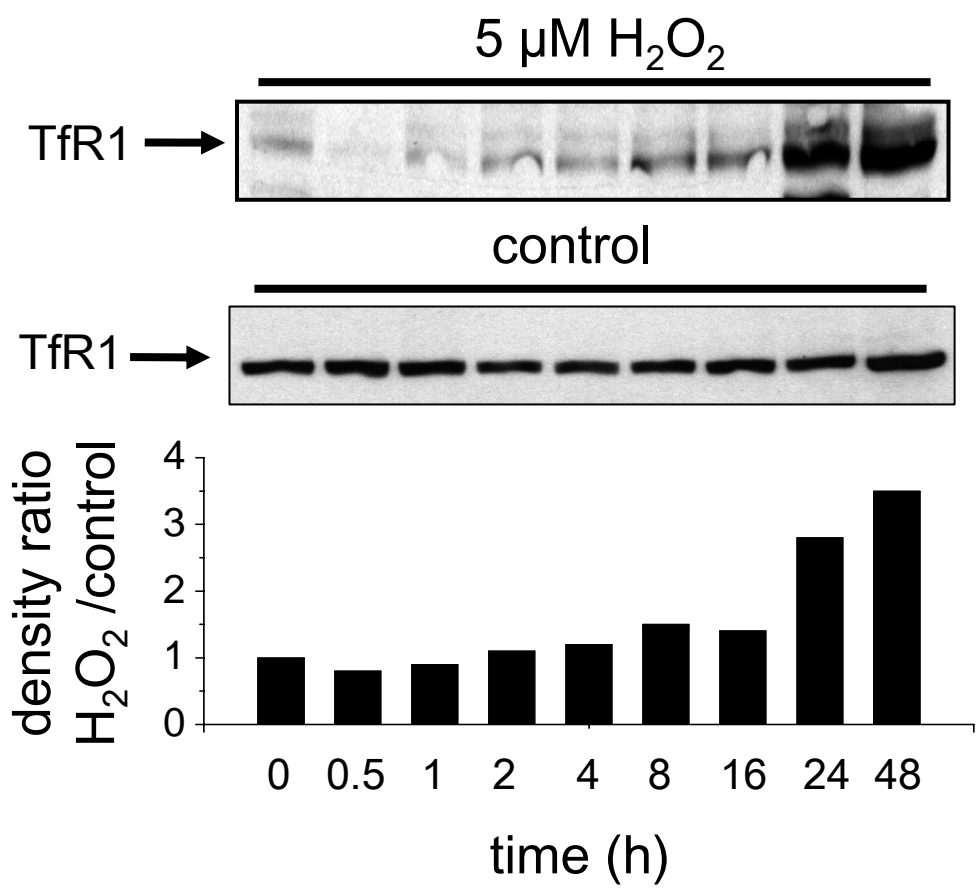


Fig. 2A

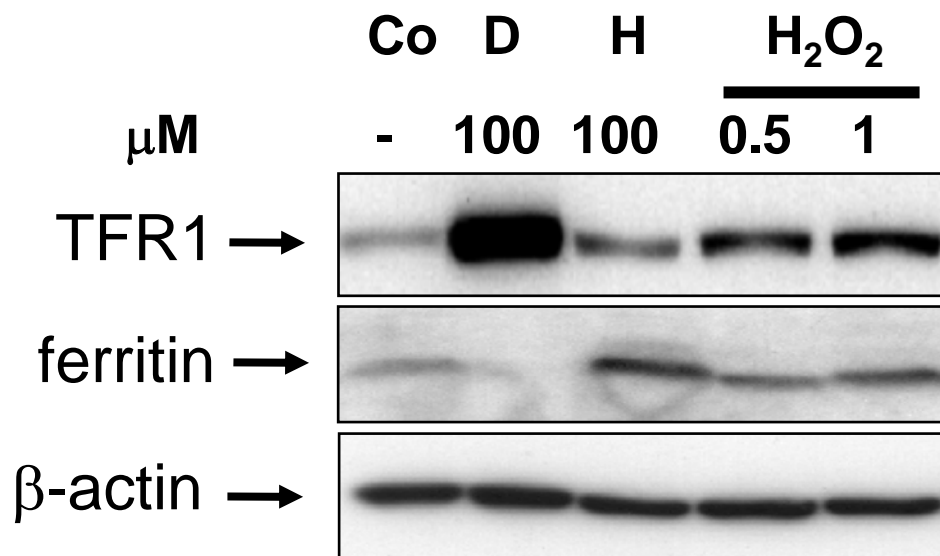


Fig. 2B

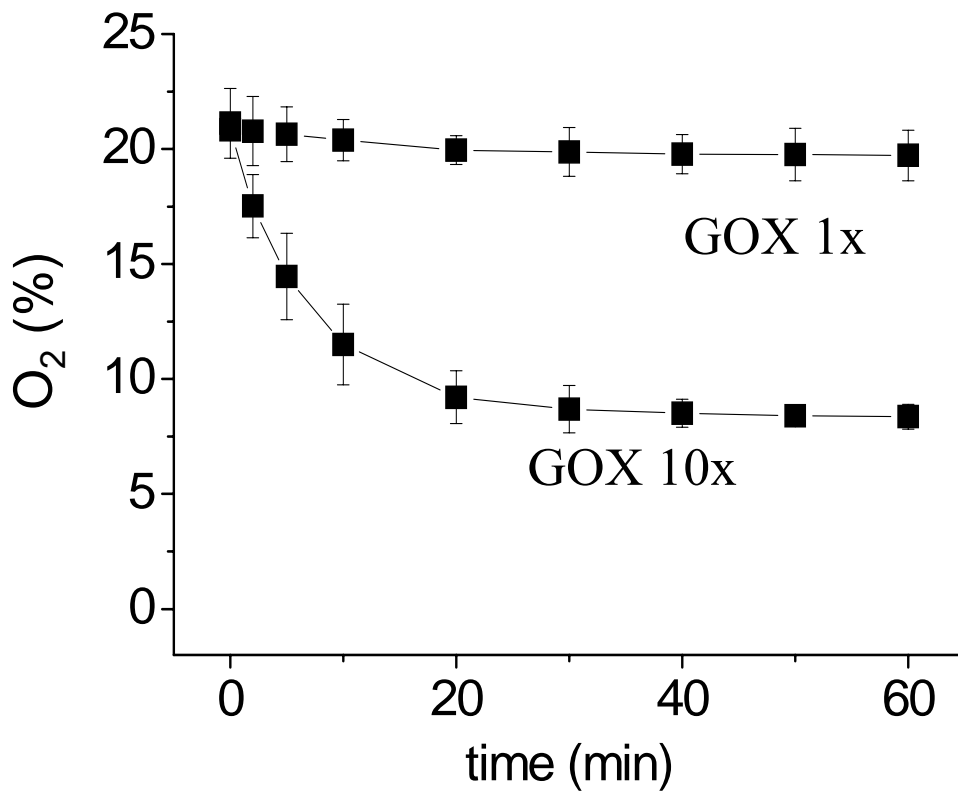


Fig. 3A

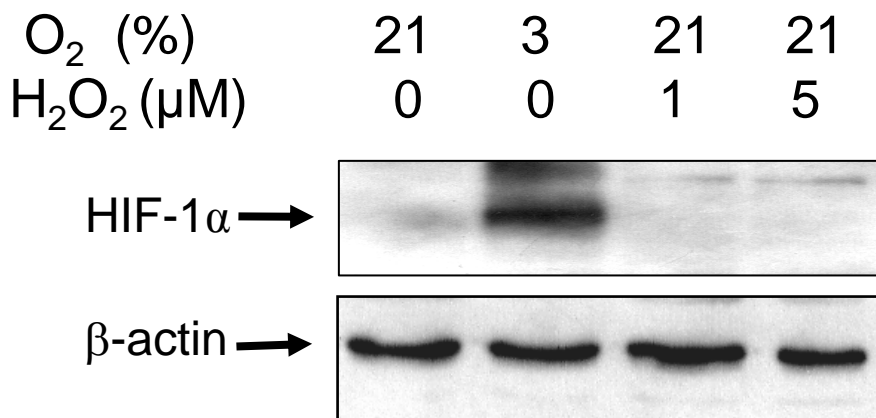


Fig. 3B

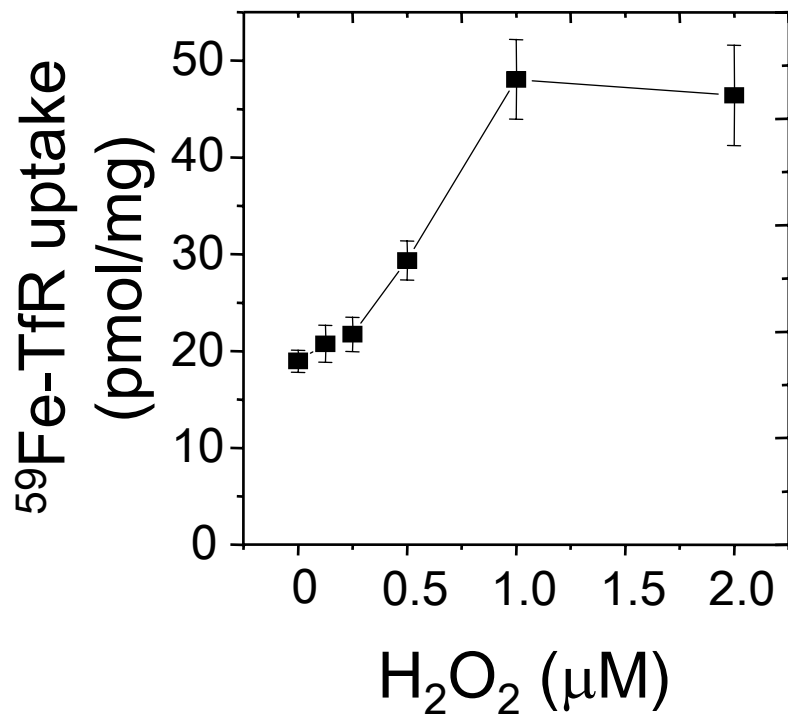


Fig. 4A

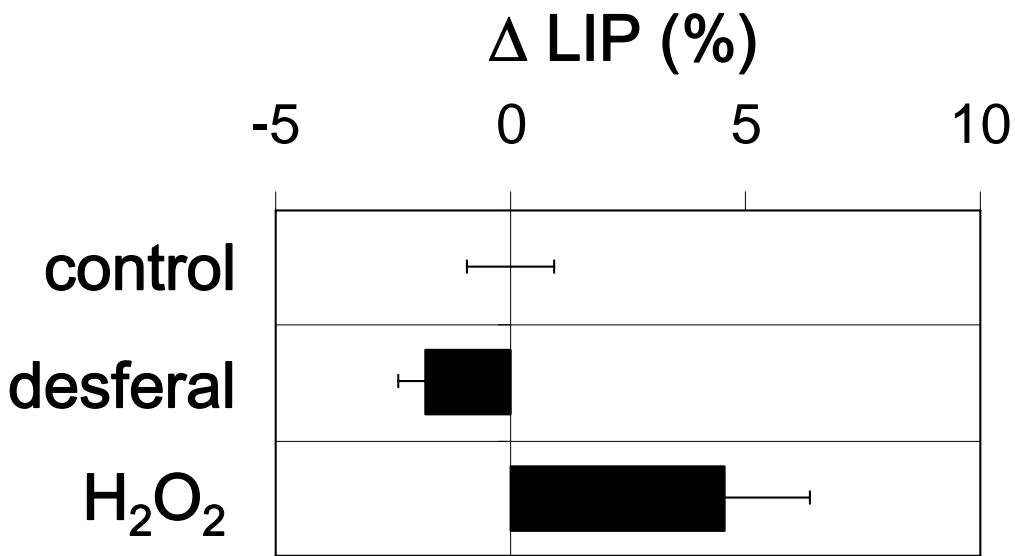


Fig. 4B

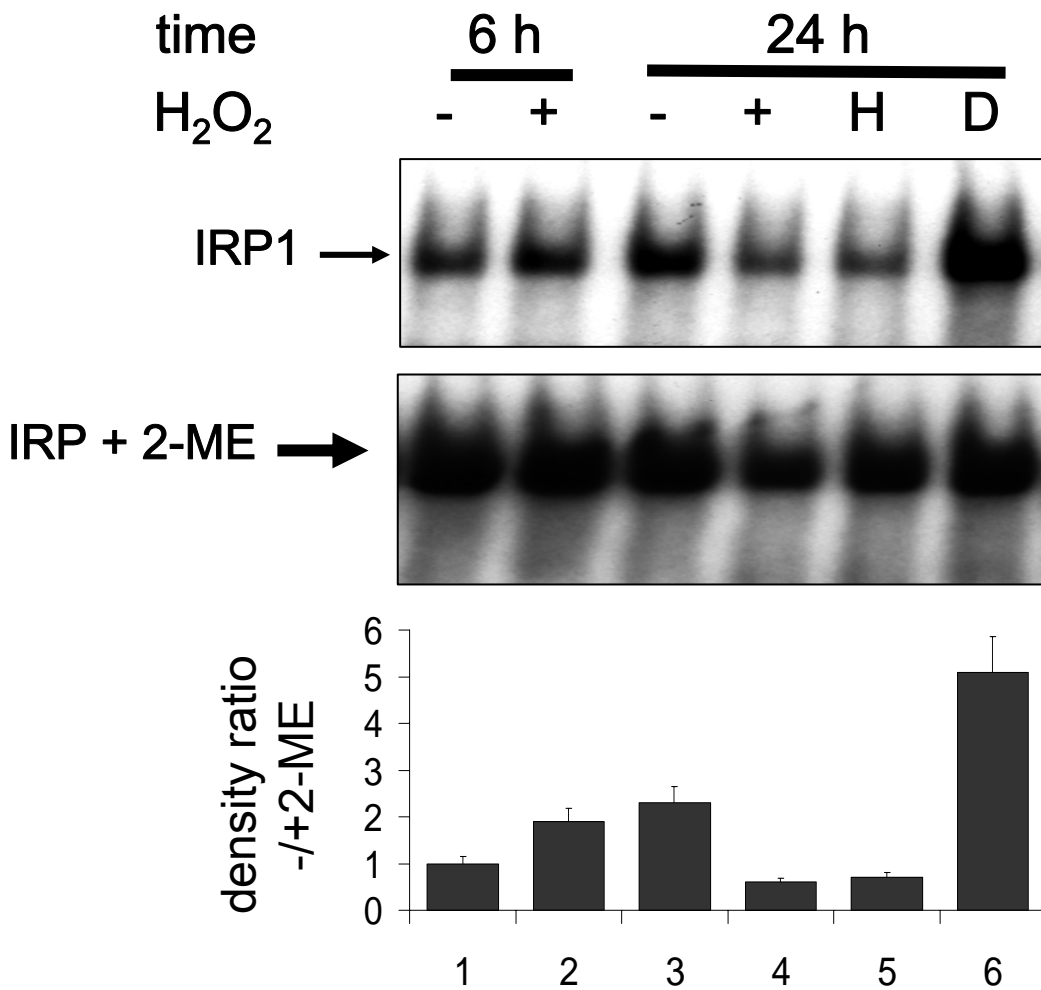


Fig. 5A

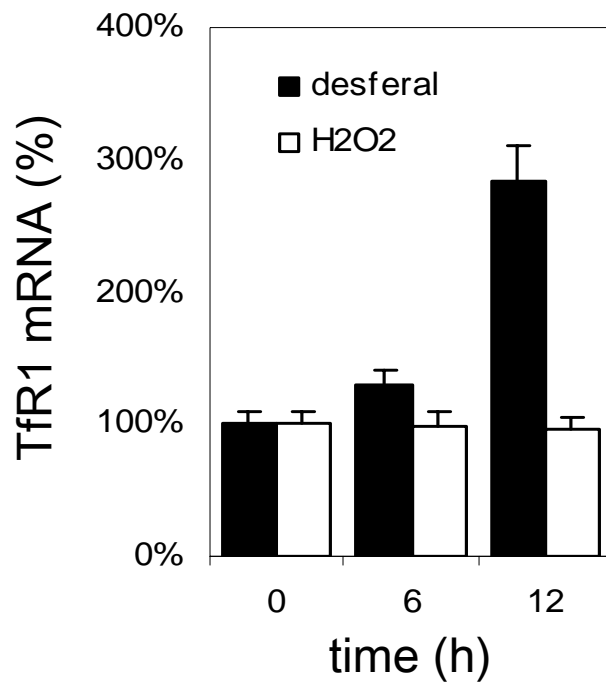


Fig. 5B

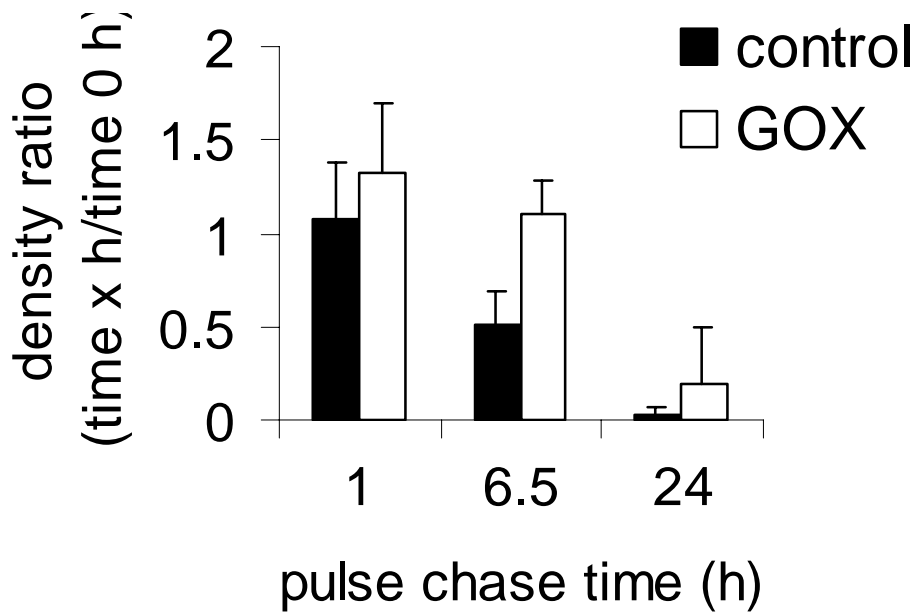
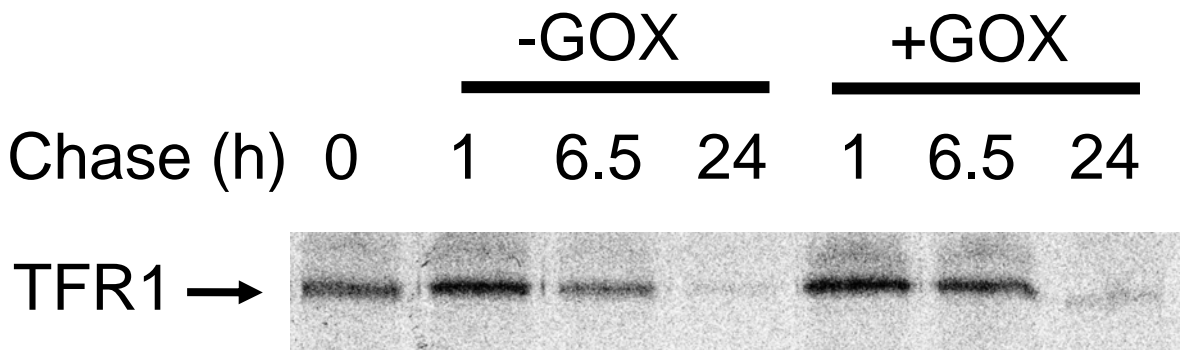


Fig. 6

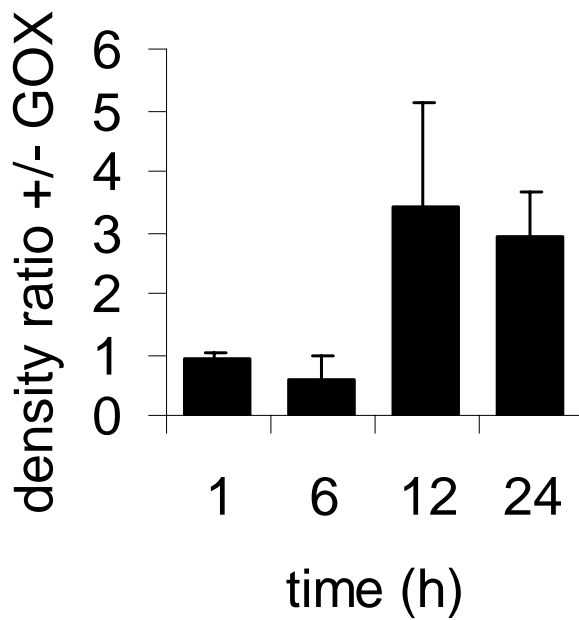
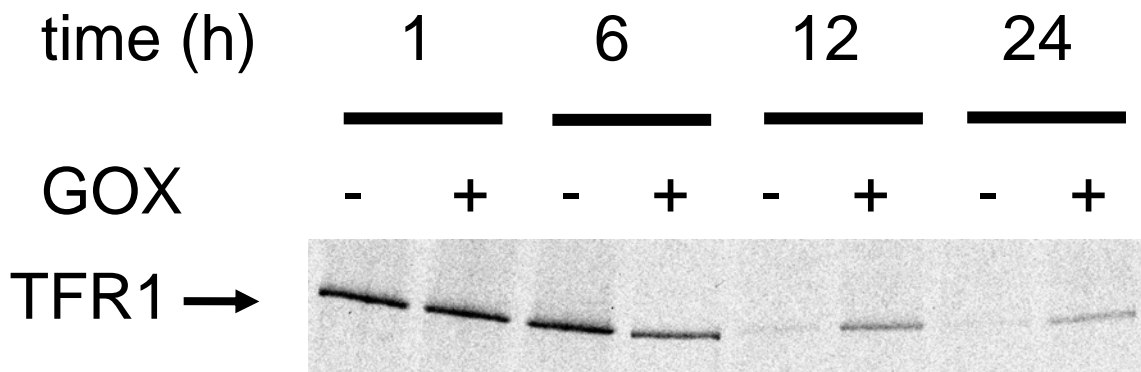


Fig. 7

FIGURE LEGENDS

Fig. 1. Exposure of cultured cells to sustained non-toxic H₂O₂.

(A) Combination of glucose oxidase and catalase (GOX/CAT) is able to maintain stable H₂O₂ concentrations over 24 hours in culture medium (DMEM). H₂O₂ was determined at different time points using the luminol/hypochlorite assay (see *materials and method*). The medium was replaced every twelve hours. Final enzyme activities: $k_{\text{CAT}} = 4.8 \times 10^{-3} \text{ s}^{-1}$ and $k_{\text{GOX}} = 2.4 \times 10^{-8} \text{ M s}^{-1}$.

(B) B6 fibroblasts were exposed to varying stable concentrations of H₂O₂ for 24 h in the presence of either 1:20.000 GOX ($k_{\text{GOX}} = 1.2 \times 10^{-7} \text{ M s}^{-1}$) or 1:100.000 GOX ($k_{\text{GOX}} = 2.4 \times 10^{-8} \text{ M s}^{-1}$) and cell viability was determined with the MTT assay. Variation of H₂O₂ concentration at the fixed amounts of GOX were achieved by increasing activities of external catalase. Each point reflects the average of eight measurements; *bars*, SD.

Fig. 2. Sustained H₂O₂ induced expression of TfR1 without repression of ferritin.

(A) B6 fibroblasts were exposed to stable concentrations of 5 μM H₂O₂ similar as described in Fig. 1A and expression of TfR1 was analyzed by Western blotting (*upper panel*). The *middle panel* shows TfR1 expression of the untreated control. The *lower panel* shows the ratio of H₂O₂-treated versus untreated controls as obtained by densitometry. The depicted experiment is representative of 3 independent measurements.

(B) B6 fibroblasts were treated for 24 h with the iron chelator desferroxamine (D), hemine (H), two different sustained concentrations of H₂O₂ and expression of TfR1, ferritin and β -actin was determined by Western blotting. In contrast to iron depletion by

desferroxamine, sustained H_2O_2 slightly increases ferritin levels in addition to TfR1 induction. The depicted experiment is representative of 3 independent measurements.

Fig. 3. GOX induces TfR1 expression by H_2O_2 in the absence of hypoxia.

(A) GOX activities that are sufficient to induce TfR1 (GOX 1x) do not change oxygen levels while high activities of GOX (GOX 10x) are able to induce hypoxia in the cell culture medium. Oxygen levels were measured with an oxygen electrode in the presence of varying GOX activities in a 10 cm culture dish containing 45 ml medium and 25 mM glucose. GOX 1x corresponds to $k_{\text{GOX}} = 3.0 \times 10^{-8} \text{ M s}^{-1}$. (B) Expression of HIF-1 α was measured in HepG2 cells that were exposed to different levels of sustained H_2O_2 . An oxygen chamber (6% oxygen) was used as positive control. HIF1 α was rapidly induced within 4 hours. No HIF1 α induction was observed with the GOX/CAT system (GOX 1x) generating 1 or 10 μM of sustained H_2O_2 although TfR1 is induced under these conditions (see Fig. 2). Catalase was used to adjust H_2O_2 levels. *Lanes (medium volume, k_{GOX} , k_{CAT}):* lane 1 – 10 ml, 0,0; lane 2 – 10 ml, 3% oxygen, lane 3 – 10 ml, $2.4 \times 10^{-8} \text{ M s}^{-1}$, $2.4 \times 10^{-2} \text{ s}^{-1}$, lane 4 – 10 ml, $4.8 \times 10^{-8} \text{ M s}^{-1}$, $4.8 \times 10^{-3} \text{ s}^{-1}$. The depicted experiment is representative of 3 independent measurements.

Fig. 4. TfR1 expression is functional and leads to accumulation of the intracellular labile iron pool (LIP).

(A) The uptake of ^{59}Fe -labeled diferric transferrin is induced in the presence of continuous release of H_2O_2 over 24 hours. B6 fibroblasts were exposed to GOX/CAT to

obtain sustained H₂O₂ concentrations as indicated. Each point reflects the average of five measurements; *bars*, SD.

(B) Increase of labile iron pool in the presence of a continuous non-toxic flux of H₂O₂ over 24 hours in B6 fibroblasts. Conditions are similar as described in Fig. 1. 100 μM desferal was used as negative control to deplete B6 fibroblasts of iron. The depicted experiment is representative of eight independent measurements; *bars*, SD.

Fig. 5. H₂O₂ induces TfR1 expression in B6 cells independently of the IRE/IRP network.

(A) Cytoplasmic extracts (25 μg) were analyzed by EMSA with 25,000 cpm of ³²P-labeled IRE probe (*upper panel*) or presence of 2% 2-mercaptoethanol (*medium panel*). The *lower panel* shows the ratio of 2-mercaptoethanol-treated (loading control) versus untreated lysates as obtained by densitometry. IRP1 activity was assessed in the absence or presence of H₂O₂ for 6 or 24 h (lanes 1-4). Treatments with 100 μM desferrioxamine or hemin were used as positive and negative control, respectively (lane 5 and 6). Other conditions are as described in Fig. 1. The depicted results are representative of 3 independent experiments.

(B) Mouse B6 fibroblasts were treated with sustained H₂O₂ using a GOX/CAT system as in Fig. 1. TfR1 mRNA levels were analyzed by quantitative RT-PCR and expressed relative to β-actin mRNA. Data from 3 independent experiments are shown (mean ±SD). Iron depletion in the presence of 100 μM desferrioxamine served as positive control strongly inducing TfR1 mRNA via IRP1 as shown in Fig. 5A.

Fig. 6. H₂O₂ induces TfR1 expression in B6 cells independently of protein stability

B6 cells were pulsed for 1 hour with [³⁵S] methionine and subsequently either treated or untreated with GOX for 1, 6, 12 or 24 hours. Immunoprecipitated TfR1 was analysed by SDS/PAGE and visualized by autoradiography (A). Radioactive bands were quantified by phosphorimaging (B). Densitometry data is represented as ratio of a chase time point over time 0.

Fig. 7. H₂O₂ induces TfR1 expression in B6 cells via direct stimulation of translation.

B6 cells were either treated or untreated with GOX for 1, 6, 12 and 24 h. Following the indicated time points, cells were pulsed for 1 hour with [³⁵S] methionine. Immunoprecipitated TfR1 was analysed by SDS/PAGE and visualized by autoradiography (A). Radioactive bands were quantified by phosphorimaging (B). Densitometry data is represented as GOX treated cells over untreated cells.

CHAPTER V. DISCUSSION

In 2004, the discovery of HJV [2] as the second gene responsible for JH led us to engineer overexpressing cell models for both WT and disease associated mutant G320V HJV. This system was used to observe how HJV reacts to different sources of iron. Surprisingly, the only detected effect of these treatments was the release of sHJV upon hemin treatment. Interestingly, modulation of intracellular heme failed to promote sHJV release.

As observed in Chapter II, Fig. 2A, 2B, 3E and 3F, ferritin induction upon treatment with different iron sources did not match that of 100 μ M hemin treatment. In fact, Fe-SIH was the only iron source to match a 100 μ M hemin induction of ferritin but caused no release (data not shown). Taken together, the iron status in the cell as reflected by ferritin levels does not modulate sHJV release.

Previously published data reported that basal shedding of sHJV was inhibited by holo-Tf treatment [1, 106, 107]. In contrast, the overexpressing cell models used in Chapter II lacked basal release of sHJV. However, continuous release was observed in our differentiated muscle cells. We speculate that the reason for this discrepancy may be linked to the levels of neogenin in our H1299 cells. Neogenin has been shown to mediate shedding of sHJV [107].

During the early stages of hemin treatment, it seems that the release of WT sHJV is more pronounced than in the mutant form. However, in a prolonged 24 hour treatment, the amounts of released WT and mutant HJV were similar. This is indicative that the rate of processing during regulated release of sHJV is compromised. This is consistent with previous work illustrating defective processing of G320V mutant HJV in transiently transfected cells.

Although not completely resolved, we gained valuable insight into the mechanisms that mediate hemin induced release of sHjv. The involvement of HO-1 activity and the secretory pathway in sHjv release were ruled out. This suggests that the mechanism of release is most likely by cleavage from the plasma membrane and is currently being addressed with localization experiments. Cleavage from the membrane may occur through either PI-PLC or a number of proteases. The origin of these proteolytic factors was not in the fetal bovine serum used in cell culture. This implies that hemin may promote the activation of a factor(s) that originates from the cell.

Under more physiologically relevant conditions, sHjv release was observed in muscle cells and upon treatment with human hemolysates. Although the marked release of sHjv upon hemin treatment was intriguing, the physiological significance behind this phenomenon was metagrobolizing. Having established that hemolysis (represented experimentally by hemin, hemoglobin and human hemolysate), was a potent promoter of sHjv release, we turned to animal models to understand the physiological relevance.

Injection of mice with the hemolytic inducing agent PHZ, promoted a significant and prolonged increase in serum sHjv. The elevated and sustained levels of sHjv were consistent with our in vitro data. To see if this increase had any physiological impact on iron metabolism we measured hepcidin expression. Consistent with previously published reports [174, 205], a robust transient increase in hepatic hepcidin followed by a significant suppression was observed in these hemolytic mice. It is well established that the suppression of hepcidin following a lag upon injection occurs by an unidentified erythroid regulator. This erythroid regulator is thought to mobilize iron stores and increase absorption to meet the demands for erythropoiesis. In contrast, the transient

increase observed in past reports received very little attention. Physiologically, this induction could favor reutilization of heme iron from haptoglobin and hemopexin scavenging systems for erythropoiesis. We propose that the early induction of hepcidin expression occurs through a novel positive regulatory role for sHjv.

This proposal contradicts previously published reports suggesting that sHjv is a negative regulator of hepcidin expression. However, it should be carefully noted that all work previously published studying the function of sHjv have utilized truncated and recombinant forms [1, 4, 5]. Please refer to section “11.4.1.3.6.3. Soluble Hjv” in Chapter II for a comprehensive review of the different forms used to illustrate negative regulation of hepcidin expression by sHjv.

To address this conflicting issue, conditioned media containing *physiologically made* WT or G320V sHjv from hemin treated cells was applied to target hepatoma cells. We demonstrate that conditioned media with WT sHjv significantly induced hepcidin expression in hepatomas, whereas this acclivity was attenuated with G320V sHjv. Furthermore, liver cells treated with sera from healthy volunteers displayed augmented hepcidin mRNA levels, though sera from diseased patients blunted this response. In addition, a blot of sera from healthy volunteers and JH patients revealed that sHjv was present in relatively similar amounts. This suggests that G320V is a mutation affecting the function of sHjv. Taken together, sHjv released upon hemin treatment is necessary to positively regulate hepcidin expression where this response is blunted in JH patients with the G320V mutation.

This observation brings novel and unique insight into understanding the pathophysiology of JH. Intravascular hemolysis normally occurs in 10%-20% of red

blood cells [206], which suggests that sHjv shedding in response to heme may have a (patho) physiological role. This further alludes that JH patients with a G320V mutation lack this handling mechanism of hemolysis which may contribute to their iron overload pathology.

Importantly, positive regulation of hepcidin by sHjv was not only restricted to hemolytic conditions but also during development.

During the course of a developing mouse, hepcidin and Hjv mRNA expression in the liver have been shown to be differentially regulated [59, 115, 203]. We observed that the unique expression pattern of hepcidin from E14.5 to day 56 of its life, significantly correlated with sHjv levels present in the circulation. It should be noted that the positive correlation was strongest up until day 15. We speculate that other overriding factors take over after day 15 and are responsible for hepcidin induction until day 56 (and possibly beyond).

Mice injected with iron dextran or fed either a low or high iron diet displayed no changes in sHjv levels. These results were consistent with our in vitro data which showed no effect of sHjv release when treated with different sources of iron. This observation is in contrast to a previously published report where mice on an iron deficient diet for 21 days had significantly lower circulating sHjv [107]. When comparing our data with those reported, we observe two differences that may explain this discrepancy. Firstly, we are using different mouse strains from those published in the report. Secondly, transferrin saturation during a low iron diet in the reported mice was significantly lower than ours.

Taken together, we provide evidence of a novel function of predominantly muscle-derived sHjv to either directly or indirectly activate hepcidin in the liver during periods of hemolysis.

Chapter III takes a more in depth look at the molecular mechanisms of hepcidin/macrophage interaction. A co-culture system was used which consisted of hepcidin producing hepatomas and monocytes. Hepcidin production was achieved by either IL-6 stimulation or overexpression in hepatomas. Consistent with a previous report [62], we observed a significant increase in hepcidin expression 1-2 hours after IL-6 treatment.

As illustrated in Chapter III, hepcidin producing hepatomas are capable of inhibiting iron export by ~30-35% in co-cultured monocytes. The mechanism of iron export inhibition is probably via hepcidin binding, internalizing and degrading the iron exporter ferroportin. To date, in vitro data have failed to produce a 100% hepcidin derived inhibition of iron export from macrophages. More specifically, macrophages treated with chemically synthesized hepcidin undergo a maximum 51% inhibition of iron export in comparison to untreated cells [7]. The 51% inhibition was accompanied by a significant decrease in the iron exporter ferroportin in these macrophages [7]. If we assume that in vivo, a robust induction of hepcidin is capable of exerting a maximum inhibition of ~ 50%, then serum iron is expected to drop by 12.5% every hour. To calculate 12.5%: every 24 hours, approximately 20 mg of iron flows through a plasma transferrin compartment that contains at any moment about 3 mg of iron. Thus, every 3-4 hours there is a complete turnover of plasma iron at an approximate rate of 0.83 mg/hour. A 100% inhibition of plasma turnover would cause a ~25% decrease in serum iron/hour

(0.83 mg/hour divided by 3 mg equals ~0.25, multiplied by 100% is ~25%). Hence, 50% inhibition would be 12.5% serum iron/hour. This rate of 12.5% serum iron/hour is almost in range with a 34% reduction in serum iron observed in humans 2 hours after IL-6 infusion [62].

Importantly, inhibition of monocytic iron export by physiologically generated hepcidin further resulted in increased ferritin synthesis in an IRP2 dependent mechanism. Taken together, we illustrate through co-culture studies that hepcidin is a potent inhibitor of macrophage iron export. Furthermore, hepcidin induced iron retention within macrophages is the most likely the cause of hypoferremia in patients with ACD.

Hypoferremia observed in patients with ACD have increased iron retention in the RES. Containment and redistribution of iron into the RES deprives invading pathogens of their necessary iron. In addition, iron may also accumulate in the parenchyma of the liver which can drive the progression of fibrosis and end-stage liver disease in common liver pathologies such as chronic hepatitis C or alcoholic steatohepatitis.

In Chapter IV, we show that cells exposed to chronic H₂O₂ undergo changes in iron homeostasis. More specifically, we developed a glucose oxidase/catalase (GOX/CAT) system that generated non-toxic levels of H₂O₂ for a prolonged period of time. The 5 μM H₂O₂ generated in this system was similar to those produced by leukocytes in vivo (<10 μM) [284]. B6 fibroblasts and Huh7 hepatomas exposed to these levels, dramatically upregulated TfR1 levels in an IRP/IRE independent mechanism. In contrast, previous work illustrated that a transient and high dose treatment of H₂O₂ rapidly induced IRP1 binding activity which was sufficient to increase TfR1 levels [158]. However, since H₂O₂ is rapidly degraded, transient pulses of H₂O₂ does not reflect the

continuous release by inflammatory cells. Thus our GOX/CAT system, which provides sustained and non-toxic levels of H₂O₂ to cells, mimics a chronic inflammatory condition.

Having ruled out an IRP/IRE dependent mechanism of TfR1 induction, we explored other possibilities. Because GOX activity requires the consumption of oxygen, the possibility of HIF-1 α dependent induction of TfR1 as a result of hypoxia was investigated. Even at high concentrations of GOX, % oxygen was not sufficiently decreased to promote HIF-1 α levels. Thus, TfR1 induction was not a result of hypoxia. Furthermore, elevated TfR1 levels exposed to sustained and non-toxic levels of H₂O₂ were independent of increased protein stability.

Interestingly, the mechanism in which H₂O₂ increased the levels of TfR1 was via direct stimulation of translation. Oxidative stress has previously been shown to modulate translation but this control is complex and depends highly on conditions and cell type [273-278]. Work is currently underway to further define the translational activation of TfR1 under these inflammatory conditions.

TfR1 upregulation by H₂O₂ was shown to be functional and resulted in iron accumulation. Although a modest increase in ferritin was observed, a more significant increase in the labile iron pool and uptake of radioactively labelled holo-Tf was detected.

Taken together, during inflammatory conditions, chronic exposure to H₂O₂ released by inflammatory cells may induce iron accumulation in the liver parenchyma via direct stimulation of TfR1 translation. This accumulation on one hand serves as a protective mechanism to deprive pathogens of iron. On the other hand, continued accumulation could damage the cells themselves.

In conclusion, iron overload in the liver may be defined as elevated iron retention in the RES or increased iron accumulation in the parenchyma. In ACD, the body responds to an invading pathogen by restricting iron in the RES by increasing hepcidin production. Certain types of inflammatory conditions such as those that develop fibrosis or end-stage liver disease, display increased iron accumulation in the parenchyma. The mechanism of increased iron uptake in the parenchyma is mediated by H₂O₂ stimulation of TfR1 translation. Dangerous iron deposits in the parenchyma are also observed during JH. Patients with this genetic disease, express inappropriately low levels of hepcidin. As a consequence, elevated ferroportin levels increase iron mobilization from stores (and increased iron absorption) and subsequently saturates serum transferrin.

When all is said and done, many non-mutually exclusive molecular mechanisms drive the alterations in iron homeostasis observed during hemochromatosis and anemia.

REFERENCES

1. Lin, L., Y.P. Goldberg, and T. Ganz, *Competitive regulation of hepcidin mRNA by soluble and cell-associated hemojuvelin*. Blood, 2005. **106**: p. 2884-2889.
2. Papanikolaou, G., et al., *Mutations in HFE2 cause iron overload in chromosome 1q-linked juvenile hemochromatosis*. Nat. Genet., 2004. **36**: p. 77-82.
3. Babitt, J.L., et al., *Bone morphogenetic protein signaling by hemojuvelin regulates hepcidin expression*. Nat. Genet., 2006. **38**: p. 531-539.
4. Babitt, J.L., et al., *Modulation of bone morphogenetic protein signaling in vivo regulates systemic iron balance*. J Clin Invest, 2007. **117**(7): p. 1933-9.
5. Lin, L., et al., *Iron-transferrin regulates hepcidin synthesis in primary hepatocyte culture through hemojuvelin and BMP2/4*. Blood, 2007.
6. Nemeth, E., et al., *Hepcidin regulates cellular iron efflux by binding to ferroportin and inducing its internalization*. Science, 2004. **306**: p. 2090-2093.
7. Knutson, M.D., et al., *Iron release from macrophages after erythrophagocytosis is up-regulated by ferroportin 1 overexpression and down-regulated by hepcidin*. Proc. Natl. Acad. Sci. USA, 2005. **102**: p. 1324-1328.
8. Hirayama, M., et al., *Regulation of iron metabolism in HepG2 cells: a possible role for cytokines in the hepatic deposition of iron*. Hepatology, 1993. **18**: p. 874-880.
9. Upton, R.L., et al., *Variable tissue expression of transferrin receptors: relevance to acute respiratory distress syndrome*. Eur. Respir. J., 2003. **22**: p. 335-341.
10. Pantopoulos, K., et al., *Differences in the regulation of iron regulatory protein 1 (IRP1) by extra- and intracellular oxidative stress*. J. Biol. Chem., 1997. **272**: p. 9802-9808.
11. Finkel, T. and N.J. Holbrook, *Oxidants, oxidative stress and the biology of ageing*. Nature, 2000. **408**(6809): p. 239-47.
12. Halliwell, B., J.M. Gutteridge, and C.E. Cross, *Free radicals, antioxidants, and human disease: where are we now?* J Lab Clin Med, 1992. **119**(6): p. 598-620.
13. Le Bras, M., et al., *Reactive oxygen species and the mitochondrial signaling pathway of cell death*. Histol Histopathol, 2005. **20**(1): p. 205-19.
14. Gunshin, H., et al., *Cloning and characterization of a mammalian proton-coupled metal-ion transporter*. Nature, 1997. **388**(6641): p. 482-8.
15. Mims, M.P. and J.T. Prechal, *Divalent metal transporter 1*. Hematology, 2005. **10**(4): p. 339-45.
16. Mims, M.P., et al., *Identification of a human mutation of DMT1 in a patient with microcytic anemia and iron overload*. Blood, 2005. **105**(3): p. 1337-42.
17. Donovan, A., et al., *Positional cloning of zebrafish ferroportin1 identifies a conserved vertebrate iron exporter*. Nature, 2000. **403**(6771): p. 776-81.
18. McKie, A.T., et al., *A novel duodenal iron-regulated transporter, IREG1, implicated in the basolateral transfer of iron to the circulation*. Mol Cell, 2000. **5**(2): p. 299-309.
19. Abboud, S. and D.J. Haile, *A novel mammalian iron-regulated protein involved in intracellular iron metabolism*. J Biol Chem, 2000. **275**(26): p. 19906-12.
20. Hellman, N.E. and J.D. Gitlin, *Ceruloplasmin metabolism and function*. Annu Rev Nutr, 2002. **22**: p. 439-58.

21. Jeong, S.Y. and S. David, *Glycosylphosphatidylinositol-anchored ceruloplasmin is required for iron efflux from cells in the central nervous system*. J Biol Chem, 2003. **278**(29): p. 27144-8.
22. Ponka, P., C. Beaumont, and D.R. Richardson, *Function and regulation of transferrin and ferritin*. Semin Hematol, 1998. **35**(1): p. 35-54.
23. Kawabata, H., et al., *Expression of transferrin receptor 2 in normal and neoplastic hematopoietic cells*. Blood, 2001. **98**(9): p. 2714-9.
24. Kawabata, H., et al., *Molecular cloning of transferrin receptor 2. A new member of the transferrin receptor-like family*. J Biol Chem, 1999. **274**(30): p. 20826-32.
25. Levy, J.E., et al., *Transferrin receptor is necessary for development of erythrocytes and the nervous system*. Nat. Genet., 1999. **21**: p. 396-399.
26. Harrison, P.M. and P. Arosio, *The ferritins: molecular properties, iron storage function and cellular regulation*. Biochim Biophys Acta, 1996. **1275**(3): p. 161-203.
27. Theil, E.C., *Ferritin: at the crossroads of iron and oxygen metabolism*. J Nutr, 2003. **133**(5 Suppl 1): p. 1549S-53S.
28. Ferreira, C., et al., *Early embryonic lethality of H ferritin gene deletion in mice*. J Biol Chem, 2000. **275**(5): p. 3021-4.
29. Ferreira, C., et al., *H ferritin knockout mice: a model of hyperferritinemia in the absence of iron overload*. Blood, 2001. **98**(3): p. 525-32.
30. Liu, X., W. Jin, and E.C. Theil, *Opening protein pores with chaotropes enhances Fe reduction and chelation of Fe from the ferritin biomineral*. Proc Natl Acad Sci U S A, 2003. **100**(7): p. 3653-8.
31. Radisky, D.C. and J. Kaplan, *Iron in cytosolic ferritin can be recycled through lysosomal degradation in human fibroblasts*. Biochem J, 1998. **336** (Pt 1): p. 201-5.
32. Levi, S., et al., *A human mitochondrial ferritin encoded by an intronless gene*. J Biol Chem, 2001. **276**(27): p. 24437-40.
33. Cazzola, M., et al., *Mitochondrial ferritin expression in erythroid cells from patients with sideroblastic anemia*. Blood, 2003. **101**(5): p. 1996-2000.
34. Roetto, A., et al., *Pathogenesis of hyperferritinemia cataract syndrome*. Blood Cells Mol Dis, 2002. **29**(3): p. 532-5.
35. Rouault, T.A., *Post-transcriptional regulation of human iron metabolism by iron regulatory proteins*. Blood Cells Mol Dis, 2002. **29**(3): p. 309-14.
36. LaVaute, T., et al., *Targeted deletion of the gene encoding iron regulatory protein-2 causes misregulation of iron metabolism and neurodegenerative disease in mice*. Nat Genet, 2001. **27**(2): p. 209-14.
37. Samaniego, F., et al., *Molecular characterization of a second iron-responsive element binding protein, iron regulatory protein 2. Structure, function, and post-translational regulation*. J Biol Chem, 1994. **269**(49): p. 30904-10.
38. Cairo, G. and A. Pietrangelo, *Iron regulatory proteins in pathobiology*. Biochem J, 2000. **352** Pt 2: p. 241-50.
39. Fillebeen, C. and K. Pantopoulos, *Redox control of iron regulatory proteins*. Redox Rep, 2002. **7**(1): p. 15-22.
40. Pantopoulos, K., *Iron metabolism and the IRE/IRP regulatory system: an update*. Ann. N Y Acad. Sci., 2004. **1012**: p. 1-13.

41. Pantopoulos, K. and M.W. Hentze, *Rapid responses to oxidative stress mediated by iron regulatory protein*. *Embo J*, 1995. **14**(12): p. 2917-24.
42. Pantopoulos, K., et al., *Differences in the regulation of iron regulatory protein-1 (IRP-1) by extra- and intracellular oxidative stress*. *J Biol Chem*, 1997. **272**(15): p. 9802-8.
43. Guo, B., Y. Yu, and E.A. Leibold, *Iron regulates cytoplasmic levels of a novel iron-responsive element-binding protein without aconitase activity*. *J Biol Chem*, 1994. **269**(39): p. 24252-60.
44. Henderson, B.R. and L.C. Kuhn, *Differential modulation of the RNA-binding proteins IRP-1 and IRP-2 in response to iron. IRP-2 inactivation requires translation of another protein*. *J Biol Chem*, 1995. **270**(35): p. 20509-15.
45. Guo, B., et al., *Iron regulates the intracellular degradation of iron regulatory protein 2 by the proteasome*. *J Biol Chem*, 1995. **270**(37): p. 21645-51.
46. Iwai, K., R.D. Klausner, and T.A. Rouault, *Requirements for iron-regulated degradation of the RNA binding protein, iron regulatory protein 2*. *Embo J*, 1995. **14**(21): p. 5350-7.
47. Pantopoulos, K. and M.W. Hentze, *Nitric oxide signaling to iron-regulatory protein: direct control of ferritin mRNA translation and transferrin receptor mRNA stability in transfected fibroblasts*. *Proc Natl Acad Sci U S A*, 1995. **92**(5): p. 1267-71.
48. Recalcati, S., et al., *Nitric oxide-mediated induction of ferritin synthesis in J774 macrophages by inflammatory cytokines: role of selective iron regulatory protein-2 downregulation*. *Blood*, 1998. **91**(3): p. 1059-66.
49. Bouton, C., L. Oliveira, and J.C. Drapier, *Converse modulation of IRP1 and IRP2 by immunological stimuli in murine RAW 264.7 macrophages*. *J Biol Chem*, 1998. **273**(16): p. 9403-8.
50. Kim, S. and P. Ponka, *Effects of interferon-gamma and lipopolysaccharide on macrophage iron metabolism are mediated by nitric oxide-induced degradation of iron regulatory protein 2*. *J Biol Chem*, 2000. **275**(9): p. 6220-6.
51. Kim, S. and P. Ponka, *Nitrogen monoxide-mediated control of ferritin synthesis: implications for macrophage iron homeostasis*. *Proc Natl Acad Sci U S A*, 2002. **99**(19): p. 12214-9.
52. Pantopoulos, K., G. Weiss, and M.W. Hentze, *Nitric oxide and oxidative stress (H₂O₂) control mammalian iron metabolism by different pathways*. *Mol Cell Biol*, 1996. **16**(7): p. 3781-8.
53. Boccio, J.R. and V. Iyengar, *Iron deficiency: causes, consequences, and strategies to overcome this nutritional problem*. *Biol. Trace Elem. Res.*, 2003. **94**: p. 1-32.
54. Weiss, G., *Pathogenesis and treatment of anaemia of chronic disease*. *Blood Rev.*, 2002. **16**: p. 87-96.
55. Bomford, A., *Genetics of haemochromatosis*. *Lancet*, 2002. **360**: p. 1673-1681.
56. Pippard, M.J., *Secondary iron overload*. *Iron metabolism in health and disease*, ed. J.H. Brock, et al. 1994, London: W. B. Saunders Company Ltd. 271-309.
57. Krause, A., et al., *LEAP-1, a novel highly disulfide-bonded human peptide, exhibits antimicrobial activity*. *FEBS Lett.*, 2000. **480**: p. 147-150.

58. Nicolas, G., et al., *Lack of hepcidin gene expression and severe tissue iron overload in upstream stimulatory factor 2 (USF2) knockout mice*. Proc. Natl. Acad. Sci. USA, 2001. **98**: p. 8780-8785.
59. Nicolas, G., et al., *Severe iron deficiency anemia in transgenic mice expressing liver hepcidin*. Proc. Natl. Acad. Sci. USA, 2002. **99**: p. 4596-4601.
60. Nemeth, E., et al., *The N-terminus of hepcidin is essential for its interaction with ferroportin: structure-function study*. Blood, 2005.
61. De Domenico, I., et al., *The molecular basis of ferroportin-linked hemochromatosis*. Proc. Natl. Acad. Sci. USA, 2005. **102**: p. 8955-8960.
62. Nemeth, E., et al., *IL-6 mediates hypoferremia of inflammation by inducing the synthesis of the iron regulatory hormone hepcidin*. J. Clin. Invest., 2004. **113**: p. 1271-1276.
63. Pigeon, C., et al., *A new mouse liver-specific gene, encoding a protein homologous to human antimicrobial peptide hepcidin, is overexpressed during iron overload*. J. Biol. Chem., 2001. **276**: p. 7811-7819.
64. Camaschella, C., et al., *The gene TFR2 is mutated in a new type of haemochromatosis mapping to 7q22*. Nat. Genet., 2000. **25**: p. 14-15.
65. Feder, J.N., et al., *A novel MHC class I-like gene is mutated in patients with hereditary haemochromatosis*. Nature Genet., 1996. **13**: p. 399-408.
66. Roetto, A., et al., *Mutant antimicrobial peptide hepcidin is associated with severe juvenile hemochromatosis*. Nat. Genet., 2003. **33**: p. 21-22.
67. Feder, J.N., et al., *The hemochromatosis founder mutation in HLA-H disrupts β_2 -microglobulin interaction and cell surface expression*. J. Biol. Chem., 1997. **272**: p. 14025-14028.
68. Zhou, X.Y., et al., *HFE gene knockout produces mouse model of hereditary hemochromatosis*. Proc. Natl. Acad. Sci. USA, 1998. **95**: p. 2492-2497.
69. Bahram, S., et al., *Experimental hemochromatosis due to MHC class I HFE deficiency: immune status and iron metabolism*. Proc. Natl. Acad. Sci. USA, 1999. **96**: p. 13312-13317.
70. Levy, J.E., et al., *The C282Y mutation causing hereditary hemochromatosis does not produce a null allele*. Blood, 1999. **94**: p. 9-11.
71. Fleming, R.E., et al., *Mouse strain differences determine severity of iron accumulation in Hfe knockout model of hereditary hemochromatosis*. Proc. Natl. Acad. Sci. USA, 2001. **98**: p. 2707-2711.
72. Dupic, F., et al., *Inactivation of the hemochromatosis gene differentially regulates duodenal expression of iron-related mRNAs between mouse strains*. Gastroenterology, 2002. **122**: p. 745-751.
73. Lebrón, J.A., A.P. West, Jr., and P.J. Bjorkman, *The hemochromatosis protein HFE competes with transferrin for binding to the transferrin receptor*. J. Mol. Biol., 1999. **294**: p. 239-245.
74. Bennett, M.J., J.A. Lebron, and P.J. Bjorkman, *Crystal structure of the hereditary haemochromatosis protein HFE complexed with transferrin receptor*. Nature, 2000. **403**: p. 46-53.
75. Feder, J.N., et al., *The hemochromatosis gene product complexes with the transferrin receptor and lowers its affinity for ligand binding*. Proc. Natl. Acad. Sci. USA, 1998. **95**: p. 1472-1477.

76. Roy, C.N., et al., *The hereditary hemochromatosis protein, HFE, specifically regulates transferrin-mediated iron uptake in HeLa cells.* J. Biol. Chem., 1999. **274**: p. 9022-9028.
77. Roy, C.N. and C.A. Enns, *Iron homeostasis: new tales from the crypt.* Blood, 2000. **96**: p. 4020-4027.
78. Spasic, M.V., et al., *Physiologic systemic iron metabolism in mice deficient for duodenal Hfe.* Blood, 2007. **109**: p. 4511-4517.
79. Kawabata, H., et al., *Molecular cloning of transferrin receptor 2. A new member of the transferrin receptor-like family.* J. Biol. Chem., 1999. **274**: p. 20826-20832.
80. Kawabata, H., et al., *Expression of transferrin receptor 2 in normal and neoplastic hematopoietic cells.* Blood, 2001. **98**: p. 2714-2719.
81. Kawabata, H., et al., *Transferrin receptor 2- $\{\alpha\}$ supports cell growth both in iron-chelated cultured cells and in vivo.* J. Biol. Chem., 2000. **275**: p. 16618-16625.
82. Johnson, M.B. and C.A. Enns, *Diferic transferrin regulates transferrin receptor 2 protein stability.* Blood, 2004. **104**: p. 4287-4293.
83. Johnson, M.B., et al., *Transferrin receptor 2: evidence for ligand-induced stabilization and redirection to a recycling pathway.* Mol Biol Cell, 2007. **18**(3): p. 743-54.
84. Fleming, R.E., et al., *Transferrin receptor 2: continued expression in mouse liver in the face of iron overload and in hereditary hemochromatosis.* Proc. Natl. Acad. Sci. USA, 2000. **97**: p. 2214-2219.
85. Wallace, D.F., et al., *First phenotypic description of transferrin receptor 2 knockout mouse, and the role of hepcidin.* Gut, 2005. **54**: p. 980-986.
86. Huang, F.W., et al., *A mouse model of juvenile hemochromatosis.* J. Clin. Invest., 2005. **115**: p. 2187-2191.
87. Niederkofler, V., R. Salie, and S. Arber, *Hemojuvelin is essential for dietary iron sensing, and its mutation leads to severe iron overload.* J. Clin. Invest., 2005. **115**: p. 2180-2186.
88. Rodriguez, A., P. Pan, and S. Parkkila, *Expression studies of neogenin and its ligand hemojuvelin in mouse tissues.* J. Histochem. Cytochem., 2007. **55**: p. 85-96.
89. Kuninger, D., et al., *Complex biosynthesis of the muscle-enriched iron regulator RGMc.* J. Cell Sci., 2006. **119**: p. 3273-3283.
90. Zhang, A.S., et al., *Interaction of HJV with neogenin results in iron accumulation in HEK293 cells.* J. Biol. Chem., 2005. **280**: p. 33885-33894.
91. Voet, D. and J.G. Voet, *Biochemistry.* 3rd ed. 2004, Hoboken, NJ: J. Wiley & Sons. xv, 1591.
92. Ludbrook, S.B., et al., *The integrin α v β 3 is a receptor for the latency-associated peptides of transforming growth factors β 1 and β 3.* Biochem J, 2003. **369**(Pt 2): p. 311-8.
93. Collins, J.F., *Gene chip analyses reveal differential genetic responses to iron deficiency in rat duodenum and jejunum.* Biol Res, 2006. **39**(1): p. 25-37.
94. Maeda, Y., H. Ashida, and T. Kinoshita, *CHO glycosylation mutants: GPI anchor.* Methods Enzymol, 2006. **416**: p. 182-205.

95. Lanzara, C., et al., *The spectrum of hemojuvelin gene mutations in 1q-linked juvenile hemochromatosis*. Blood, 2004. **11**: p. 4317-4321.
96. Gehrke, S.G., et al., *HJV gene mutations in European patients with juvenile hemochromatosis*. Clin Genet, 2005. **67**(5): p. 425-8.
97. Lee, P.L., et al., *Genetic abnormalities and juvenile hemochromatosis: mutations of the HJV gene encoding hemojuvelin*. Blood, 2004.
98. Beutler, L. and E. Beutler, *Hematologically important mutations: iron storage diseases*. Blood Cells Mol Dis, 2004. **33**(1): p. 40-4.
99. Daraio, F., et al., *Juvenile hemochromatosis due to G320V/Q116X compound heterozygosity of hemojuvelin in an Irish patient*. Blood Cells Mol Dis, 2005. **35**(2): p. 174-6.
100. Koyama, C., et al., *Three patients with middle-age-onset hemochromatosis caused by novel mutations in the hemojuvelin gene*. J Hepatol, 2005. **43**(4): p. 740-2.
101. Huang, F.W., et al., *Identification of a novel mutation (C321X) in HJV*. Blood, 2004. **104**: p. 2176-2177.
102. Lee, P., et al., *A juvenile hemochromatosis patient homozygous for a novel deletion of cDNA nucleotide 81 of hemojuvelin*. Acta Haematol, 2006. **115**(1-2): p. 123-7.
103. Janosi, A., et al., *Homozygosity for a novel nonsense mutation (G66X) of the HJV gene causes severe juvenile hemochromatosis with fatal cardiomyopathy*. Blood, 2005. **105**(1): p. 432.
104. Lee, P.L., et al., *Hemojuvelin (HJV) mutations in persons of European, African-American and Asian ancestry with adult onset haemochromatosis*. Br J Haematol, 2004. **127**(2): p. 224-9.
105. Camus, L.M. and L.A. Lambert, *Molecular evolution of hemojuvelin and the repulsive guidance molecule family*. J Mol Evol, 2007. **65**(1): p. 68-81.
106. Silvestri, L., et al., *Defective targeting of hemojuvelin to plasma membrane is a common pathogenetic mechanism in juvenile hemochromatosis*. Blood, 2007: p. in press.
107. Zhang, A.S., et al., *Evidence that inhibition of hemojuvelin shedding in response to iron is mediated through neogenin*. J. Biol. Chem., 2007: p. in press.
108. Zhang, L. and R.S. Jope, *Oxidative stress differentially modulates phosphorylation of ERK, p38 and CREB induced by NGF or EGF in PC12 cells*. Neurobiol. Aging, 1999. **20**(3): p. 271-278.
109. Huang, J. and R.J. Schneider, *Adenovirus inhibition of cellular protein synthesis involves inactivation of cap-binding protein*. Cell, 1991. **65**: p. 271-280.
110. Samad, T.A., et al., *DRAGON, a bone morphogenetic protein co-receptor*. J Biol Chem, 2005. **280**(14): p. 14122-9.
111. Babbitt, J.L., et al., *Repulsive guidance molecule (RGMa), a DRAGON homologue, is a bone morphogenetic protein co-receptor*. J Biol Chem, 2005. **280**(33): p. 29820-7.
112. Miyazono, K., K. Kusanagi, and H. Inoue, *Divergence and convergence of TGF-beta/BMP signaling*. J Cell Physiol, 2001. **187**(3): p. 265-76.
113. Truksa, J., et al., *Bone morphogenetic proteins 2, 4, and 9 stimulate murine hepcidin 1 expression independently of Hfe, transferrin receptor 2 (Tfr2), and IL-6*. Proc. Natl. Acad. Sci. USA, 2006. **103**: p. 10289-10293.

114. Wang, R.H., et al., *A role of SMAD4 in iron metabolism through the positive regulation of hepcidin expression*. Cell Metab., 2005. **2**: p. 399-409.
115. Krijt, J., et al., *Expression of Rgmc, the murine ortholog of hemojuvelin gene, is modulated by development and inflammation, but not by iron status or erythropoietin*. Blood, 2004. **104**: p. 4308-4310.
116. Nemeth, E., et al., *Hepcidin, a putative mediator of anemia of inflammation, is a type II acute-phase protein*. Blood, 2003. **101**: p. 2461-2463.
117. Lee, P., et al., *The IL-6- and lipopolysaccharide-induced transcription of hepcidin in HFE-, transferrin receptor 2-, and beta 2-microglobulin-deficient hepatocytes*. Proc. Natl. Acad. Sci. USA, 2004. **101**: p. 9263-9265.
118. Schmidtmer, J. and D. Engelkamp, *Isolation and expression pattern of three mouse homologues of chick Rgm*. Gene Expr Patterns, 2004. **4**(1): p. 105-10.
119. Oldekamp, J., et al., *Expression pattern of the repulsive guidance molecules RGM A, B and C during mouse development*. Gene Expr Patterns, 2004. **4**(3): p. 283-8.
120. Niederkofler, V., et al., *Repulsive guidance molecule (RGM) gene function is required for neural tube closure but not retinal topography in the mouse visual system*. J Neurosci, 2004. **24**(4): p. 808-18.
121. Brinks, H., et al., *The repulsive guidance molecule RGMa is involved in the formation of afferent connections in the dentate gyrus*. J Neurosci, 2004. **24**(15): p. 3862-9.
122. Monnier, P.P., et al., *RGM is a repulsive guidance molecule for retinal axons*. Nature, 2002. **419**: p. 392-395.
123. Rajagopalan, S., et al., *Neogenin mediates the action of repulsive guidance molecule*. Nat Cell Biol, 2004. **6**(8): p. 756-62.
124. Matsunaga, E., et al., *RGM and its receptor neogenin regulate neuronal survival*. Nat Cell Biol, 2004. **6**(8): p. 749-55.
125. Fortier, A., et al., *Single gene effects in mouse models of host: pathogen interactions*. J Leukoc Biol, 2005. **77**(6): p. 868-77.
126. Goetz, D.H., et al., *The neutrophil lipocalin NGAL is a bacteriostatic agent that interferes with siderophore-mediated iron acquisition*. Mol. Cell, 2002. **10**: p. 1033-1043.
127. Yang, J., et al., *An iron delivery pathway mediated by a lipocalin*. Mol. Cell, 2002. **10**: p. 1045-1056.
128. Flo, T.H., et al., *Lipocalin 2 mediates an innate immune response to bacterial infection by sequestering iron*. Nature, 2004. **432**: p. 917-921.
129. Gangaidzo, I.T., et al., *Association of pulmonary tuberculosis with increased dietary iron*. J Infect Dis, 2001. **184**(7): p. 936-9.
130. Vadillo, M., et al., *Multiple liver abscesses due to Yersinia enterocolitica discloses primary hemochromatosis: three cases reports and review*. Clin Infect Dis, 1994. **18**(6): p. 938-41.
131. Yamashiro, K.M., et al., *Pasteurella pseudotuberculosis. Acute sepsis with survival*. Arch Intern Med, 1971. **128**(4): p. 605-8.
132. Nicolas, G., et al., *The gene encoding the iron regulatory peptide hepcidin is regulated by anemia, hypoxia, and inflammation*. J. Clin. Invest., 2002. **110**: p. 1037-1044.

133. Shike, H., et al., *Bass hepcidin is a novel antimicrobial peptide induced by bacterial challenge*. Eur. J. Biochem., 2002. **269**: p. 2232-2237.
134. Inamura, J., et al., *Upregulation of hepcidin by interleukin-1beta in human hepatoma cell lines*. Hepatol Res, 2005. **33**(3): p. 198-205.
135. Lee, P., et al., *Regulation of hepcidin transcription by interleukin-1 and interleukin-6*. Proc. Natl. Acad. Sci. USA, 2005. **102**: p. 1906-1910.
136. Wrighting, D.M. and N.C. Andrews, *Interleukin-6 induces hepcidin expression through STAT3*. Blood, 2006. **108**: p. 3204-3209.
137. Verga Falzacappa, M.V., et al., *STAT3 mediates hepatic hepcidin expression and its inflammatory stimulation*. Blood, 2007. **109**: p. 353-358.
138. Pietrangelo, A., et al., *STAT3 is required for IL-6-gp130-dependent activation of hepcidin in vivo*. Gastroenterology, 2007. **132**: p. 294-300.
139. Cartwright, G.E., *The anemia of chronic disorders*. Semin Hematol, 1966. **3**(4): p. 351-75.
140. Matzner, Y., et al., *Prevalence and causes of anemia in elderly hospitalized patients*. Gerontology, 1979. **25**(2): p. 113-9.
141. Sullivan, P.S., et al., *Epidemiology of anemia in human immunodeficiency virus (HIV)-infected persons: results from the multistate adult and adolescent spectrum of HIV disease surveillance project*. Blood, 1998. **91**(1): p. 301-8.
142. Nissenson, A.R., L.T. Goodnough, and R.W. Dubois, *Anemia: not just an innocent bystander?* Arch Intern Med, 2003. **163**(12): p. 1400-4.
143. van Iperen, C.E., A. van de Wiel, and J.J. Marx, *Acute event-related anaemia*. Br J Haematol, 2001. **115**(4): p. 739-43.
144. Maury, C.P., et al., *Tumor necrosis factor alpha, its soluble receptor I, and -308 gene promoter polymorphism in patients with rheumatoid arthritis with or without amyloidosis: implications for the pathogenesis of nephropathy and anemia of chronic disease in reactive amyloidosis*. Arthritis Rheum, 2003. **48**(11): p. 3068-76.
145. Gasche, C., et al., *Prediction of response to iron sucrose in inflammatory bowel disease-associated anemia*. Am J Gastroenterol, 2001. **96**(8): p. 2382-7.
146. Wilson, A., E. Reyes, and J. Ofman, *Prevalence and outcomes of anemia in inflammatory bowel disease: a systematic review of the literature*. Am J Med, 2004. **116 Suppl 7A**: p. 44S-49S.
147. Harrison, L.B., D. Shasha, and P. Homel, *Prevalence of anemia in cancer patients undergoing radiotherapy: prognostic significance and treatment*. Oncology, 2002. **63 Suppl 2**: p. 11-8.
148. Ludwig, H., et al., *Prediction of response to erythropoietin treatment in chronic anemia of cancer*. Blood, 1994. **84**(4): p. 1056-63.
149. Rizzo, J.D., et al., *Use of epoetin in patients with cancer: evidence-based clinical practice guidelines of the American Society of Clinical Oncology and the American Society of Hematology*. J Clin Oncol, 2002. **20**(19): p. 4083-107.
150. Collins, A.J., et al., *Death, hospitalization, and economic associations among incident hemodialysis patients with hematocrit values of 36 to 39%*. J Am Soc Nephrol, 2001. **12**(11): p. 2465-73.
151. Muller, H.M., et al., *Characteristics and clinical relevance of chronic anemia in adult heart transplant recipients*. Clin Transplant, 2001. **15**(5): p. 343-8.

152. Frost, A.E. and C.A. Keller, *Anemia and erythropoietin levels in recipients of solid organ transplants. The Multi-Organ Transplant Group.* Transplantation, 1993. **56**(4): p. 1008-11.
153. Maheshwari, A., R. Mishra, and P.J. Thuluvath, *Post-liver-transplant anemia: etiology and management.* Liver Transpl, 2004. **10**(2): p. 165-73.
154. Geiszt, M. and T.L. Leto, *The Nox family of NAD(P)H oxidases: host defense and beyond.* J Biol Chem, 2004. **279**(50): p. 51715-8.
155. Martins, E.A., R.L. Robalinho, and R. Meneghini, *Oxidative stress induces activation of a cytosolic protein responsible for control of iron uptake.* Arch Biochem Biophys, 1995. **316**(1): p. 128-34.
156. Pantopoulos, K. and M.W. Hentze, *Rapid responses to oxidative stress mediated by iron regulatory protein.* EMBO J., 1995. **14**: p. 2917-2924.
157. Mueller, S., et al., *IRP1 activation by extracellular oxidative stress in the perfused rat liver.* J. Biol. Chem., 2001. **276**: p. 23192-23196.
158. Caltagirone, A., G. Weiss, and K. Pantopoulos, *Modulation of cellular iron metabolism by hydrogen peroxide. Effects of H₂O₂ on the expression and function of iron-responsive element-containing mRNAs in B6 fibroblasts.* J. Biol. Chem., 2001. **276**: p. 19738-19745.
159. Ludwiczek, S., et al., *Cytokine-mediated regulation of iron transport in human monocytic cells.* Blood, 2003. **101**(10): p. 4148-54.
160. Tilg, H., et al., *Role of IL-10 for induction of anemia during inflammation.* J. Immunol., 2002. **169**: p. 2204-2209.
161. Kazemi-Shirazi, L., et al., *The relation of iron status and hemochromatosis gene mutations in patients with chronic hepatitis C.* Gastroenterology, 1999. **116**: p. 127-134.
162. Piperno, A., et al., *Hepatic iron overload in patients with chronic viral hepatitis: role of HFE gene mutations.* Hepatology, 1998. **28**: p. 1105-1109.
163. Haque, S., et al., *Iron overload in patients with chronic hepatitis C: a clinicopathologic study.* Hum Pathol, 1996. **27**: p. 1277-1281.
164. Riggio, O., et al., *Iron overload in patients with chronic viral hepatitis: how common is it?* Am J Gastroenterol., 1997. **92**: p. 1298-1301.
165. Bonkovsky, H.L., R.W. Lambrecht, and Y. Shan, *Iron as a co-morbid factor in nonhemochromatotic liver disease.* Alcohol, 2003. **30**: p. 137-144.
166. Means, R.T., Jr., *Recent developments in the anemia of chronic disease.* Curr Hematol Rep, 2003. **2**(2): p. 116-21.
167. Denz, H., et al., *Association between the activation of macrophages, changes of iron metabolism and the degree of anaemia in patients with malignant disorders.* Eur J Haematol, 1992. **48**(5): p. 244-8.
168. Wang, C.Q., K.B. Udupa, and D.A. Lipschitz, *Interferon-gamma exerts its negative regulatory effect primarily on the earliest stages of murine erythroid progenitor cell development.* J Cell Physiol, 1995. **162**(1): p. 134-8.
169. Taniguchi, S., et al., *Interferon gamma downregulates stem cell factor and erythropoietin receptors but not insulin-like growth factor-I receptors in human erythroid colony-forming cells.* Blood, 1997. **90**(6): p. 2244-52.
170. Jelkmann, W., *Proinflammatory cytokines lowering erythropoietin production.* J Interferon Cytokine Res, 1998. **18**(8): p. 555-9.

171. Maciejewski, J.P., et al., *Nitric oxide suppression of human hematopoiesis in vitro. Contribution to inhibitory action of interferon-gamma and tumor necrosis factor-alpha*. J Clin Invest, 1995. **96**(2): p. 1085-92.
172. Finch, C., *Regulators of iron balance in humans*. Blood, 1994. **84**: p. 1697-1702.
173. Pak, M., et al., *Suppression of hepcidin during anemia requires erythropoietic activity*. Blood, 2006. **108**: p. 3730-3735.
174. Vokurka, M., et al., *Hepcidin mRNA levels in mouse liver respond to inhibition of erythropoiesis*. Physiol. Res., 2006. **55**: p. 667-674.
175. Garby, L. and W.D. Noyes, *Studies on hemoglobin metabolism. I. The kinetic properties of the plasma hemoglobin pool in normal man*. J Clin Invest, 1959. **38**: p. 1479-83.
176. Fisman, D.N., *Hemophagocytic syndromes and infection*. Emerg Infect Dis, 2000. **6**(6): p. 601-8.
177. Ponka, P., *Cell biology of heme*. Am J Med Sci, 1999. **318**(4): p. 241-56.
178. Delaby, C., et al., *A physiological model to study iron recycling in macrophages*. Exp Cell Res, 2005. **310**(1): p. 43-53.
179. Knutson, M. and M. Wessling-Resnick, *Iron metabolism in the reticuloendothelial system*. Crit. Rev. Biochem. Mol. Biol., 2003. **38**: p. 61-88.
180. Wejman, J.C., et al., *Structure and assembly of haptoglobin polymers by electron microscopy*. J Mol Biol, 1984. **174**(2): p. 343-68.
181. Wejman, J.C., et al., *Structure of haptoglobin and the haptoglobin-hemoglobin complex by electron microscopy*. J Mol Biol, 1984. **174**(2): p. 319-41.
182. Kristiansen, M., et al., *Identification of the haemoglobin scavenger receptor*. Nature, 2001. **409**(6817): p. 198-201.
183. Dhaliwal, G., P.A. Cornett, and L.M. Tierney, Jr., *Hemolytic anemia*. Am Fam Physician, 2004. **69**(11): p. 2599-606.
184. Andriopoulos, B. and K. Pantopoulos, *Regulation of iron metabolism at the cellular and systemic level*, in *Recent Research Developments in Molecular and Cellular Biology*. 2004. p. 1-22.
185. Ponka, P. and B. Andriopoulos, *Iron can boost hepcidin both ways*. Blood, 2007. **110**(6): p. 1703-1704.
186. Dunn, L.L., Y.S. Rahmanto, and D.R. Richardson, *Iron uptake and metabolism in the new millennium*. Trends Cell Biol, 2007. **17**(2): p. 93-100.
187. Camaschella, C., A. Roetto, and M. De Gobbi, *Juvenile hemochromatosis*. Semin. Hematol., 2002. **39**: p. 242-248.
188. Pietrangelo, A., *Juvenile hemochromatosis*. J. Hepatol., 2006. **45**: p. 892-894.
189. Roetto, A., et al., *Juvenile hemochromatosis locus maps to chromosome 1q*. Am. J. Hum. Genet., 1999. **64**: p. 1388-1393.
190. Rivard, S.R., et al., *Juvenile hemochromatosis locus maps to chromosome 1q in a French Canadian population*. Eur. J. Hum. Genet., 2003. **11**: p. 585-589.
191. Papanikolaou, G., et al., *Linkage to chromosome 1q in Greek families with juvenile hemochromatosis*. Blood Cells Mol. Dis., 2001. **27**: p. 744-749.
192. Papanikolaou, G., et al., *Genetic heterogeneity underlies juvenile hemochromatosis phenotype: analysis of three families of northern Greek origin*. Blood Cells Mol. Dis., 2002. **29**(2): p. 168-73.

193. Nemeth, E. and T. Ganz, *Regulation of iron metabolism by hepcidin*. Annu. Rev. Nutr., 2006. **26**: p. 323-342.
194. Donovan, A., et al., *The iron exporter ferroportin/Slc40a1 is essential for iron homeostasis*. Cell Metabolism, 2005. **1**: p. 191-200.
195. Bridle, K.R., et al., *Disrupted hepcidin regulation in HFE-associated haemochromatosis and the liver as a regulator of body iron homeostasis*. Lancet, 2003. **361**: p. 669-673.
196. Nemeth, E., et al., *Hepcidin is decreased in TFR2 hemochromatosis*. Blood, 2005. **105**: p. 1803-1806.
197. van den Eijnde, S.M., et al., *Transient expression of phosphatidylserine at cell-cell contact areas is required for myotube formation*. J. Cell Sci., 2001. **114**: p. 3631-3642.
198. Wang, J. and K. Pantopoulos, *Conditional de-repression of ferritin synthesis in cells expressing a constitutive IRP1 mutant*. Mol. Cell. Biol., 2002. **22**: p. 4638-4651.
199. Courselaud, B., et al., *C/EBPalpha regulates hepatic transcription of hepcidin, an antimicrobial peptide and regulator of iron metabolism. Cross-talk between C/EBP pathway and iron metabolism*. J. Biol. Chem., 2002. **277**: p. 41163-41170.
200. Ryter, S.W., J. Alam, and A.M. Choi, *Heme oxygenase-1/carbon monoxide: from basic science to therapeutic applications*. Physiol. Rev., 2006. **86**: p. 583-650.
201. Dinter, A. and E.G. Berger, *Golgi-disturbing agents*. Histochem. Cell Biol., 1998. **109**: p. 571-590.
202. Liu, C.Y. and R.J. Kaufman, *The unfolded protein response*. J. Cell Sci., 2003. **116**: p. 1861-1862.
203. Nicolas, G., et al., *Constitutive hepcidin expression prevents iron overload in a mouse model of hemochromatosis*. Nat. Genet., 2003. **34**: p. 97-101.
204. Andrews, N.C. and P.J. Schmidt, *Iron homeostasis*. Annu. Rev. Physiol., 2007. **69**: p. 69-85.
205. Frazer, D.M., et al., *Delayed hepcidin response explains the lag period in iron absorption following a stimulus to increase erythropoiesis*. Gut, 2004. **53**: p. 1509-1515.
206. Moestrup, S.K. and H.J. Moller, *CD163: a regulated hemoglobin scavenger receptor with a role in the anti-inflammatory response*. Ann. Med., 2004. **36**: p. 347-354.
207. Kulaksiz, H., et al., *Pro-hepcidin: expression and cell specific localisation in the liver and its regulation in hereditary haemochromatosis, chronic renal insufficiency, and renal anaemia*. Gut, 2004. **53**: p. 735-743.
208. Ganz, T., *Hepcidin in iron metabolism*. Curr. Opin. Hematol., 2004. **11**: p. 251-254.
209. Hentze, M.W., M.U. Muckenthaler, and N.C. Andrews, *Balancing acts; molecular control of mammalian iron metabolism*. Cell, 2004. **117**: p. 285-297.
210. Fleming, R.E., *Advances in understanding the molecular basis for the regulation of dietary iron absorption*. Curr. Opin. Gastroenterol., 2005. **21**: p. 201-206.
211. Pietrangelo, A., *Hereditary hemochromatosis--a new look at an old disease*. N. Engl. J. Med., 2004. **350**: p. 2383-2397.

212. Gehrke, S.G., et al., *Expression of hepcidin in hereditary hemochromatosis: evidence for a regulation in response to serum transferrin saturation and non-transferrin-bound iron*. Blood, 2003. **102**: p. 371-376.
213. Papanikolaou, G., et al., *Hepcidin in iron overload disorders*. Blood, 2005. **105**: p. 4103-4105.
214. Ahmad, K.A., et al., *Decreased liver hepcidin expression in the hfe knockout mouse*. Blood Cells Mol. Dis., 2002. **29**: p. 361-366.
215. Muckenthaler, M., et al., *Regulatory defects in liver and intestine implicate abnormal hepcidin and Cybrd1 expression in mouse hemochromatosis*. Nat. Genet., 2003. **34**: p. 102-107.
216. Kawabata, H., et al., *Expression of hepcidin is down-regulated in TfR2 mutant mice manifesting a phenotype of hereditary hemochromatosis*. Blood, 2005. **105**: p. 376-381.
217. Adamsky, K., et al., *Decreased hepcidin mRNA expression in thalassemic mice*. Br J Haematol, 2004. **124**(1): p. 123-124.
218. Roy, C.N. and N.C. Andrews, *Anemia of inflammation: the hepcidin link*. Curr. Opin. Hematol., 2005. **12**: p. 107-111.
219. Weiss, G. and L.T. Goodnough, *Anemia of chronic disease*. N. Engl. J. Med., 2005. **352**: p. 1011-1023.
220. Hallaway, P.E., et al., *Modulation of deferoxamine toxicity and clearance by covalent attachment to biocompatible polymers*. Proc. Natl. Acad. Sci. USA, 1989. **86**: p. 10108-10112.
221. Galy, B., et al., *Altered body iron distribution and microcytosis in mice deficient for iron regulatory protein 2 (IRP2)*. Blood, 2005. **106**: p. 2580-2589.
222. Delaby, C., et al., *The presence of the iron exporter ferroportin at the plasma membrane of macrophages is enhanced by iron loading and downregulated by hepcidin*. Blood, 2005. **106**: p. 3979-3984.
223. Harrison, P.M. and P. Arosio, *The ferritins: molecular properties, iron storage function and cellular regulation*. Biochim. Biophys. Acta, 1996. **1275**: p. 161-203.
224. Cartwright, G.E., et al., *The anemia of infection. I. Hypoferremia, hypercupremia, and alterations in porphyrin metabolism in patients*. J Clin Invest, 1946. **25**: p. 65-80.
225. Hirayama, M., et al., *Regulation of iron metabolism in HepG2 cells: a possible role for cytokines in the hepatic deposition of iron*. Hepatology, 1993. **18**(4): p. 874-80.
226. Schäfer, K.-H., *Über den Einfluß von Infektionen und ähnlichen Vorgängen auf den Eisenstoffwechsel*. Zeitschrift für die gesamte experimentelle Medizin, 1942. **110**: p. 678-696.
227. Kazemi-Shirazi, L., et al., *The relation of iron status and hemochromatosis gene mutations in patients with chronic hepatitis C*. Gastroenterology, 1999. **116**(1): p. 127-34.
228. Piperno, A., et al., *Hepatic iron overload in patients with chronic viral hepatitis: role of HFE gene mutations*. Hepatology, 1998. **28**(4): p. 1105-9.
229. Haque, S., et al., *Iron overload in patients with chronic hepatitis C: a clinicopathologic study*. Hum Pathol, 1996. **27**(12): p. 1277-81.

230. Riggio, O., et al., *Iron overload in patients with chronic viral hepatitis: how common is it?* Am J Gastroenterol, 1997. **92**(8): p. 1298-1301.
231. Bonkovsky, H.L., R.W. Lambrecht, and Y. Shan, *Iron as a co-morbid factor in nonhemochromatotic liver disease.* Alcohol, 2003. **30**(2): p. 137-44.
232. Mueller, S., N.H. Afdhal, and D. Schuppan, *Iron, HCV, and liver cancer: hard metal setting the pace?* Gastroenterology, 2006. **130**(7): p. 2229-34.
233. Kondo, H., et al., *Iron metabolism in the erythrophagocytosing Kupffer cell.* Hepatology, 1988. **8**(1): p. 32-8.
234. Konijn, A.M., *Iron metabolism in inflammation.* Baillieres Clin Haematol, 1994. **7**(4): p. 829-49.
235. Freireich, E.J., et al., *The effect of inflammation on the utilization of erythrocyte and transferrin-bound radioiron for red cell production.* Blood, 1957. **12**: p. 972-982.
236. Nemeth, E., et al., *IL-6 mediates hypoferremia of inflammation by inducing the synthesis of the iron regulatory hormone hepcidin.* J Clin Invest, 2004. **113**(9): p. 1271-6.
237. Roy, C.N., et al., *An Hfe-dependent pathway mediates hyposideremia in response to lipopolysaccharide-induced inflammation in mice.* Nat Genet, 2004. **36**(5): p. 481-5.
238. Ganz, T., *Hepcidin, a key regulator of iron metabolism and mediator of anemia of inflammation.* Blood, 2003. **102**(3): p. 783-788.
239. Roy, C.N. and N.C. Andrews, *Anemia of inflammation: the hepcidin link.* Curr Opin Hematol, 2005. **12**(2): p. 107-11.
240. Nemeth, E., et al., *Hepcidin regulates cellular iron efflux by binding to ferroportin and inducing its internalization.* Science, 2004. **306**(5704): p. 2090-3.
241. Upton, R.L., et al., *Variable tissue expression of transferrin receptors: relevance to acute respiratory distress syndrome.* Eur Respir J, 2003. **22**(2): p. 335-41.
242. Klebanoff, S.J., *In inflammation: basic principles and clinical correlates*, R. Snyderman, Editor. 1988, Raven Press: New York. p. 391-444.
243. Hentze, M.W., M.U. Muckenthaler, and N.C. Andrews, *Balancing acts: molecular control of mammalian iron metabolism.* Cell, 2004. **117**(3): p. 285-97.
244. Martins, E.A., R.L. Robalinho, and R. Meneghini, *Oxidative stress induces activation of a cytosolic protein responsible for control of iron uptake.* Arch. Biochem. Biophys., 1995. **316**(1): p. 128-34.
245. Pantopoulos, K. and M.W. Hentze, *Rapid responses to oxidative stress mediated by iron regulatory protein.* EMBO J., 1995. **14**(12): p. 2917-2924.
246. Mueller, S., et al., *IRP1 activation by extracellular oxidative stress in the perfused rat liver.* J. Biol. Chem., 2001. **276**(25): p. 23192-6.
247. Pantopoulos, K., et al., *Differences in the regulation of IRP-1 (iron regulatory protein-1) by extra- and intracellular oxidative stress.* J. Biol. Chem., 1997. **272**: p. 9802-9808.
248. Caltagirone, A., G. Weiss, and K. Pantopoulos, *Modulation of cellular iron metabolism by hydrogen peroxide. Effects of H₂O₂ on the expression and function of iron-responsive element-containing mRNAs in B6 fibroblasts.* J. Biol. Chem., 2001. **22**: p. 22.

249. Lok, C.N. and P. Ponka, *Identification of a hypoxia response element in the transferrin receptor gene*. J. Biol. Chem., 1999. **274**(34): p. 24147-24152.
250. Tacchini, L., et al., *Transferrin receptor induction by hypoxia. HIF-1-mediated transcriptional activation and cell-specific post-transcriptional regulation*. J. Biol. Chem., 1999. **274**(34): p. 24142-6.
251. Guzy, R.D., et al., *Mitochondrial complex III is required for hypoxia-induced ROS production and cellular oxygen sensing*. Cell Metab, 2005. **1**(6): p. 401-8.
252. Mueller, S., *Sensitive and nonenzymatic measurement of hydrogen peroxide in biological systems*. Free Radic. Biol. Med., 2000. **29**(5): p. 410-5.
253. Mueller, S., et al., *A chemiluminescence approach to study the regulation of iron metabolism by oxidative stress*, in *Bioluminescence and chemiluminescence: molecular reporting with photons*, P.E. Stanley, Editor. 1997, John Wiley & Sons Ltd: Baffins Lane, Chichester, Sussex. p. 338-341.
254. Mütze, S., et al., *Myeloperoxidase-derived hypochlorous acid antagonizes the oxidative stress-mediated activation of iron regulatory protein 1*. J. Biol. Chem., 2003. **278**(42): p. 40542-9.
255. Mueller, S., H.D. Riedel, and W. Stremmel, *Direct evidence for catalase as the predominant H₂O₂ -removing enzyme in human erythrocytes*. Blood, 1997. **90**(12): p. 4973-4978.
256. Mueller, S. and K. Pantopoulos, *Activation of iron regulatory protein-1 (IRP1) by oxidative stress*. Methods Enzymol., 2002. **348**: p. 324-337.
257. Rost, D., et al., *Liver-homing of purified glucose oxidase: A novel in vivo model of physiological hepatic oxidative stress (H₂O₂)*. J Hepatol, 2006.
258. Breuer, W., et al., *Transport of iron and other transition metals into cells as revealed by a fluorescent probe*. Am J Physiol, 1995. **268**(6 Pt 1): p. C1354-61.
259. Breuer, W., S. Epsztejn, and Z.I. Cabantchik, *Iron acquired from transferrin by K562 cells is delivered into a cytoplasmic pool of chelatable iron(II)*. J. Biol. Chem., 1995. **270**(41): p. 24209-15.
260. Laskey, J., et al., *Evidence that transferrin supports cell proliferation by supplying iron for DNA synthesis*. Exp Cell Res, 1988. **176**(1): p. 87-95.
261. Riedel, H.D., et al., *HFE downregulates iron uptake from transferrin and induces iron-regulatory protein activity in stably transfected cells*. Blood, 1999. **94**(11): p. 3915-21.
262. Mueller, S., E. Cadenas, and A.H. Schonthal, *p21WAF1 regulates anchorage-independent growth of HCT116 colon carcinoma cells via E-cadherin expression*. Cancer. Res., 2000. **60**(1): p. 156-63.
263. Mueller, S. and J. Arnhold, *Fast and sensitive chemiluminescence determination of H₂O₂ concentration in stimulated human neutrophils*. J. Biolumin. Chemilumin., 1995. **10**(4): p. 229-237.
264. Sureda, A., et al., *Extracellular H₂O₂ and not superoxide determines the compartment-specific activation of transferrin receptor by iron regulatory protein 1*. Free Radic Res, 2005. **39**(8): p. 817-24.
265. Wang, J., G. Chen, and K. Pantopoulos, *Inhibition of transferrin receptor 1 transcription by a cell density response element*. Biochem. J., 2005. **392**: p. 392, 383-388.

266. Katschinski, D.M., et al., *Heat induction of the unphosphorylated form of hypoxia-inducible factor-1alpha is dependent on heat shock protein-90 activity*. J Biol Chem, 2002. **277**(11): p. 9262-7.
267. Volland, W., *Untersuchungen über den intermediären Eisenstoffwechsel nach wiederholter Injektion artfremden Serums*. Klinische Wochenschrift, 1940. **19**: p. 1242.
268. Quastel, M.R. and J.F. Ross, *The effect of acute inflammation on the utilization and distribution of transferrin-bound and erythrocyte radioiron*. Blood, 1966. **28**: p. 738-757.
269. Knutson, M.D., et al., *Iron release from macrophages after erythrophagocytosis is up-regulated by ferroportin 1 overexpression and down-regulated by hepcidin*. Proc Natl Acad Sci U S A, 2005. **102**(5): p. 1324-8.
270. BelAiba, R.S., et al., *Redox-sensitive regulation of the HIF pathway under non-hypoxic conditions in pulmonary artery smooth muscle cells*. Biol Chem, 2004. **385**(3-4): p. 249-57.
271. Coronella-Wood, J., et al., *c-Fos phosphorylation induced by H₂O₂ prevents proteasomal degradation of c-Fos in cardiomyocytes*. J Biol Chem, 2004. **279**(32): p. 33567-74.
272. Reinheckel, T., et al., *Differential impairment of 20S and 26S proteasome activities in human hematopoietic K562 cells during oxidative stress*. Arch Biochem Biophys, 2000. **377**(1): p. 65-8.
273. Patel, J., et al., *Cellular stresses profoundly inhibit protein synthesis and modulate the states of phosphorylation of multiple translation factors*. Eur J Biochem, 2002. **269**(12): p. 3076-85.
274. Cobelens, P.M., et al., *Hydrogen peroxide impairs GRK2 translation via a calpain-dependent and cdk1-mediated pathway*. Cell Signal, 2007. **19**(2): p. 269-77.
275. MacCallum, P.R., et al., *Cap-dependent and hepatitis C virus internal ribosome entry site-mediated translation are modulated by phosphorylation of eIF2alpha under oxidative stress*. J Gen Virol, 2006. **87**(Pt 11): p. 3251-62.
276. Kang, K.R. and S.Y. Lee, *Effect of serum and hydrogen peroxide on the Ca²⁺/calmodulin-dependent phosphorylation of eukaryotic elongation factor 2(eEF-2) in Chinese hamster ovary cells*. Exp Mol Med, 2001. **33**(4): p. 198-204.
277. O'Loghlen, A., et al., *Reversible inhibition of the protein phosphatase 1 by hydrogen peroxide. Potential regulation of eIF2 alpha phosphorylation in differentiated PC12 cells*. Arch Biochem Biophys, 2003. **417**(2): p. 194-202.
278. Shenberger, J.S., M.H. Adams, and S.G. Zimmer, *Oxidant-induced hypertrophy of A549 cells is accompanied by alterations in eukaryotic translation initiation factor 4E and 4E-binding protein-1*. Am J Respir Cell Mol Biol, 2002. **27**(2): p. 250-6.
279. Luciani, N., et al., *Stimulation of translation by reactive oxygen species in a cell-free system*. Biochimie, 1995. **77**(3): p. 182-9.
280. Casano, L.M., M. Martin, and B. Sabater, *Hydrogen peroxide mediates the induction of chloroplastic Ndh complex under photooxidative stress in barley*. Plant Physiol, 2001. **125**(3): p. 1450-8.

281. Zhang, A., et al., *The OxyS regulatory RNA represses rpoS translation and binds the Hfq (HF-I) protein*. *Embo J*, 1998. **17**(20): p. 6061-8.
282. Kotamraju, S., et al., *Transferrin receptor-dependent iron uptake is responsible for doxorubicin-mediated apoptosis in endothelial cells: role of oxidant-induced iron signaling in apoptosis*. *J Biol Chem*, 2002. **277**(19): p. 17179-87.
283. Mueller, S., *Iron regulatory protein 1 as a sensor of reactive oxygen species*. *Biofactors*, 2005. **24**(1-4): p. 171-81.
284. Mueller, S., et al., *A chemiluminescence approach to study the regulation of iron metabolism by oxidative stress*. *Bioluminescence and Chemiluminescence*, ed. J.W. Hastings, Kricka, L. J. Stanley, P. E. 1997, Baffins Lane, Chichester, Sussex: John Wiley & Sons Ltd. 338-341.

ABREVIATIONS

μ, micro

β2M, beta 2 microglobulin

ACD, anemia of chronic disease

AI, anemia of inflammation

ALAS2, aminolevulinate synthase 2

ANOVA, analysis of variance

BMP, bone morphogenic protein

bp, base pairs

BRE, bone morphogenic response element

CAT, catalase

Cd, cadmium

cHjv, cellular hemojuvelin

Co, cobalt

Cp, ceruloplasmin

Ctrl, control

Cu, copper

DcytB, D cytochrome B

DFO, desferrioxamine

DMEM, Dulbecco's modified Eagle's medium

DMOG, dimethyl-oxalyl-glycine

DMT1, divalent metal transporter 1

DNA, deoxyribonucleic acid

ECL, enhanced chemiluminescence

EMSA, electrophoretic mobility shift assay

FAC, ferric ammonium citrate

FBS, fetal bovine serum

Fe, iron

FeSO₄, ferrous sulphate

Fpn1, ferroportin

g, grams

G6PD, glucose-6-phosphate dehydrogenase

GFP, green fluorescent protein

GOX, glucose oxidase

gp, glycoprotein

GPI, glycosylphosphatidylinositol

h, hour

H⁺, hydrogen

H₂O₂, hydrogen peroxide

HA, hemagglutinin

HFE, hemochromatosis gene or protein

HH, hereditary hemochromatosis

HIF, hypoxia-inducible factor

Hjv, hemojuvelin

HMW, high molecular weight

HO-1, heme oxygenase-1

Holo-Tf, holo-transferrin

Hp, hephaestin

HS, horse serum

IB, immunoblot

IDA, iron deficiency anemia

IFN, interferon

IL, interleukin

IP, immunoprecipitation

IRE, iron-responsive element

IRP1, iron regulatory protein 1

IRP2, iron regulatory protein 2

JAK, janus kinases

JH, juvenile hemochromatosis

kb, kilobase

kDa, kilo Dalton

L, liter

LAP, latency associated peptides

LEAP-1, liver-expressed antimicrobial peptide

LIP, labile iron pool

LPS, lipopolysaccharide

m, milli

Min, minutes

Mn, manganese

mRNA, messenger ribonucleic acid

MTT, 3-(4,5-dimethylthiazol-2-yl)-2,5-diphenyltetrazolium bromide

n, nano

NADPH, nicotinamide adenine dinucleotide phosphate-oxidase

NGAL, neutral gelatinase-associated lipocalin

Ni, nickel

NO, nitric oxide

NRAMP, natural resistance-associated macrophage protein

O₂, oxygen

OCl⁻, hypochlorite

ONOO⁻, peroxynitrite

Pb, lead

PBS, phosphate-buffered saline

PHZ, phenylhydrazine

PI-PLC, phosphatidylinositol-specific phospholipase C

RES, reticuloendothelial system

RGM, repulsive guidance molecule

RNase, ribonuclease

ROI, reactive oxygen intermediates

RT-PCR, real-time polymerase chain reaction

SD, standard deviation

sHjv, soluble hemojuvelin

SLC40A, solute carrier family 40

SnPPIX, tin protoporphyrin IX

STAT, signal transducers and activators of transcription

t, time

TBS, tris-buffered saline

tet, tetracycline

Tf, transferrin

TfR1, transferrin receptor 1

TGF β , Transforming growth factor β

TIBC, total iron binding capacity

TNF, tumor necrosis factor

USF2, upstream stimulatory factor

UTR, untranslated region

vWF, von Willebrand factor

WT, wild-type

Zn, zinc

REFEREED PAPERS IN PUBLISHED FORMAT

Hepcidin generated by hepatoma cells inhibits iron export from co-cultured THP1 monocytes[☆]

Bill Andriopoulos¹, Kostas Pantopoulos^{1,2,*}

¹Lady Davis Institute for Medical Research, Sir Mortimer B. Davis Jewish General Hospital, 3755 Cote-Ste-Catherine Road, Montreal, Que., Canada H3T 1E2

²Department of Medicine, McGill University, Montreal, Que., Canada

Background/Aims: The antimicrobial peptide hepcidin is generated in the liver and released into the circulation in response to iron, oxygen and inflammatory signals. Hepcidin serves as a hormonal regulator of duodenal iron absorption and iron trafficking in the reticuloendothelial system. The aim of this study is to explore the effects of this regulatory peptide in macrophage iron metabolism.

Methods: Hepcidin-mediated iron efflux and parameters of cellular iron homeostasis were studied in THP1 monocytic cells co-cultured with hepcidin-producing hepatic cells.

Results: Stimulation of hepcidin expression in Huh7 cells with interleukin-6 promoted a significant ~30% decrease in ⁵⁹Fe efflux from THP1 cells, previously loaded with ⁵⁹Fe-transferrin. Similar results were obtained with HepG2 cells transfected with a hepcidin cDNA. Importantly, hepcidin expression from Huh7 cells elicited a decrease in the levels of the iron-sensitive post-transcriptional regulator IRP2 in THP1 cells, accompanied by de novo synthesis of the iron storage protein ferritin.

Conclusions: Physiologically generated hepcidin inhibits iron efflux and promotes iron accumulation in monocytic cells, mimicking a pathophysiological response commonly observed in the anemia of inflammation. Our results highlight the crucial role of hepcidin in the control of macrophage iron homeostasis.

© 2005 European Association for the Study of the Liver. Published by Elsevier B.V. All rights reserved.

Keywords: Ferroportin; Hemochromatosis; Anemia of chronic disease; HFE; Hemojuvelin

1. Introduction

Hepcidin, a conserved cysteine-rich peptide of 20–25 aminoacids, is produced in the liver and functions as the principal hormonal regulator of body iron homeostasis [1–3]. Hepcidin negatively regulates iron absorption in the duodenum and transport in reticuloendothelial cells by

controlling the levels of the iron exporter ferroportin [4,5]. The expression of hepcidin is turned off in response to low body iron stores, anemia or hypoxia [6]. On the other hand, hepcidin is induced by iron overload [7] or by inflammatory signals via interleukins IL-1 or IL-6 [8,9]. Misregulation of hepcidin expression is associated with a broad spectrum of iron-related disorders.

Genetic mutations leading to complete silencing of hepcidin are etiologically linked to a rare form of juvenile hemochromatosis [10], an early onset disease of iron overload characterized by pathological iron absorption and deposition within parenchymal cells with a relative sparing of macrophages [11]. More common forms of hereditary hemochromatosis (caused by mutations in HFE, TfR2 or HJV) [11] correlate with various degrees of hepcidin deficiency [12–15]. Likewise, hepcidin is suppressed in patients with thalassemia syndromes but increases in patients with ‘ferroportin disease’ [16]. Similar phenotypes have been described in

Received 22 August 2005; received in revised form 26 October 2005; accepted 29 October 2005; available online 5 December 2005

[☆] Supported by grants from the Anemia Institute for Research and Education (AIRE) and from the Ministère de la Recherche, de la Science et de la Technologie (MRST).

* Corresponding author. Address: Department of Medicine, Lady Davis Institute for Medical Research, Sir Mortimer B. Davis Jewish General Hospital, 3755 Cote-Ste-Catherine Road, McGill University, Montreal, Que., Canada H3T 1E2. Tel.: +1 514 340 8260x5293; fax: +1 514 340 7502.

E-mail address: kostas.pantopoulos@mcgill.ca (K. Pantopoulos).

mouse models of hemochromatosis [17–23] and thalassemia [24]. Transgenic mice over-expressing hepcidin from a liver-specific promoter show profound defects in materno-fetal iron transport and display severe iron deficiency anemia [25].

Hepcidin levels are normally elevated following iron ingestion or infection [9]. The upregulation of hepcidin expression by inflammatory signals is tightly linked to the ‘anemia of chronic disease’ (ACD) or ‘anemia of inflammation’ (AI) [26,27]. This condition is characterized by hypoferremia due to iron retention within macrophages and decreased iron absorption. The withholding of iron may be protective against growing bacteria but eventually limits erythropoiesis. Even though the development of ACD depends on multiple factors [27], hepcidin is considered as the key mediator for the diversion of iron traffic by controlling the stability of ferroportin [4,5], which is unique in its capacity to export iron from macrophages and intestinal cells [28].

The experimental evidence supporting this mechanism was based on the direct binding of human hepcidin to transfected mouse ferroportin-GFP in HEK293 and HeLa cells, promoting its internalization and lysosomal degradation [4,5]. In a separate study, synthetic human hepcidin inhibited iron export and decreased the levels of transfected murine ferroportin in J774 macrophages [29]. These data are consistent with a function of hepcidin as a principal regulator of iron efflux from macrophages.

Considering that the effector (hepcidin) and the target (ferroportin) are expressed in different cell types, the above mechanism would require cell-to-cell communication between hepcidin-producing hepatocytes with macrophages. To further validate the molecular basis of hepcidin regulatory activity under physiologically relevant conditions, we establish here a co-culture model of Huh7 or HepG2 hepatoma and THP1 monocytic cells. We demonstrate that hepcidin generated by hepatoma cells is capable of regulating iron metabolism in neighboring monocytes.

2. Materials and methods

2.1. Materials

Hemin, IL-6 and ceruloplasmin were purchased from Sigma (St Louis, MI). Desferrioxamine (DFO) was from Novartis (Dorval, QC, Canada). High molecular weight desferrioxamine (HMW-DFO), a non-permeable hydroxyethyl starch conjugate [30], was obtained from Biomedical Frontiers (Minneapolis, MN).

2.2. Cell culture

Human Huh7 and HepG2 hepatoma cells and H1299 lung cancer cells were grown in Dulbecco’s modified Eagle’s medium supplemented with 10% heat-inactivated fetal bovine serum, 100 units/ml penicillin, and 100 µg/ml streptomycin. Media for Huh7 and HepG2 cells also contained 1% non-essential amino acids. Human THP1 monocytic cells were cultured in supplemented RPMI.

2.3. Co-culture experiments

THP1 suspension cells were inserted into a co-culture cartridge (BD Falcon), which was placed on top of 6-well dishes containing monolayers of 0.2×10^6 Huh7, HepG2 or H1299 cells. Co-culture experiments were performed in serum-free RPMI to avoid possible interference of serum transferrin on iron uptake and release.

2.4. Generation of HepG2 hepcidin transfectants

Human hepcidin cDNA (kindly provided by Dr M. Muckenthaler, University of Heidelberg, Germany) was digested out of the parent pDNR-LIB vector with EcoR1 and Xho1 and ligated into pcDNA3. The construct was transfected into HepG2 cells by Lipofectamine Plus (Invitrogen) and stable clones were selected and maintained in the presence of 500 µg/ml G418 (Invitrogen).

2.5. Iron release assays

^{59}Fe -labelled transferrin (Tf) was prepared as previously described [31]. THP1 suspension cells were loaded overnight with 5 µM ^{59}Fe -Tf in serum-free RPMI. Subsequently, the cells were harvested by centrifugation at 4 °C and washed 4× with ice-cold RPMI to remove traces of soluble ^{59}Fe -Tf. Under these conditions, less than ~0.1% of radioactivity could be extracted after the second wash, indicating complete removal of non-internalized transferrin. Aliquots of 2×10^5 cells were resuspended in pre-warmed serum-free RPMI containing 100 µM HMW-DFO and immediately placed into a CO₂ incubator at 37 °C either alone, or in co-culture with other cells. Radioactivity in the supernatant, corresponding to ^{59}Fe release, and in THP1 cells was monitored at specified time intervals on a γ-counter. To calculate the percentage of ^{59}Fe release, the amount of soluble radioactivity was divided by the total amount of radioactivity in media and THP1 cells.

2.6. Western blotting

Cells were lysed in cytoplasmic lysis buffer (1% Triton X-100, 300 mM NaCl and 50 mM Tris/HCl; pH 7.4). Cell debris was cleared by centrifugation and protein concentration was measured with the Bradford reagent (BioRad). Cell lysates (15 µg) were resolved by SDS/PAGE and proteins transferred onto nitrocellulose filters. The blots were saturated with 10% non-fat milk in Tris-buffered saline (TBS) and probed overnight at 4 °C with 1:500 diluted ferritin (DakoCytomation Inc.) or IRP2 [32] antibodies. After 3× washes with TBS containing 0.1% (v/v) Tween 20, the blots were further incubated for 2 h at room temperature with 1:5000 diluted goat anti-rabbit IgG (Sigma). Detection of the peroxidase-coupled secondary antibodies was performed with the ECL[®] method (Amersham). The blots were quantified by densitometry.

2.7. Metabolic labeling with ^{35}S -methionine/cysteine and immunoprecipitation of ferritin

THP1 cells were metabolically labeled during co-culture with (50 µCi/ml) *trans*-[^{35}S]label, a mixture of 70:30 ^{35}S -methionine/cysteine (ICN). Cytoplasmic lysates (160 µg) were subjected to quantitative immunoprecipitation with 5 µl ferritin antibody (Roche). Immunoprecipitated proteins were analysed by SDS/PAGE and visualized by autoradiography. Radioactive bands were quantified by phosphorimaging.

2.8. Northern blotting

Cells were lysed with the Trizol reagent (Invitrogen) and RNA was prepared according to the manufacturer’s recommendations. Total cellular RNA (10 µg) was electrophoretically resolved on a denaturing agarose gel, transferred onto nylon membranes, and hybridized to ^{32}P -labeled human hepcidin or β-actin cDNA probes. Autoradiograms were quantified by phosphorimaging.

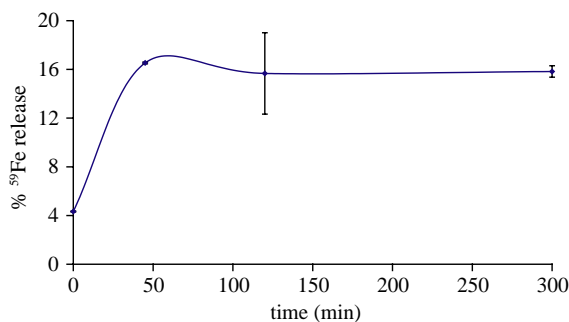


Fig. 1. Kinetics of ^{59}Fe release from THP1 monocytic cells. The cells were loaded with $5\ \mu\text{M}$ ^{59}Fe -Tf for 16 h and the release of ^{59}Fe in serum-free media was measured at the indicated time intervals. The media contained $100\ \mu\text{M}$ HMW-DFO to capture and solubilize ^{59}Fe . Iron release is expressed as percentage of the total amount of soluble ^{59}Fe in media divided by ^{59}Fe in both media and cells. Values correspond to triplicate experiments (mean \pm SD). [This figure appears in colour on the web.]

2.9. Statistical analysis

Data are shown as means \pm SD. Statistical analysis was performed by one-way ANOVA test with the Prism GraphPad Software (version 4.0c).

3. Results

3.1. ^{59}Fe uptake and release from THP1 monocytic cells

Human THP1 monocytic cells were utilized as a model to study the effects of hepcidin on the regulation of macrophage iron metabolism. We first established conditions for iron release assays. The cells were loaded overnight with ^{59}Fe -Tf and the efflux of ^{59}Fe in serum-free media was measured on a γ -counter. In preliminary experiments we noticed that $\sim 20\%$ of released radioactivity could not be recovered and remained attached to the plastic dish. Complete solubilization of

released ^{59}Fe was accomplished by employing HMW-DFO as an iron acceptor. The addition of bovine ceruloplasmin at concentrations of 0.2 or $0.6\ \mu\text{g}/\text{ml}$ did not appreciably alter the amount of soluble radioactivity (data not shown). A typical time course experiment under optimized conditions is shown in Fig. 1. The efflux of ^{59}Fe was fast and reached a plateau within 45–60 min, possibly due to the absence of other iron sources in the serum-free media. The plateau was maintained for up to 5 h. The fraction of released radioactivity corresponded to $\sim 16\%$ of the amount of internalized ^{59}Fe . Thus, under these experimental conditions, iron efflux from THP1 cells only occurs for 45–60 min following termination of external iron supply.

3.2. Generation of hepcidin by Huh7 or HepG2 hepatoma cells inhibits ^{59}Fe release from co-cultured THP1 monocytes

Because hepcidin is exclusively produced by hepatocytes [1–3], we utilized Huh7 hepatoma cells as physiological source of the peptide. As expected [33], a treatment with $20\ \text{ng}/\text{ml}$ IL-6 for 2 h dramatically induced hepcidin mRNA expression in Huh7 cells, but not in control H1299 lung cancer cells (Fig. 2A). In a time course experiment, hepcidin mRNA levels peaked within 1–2 h and remained elevated after 6 h of IL-6 treatment, while under these conditions the expression of control β -actin mRNA did not change (Fig. 2B). We next examined how physiologically generated hepcidin controls macrophage iron efflux. Huh7 cells, previously treated with IL-6, or not, or H1299 cells, were co-cultured with [^{59}Fe -Tf]-loaded THP1 monocytes. When co-cultured with [IL-6]-treated Huh7 cells, THP1 monocytes released $\sim 30\%$ less ^{59}Fe as compared to control (Fig. 2C). The effect was statistically significant ($p < 0.05$) and suggests that hepcidin generated by Huh7 cells in response to IL-6 inhibits iron efflux from THP1 monocytes.

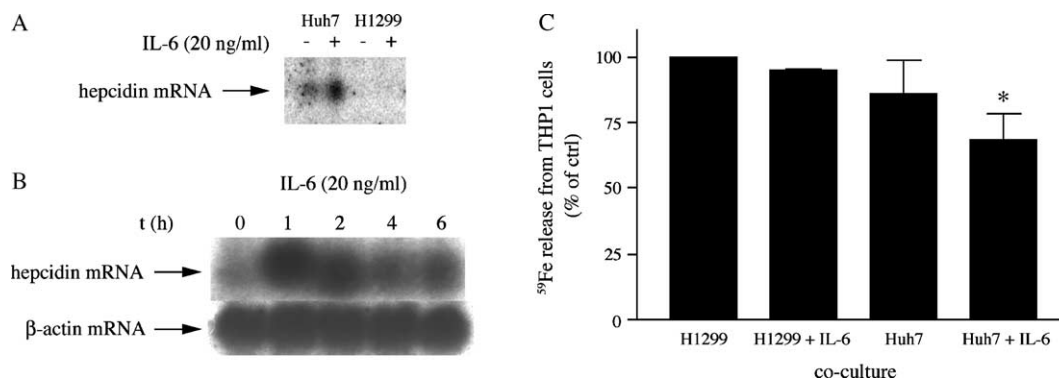


Fig. 2. The expression of hepcidin from Huh7 hepatoma cells inhibits ^{59}Fe release in THP1 monocytes. (A) Huh7 hepatoma and H1299 lung cancer cells were treated with $20\ \text{ng}/\text{ml}$ IL-6 for 2 h and the expression of hepcidin mRNA was analyzed by Northern blotting. (B) Huh7 cells were treated with $20\ \text{ng}/\text{ml}$ IL-6 and the expression of hepcidin (top) and β -actin (bottom) mRNAs at the indicated time intervals was analyzed by Northern blotting. (C) THP1 monocytes were loaded with $5\ \mu\text{M}$ ^{59}Fe -Tf for 16 h and co-cultured for 4 h with H1299 or Huh7 cells, previously treated with $20\ \text{ng}/\text{ml}$ IL-6 for 2 h or not. The release of ^{59}Fe was monitored in serum-free media containing $100\ \mu\text{M}$ HMW-DFO. Iron release, calculated from the total amount of soluble ^{59}Fe in media divided by ^{59}Fe in both media and cells, is expressed as percentage of control (co-culture with H1299 cells). Values correspond to triplicate experiments (mean \pm SD). * $p < 0.05$ versus control (one-way ANOVA test).

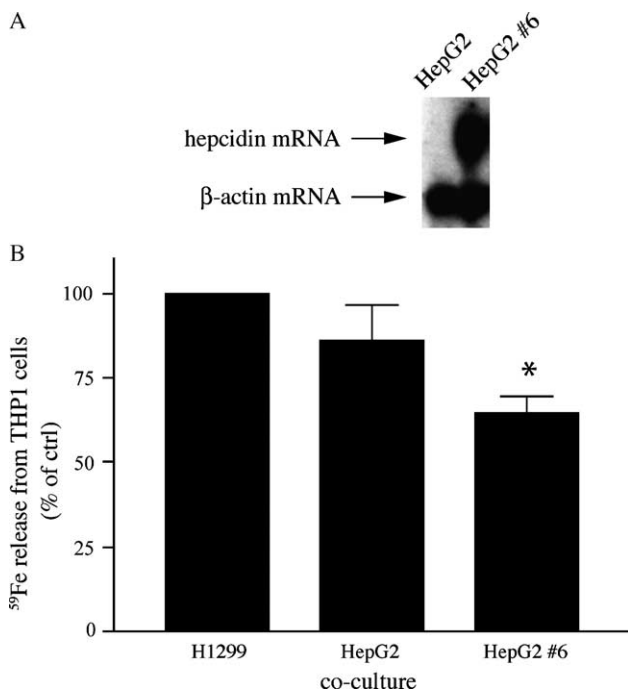


Fig. 3. The expression of hepcidin from HepG2 hepatoma cells inhibits ^{59}Fe release in THP1 monocytes. (A) Northern blot analysis of hepcidin (top) and β -actin (bottom) mRNAs in parent HepG2 cells and in HepG2 #6, stably transfected with a hepcidin cDNA. (B) THP1 monocytes were loaded with $5\ \mu\text{M}$ ^{59}Fe -Tf for 16 h and co-cultured for 4 h with either control H1299 lung cancer cells, parent HepG2 cells, or HepG2 #6. The release of ^{59}Fe was monitored in serum-free media containing $100\ \mu\text{M}$ HMW-DFO. Iron release, calculated from the total amount of soluble ^{59}Fe in media divided by ^{59}Fe in both media and cells, is expressed as percentage of control (co-culture with H1299 cells). Values correspond to triplicate experiments (mean \pm SD). * $p < 0.05$ versus control (one-way ANOVA test).

In co-cultures with untreated Huh7 cells, which express low levels of hepcidin mRNA (Fig. 2A), a $\sim 15\%$ decrease in ^{59}Fe release from THP1 monocytes was observed. Trypan blue exclusion assays showed that under all experimental conditions cell viability was not affected, confirming that the release of ^{59}Fe was not due to cell decay.

It could be argued that the above described inhibition in ^{59}Fe release may not be directly mediated by hepcidin but rather depend on other, possibly pleiotropic effects of IL-6. To achieve high levels of hepcidin expression in the absence of IL-6 stimulation, a hepcidin cDNA was transfected into HepG2 hepatoma cells and stable clones were selected. Northern blot analysis shows that hepcidin mRNA expression is dramatically upregulated in HepG2 clone #6 (Fig. 3A). The effects of hepcidin on iron release were evaluated in co-culture assays of HepG2 #6, parent HepG2, or control H1299 cells with [^{59}Fe -Tf]-loaded THP1 monocytes. In the presence of HepG2 #6, the release of ^{59}Fe from THP1 monocytes was statistically significantly ($p < 0.05$) decreased by $\sim 35\%$ as compared to control (Fig. 3B), in agreement with the data obtained with [IL-6]-stimulated Huh7 cells. Likewise, in co-culture with

parent HepG2 cells, a smaller ($\sim 14\%$) decrease in ^{59}Fe release was apparent, as with untreated Huh7 cells. Taken together, the results in Figs. 2 and 3 suggest that physiologically produced hepcidin inhibits iron efflux from target monocytes.

3.3. Hepcidin generated by Huh7 cells elicits responses to iron loading in co-cultured THP1 monocytes

The hepcidin-mediated inhibition of ^{59}Fe release from THP1 cells implies that physiologically generated hepcidin may have the capacity to alter their overall iron status. To examine this, THP1 cells were co-cultured with Huh7 hepatoma or control H1299 cells and the expression of the cytoplasmic post-transcriptional regulator IRP2, which is sensitive to proteasomal degradation in response to iron loading [34], was analyzed by Western blotting. The co-culture with [IL-6]-stimulated Huh7 cells promoted a profound ($\sim 66\%$) decrease in the steady-state levels of IRP2 in THP1 cells (Fig. 4). The decrease was more modest ($\sim 13\%$) in the absence of IL-6 treatment (lane 2). Consistently with the data in Fig. 2, a treatment of control H1299 cells with IL-6 did not affect IRP2 levels in co-cultured THP1 cells (supplemental Fig. 1A). These findings support the idea that hepcidin-mediated inhibition of iron efflux results in accumulation of intracellular iron within THP1 cells, which is sensed by IRP2 and promotes its degradation.

The reduction of IRP2 levels is expected to de-repress ferritin mRNA translation; this in turn leads to storage and detoxification of excess iron [2,34]. An immunoprecipitation assay with ferritin antibodies following metabolic labeling of the co-cultured cells with ^{35}S -methionine/cysteine revealed that [IL-6]-stimulated Huh7 cells

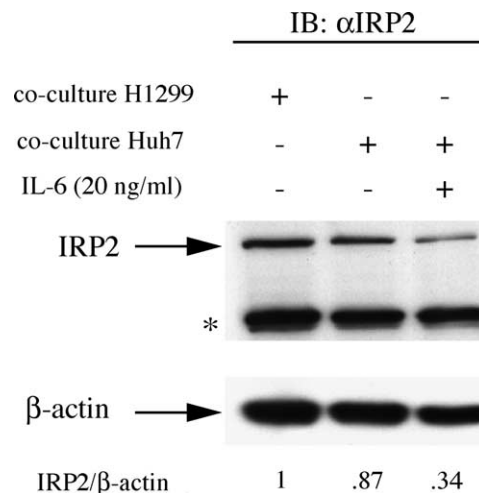


Fig. 4. The generation of hepcidin by Huh7 hepatoma cells decreases IRP2 levels in THP1 monocytes. THP1 monocytes were co-cultured for 4 h with either control H1299 lung cancer cells, Huh7 cells, or Huh7 cells previously treated with $20\ \text{ng/ml}$ IL-6 for 2 h. The expression of IRP2 (top) and β -actin (bottom) in THP1 cells was analyzed by Western blotting. IRP2/ β -actin ratios were quantified by densitometry. *Denotes an apparently non-specific band.

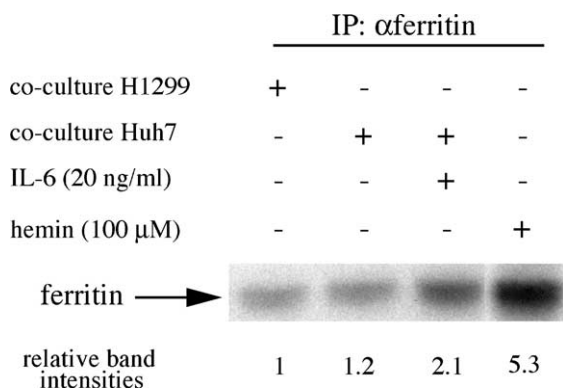


Fig. 5. The generation of hepcidin by Huh7 hepatoma cells stimulates ferritin synthesis in THP1 monocytes. THP1 monocytes were co-cultured for 2 h with either control H1299 lung cancer cells, or Huh7 cells, or Huh7 cells previously treated with 20 ng/ml IL-6 for 2 h. Subsequently, the co-cultured cells were metabolically labeled with (50 μ Ci/ml) *trans*-[35 S]label for 2 h. Lysates from THP1 cells were subjected to quantitative immunoprecipitation with ferritin antibodies. Immunoprecipitated material was analyzed by SDS-PAGE on a 15% gel and newly synthesized ferritin (arrow) was visualized by autoradiography. The relative band intensities were quantified by phosphorimaging.

triggered a 2.1-fold increase in de novo ferritin synthesis in THP1 cells (Fig. 5, lanes 1–3). As expected, a treatment with hemin fully de-repressed ferritin synthesis by 5.3-fold (lane 4), while a co-culture with [IL-6]-stimulated control H1299 cells did not affect ferritin mRNA translation in THP1 cells (supplemental Fig. 1B). We conclude that physiologically generated hepcidin modulates iron homeostasis and yields an iron-rich phenotype in THP1 monocytes via inhibition of iron efflux.

4. Discussion

The antimicrobial peptide hepcidin has emerged as a major hormonal regulator of systemic iron homeostasis. Overwhelming genetic data, suggested that hepcidin negatively regulates dietary iron absorption in the duodenum and the recycling of iron from senescent red blood cells via reticuloendothelial macrophages [1,3,26]. Biochemical experiments revealed that hepcidin binds to transfected GFP-ferroportin and regulates its subcellular localization and stability [4,5]. The iron exporter ferroportin mediates iron efflux from macrophages, which is crucial for the maintenance of a dynamic pool of transferrin-bound iron in plasma and the delivery of the metal to developing erythroid cells and other tissues [2]. The potential of hepcidin to control ferroportin expression provides a framework to understand the function of this peptide. Nevertheless, the functional characterization of hepcidin is far from completed and important physiological aspects remain largely unexplored. This prompted us to study the effects of

hepcidin on macrophage iron efflux and on overall macrophage iron metabolism.

Because hepcidin is generated by hepatocytes and serves as a signal to target macrophages (and enterocytes), we established a physiologically relevant co-culture model of hepcidin-producing hepatoma cells and target THP1 monocytic cells. We previously optimized conditions for an iron release assay: THP1 cells were loaded with 59 Fe-Tf and the release of 59 Fe in serum-free media was monitored in the presence of HMW-DFO as an iron acceptor (Fig. 1). The induction of endogenous hepcidin by Huh7 cells in response to stimulation with IL-6, or the over-expression of a hepcidin cDNA in transfected HepG2 cells, appreciably reduced the release of 59 Fe from co-cultured THP1 monocytes by 30–35% (Figs. 2 and 3). These statistically significant values ($p < 0.05$) compare to 59 Fe release in control co-culture experiments with H1299 lung cancer cells. A consistent, yet smaller decrease (~15%) that did not reach statistical significance was apparent when 59 Fe release from THP1 monocytes was compared between co-cultures with control H1299 cells that do not express any hepcidin (Fig. 2A), and co-cultures with unstimulated Huh7 or untransfected HepG2 cells. This effect could be attributed to basal expression of hepcidin in the hepatic cells.

The data in Figs. 2 and 3 directly demonstrate that physiologically generated hepcidin controls iron efflux from monocytic cells. They also corroborate biochemical experiments documenting inhibition of iron efflux due to hepcidin-mediated relocalization and lysosomal degradation of transfected ferroportin [4,5,29]. Moreover, they strongly suggest that hepcidin produced by hepatoma cells likely targets endogenous ferroportin from co-cultured THP1 cells for degradation. Experiments are underway to validate this hypothesis, which is further supported by recent data showing that exposure of bone marrow-derived macrophages to synthetic hepcidin decreases levels of endogenous ferroportin [35].

Importantly, the capacity of physiologically generated hepcidin to inhibit 59 Fe release from THP1 cells correlates with a reduction of IRP2 levels (Fig. 4) and the concomitant de-repression of ferritin synthesis (Fig. 5). Because IRP2 is sensitive to iron-dependent degradation [34], assessment of its steady-state levels serves as a reliable marker of cellular iron status [4]. Thus, low IRP2 levels are indicative of an iron-replete state. The observed increase in de novo synthesis of ferritin, that stores and detoxifies excess intracellular iron [36], is in agreement with the well-established function of IRP2 as a repressor of ferritin mRNA translation [2,34].

In summary, the data presented here show that hepcidin generated by hepatic cells inhibits iron efflux from target monocytes and activates homeostatic responses in these cells to handle iron accumulation. These findings are fully consistent with a function of hepcidin in controlling the degree of iron load in macrophages and with the proposed

causative relationship of pathological hepcidin expression with the development of ACD.

Acknowledgements

We thank Dr M. Muckenthaler (University of Heidelberg) for the hepcidin cDNA and Drs B. Galy and M. W. Hentze (EMBL, Heidelberg) for the IRP2 antisera. KP holds a senior career award from the Fonds de la recherche en santé du Québec (FRSQ).

Supplementary Material

Supplementary data associated with this article can be found, in the online version, at [doi:10.1016/j.jhep.2005.10.025](https://doi.org/10.1016/j.jhep.2005.10.025)

References

- [1] Ganz T. Hepcidin in iron metabolism. *Curr Opin Hematol* 2004;11:251–254.
- [2] Hentze MW, Muckenthaler MU, Andrews NC. Balancing acts: molecular control of mammalian iron metabolism. *Cell* 2004;117:285–297.
- [3] Fleming RE. Advances in understanding the molecular basis for the regulation of dietary iron absorption. *Curr Opin Gastroenterol* 2005;21:201–206.
- [4] Nemeth E, Tuttle MS, Powelson J, Vaughn MB, Donovan A, Ward DM, et al. Hepcidin regulates cellular iron efflux by binding to ferroportin and inducing its internalization. *Science* 2004;306:2090–2093.
- [5] De Domenico I, Ward DM, Nemeth E, Vaughn MB, Musci G, Ganz T, et al. The molecular basis of ferroportin-linked hemochromatosis. *Proc Natl Acad Sci USA* 2005;102:8955–8960.
- [6] Nicolas G, Chauvet C, Viatte L, Danan JL, Bigard X, Devaux I, et al. The gene encoding the iron regulatory peptide hepcidin is regulated by anemia, hypoxia, and inflammation. *J Clin Invest* 2002;110:1037–1044.
- [7] Pigeon C, Ilyin G, Courselaud B, Leroyer P, Turlin B, Brissot P, et al. A new mouse liver-specific gene, encoding a protein homologous to human antimicrobial peptide hepcidin, is overexpressed during iron overload. *J Biol Chem* 2001;276:7811–7819.
- [8] Lee P, Peng H, Gelbart T, Wang L, Beutler E. Regulation of hepcidin transcription by interleukin-1 and interleukin-6. *Proc Natl Acad Sci USA* 2005;102:1906–1910.
- [9] Nemeth E, Rivera S, Gabayan V, Keller C, Taudorf S, Pedersen BK, et al. IL-6 mediates hypoferrinemia of inflammation by inducing the synthesis of the iron regulatory hormone hepcidin. *J Clin Invest* 2004;113:1271–1276.
- [10] Roetto A, Papanikolaou G, Politou M, Alberti F, Girelli D, Christakis J, et al. Mutant antimicrobial peptide hepcidin is associated with severe juvenile hemochromatosis. *Nat Genet* 2003;33:21–22.
- [11] Pietrangelo A. Hereditary hemochromatosis—a new look at an old disease. *N Engl J Med* 2004;350:2383–2397.
- [12] Bridle KR, Frazer DM, Wilkins SJ, Dixon JL, Purdie DM, Crawford DH, et al. Disrupted hepcidin regulation in HFE-associated haemochromatosis and the liver as a regulator of body iron homeostasis. *Lancet* 2003;361:669–673.
- [13] Nemeth E, Roetto A, Garozzo G, Ganz T, Camaschella C. Hepcidin is decreased in TFR2 hemochromatosis. *Blood* 2005;105:1803–1806.
- [14] Papanikolaou G, Samuels ME, Ludwig EH, MacDonald ML, Franchini PL, Dube MP, et al. Mutations in HFE2 cause iron overload in chromosome 1q-linked juvenile hemochromatosis. *Nat Genet* 2004;36:77–82.
- [15] Gehrke SG, Kulaksiz H, Herrmann T, Riedel HD, Bents K, Veltkamp C, et al. Expression of hepcidin in hereditary hemochromatosis: evidence for a regulation in response to serum transferrin saturation and non-transferrin-bound iron. *Blood* 2003;102:371–376.
- [16] Papanikolaou G, Tzilianos M, Christakis JI, Bogdanos D, Tsimirika K, MacFarlane J, et al. Hepcidin in iron overload disorders. *Blood* 2005;105:4103–4105.
- [17] Nicolas G, Bennoun M, Devaux I, Beaumont C, Grandchamp B, Kahn A, et al. Lack of hepcidin gene expression and severe tissue iron overload in upstream stimulatory factor 2 (USF2) knockout mice. *Proc Natl Acad Sci USA* 2001;98:8780–8785.
- [18] Ahmad KA, Ahmann JR, Migas MC, Waheed A, Britton RS, Bacon BR, et al. Decreased liver hepcidin expression in the hfe knockout mouse. *Blood Cells Mol Dis* 2002;29:361–366.
- [19] Muckenthaler M, Roy CN, Custodio AO, Minana B, DeGraaf J, Montross LK, et al. Regulatory defects in liver and intestine implicate abnormal hepcidin and cybrd1 expression in mouse hemochromatosis. *Nat Genet* 2003;34:102–107.
- [20] Kawabata H, Fleming RE, Gui D, Moon SY, Saitoh T, O’Kelly J, et al. Expression of hepcidin is down-regulated in Tfr2 mutant mice manifesting a phenotype of hereditary hemochromatosis. *Blood* 2005;105:376–381.
- [21] Wallace DF, Summerville L, Lusby PE, Subramaniam VN. First phenotypic description of transferrin receptor 2 knockout mouse, and the role of hepcidin. *Gut* 2005;54:980–986.
- [22] Huang FW, Pinkus JL, Pinkus GS, Fleming MD, Andrews NC. A mouse model of juvenile hemochromatosis. *J Clin Invest* 2005;115:2187–2191.
- [23] Niederkofler V, Salie R, Arber S. Hemojuvelin is essential for dietary iron sensing, and its mutation leads to severe iron overload. *J Clin Invest* 2005;115:2180–2186.
- [24] Adamsky K, Weizer O, Amarglio N, Breda L, Harmelin A, Rivella S, et al. Decreased hepcidin mRNA expression in thalassemic mice. *Br J Haematol* 2004;124:123–124.
- [25] Nicolas G, Bennoun M, Porteu A, Mativet S, Beaumont C, Grandchamp B, et al. Severe iron deficiency anemia in transgenic mice expressing liver hepcidin. *Proc Natl Acad Sci USA* 2002;99:4596–4601.
- [26] Roy CN, Andrews NC. Anemia of inflammation: the hepcidin link. *Curr Opin Hematol* 2005;12:107–111.
- [27] Weiss G, Goodnough LT. Anemia of chronic disease. *N Engl J Med* 2005;352:1011–1023.
- [28] Donovan A, Lima CA, Pinkus JL, Pinkus GS, Zon LI, Robine S, et al. The iron exporter ferroportin/Slc40a1 is essential for iron homeostasis. *Cell Metab* 2005;1:191–200.
- [29] Knutson MD, Oukka M, Koss LM, Aydemir F, Wessling-Resnick M. Iron release from macrophages after erythrophagocytosis is up-regulated by ferroportin 1 overexpression and down-regulated by hepcidin. *Proc Natl Acad Sci USA* 2005;102:1324–1328.
- [30] Hallaway PE, Eaton JW, Panter SS, Hedlund BE. Modulation of deferoxamine toxicity and clearance by covalent attachment to biocompatible polymers. *Proc Natl Acad Sci USA* 1989;86:10108–10112.
- [31] Caltagirone A, Weiss G, Pantopoulos K. Modulation of cellular iron metabolism by hydrogen peroxide. Effects of H₂O₂ on the expression and function of iron-responsive element-containing mRNAs in B6 fibroblasts. *J Biol Chem* 2001;276:19738–19745.
- [32] Galy B, Ferring D, Minana B, Bell O, Janser HG, Muckenthaler M, et al. Altered body iron distribution and microcytosis in mice deficient for iron regulatory protein 2 (IRP2). *Blood* 2005;106:2580–2589.

- [33] Nemeth E, Valore EV, Territo M, Schiller G, Lichtenstein A, Ganz T. Hepcidin, a putative mediator of anemia of inflammation, is a type II acute-phase protein. *Blood* 2003;101:2461–2463.
- [34] Pantopoulos K. Iron metabolism and the IRE/IRP regulatory system: an update. *Ann NY Acad Sci* 2004;1012:1–13.
- [35] Delaby C, Pilard N, Goncalves AS, Beaumont C, Canonne-Hergaux F. The presence of the iron exporter ferroportin at the plasma membrane of macrophages is enhanced by iron loading and downregulated by hepcidin. *Blood* 2005; 106:3979–3984.
- [36] Harrison PM, Arosio P. The ferritins: molecular properties, iron storage function and cellular regulation. *Biochim Biophys Acta* 1996; 1275:161–203.

Sustained Hydrogen Peroxide Induces Iron Uptake by Transferrin Receptor-1 Independent of the Iron Regulatory Protein/Iron-responsive Element Network*

Received for publication, March 22, 2007 Published, JBC Papers in Press, May 21, 2007, DOI 10.1074/jbc.M702463200

Bill Andriopoulos[‡], Stephan Hegedüs[§], Julia Mangin[§], Hans-Dieter Riedel[§], Ulrike Hebling[§], Jian Wang[‡], Kostas Pantopoulos^{‡¶}, and Sebastian Mueller^{§||1}

From the [§]Department of Internal Medicine, Salem Medical Center, University of Heidelberg, Zeppelinstrasse 11-33, 69121 Heidelberg, Germany, the [‡]Lady Davis Institute for Medical Research, Sir Mortimer B. Davis Jewish General Hospital, 3755 Cote-Ste-Catherine Road, Montreal, Quebec H3T 1E2, Canada, the [¶]Department of Medicine, McGill University, Montreal, Quebec H3T 1E2, Canada, and the ^{||}Division of Gastroenterology and Hepatology, Beth Israel Deaconess Medical Center, Harvard Medical School, Boston, Massachusetts 02215

Local and systemic inflammatory conditions are characterized by the intracellular deposition of excess iron, which may promote tissue damage via Fenton chemistry. Because the Fenton reactant H₂O₂ is continuously released by inflammatory cells, a tight regulation of iron homeostasis is required. Here, we show that exposure of cultured cells to sustained low levels of H₂O₂ that mimic its release by inflammatory cells leads to up-regulation of transferrin receptor 1 (TfR1), the major iron uptake protein. The increase in TfR1 results in increased transferrin-mediated iron uptake and cellular accumulation of the metal. Although iron regulatory protein 1 is transiently activated by H₂O₂, this response is not sufficient to stabilize TfR1 mRNA and to repress the synthesis of the iron storage protein ferritin. The induction of TfR1 is also independent of transcriptional activation via hypoxia-inducible factor 1 α or significant protein stabilization. In contrast, pulse experiments with ³⁵S-labeled methionine/cysteine revealed an increased rate of TfR1 synthesis in cells exposed to sustained low H₂O₂ levels. Our results suggest a novel mechanism of iron accumulation by sustained H₂O₂, based on the translational activation of TfR1, which could provide an important (patho)physiological link between iron metabolism and inflammation.

Systemic iron homeostasis undergoes typical changes during inflammatory or infectious conditions. A decrease in plasma iron concentration limits the availability of the metal for erythropoiesis, ultimately leading to the so-called anemia of chronic disease (1). In addition to iron retention within the reticuloendothelial system, parenchymal cells such as hepatocytes also accumulate iron under inflammatory conditions (2–8), and this iron deposition has been identified as an important factor

in tissue damage by free radicals (9). In addition, hepatic iron accumulation appears to be an important cofactor in the development of fibrosis and end stage liver disease in such common chronic liver pathologies such as hepatitis C or alcoholic steatohepatitis (4–8).

Significant progress has been made toward understanding the molecular basis of iron retention within the reticuloendothelial system during inflammation (10–12). The mechanism involves the interleukin-6-mediated induction of the iron-regulatory peptide hepcidin (13, 14), which inhibits iron efflux from macrophages and intestinal enterocytes (15, 16) by binding to and promoting the degradation of the transporter ferroportin 1 (IREG1 or MTP1) (17). The ensuing hypoferrremia is thought to be part of a physiological defense strategy to deplete invading bacteria from the growth-essential iron. Thus far, the possibility that inflammation-mediated accumulation of iron in parenchymal cells may also contribute to hypoferrremia has not received much attention. Nevertheless, the expression of transferrin receptor 1 (TfR1),² the major iron uptake protein, is induced in several models of inflammation (2, 18).

Upon activation, inflammatory cells such as neutrophils and macrophages undergo an “oxidative burst” that results in the release of large amounts of reactive oxygen species to kill invading bacteria (19). The membrane-associated NADPH-oxidase (NOX2) first generates superoxide that is rapidly dismutated to the more stable H₂O₂ by superoxide dismutases (20). Thus, during inflammation, cells and tissues are exposed to sustained concentrations of H₂O₂ demanding a tight regulation of iron homeostasis to prevent tissue damage via Fenton and Fenton-like reactions. The activation of iron regulatory protein 1 (IRP1) by H₂O₂ has been proposed as a regulatory link between cellular iron homeostasis and inflammation. IRP1 regulates the expression of several proteins by post-transcriptional mechanisms. In iron-deficient cells, the mRNA of TfR1 is stabilized upon binding of IRP1 and IRP2 to iron-responsive elements (IREs) within

* This work was supported by grants from the University of Heidelberg, the Alexander von Humboldt foundation the Canadian Liver Foundation, the Deutsche Forschungsgemeinschaft, the Dietmar Hopp Foundation, and the Canadian Institutes of Health Research. The costs of publication of this article were defrayed in part by the payment of page charges. This article must therefore be hereby marked “advertisement” in accordance with 18 U.S.C. Section 1734 solely to indicate this fact.

¹ To whom correspondence should be addressed: Beth Israel Deaconess Medical Center, Harvard Medical School, 330 Brookline Ave., Dana 501, Boston, MA 02215. Tel.: 617-667-0571; Fax: 617-667-2767; E-mail: smueller@bidmc.harvard.edu or sebastian.mueller@urz.uni-heidelberg.de.

² The abbreviations used are: TfR1, transferrin receptor 1; CAT, catalase; EMSA, electrophoretic mobility shift assay; GOX, glucose oxidase; IRE, iron-responsive element; IRP1, iron regulatory protein 1; LIP, labile iron pool; HIF, hypoxia-inducible factor; PBS, phosphate-buffered saline; MTT, 3-(4,5-dimethylthiazol-2-yl)-2,5-diphenyltetrazolium bromide; DMEM, Dulbecco’s modified Eagle’s medium; RT, reverse transcription.

Sustained H₂O₂ Induces Iron Uptake by TfR1

its 3'-untranslated region (21). Earlier work showed that the IRE binding activity of IRP1 is induced by H₂O₂ (22, 23). Thus, exposure of cultured cells or intact rat liver to H₂O₂ at quantities that are commonly released by inflammatory cells rapidly activate IRP1 within 30–60 min (24, 25). Importantly, IRP1 activation by H₂O₂ was sufficient to increase TfR1 expression in B6 fibroblasts (26). TfR1 expression is also controlled transcriptionally; one mechanism involves the hypoxia-inducible factor 1 α (HIF-1 α), which binds to a conserved binding site within the TfR1 promoter (27, 28). HIF-1 α is activated in response to hypoxia, but up-regulation of HIF-1 α has also been linked to mitochondria-derived oxidative stress (29).

Transient pulses of H₂O₂ are commonly employed to study the effects of this reactive oxygen intermediate in biochemical pathways. Such conditions, however, hardly mimic the continuous release of H₂O₂ from inflammatory cells because H₂O₂ is degraded rapidly by cultured cells (30). We have previously employed an enzymatic system for H₂O₂ generation at steady-state levels based on glucose oxidase (GOX) and catalase (CAT) (25, 30–32). For methodological reasons, however, these studies were restricted to relatively short time intervals (24, 25). In an optimized setting, we expose here cultured cells to a sustained flux of H₂O₂ at low, nontoxic concentrations that mimic the H₂O₂ release by inflammatory cells in terms of time and dose response. We show that such conditions induce the expression of TfR1, which is associated with increased transferrin-mediated iron uptake and intracellular iron accumulation. Neither IRP1 nor HIF-1 α are involved in the up-regulation of TfR1 in response to such sustained low levels of H₂O₂. Moreover, H₂O₂ does not block TfR1 turnover but significantly stimulates TfR1 expression at the translational level. We suggest that H₂O₂-mediated iron uptake via translational induction of TfR1 could be a general mechanism that contributes to iron accumulation and tissue damage under conditions of inflammation.

EXPERIMENTAL PROCEDURES

Reagents—Luminol, NaOCl, phosphate-buffered saline (PBS), Hanks' buffer, H₂O₂, catalase, tetrazolium salt (MTT), glucose oxidase, and sodium azide were purchased from Sigma. Dulbecco's modified Eagle's medium (DMEM), McCoy's 5A medium, and penicillin/streptomycin were purchased from Invitrogen. Fetal calf serum was purchased from Greiner Labortechnik. Stock solutions of luminol, NaOCl, and H₂O₂ were prepared as described recently (32).

Cell Culture—Human HepG2, HeLa, and HT29 cells were grown in DMEM supplemented with 2 mM glutamine, 4.5 g/liter glucose, 100 units/ml penicillin, 0.1 ng/ml streptomycin, and 10% fetal calf serum. Human colonic carcinoma HCT116 cells were grown in McCoy's 5A medium, and murine B6 fibroblasts were grown in supplemented DMEM containing 1000 mg/liter of glucose. The cells were maintained in an incubator at 37 °C with 5% CO₂.

Determination of Enzymatic Activities for Catalase and GOX—Enzymatic activities of GOX and catalase were determined at submicromolar H₂O₂ concentrations prior to the experiment using a sensitive chemiluminescence technique (31, 33). Continuous measurements on supernatants of cultured cells con-

firmed the maintenance of steady-state concentrations of H₂O₂ during each experiment (30).

Electrophoretic Mobility Shift Assay (EMSA)—EMSAs were performed as described previously using a radiolabeled human ferritin H-chain IRE probe (34). RNA-protein complex formation was quantified by densitometric scanning of the depicted autoradiographs.

Western Blotting—The cells were solubilized directly in radioimmune precipitation assay lysis buffer, and lysates were immediately boiled for 10 min. Equal aliquots were resolved by SDS/PAGE on 8% gels, and proteins were transferred on to nitrocellulose filters. The blots were saturated with 5% nonfat milk in PBS and probed with 1:4000 TfR1 (Zymed Laboratories Inc., San Francisco, CA), 1:250 HIF-1 α mouse (Biosciences, Heidelberg, Germany), or 1:500 β -actin (Sigma) antibodies. After washing with Tris-buffered saline containing 0.05% (v/v) Tween 20, the blots were further incubated with horseradish peroxidase-conjugated secondary antibodies using the following dilutions: TfR monoclonal antibodies with rabbit anti-mouse IgG 1:6000, β -actin antibodies with goat anti-rabbit IgG 1:10000, and HIF-1 α mouse antibodies with goat anti-mouse IgG 1:10000 dilution. Glucose oxidase was detected with a previously developed anti-GOX polyclonal antibody (35) in conjunction with an horseradish peroxidase-conjugated anti-guinea pig secondary antibody (Dianova, Hamburg, Germany) at a dilution of 1:3000. Detection of the horseradish peroxidase-coupled secondary antibodies was performed with the ECL[®] method (Amersham Biosciences). The blots were quantified by densitometric scanning using the TotalLab software version 1.11 (Nonlinear Dynamics Inc., Durham, NC).

Determination of the Labile Iron Pool (LIP)—The LIP was measured using the metal-sensitive fluorescence probe calcein (36, 37). We modified the technique to allow LIP detection of attached cells. Briefly, the cells were first treated for over 24 h in the presence of H₂O₂ or the membrane-impermeable iron chelator desferal (desferrioxamine). The cells were then washed twice with PBS and loaded with calcein-acetoxymethyl ester at a final concentration of 5 μ M for 30 min (from a 10 mM stock solution in dimethyl sulfoxide). First fluorescence readings (F1) were taken using a Fluostar (BMG Labtechnologies GmbH, Offenburg, Germany) in bottom read technique with a fluorescein optical filter (excitation, 465–495 nm; emission, 505 nm). Subsequently, the cells were depleted of iron in the presence of the membrane-permeable iron chelator salicylaldehyde isonicotinoyl hydrazone for 30 min (38), and a second measurement of fluorescence was performed (F2). After background subtraction, this protocol allowed us to determine the F2/F1 ratio as relative indicator of LIP independent of the cell number and distribution within the wells.

Northern Blotting—RNA prepared with the TRIzol[®] reagent (Invitrogen) was analyzed by Northern blotting with ³²P-radio-labeled mouse TfR1, hepcidin, or rat β -actin cDNA probes (23).

Oxygen Measurements and Induction of Hypoxia—Oxygen was measured using a computer-driven oxygen electrode Oxi 325-B (WTW, Weilheim, Germany). The electrode was calibrated with air-saturated water (21%). Permanent magnetic stirring was necessary to facilitate oxygen exchange at the membrane side of the oxygen electrode. To induce hypoxia, an

custom-made oxygen chamber was used and equilibrated with a prepared gas mixture of 3% oxygen, 5% carbon dioxide, and 92% nitrogen (Lifegas).

Iron Uptake Experiments—Transferrin-mediated iron uptake experiments were carried out as described in Ref. 39. Briefly, uptake experiments of ^{59}Fe -labeled diferric transferrin (holotransferrin) were performed in 6-cm dishes at 37 °C for 30 min in 1 ml of buffer A (140 mM NaCl, 5 mM KCl, 1 mM CaCl_2 , 1 mM MgCl_2 , 5 mM NaH_2PO_4 , and 5 mM HEPES, pH 7.4). The cells were washed five times with ice-cold PBS and then lysed with 1 ml 1 M NaOH. Radioactivity of lysates was determined using a Cobra II Auto Gamma counter (Canberra Packard, Meriden, CT). For all of the uptake experiments, the controls were incubated on ice to determine nonspecific binding of holotransferrin to the cell membrane. The 0 °C values were subtracted from the 37 °C values to determine net uptake rates.

Analysis of TfR1 mRNA Levels by Quantitative RT-PCR—Total RNA was isolated from cell culture using the TRIzol® reagent (Invitrogen). TfR1 and control β -actin mRNA transcripts were quantified by a two-step RT-PCR with the Applied Biosystems 7500 real time PCR system. cDNA synthesis was performed with a first strand cDNA synthesis kit for RT-PCR (Invitrogen), according to the manufacturer's instructions. Transcripts were amplified in duplicates with specific sense and antisense QuantiTect® primers (Qiagen). The thermal cycler profile consisted of a total reaction volume of 50 μl that underwent a 95 °C activation for 10 min, followed by 40 repetitions of the following three steps: 95 °C denaturation for 15 s, annealing at 55 °C for 30 s, and a 33-s extension period at 72 °C. Transcripts were detected with the QuantiTect SYBR® Green kit. TfR1/ β -actin ratios were calculated using LightCycler sequence detection software v1.2.

TfR1 Protein Stability and Synthesis—For protein stability, the cells were metabolically labeled for 1 h with (50 $\mu\text{Ci/ml}$) trans- ^{35}S label, a mixture of 70:30 [^{35}S]methionine/cysteine (ICN, Irvine, CA) in RPMI methionine/cysteine-free medium prior to GOX treatment. Following the 1-h pulse, the cells were chased with cold medium in the absence or presence of GOX treatment. In contrast, the rate of protein synthesis was determined by first incubating the cells in cold medium with or without GOX and subsequently metabolically labeling the cells for 1 h. Following both the protein stability and synthesis studies, the cells were lysed with radioimmune precipitation assay buffer, and 1 mg of lysates was subjected to quantitative immunoprecipitation with 2 μl of mouse monoclonal TfR (Zymed Laboratories Inc., San Francisco, CA). Immunoprecipitated proteins were analyzed by SDS/PAGE and visualized by autoradiography. Radioactive bands were quantified by phosphorimaging.

Cytotoxicity Studies—Cell viability was determined with the MTT assay (40). Briefly, conversion of the tetrazolium salt (MTT) into a blue formazan product was detected using a 96-well plate reader (Fluostar, BMG Labtechnologies GmbH, Offenburg, Germany) at 570 nm. The cells were treated with different activities of glucose oxidase and catalase in culture medium for 24 h in 96-well plates at 37 °C. After two washing steps with PBS, MTT was added to each well (0.5 mg/ml), the cells were incubated for further 4 h at 37 °C and, finally, 10%

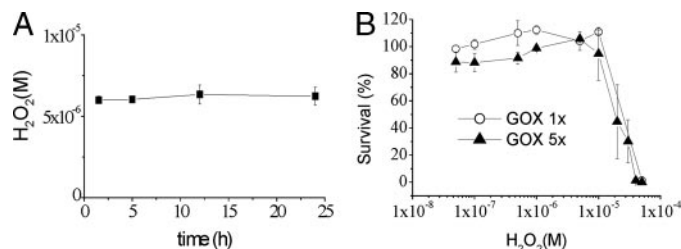


FIGURE 1. Exposure of cultured cells to sustained nontoxic H_2O_2 . A, combination of glucose oxidase and catalase (GOX/CAT) is able to maintain stable H_2O_2 concentrations over 24 h in culture medium (DMEM, high glucose). H_2O_2 was determined at different time points using the luminol/hypochlorite assay (see "Experimental Procedures"). Final enzyme activities: $k_{\text{CAT}} = 4.8 \times 10^{-3} \text{ s}^{-1}$ and $k_{\text{GOX}} = 3 \times 10^{-8} \text{ M s}^{-1}$. B, B6 fibroblasts were exposed to varying stable concentrations of H_2O_2 for 24 h in the presence of two different GOX concentrations with GOX 1 \times corresponding to $k_{\text{GOX}} = 3 \times 10^{-8} \text{ M s}^{-1}$. Cell viability was determined with the MTT assay. Variation of H_2O_2 concentration at the fixed amounts of GOX were achieved by increasing activities of external catalase. Each point reflects the average of eight measurements. Bars, S.D.

SDS in 0.01 M HCl was added to lyse the cells. The samples were incubated overnight, and the absorbance was measured.

RESULTS

Generation of Sustained H_2O_2 in Cultured Cells under Nontoxic Conditions—Optimization of the previously developed GOX/CAT system (30–32) allowed us to expand H_2O_2 exposure times up to several days, thus mimicking, with respect to oxidative stress, a chronic inflammatory response. Levels and flux of H_2O_2 by GOX are lower or resemble those of activated leukocytes *in vivo* (0.2 $\mu\text{M s}^{-1}$ or $<10 \mu\text{M}$) (41). Using an ultrasensitive H_2O_2 assay (30, 41), we show (Fig. 1A) that H_2O_2 is maintained at a constant concentration of $\sim 5 \mu\text{M}$ over the entire time interval of 24 h, indicating that GOX remains stable under these experimental conditions and the substrates glucose and oxygen are not depleted. Cell cultures could be exposed to GOX/CAT over several days, and such experiments were only limited by cellular confluence and eventual growth arrest. The media were always replaced every 12 or 24 h to prevent glucose depletion. We then examined whether under the above experimental conditions toxicity/growth inhibition was associated with H_2O_2 concentrations or flux by varying GOX amounts or ratios of GOX/CAT (32, 42). As demonstrated in Fig. 1B, toxicity depended solely on the levels of H_2O_2 and was independent of the flux. Both GOX 1 \times and GOX 5 \times inhibited cell growth when H_2O_2 levels exceeded a concentration of 10 μM H_2O_2 . Interestingly, B6 cells that were incubated with increasing GOX without the additional external catalase also showed growth inhibition at a steady-state concentration of 10 μM H_2O_2 because of the low cellular catalase activity of 0.001 s^{-1} (31). Thus, toxicity of a GOX/CAT system only depends on the concentration of H_2O_2 (defined by the ratio of GOX/CAT) and not the H_2O_2 generation rate (defined by the GOX activity), which could be linked to consumption or other metabolites. No changes in cell growth were observed with H_2O_2 concentrations below 5 μM , and these nontoxic conditions are tolerated well over 24 h.

Sustained Exposure of Cultured Cells to Nontoxic H_2O_2 Concentrations Up-regulates TfR1—Long term exposure of B6 fibroblasts over 48 h to low H_2O_2 concentrations was accompanied by a strong induction of TfR1 expression (Fig.

Sustained H₂O₂ Induces Iron Uptake by TfR1

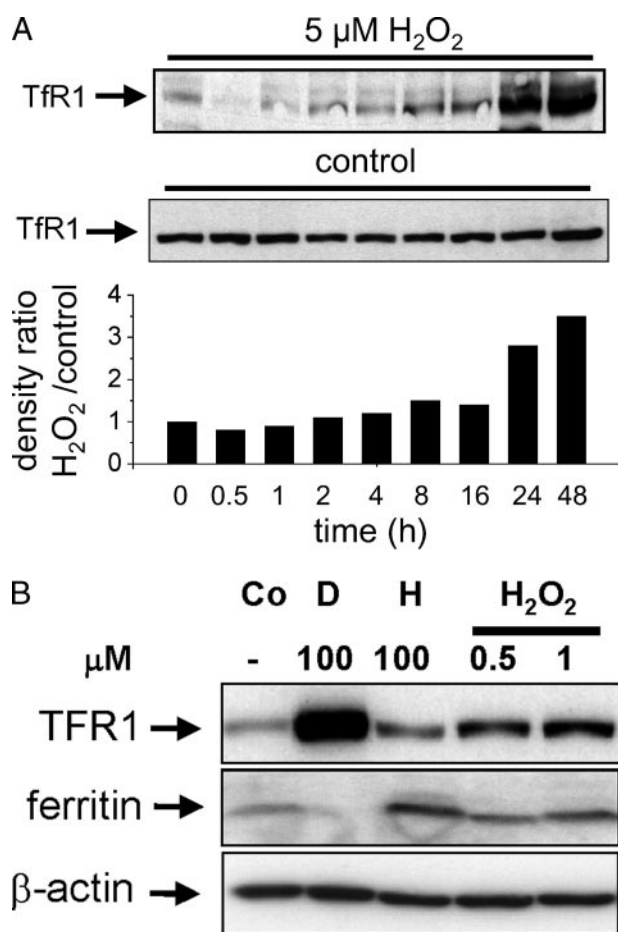


FIGURE 2. Sustained H₂O₂ up-regulates TfR1 without repression of ferritin. *A*, B6 fibroblasts were exposed to stable concentrations of 5 μM H₂O₂ similar as described in the legend to Fig. 1*A*, and expression of TfR1 was analyzed by Western blotting (*top panel*). The *middle panel* shows TfR1 expression of the untreated control. The *bottom panel* shows the ratio of H₂O₂-treated versus untreated controls as obtained by densitometry. The depicted experiment is representative of three independent measurements. *B*, B6 fibroblasts were treated for 24 h with the iron chelator desferrioxamine (*D*), hemine (*H*), two different sustained concentrations of H₂O₂, and expression of TfR1, ferritin, and β -actin was determined by Western blotting. In contrast to iron depletion by desferrioxamine, sustained H₂O₂ slightly increases ferritin levels in addition to TfR1 induction. The depicted experiment is representative of three independent measurements.

2*A*). A slight increase (40%) of TfR1 steady-state levels was observed after 8 h, whereas maximal activation (~ 3.5 -fold) was manifested after 24 h and sustained up to 48 h. Excess of catalase completely blocked TfR1 up-regulation (not shown). Thus, H₂O₂ not only antagonized the previously reported inhibiting effect of cell growth on TfR1 expression (43) but further increased TfR1 expression. The ratios of TfR1 densities from H₂O₂-treated and control cells are shown in the *bottom panel* of Fig. 2*A*. In contrast to iron-depleting conditions, the iron storage protein ferritin was slightly up-regulated in H₂O₂-treated cells and more so with iron loading with hemine (Fig. 2*B*). Thus, prolonged exposure of B6 cells to nontoxic H₂O₂ concentrations strongly activates TfR1 expression and slightly up-regulates ferritin. Importantly, these data were corroborated in additional cell lines of various tissue origin (HeLa, HepG2, HCT116, and HT29).

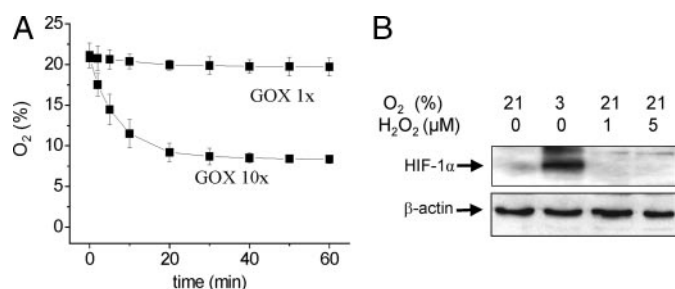


FIGURE 3. GOX induces expression of TfR1 via H₂O₂ in the absence of hypoxia. *A*, GOX activities that are sufficient to induce TfR1 (GOX 1 \times) do not change oxygen levels, whereas high activities of GOX (GOX 10 \times) are able to induce mild hypoxia in the cell culture medium. The oxygen levels were measured with an oxygen electrode in the presence of varying GOX activities in a 10-cm culture dish containing 45 ml of medium and 25 mM glucose. GOX 1 \times corresponds to $k_{\text{GOX}} = 3.0 \times 10^{-8} \text{ M s}^{-1}$. *B*, expression of HIF-1 α was measured in HepG2 cells that were exposed to different levels of sustained H₂O₂. An oxygen chamber (3% oxygen) was used as positive control. HIF-1 α was rapidly induced within 6 h. No HIF-1 α induction was observed with the GOX/CAT system (GOX 1 \times) generating 1 or 5 μM of sustained H₂O₂, although TfR1 is induced under these conditions (see Fig. 2). Catalase was used to adjust H₂O₂ levels. *Lanes* (medium volume, k_{GOX} , k_{CAT}): *lane 1*, 10 ml, 0, 0; *lane 2*, 10 ml, 3% oxygen; *lane 3*, 10 ml, $3 \times 10^{-8} \text{ M s}^{-1}$, $2.4 \times 10^{-2} \text{ s}^{-1}$; *lane 4*, 10 ml, $3 \times 10^{-8} \text{ M s}^{-1}$, $4.8 \times 10^{-3} \text{ s}^{-1}$. The depicted experiment is representative of three independent measurements.

TfR1 Up-regulation in Cells Exposed to GOX/CAT Is Mediated Solely by H₂O₂ and Not Hypoxia—In the GOX/CAT system, the ratio of GOX/CAT activities determines the concentration of H₂O₂, whereas GOX defines the consumption rate of oxygen (30). At higher concentrations, GOX significantly decreases oxygen levels in the culture medium (Fig. 3*A*). Because hypoxia (27, 28) and oxidative stress (29) have been shown to induce TfR1 expression via the transcription factor HIF-1 α , we next studied whether exposure of cells to sustained H₂O₂ at our conditions increases expression of HIF-1 α . Hepatoma HepG2 cells that express HIF-1 α in response to hypoxia (44) were exposed for 6 h to different concentrations of H₂O₂ generated by the GOX/CAT system that are known to induce TfR1 (Fig. 2), and HIF-1 α was determined by Western blotting (Fig. 3*B*). The cells that were incubated with 3% oxygen using an oxygen chamber served as a positive control. As expected, HIF-1 α expression is only induced at 3% oxygen (*lane 2*), whereas the application of GOX/CAT at an H₂O₂ flux that results in TfR1 activation (as in Fig. 2) did not stimulate HIF-1 α expression (*lane 3* and 4). We conclude that sustained H₂O₂ activates TfR1 specifically and in the absence of hypoxia.

H₂O₂-mediated Up-regulation of TfR1 Is Functional and Results in Intracellular Accumulation of Iron—We next addressed the question of whether TfR1 up-regulation in response to sustained H₂O₂ is physiologically significant. Transferrin-mediated iron uptake was measured by exposing B6 cells to various steady-state H₂O₂ concentrations over 24 h in the presence of ⁵⁹Fe-loaded and purified transferrin. Fig. 4*A* demonstrates a significant H₂O₂-dependent increase in ⁵⁹Fe uptake 2.4-fold. We then assessed the effects of the prolonged H₂O₂ treatment on the LIP using a modified calcein assay (36, 37). Iron depletion by desferrioxamine was used as negative control. Fig. 4*B* shows that the LIP is clearly increased in B6 fibroblasts upon exposure to a H₂O₂ flux over 24 h. Similar responses of LIP were found with all other cell lines (data not shown).

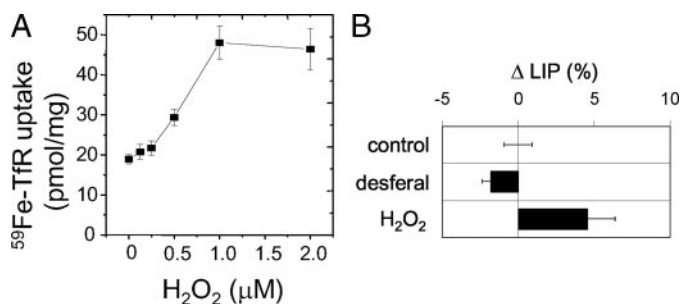


FIGURE 4. Sustained H₂O₂ increases transferrin-mediated iron uptake and the intracellular LIP. *A*, the uptake of ⁵⁹Fe-labeled diferric transferrin is induced in the presence of continuous release of H₂O₂ over 24 h. B6 fibroblasts were exposed to GOX/CAT to obtain sustained H₂O₂ concentrations as indicated. Each point reflects the average of five measurements. *Bars*, S.D. *B*, increase of labile iron pool in the presence of a continuous nontoxic flux of H₂O₂ over 24 h in B6 fibroblasts. The conditions are similar to those described in the legend to Fig. 1. 100 μM desferal (desferrioxamine) was used as negative control to deplete B6 fibroblasts of iron. The depicted experiment is representative of eight independent measurements. *Bars*, S.D.

Stimulated Iron Uptake by Sustained H₂O₂ Is Independent of the IRE/IRP Regulatory System—Earlier studies had shown that H₂O₂ rapidly activates IRP1 in cultured cells (22, 23) and in perfused rat liver (24) and that H₂O₂-mediated activation of IRP1 was sufficient to increase TfR1 mRNA and protein levels (26). A threshold of ~10 μM was defined as the minimal concentration required for IRP1 activation within 30–60 min (25); however, methodological constraints did not allow H₂O₂ exposure times longer than 60 min. The optimized H₂O₂ models presented herein enabled us to evaluate IRP1 activity by EMSA after prolonged H₂O₂ treatments. Exposure of B6 cells to steady-state concentrations of ~5 μM H₂O₂ was associated with an initial modest activation of IRP1 that was detectable up to 6 h (Fig. 5*A*, lanes 1 and 2). However, IRP1 activity declined within the next 24 h of H₂O₂ treatment (lanes 3–4), to the same degree observed in response to iron-loading with hemin (lane 5). As expected, the iron chelator desferrioxamine drastically activated IRP1 (lane 6). In contrast to iron overload with hemin, however, incubation of cell lysates with 2-mercaptoethanol that activates IRP1 *in vitro* indicated also decreased IRP1 protein levels. Moreover, TfR1 mRNA levels were not increased in response to H₂O₂ as determined by quantitative RT-PCR (Fig. 5*B*). Thus, it appears that the sustained exposure of cells to such low, nontoxic H₂O₂ concentrations only modestly and transiently induces IRP1 activity, and this response is not sufficient to stabilize TfR1 mRNA.

Increased Levels of TfR1 during Sustained H₂O₂ Is Independent of TfR1 Stability but Involves Stimulation of TfR1 Synthesis—Expression of TfR1 is typically controlled at the level of transcription or stabilization of its mRNA via IRPs. Because these mechanisms were excluded, we next studied whether TfR1 levels were affected by either protein stability or synthesis. To measure protein stability in cells with or without sustained H₂O₂ treatment, B6 cells were pulsed with [³⁵S]methionine/cysteine for 1 h (time 0) and chased for 1, 6.5, and 24 h (Fig. 6). The cells were then lysed, and TfR1 levels were determined by quantitative immunoprecipitation and autoradiography. After 1 and 6 h of chase, TfR1 expression appeared to be slightly higher in cells treated with H₂O₂ than in control cells. However, a 24-h treatment with H₂O₂ did not affect the stability of TfR1.

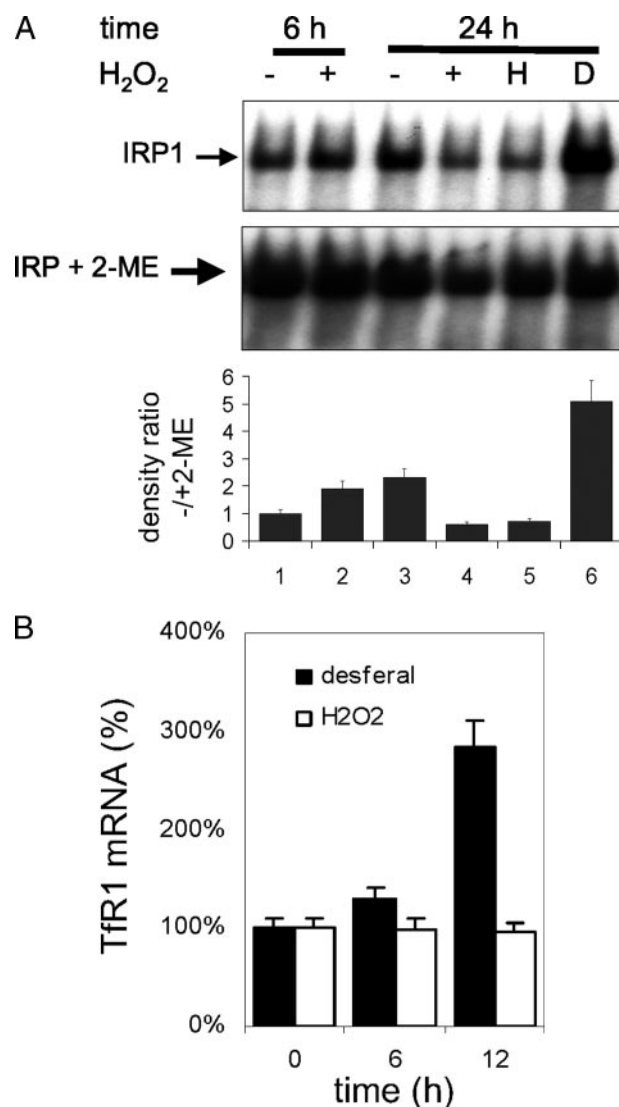


FIGURE 5. Sustained H₂O₂ up-regulates TfR1 independently of the IRE/IRP network. *A*, cytoplasmic extracts (25 μg) were analyzed by EMSA with 25,000 cpm of ³²P-labeled IRE probe (top panel) or presence of 2% 2-mercaptoethanol (middle panel). The bottom panel shows the ratio of 2-mercaptoethanol-treated (loading control) versus untreated lysates as obtained by densitometry. IRP1 activity was assessed in the absence or presence of H₂O₂ for 6 or 24 h (lanes 1–4). Treatments with 100 μM desferrioxamine or hemin were used as positive and negative controls, respectively (lane 5 and 6). Other conditions are as described in the legend to Fig. 1. The depicted results are representative of three independent experiments. *B*, mouse B6 fibroblasts were treated with sustained H₂O₂ using a GOX/CAT system as in Fig. 1. TfR1 mRNA levels were analyzed by quantitative RT-PCR and expressed relative to β-actin mRNA. Data from three independent experiments are shown (means ± S.D.). Iron depletion in the presence of 100 μM desferrioxamine served as positive control strongly inducing TfR1 mRNA via IRP1 as shown in Fig. 5*A*.

We conclude that the surge of TfR1 levels during H₂O₂ treatment is independent of TfR1 stabilization. We next addressed whether the rate of protein synthesis played a role in the elevated levels of TfR1 during H₂O₂ treatment. The cells were treated with GOX for 1, 6, 12, and 24 h and subsequently pulsed with the [³⁵S]methionine/cysteine for 1 h (Fig. 7). The cells were then lysed, and TfR1 synthesis was analyzed by quantitative immunoprecipitation and autoradiography. As shown in Fig. 7, the rate of TfR1 synthesis was relatively unchanged in comparison with nontreated cells following 1 and 6 h of GOX

Sustained H_2O_2 Induces Iron Uptake by Tfr1

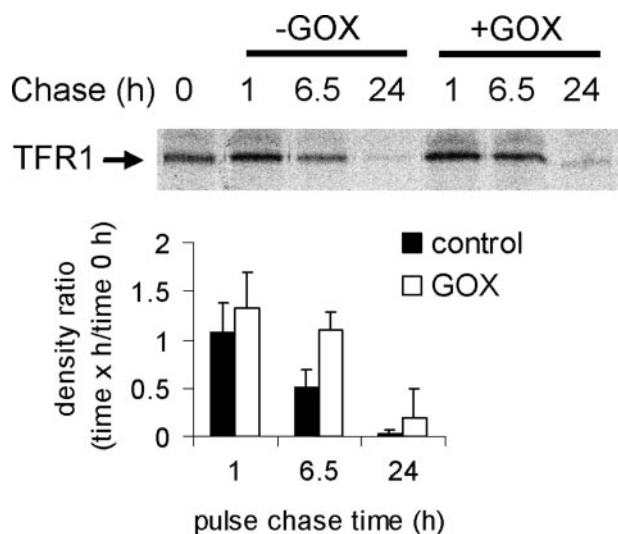


FIGURE 6. Tfr1 up-regulation by H_2O_2 is independent of protein stability. B6 cells were pulsed for 1 h with [^{35}S]methionine/cysteine and chased for 1, 6.5, or 24 h with or without additional GOX. Immunoprecipitated Tfr1 was analyzed by SDS/PAGE and visualized by autoradiography (top panel). Radioactive bands were quantified by phosphorimaging (bottom panel). Densitometry data are represented as ratio of chased time versus time 0 h and reflect three independent experiments.

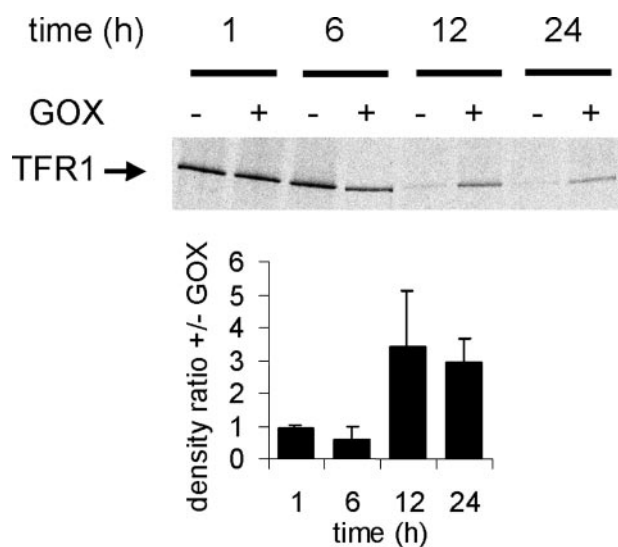


FIGURE 7. Sustained H_2O_2 induces Tfr1 synthesis via direct stimulation of translation. B6 cells were treated with GOX for 1, 6, 12, and 24 h and subsequently pulsed with the [^{35}S]methionine/cysteine for 1 h. Immunoprecipitated Tfr1 was analyzed by SDS/PAGE and visualized by autoradiography (top panel). Radioactive bands were quantified by phosphorimaging (bottom panel). Densitometry data indicate the ratio of Tfr synthesis of GOX treated versus control from three independent experiments.

treatment. In contrast, Tfr1 mRNA translation was dramatically up-regulated in H_2O_2 -exposed cells after 12 h of GOX treatment. These findings indicate a novel mechanism by which sustained H_2O_2 increases iron uptake via translational stimulation of Tfr1.

DISCUSSION

The typical changes of iron homeostasis during acute inflammation are considered to be part of the defensive immune response. In chronic inflammation, however, parenchymal cells often show increased deposits of iron that may aggravate dis-

ease progression and promote further tissue damage. Under these conditions, iron becomes especially harmful because it catalyzes the generation of free radicals from reactive oxygen species released by inflammatory cells. Here, we show that the exposure of various cell types to sustained H_2O_2 results in the up-regulation of Tfr1 expression and accumulation of iron. We also provide evidence that the mechanism for Tfr1 activation by H_2O_2 is translational.

The levels of sustained H_2O_2 utilized in our experiments are nontoxic and mimic inflammatory conditions. Thus, our experimental system provides a tool to study the alterations of iron homeostasis observed in chronic inflammation. A diversion of iron from circulation into intracellular compartments is well established. This is associated with impaired erythropoiesis, which eventually leads to the anemia of chronic disease (1, 3, 45, 46). The antimicrobial peptide hepcidin inhibits iron efflux from macrophages via ferroportin 1 (17, 47). Considering that hepcidin expression is induced by the pro-inflammatory cytokine interleukin-6, this pathway is expected to promote tissue iron accumulation and thereby plays a key role in the development of anemia of chronic disease. It is, however, possible that in addition to inhibition of iron efflux, increased iron uptake may also contribute to tissue iron accumulation in anemia of chronic disease. Our results suggest that the H_2O_2 -mediated increase of Tfr1 may account for this response.

Importantly, increased expression of Tfr1 has been observed in animal models of inflammation (2, 18). In humans, direct evidence of Tfr1 up-regulation has been recently found in patients with acute respiratory distress syndrome (18). In addition, levels of soluble Tfr receptor are associated with inflammation independent of the degree of erythropoiesis, the hypoxic response and iron status (48). During acute inflammation, the up-regulation of Tfr1 may reduce the availability of essential iron to invading bacteria and is probably beneficial for the host. In chronic inflammation, however, accumulation of iron in tissues is associated with toxicity (9) and seems to drive progression of fibrosis and end stage liver disease in such common liver pathologies such as chronic hepatitis C or alcoholic liver disease (4–8).

What is the mechanism for Tfr1 activation by low, nontoxic doses of H_2O_2 ? We first explored the role of HIF-1 α that is known to transcriptionally activate Tfr1 (27, 28) and also responds to reactive oxygen species independently of hypoxia (29, 49). However, our data clearly show that the GOX system can be calibrated to generate H_2O_2 steady-state levels in the absence of hypoxia (Fig. 3). Moreover, the H_2O_2 -mediated activation of Tfr1 expression does not require the induction of HIF-1 α . Second, we hypothesized that the mechanism may involve Tfr1 mRNA stabilization by IRP1, which is rapidly activated by H_2O_2 within 30 min to bind to IREs (22, 23, 34). As shown previously in B6 fibroblasts, IRP1 is activated by a bolus of 100 μM H_2O_2 (26). In the present study, B6 and other cells were exposed to sustained $\sim 5 \mu M$ H_2O_2 (Fig. 1), and IRP1 was only partially and temporarily activated (Fig. 5A), very likely because of H_2O_2 signaling. The absence of full IRP1 activation under these conditions is fully consistent with previous findings, showing that a concentration of $\sim 10 \mu M$ H_2O_2 was a minimum requirement to elicit the complete response (25).

Notably, IRP1 activity decreased at later time intervals (24 h) of GOX treatment, possibly because of increased intracellular iron accumulation. The observed modest alterations in IRE binding activity did not affect TfR1 mRNA levels (Fig. 5B), suggesting that the increase in TfR1 expression in GOX-treated B6 cells (Fig. 2A) is independent of IRPs. H₂O₂ has been shown to differentially affect protein degradation in mammalian cells (50, 51). However, pulse-chase experiments with [³⁵S]methionine/cysteine indicate that H₂O₂ does not affect the stability of TfR1 (Fig. 6). Studies of [³⁵S]methionine/cysteine incorporation rather demonstrate that H₂O₂ directly and significantly stimulates TfR1 synthesis.

The direct stimulation of TfR1 protein synthesis by low levels of H₂O₂ is somewhat unexpected. Proteomics data showed that H₂O₂ induces the expression of proteins that are important for translation and RNA processing (52). However, only a few studies on the oxidative modulation of translation exist, and they show a complex response depending on cell type and conditions (52–57). Thus, H₂O₂ was shown to inhibit translation (52, 53) by mechanisms such as the inhibition of the 70-kDa ribosomal protein S6 kinase (52), dephosphorylation of the eukaryotic initiation factor 4E-binding protein 1, or increased binding of this repressor protein to eukaryotic initiation factor 4E and concomitant loss of eukaryotic initiation factor 4F complexes (52, 57). Translation can also be inhibited by H₂O₂ via phosphorylation of the elongation factor eukaryotic elongation factor 2 (eEF2) (52), which was either mediated by activation of the eEF-2 specific, Ca²⁺/calmodulin-dependent protein kinase III (55) or reversible inhibition of the protein phosphatase 1 (56). On the other side, H₂O₂ has been shown to stimulate translation in cell-free systems (58), plants (59), bacteria (60), and mammalian cells (54). Importantly, the latter study indicated that the effect of H₂O₂ on translation depends on the levels of H₂O₂ and the cell sensitivity toward H₂O₂. Thus, in Huh7 cells that are moderately sensitive toward H₂O₂, translation was up-regulated even at a low level of H₂O₂.

In summary, our study establishes that sustained, nontoxic concentrations of H₂O₂ stimulate TfR1 expression by a novel translational mechanism. Hence, H₂O₂ is able to stimulate TfR1 expression both at the post-transcriptional level via IRP1 and at the translational level, which points to a potentially general mechanism of iron internalization in the presence of H₂O₂. In addition to the role of hepcidin and ferroportin on iron homeostasis during inflammation (17, 47), H₂O₂-mediated iron uptake could provide an alternative local mechanism that removes iron from the inflammatory battle field and prevents unspecific collateral tissue damage. Under conditions of chronic inflammation, however, the continued accumulation of iron could itself impose a threat to cells and tissues (2–9). In addition, translational stimulation of TfR1 expression by H₂O₂ could participate in the toxicity of chemotherapeutic anticancer agents such as doxorubicin that are known to increase TfR1 expression (61, 62). Our work underlines the importance of studying the expression of proteins in clinical and animal trials that are commonly focusing on the mRNA levels because of limited tissue availability. Our novel tool of a sustained exposure of cultured cells to H₂O₂ will help to better understand molecular mechanisms related to oxidative stress in future

studies that should also include the complex redox-sensitive regulation of translation.

Acknowledgment—We thank Dr. Prem Ponka for kindly providing us with salicylaldehyde isonicotinoyl hydrazone.

REFERENCES

- Cartwright, G. E., Lauritsen, M. A., Jones, P. J., Merrill, I. M., and Wintrobe, M. M. (1946) *J. Clin. Investig.* **25**, 65–80
- Hirayama, M., Kohgo, Y., Kondo, H., Shintani, N., Fujikawa, K., Sasaki, K., Kato, J., and Niitsu, Y. (1993) *Hepatology* **18**, 874–880
- Schäfer, K.-H. (1942) *Zeitschrift für die Gesamte Experimentelle Medizin* **110**, 678–696
- Kazemi-Shirazi, L., Datz, C., Maier-Dobersberger, T., Kaserer, K., Hackl, F., Polli, C., Steindl, P. E., Penner, E., and Ferenci, P. (1999) *Gastroenterology* **116**, 127–134
- Piperno, A., Vergani, A., Malosio, I., Parma, L., Fossati, L., Ricci, A., Bovo, G., Boari, G., and Mancina, G. (1998) *Hepatology* **28**, 1105–1109
- Haque, S., Chandra, B., Gerber, M. A., and Lok, A. S. (1996) *Hum. Pathol.* **27**, 1277–1281
- Riggio, O., Montagnese, F., Fiore, P., Folino, S., Giambartolomei, S., Gandin, C., Merli, M., Quinti, I., Violante, N., Caroli, S., Senofonte, O., and Capocaccia, L. (1997) *Am. J. Gastroenterol.* **92**, 1298–1301
- Bonkovsky, H. L., Lambrecht, R. W., and Shan, Y. (2003) *Alcohol* **30**, 137–144
- Mueller, S., Afdhal, N. H., and Schuppan, D. (2006) *Gastroenterology* **130**, 2229–2234
- Kondo, H., Saito, K., Grasso, J. P., and Aisen, P. (1988) *Hepatology* **8**, 32–38
- Konijn, A. M. (1994) *Baillieres Clin. Haematol.* **7**, 829–849
- Freireich, E. J., Miller, A., Emerson, C. P., and Ross, J. F. (1957) *Blood* **12**, 972–982
- Nemeth, E., Rivera, S., Gabayan, V., Keller, C., Taudorf, S., Pedersen, B. K., and Ganz, T. (2004) *J. Clin. Investig.* **113**, 1271–1276
- Roy, C. N., Custodio, A. O., de Graaf, J., Schneider, S., Akpan, I., Montross, L. K., Sanchez, M., Gaudino, A., Hentze, M. W., Andrews, N. C., and Muckenthaler, M. U. (2004) *Nat. Genet.* **36**, 481–485
- Ganz, T. (2003) *Blood* **102**, 783–788
- Roy, C. N., and Andrews, N. C. (2005) *Curr. Opin. Hematol.* **12**, 107–111
- Nemeth, E., Tuttle, M. S., Powelson, J., Vaughn, M. B., Donovan, A., Ward, D. M., Ganz, T., and Kaplan, J. (2004) *Science* **306**, 2090–2093
- Upton, R. L., Chen, Y., Mumby, S., Gutteridge, J. M., Anning, P. B., Nicholson, A. G., Evans, T. W., and Quinlan, G. J. (2003) *Eur. Respir. J.* **22**, 335–341
- Klebanoff, S. J. (1988) in *Phagocytic Cells: Products of Oxygen Metabolism* (Snyderman, R., ed) pp. 391–444, Raven Press, New York
- Geiszt, M., and Leto, T. L. (2004) *J. Biol. Chem.* **279**, 51715–51718
- Hentze, M. W., Muckenthaler, M. U., and Andrews, N. C. (2004) *Cell* **117**, 285–297
- Martins, E. A., Robalinho, R. L., and Meneghini, R. (1995) *Arch. Biochem. Biophys.* **316**, 128–134
- Pantopoulos, K., and Hentze, M. W. (1995) *EMBO J.* **14**, 2917–2924
- Mueller, S., Pantopoulos, K., Hübner, C. A., Stremmel, W., and Hentze, M. W. (2001) *J. Biol. Chem.* **276**, 23192–23196
- Pantopoulos, K., Mueller, S., Atzberger, A., Ansorge, W., Stremmel, W., and Hentze, M. W. (1997) *J. Biol. Chem.* **272**, 9802–9808
- Caltagirone, A., Weiss, G., and Pantopoulos, K. (2001) *J. Biol. Chem.* **276**, 19738–19745
- Lok, C. N., and Ponka, P. (1999) *J. Biol. Chem.* **274**, 24147–24152
- Tacchini, L., Bianchi, L., Bernelli-Zazzera, A., and Cairo, G. (1999) *J. Biol. Chem.* **274**, 24142–24146
- Guzy, R. D., Hoyos, B., Robin, E., Chen, H., Liu, L., Mansfield, K. D., Simon, M. C., Hammerling, U., and Schumacker, P. T. (2005) *Cell Metab.* **1**, 401–408
- Mueller, S. (2000) *Free Radic. Biol. Med.* **29**, 410–415
- Mueller, S., Pantopoulos, K., Hentze, M. W., and Stremmel, W. (1997) in *Bioluminescence and Chemiluminescence: Molecular Reporting with Pho-*

Sustained H₂O₂ Induces Iron Uptake by TfR1

- tons (Stanley, P. E., ed), pp. 338–341, John Wiley & Sons Ltd., Chichester, UK
32. Mütze, S., Hebling, U., Stremmel, W., Wang, J., Arnhold, J., Pantopoulos, K., and Mueller, S. (2003) *J. Biol. Chem.* **278**, 40542–40549
 33. Mueller, S., Riedel, H. D., and Stremmel, W. (1997) *Blood* **90**, 4973–4978
 34. Mueller, S., and Pantopoulos, K. (2002) *Methods Enzymol.* **348**, 324–337
 35. Rost, D., Welker, A., Welker, J., Millonig, G., Berger, I., Autschbach, F., Schuppan, D., and Mueller, S. (2007) *J. Hepatol.* **46**, 482–491
 36. Breuer, W., Epsztejn, S., Millgram, P., and Cabantchik, I. Z. (1995) *Am. J. Physiol.* **268**, C1354–C1361
 37. Breuer, W., Epsztejn, S., and Cabantchik, Z. I. (1995) *J. Biol. Chem.* **270**, 24209–24215
 38. Laskey, J., Webb, I., Schulman, H. M., and Ponka, P. (1988) *Exp. Cell Res.* **176**, 87–95
 39. Riedel, H. D., Muckenthaler, M. U., Gehrke, S. G., Mohr, I., Brennan, K., Herrmann, T., Fitscher, B. A., Hentze, M. W., and Stremmel, W. (1999) *Blood* **94**, 3915–3921
 40. Mueller, S., Cadenas, E., and Schonthal, A. H. (2000) *Cancer Res.* **60**, 156–163
 41. Mueller, S., and Arnhold, J. (1995) *J. Biolumin. Chemilumin.* **10**, 229–237
 42. Sureda, A., Hebling, U., Pons, A., and Mueller, S. (2005) *Free Radic. Res.* **39**, 817–824
 43. Wang, J., Chen, G., and Pantopoulos, K. (2005) *Biochem. J.* **392**, 383–388
 44. Katschinski, D. M., Le, L., Heinrich, D., Wagner, K. F., Hofer, T., Schindler, S. G., and Wenger, R. H. (2002) *J. Biol. Chem.* **277**, 9262–9267
 45. Volland, W. (1940) *Klinische Wochenschrift* **19**, 1242
 46. Quastel, M. R., and Ross, J. F. (1966) *Blood* **28**, 738–757
 47. Knutson, M. D., Oukka, M., Koss, L. M., Aydemir, F., and Wessling-Resnick, M. (2005) *Proc. Natl. Acad. Sci. U. S. A.* **102**, 1324–1328
 48. Kasvosve, I., Gomo, Z. A., Nathoo, K. J., Matibe, P., Mudenge, B., Loyevsky, M., Nekhai, S., and Gordeuk, V. R. (2006) *Clin. Chim. Acta* **371**, 130–136
 49. BelAiba, R. S., Djordjevic, T., Bonello, S., Flugel, D., Hess, J., Kietzmann, T., and Gorlach, A. (2004) *Biol. Chem.* **385**, 249–257
 50. Coronella-Wood, J., Terrand, J., Sun, H., and Chen, Q. M. (2004) *J. Biol. Chem.* **279**, 33567–33574
 51. Reinheckel, T., Ullrich, O., Sitte, N., and Grune, T. (2000) *Arch. Biochem. Biophys.* **377**, 65–68
 52. Patel, J., McLeod, L. E., Vries, R. G., Flynn, A., Wang, X., and Proud, C. G. (2002) *Eur. J. Biochem.* **269**, 3076–3085
 53. Cobelens, P. M., Kavelaars, A., Heijnen, C. J., Ribas, C., Mayor, F., Jr., and Penela, P. (2007) *Cell Signal.* **19**, 269–277
 54. MacCallum, P. R., Jack, S. C., Egan, P. A., McDermott, B. T., Elliott, R. M., and Chan, S. W. (2006) *J. Gen. Virol.* **87**, 3251–3262
 55. Kang, K. R., and Lee, S. Y. (2001) *Exp. Mol. Med.* **33**, 198–204
 56. O’Loughlin, A., Perez-Morgado, M. I., Salinas, M., and Martin, M. E. (2003) *Arch. Biochem. Biophys.* **417**, 194–202
 57. Shenberger, J. S., Adams, M. H., and Zimmer, S. G. (2002) *Am. J. Respir. Cell Mol. Biol.* **27**, 250–256
 58. Luciani, N., Hess, K., Belleville, F., and Nabet, P. (1995) *Biochimie. (Paris)* **77**, 182–189
 59. Casano, L. M., Martin, M., and Sabater, B. (2001) *Plant Physiol.* **125**, 1450–1458
 60. Zhang, A., Altuvia, S., Tiwari, A., Argaman, L., Hengge-Aronis, R., and Storz, G. (1998) *EMBO J.* **17**, 6061–6068
 61. Kotamraju, S., Chitambar, C. R., Kalivendi, S. V., Joseph, J., and Kalyanaraman, B. (2002) *J. Biol. Chem.* **277**, 17179–17187
 62. Mueller, S. (2005) *Biofactors* **24**, 171–181